UNIVERSITAT ROVIRA I VIRGILI
1,3- DIPHOSPHITE LIGANDS WITH FURANOSIDE BACKBONE: A POWERFUL TOOL IN ASYMMETRIC CATALYSIS
Aitor Gual Gozalbo
DL: T-1535-2009/ISBN: 978-84-692-4554-5

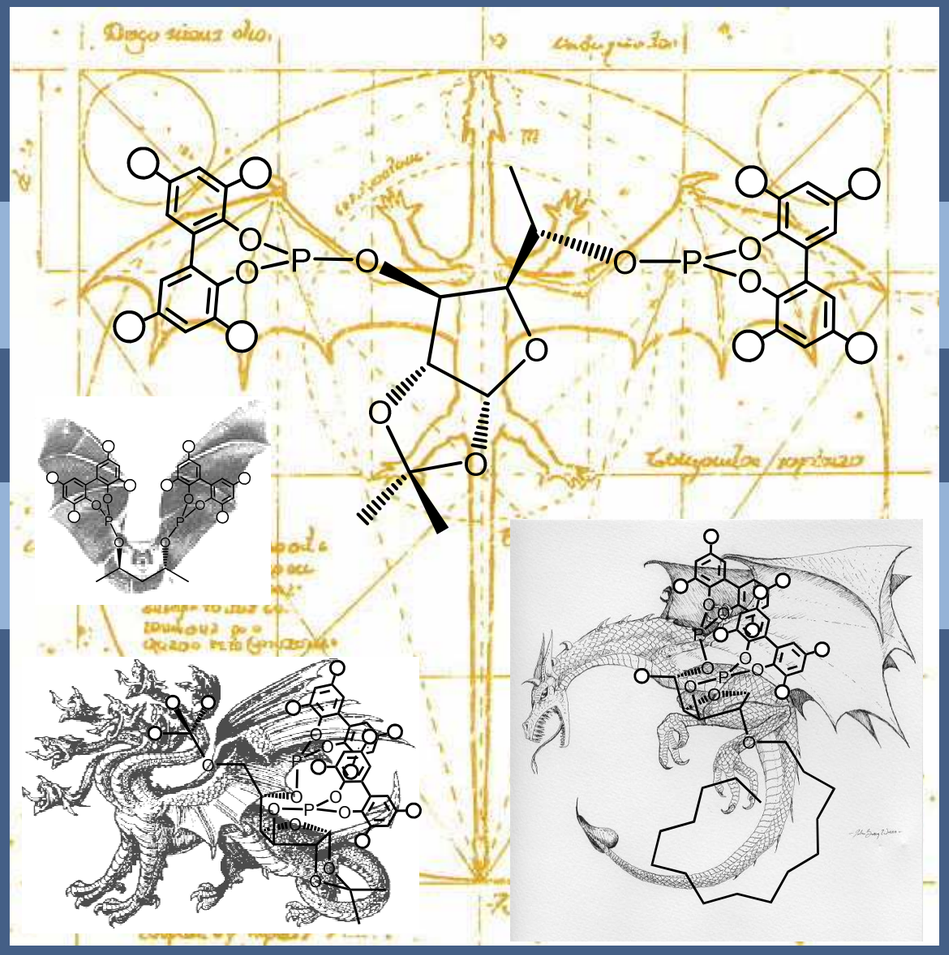

Aitor Gual Gozalbo

1,3-DIPHOSPHITE LIGANDS WITH FURANOSIDE BACKBONE: A POWERFUL TOOL IN ASYMMETRIC CATALYSIS

Aitor Gual Gozalbo

Ph- D Thesis

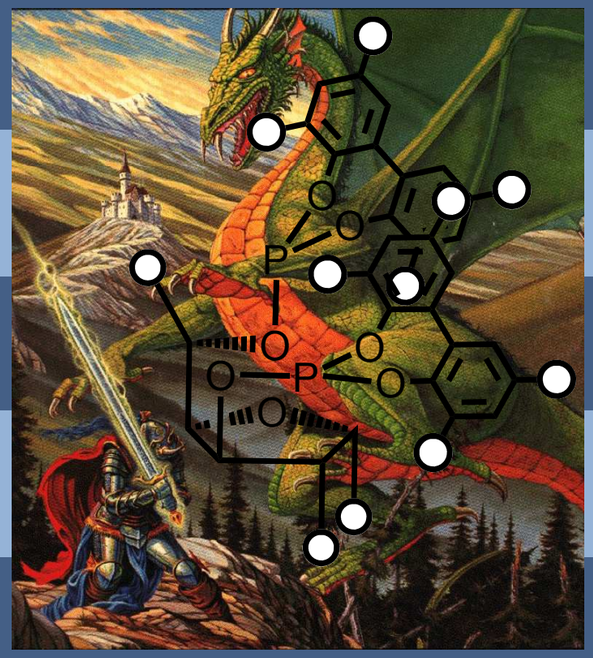

UNIVERSITAT ROVIRA I VIRGILI
TARRAGONA
2009

Tarragona 2009

UNIVERSITAT ROVIRA I VIRGILI
1,3- DIPHOSPHITE LIGANDS WITH FURANOSIDE BACKBONE: A POWERFUL TOOL IN ASYMMETRIC CATALYSIS
Aitor Gual Gozalbo
DL: T-1535-2009/ISBN: 978-84-692-4554-5

Aitor Gual Gozalbo

1,3-DIPHOSPHITE LIGANDS WITH FURANOSIDE BACKBONE: A POWERFUL TOOL IN ASYMMETRIC CATALYSIS

Ph-D Thesis

Supervised by Prof. Dr. Carmen Claver Cabrero
and Prof. Dr. Sergio Castillón Miranda

Departament
de Química Física i Inorgànica

UNIVERSITAT ROVIRA I VIRGILI

TARRAGONA
2009

UNIVERSITAT ROVIRA I VIRGILI
1,3- DIPHOSPHITE LIGANDS WITH FURANOSIDE BACKBONE: A POWERFUL TOOL IN ASYMMETRIC CATALYSIS
Aitor Gual Gozalbo
DL: T-1535-2009/ISBN: 978-84-692-4554-5

UNIVERSITAT ROVIRA I VIRGILI
1,3- DIPHOSPHITE LIGANDS WITH FURANOSIDE BACKBONE: A POWERFUL TOOL IN ASYMMETRIC CATALYSIS
Aitor Gual Gozalbo
DL: T-1535-2009/ISBN: 978-84-692-4554-5

UNIVERSITAT ROVIRA I VIRGILI

Departament de Química Física i Inorgànica

Campus Sescelades
Carrer Marcel·lí Domingo,s/n
43007 Tarragona
Tel. 977 55 81 37
Fax. 977 55 95 63

Prof. Dra. Carmen Claver Cabrero, catedràtica del Departament de Química Física i Inorgànica de la Universitat Rovira i Virgili,

CERTIFICO:

Que el present treball, titulat "**1,3-DIPHOSPHITE LIGANDS WITH FURANOSIDE BACKBONE: A POWERFUL TOOL IN ASYMMETRIC CATALYSIS**", que presenta Aitor Gual Gozalbo per a l´obtenció del títol de Doctor, ha estat realitzat sota la meva direcció i la co-direcció del Prof. Dr. Sergio Castillón Miranda, del Departament de Química Analítica i Orgànica de la Universitat Rovira i Virgili, al Departament de Química Física i Inorgànica i que acompleix els requeriments per poder optar a Menció Europea.

Tarragona, 30 d´abril de 2009

UNIVERSITAT ROVIRA I VIRGILI
1,3- DIPHOSPHITE LIGANDS WITH FURANOSIDE BACKBONE: A POWERFUL TOOL IN ASYMMETRIC CATALYSIS
Aitor Gual Gozalbo
DL: T-1535-2009/ISBN: 978-84-692-4554-5

UNIVERSITAT ROVIRA I VIRGILI
1,3- DIPHOSPHITE LIGANDS WITH FURANOSIDE BACKBONE: A POWERFUL TOOL IN ASYMMETRIC CATALYSIS
Aitor Gual Gozalbo
DL: T-1535-2009/ISBN: 978-84-692-4554-5

Agraïments/ Agradecimientos/ Acknowledgements/ Remerciements

Mi tesis ha de comenzar con el agradecimiento, por supuesto, para el Prof. Dr. Eduardo Peris de la Universitat Jaume I de Castellón, España por soportar las trastadas de aquel año en el que fue mi tutor Erasmus (alla por el 2004!...), y después de todo, ponerme en contacto con la que ha sido mi directora de tesis, la Prof. Dr. Carmen Claver. Y por supuesto, obrigado (ya casi no me acuerdo de hablar portugués) al Prof. Dr. Artur Cavacco Paulo de la Universidad de Guimaraes, Portugal por tener mucha paciencia en aquel año Erasmus que fue mi primera experiencia trabajando en investigación en un laboratorio químico. Cabe incluir dentro de estos agradecimientos a toda la gente del laboratorio de Química Textil de la Universidad de Guimarães, y por supuesto a todos mis compañeros Erasmus (especialmente a mi tocayo Domingo) y no-Erasmus que encontré por el país vecino (Alfonso Henriques, el primer rey de Portugal, nació en Guimarães).

En segundo lugar, pero el más importante en este caso, mi agradecimiento a la Prof. Dra. Carmen Claver y al Prof. Dr. Sergio Castillón por recibirme con los brazos abiertos en el grupo de investigación Química Organometálica y de Catálisis Homogénea (OMICH) de la Universidad Rovira i Virgili de Tarragona, España. Primero de todo, aunque sea bastante "CABEZON" he aprendido mucho de vosotros, y no puedo más que agradeceros para siempre que confiarais en mi para hacer una tesis en catálisis homogénea.

En tercer lugar, mi agradecimiento a todo el grupo "humano" que se encarga de planificar los cursos interuniversitarios de "Catálisis Homogénea" porqué fue una forma suave y al mismo tiempo contundente de adentrarnos en este campo de la química. Mi agradecimiento a los profesores del curso y al grupo de estudiantes que participaban (Juan Urbano "mi Hermano" y "El Licenciado"de la UHU de Huelva, Mónica y Rosa de la UJI de Castellón, Charo de UB de Barcelona, Meritxell de la UAB de Barcelona, Arnau y Ana de la Universitat de Girona, Vanesa de la URV de Tarragona, Noelia de UCLM de Ciudad Real) en aquellos cursos.

DL: T-1535-2009/ISBN: 978-84-692-4554-5

Acknowledgements/Agraïments

Referente al grupo de investigación "Química Organometálica y Catálisis Homogénea" (OMICH) de la Universidad Rovira i Virgili de Tarragona quiero agradecer a la Dra. Aurora Ruiz por su disponibilidad ante cualquier duda y por su simpatía. A la Dra. Montserrat Diéguez y al Dr. Oscar Pàmies por su trato correcto y la colaboración en la realización de experimentos de alquilación alílica con los ligandos diseñados en esta tesis. Y al resto de profesores del área agradecerles su simpatía en los momentos que hemos interaccionado: Dra. Aranzazu Orejón, Dra. Pilar Salagre, Dra. Yolanda Cesteros, Dra. Anna Maria Masdeu y Dra. Elena Fernández.

Bueno, ahora viene lo más "difícil"….porque por este grupo desde que llegué ha pasado un grupo de gente bastante grande. Así que voy a empezar por los que estaban cuando yo llegué al grupo: Marta (el primer día me dio miedo), Rosa (gracias por ayudarme a empezar), Antonio, Eugeni, Isabel Salla, Olga, Vanesa, Clara, Bianca e Yvette (graciás por enseñarme a hacer alquilación alílica), graciás por todo, hemos cantado y bailado mucho. No, no tengas miedo, Jesus, he puesto un punto y aparte porque tú te lo mereces "neng", pero tienes que saber que ahora cuando me agacho en el laboratorio siempre miro atrás. He de mencionar también a mi gran amigo Nacho de Zaragoza, que estuvo entre nosotros pero ahora está haciendo la tesis en Barcelona, un abrazo "maño".

Bueno, después de toda esta gente, recuerdo que un día llegó un tal Eduardo García, un asturiano que venía de Italia, y desde aquel día nunca fui a jugar una diana y beber una cervecita "solo". Y por supuesto el Dr. Cyril Godard, un francés que vino de York, que no sabía nada de los "CABEZONES DE CASTELLON", y para su desgracia topo conmigo "EL REY DE LOS CABEZONES" y con el que compartía más de una afición, como por ejemplo "las bicicletas". Ahora en serio, quiero agradecerle en especial al Dr. Cyril Godard por todo el tiempo que ha perdido conmigo discutiendo y porqué en gran parte esta tesis no hubiera sido posible sin él (experimentos, discusiones, correcciones y muchas cosas más). Graciás por todo. Y paso el tiempo, y los que estaban fueron acabando, y gente nueva fue comenzando. Bueno, a ver si os menciono a todos y por orden: Dr. Ali Aghmiz (también conocido como "Casillas"), Eva (futura doctora en pocos meses), Isa (gracias por leernos las noticias y por tu simpatía), Carolina (ánimo con los ligandos y no desesperes, a veces, las cosas que más cuestan son las que más valoras después), Dolores, Verónica (tendrás una

tesis fantástica), Angélica (ánimo con la tesis que casi la tienes), Ariadna, Xavi, Amadeu, Mercé, Oriol (el año que viene ganareis el campeonato), Dr. Olivier Jacquet (ahora en el ICIQ), Cristina Pubill (si soy para ti una musa píntame un retrato) y Cristina Solé. Animo a todos, que el tiempo pasa volando y cuando estas a gusto aun más, os lo digo por experiencia. También debó recordar a la futura doctora Sarah Fachetti, que compartió conmigo los últimos nueve meses de mi tesis con una intensa y dura experiencia en el mundo de la hidroformilación con ligandos monofosfitos. También tengo que agradecerle a nuestra querida Maria Jose Romero todo el esfuerzo por ayudarme con pedidos, facturas, envíos de paquetes,…etc, graciás Maria Jose.

Bueno, no puedo olvidarme de agradecer a los grupos del Departamento de Química Orgánica su colaboración "especial" y en particular al grupo de Carbohidratos (Dra. Patricia Marce, Dr. David Benito, Isidro, Pep, Irene, Antonio, Dr. Omar, Dr. Miguel Angel, Xavi) y al grupo de Polímeros (especialmente a Lucas y a Quique). También nombrar a Marisol que me ha estado informando de todo lo necesario para planear la preparación del evento y me ha quitado un peso "brutal" de encima. Finalmente, tengo que nombrar a un genio del RMN, a nuestro gran y poderoso técnico Ramon Guerrero, si él no lo puede hacer es que es imposible. Y las chicas de microscopia (Merce y Mariana) con las que compartí muchas tardes en silencio en el cuarto oscuro donde está el aparato. Además, mi agradecimiento al resto de personal de los Servicios Científico-Técnicos que en algún momento me prestó su ayuda.

Tampoco puedo olvidarme de agradecerles a los grupos con los que he colaborado su hospitalidad y su esfuerzo para que todo saliera lo mejor posible.

Prof. Dr. Bruno Chaudret and Dr. Karine Philippot from "Laboratoire de Chimie de Coordination" of Toulouse, France are acknowledged to introduce me to the synthesis of metal nanoparticles by decomposition of organometallic precursor and the synthesis of these precursors. Special thanks to Prof. Dr. Karine Philippot to improve my knowledge in the "World of the Nanoscience". I want to include Dr. Jordi Garcia Anton to teach me the lab techniques to stabilize ruthenium nanoparticles, and their characterization by TEM techniques.

UNIVERSITAT ROVIRA I VIRGILI
1,3- DIPHOSPHITE LIGANDS WITH FURANOSIDE BACKBONE: A POWERFUL TOOL IN ASYMMETRIC CATALYSIS
Aitor Gual Gozalbo
DL: T-1535-2009/ISBN: 978-84-692-4554-5

Prof. Dr. Alain Roucoux and Dr. Audrey Nowicky-Denicourt from "Ecole Nationale Supérieure de Chimie de Rennes", France are acknowledged to introduce me to the application of metal nanoparticles as catalysts for hydrogenation processes. Special thanks to Prof. Dr. Alain Roucoux and Dr. Audrey Nowitzky-Denicourt for our excellent discussions, which really helped me to improve my knowledge in the "World of the Nanoscience". I want to include Dr. Bastian Leger to teach me the lab techniques to apply metal nanoparticles as catalysts in the hydrogenation processes.

Prof. Dr. Dieter Vogt, Dr. Christian Müller and Dr. Leandra Cornelissen from I/TUe of Eindhoven, Netherlands are kindly acknowledged for their excellent and very interesting work using our designed diphosphite ligands in the in the Rh-asymmetric hydroformylation of 1,1-substituted alkenes. Special thanks to them for the interesting discussions about "the hydroformylation labyrinth". It was necessary to remark, that Dr. Leandra Cornelissen carried out an excellent and exhaustive work with my "not-easily synthesizable" ligands.

Prof. Dr. Montserrat Gomez, Dr. Emmanuelle Teuma, Dr. Fernando Fernandez and Dr. Delphine Sanhes from University of Barcelona, Spain and University Paul Sabatier of Toulouse, France are kindly acknowledged for their interest in the synthesis of diphosphites derived of their diol backbones and their application in metal-catalysed asymmetric processes.

També vull fer partíceps d'aquesta tesi a tots els meus amics (Alfredo, Xixell, Juan, Nando, Mamen, Amanda, Juan, Yanick, Toni "Pequeño", Andy, Itxell, Xavier Sala, Eva…etc) i als meus companys a la universitat de Castelló (Peré, Hueso, Raul, Ruben, Gato, Raquel, Eva, Maria,…etc). I finalment afegir una menció especial per a la GIPA.

En últim lloc, i jo diria que el factor clau per a que estiga avui aquí, vull agrair als meus pares (Rafael Vicente i Maria Dolores), a la meua germana (Gema) i a la resta de la meva família (tió Llango, avia Lola, tió Alejandro, tia Susana, Laura i Alejandro) per la confiança i el suport que m'han donat durant tots aquestos anys des de que era petit fins ara, gràcies per tot de tot cor. Finalment, vull dedicar aquesta tesi a la meva família i a la memòria dels meus avis desapareguts (Jose, Vicente i Irene).

GRÀCIES A TOTS, tots heu col·laborat en l'elaboració d'aquesta tesi, i gràcies també a la persona que estiga llegint-la.

UNIVERSITAT ROVIRA I VIRGILI
1,3- DIPHOSPHITE LIGANDS WITH FURANOSIDE BACKBONE: A POWERFUL TOOL IN ASYMMETRIC CATALYSIS
Aitor Gual Gozalbo
DL: T-1535-2009/ISBN: 978-84-692-4554-5

UNIVERSITAT ROVIRA I VIRGILI
1,3- DIPHOSPHITE LIGANDS WITH FURANOSIDE BACKBONE: A POWERFUL TOOL IN ASYMMETRIC CATALYSIS
Aitor Gual Gozalbo
DL: T-1535-2009/ISBN: 978-84-692-4554-5

UNIVERSITAT ROVIRA I VIRGILI
1,3- DIPHOSPHITE LIGANDS WITH FURANOSIDE BACKBONE: A POWERFUL TOOL IN ASYMMETRIC CATALYSIS
Aitor Gual Gozalbo
DL: T-1535-2009/ISBN: 978-84-692-4554-5

"The great tragedy of science:
the slaying of a beautiful hypothesis by an ugly fact."

Thomas Huxley

UNIVERSITAT ROVIRA I VIRGILI
1,3- DIPHOSPHITE LIGANDS WITH FURANOSIDE BACKBONE: A POWERFUL TOOL IN ASYMMETRIC CATALYSIS
Aitor Gual Gozalbo
DL: T-1535-2009/ISBN: 978-84-692-4554-5

Contents

UNIVERSITAT ROVIRA I VIRGILI
1,3- DIPHOSPHITE LIGANDS WITH FURANOSIDE BACKBONE: A POWERFUL TOOL IN ASYMMETRIC CATALYSIS
Aitor Gual Gozalbo
DL: T-1535-2009/ISBN: 978-84-692-4554-5

UNIVERSITAT ROVIRA I VIRGILI
1,3- DIPHOSPHITE LIGANDS WITH FURANOSIDE BACKBONE: A POWERFUL TOOL IN ASYMMETRIC CATALYSIS
Aitor Gual Gozalbo
DL: T-1535-2009/ISBN: 978-84-692-4554-5

Chapter 1

General Introduction: 1,3-Phosphorus ligands with furanoside backbone in metal-catalysed asymmetric processes

UNIVERSITAT ROVIRA I VIRGILI
1,3- DIPHOSPHITE LIGANDS WITH FURANOSIDE BACKBONE: A POWERFUL TOOL IN ASYMMETRIC CATALYSIS
Aitor Gual Gozalbo
DL: T-1535-2009/ISBN: 978-84-692-4554-5

The demand for chiral compounds in pharmaceutical, agrochemical and the flavour and fragrance industry has encouraged the development of methods for synthesizing such compounds. Three basic strategies make possible the production of enantiomerically pure compounds: a) the use of optically active natural molecules as building blocks, b) optical resolution via resolving agents and c) asymmetric synthesis. Asymmetric synthesis is commonly used to prepare chiral compounds. The basic principle of this method is to form a new chiral center under the influence of a chiral group. Asymmetric catalysis is part of this preparative method and makes possible the transformation of a pro-chiral or racemic substrate into a chiral product using catalytic amounts of the compounds which contain the chiral information. Homogeneous catalysis involves a catalytic system in which the substrates and the catalyst components are brought together in one phase, most often liquid, where the catalyst is usually a metal complex modified with ligands. Therefore, the ligand effects are extremely important in homogeneous catalysis by metal complexes. In enantioselective homogeneous metal catalysis the design of new ligands is perhaps the most crucial step to achieve the highest levels of reactivity and selectivity.[1] Chiral ligands are prepared following some of the general strategies mentioned above to obtain enantiopure compounds. Concerning the strategy that uses the chiral pool, carbohydrates have been widely used for preparing chiral ligands and the phosphorus derivatives were one of the most successful families of ligands in asymmetric catalysis.[2]

1.1. 1,3-Diol furanoside carbohydrate backbone

To reach the highest levels of reactivity and selectivity in catalytic enantiopure reactions, several reaction parameters must be explored and adjusted. In this optimisation process, careful selection and design of the chiral ligands are perhaps the most crucial steps, since the best ligand strongly depends on each particular reaction. One of the simplest ways to obtain chiral compounds is to transform or derivative natural chiral compounds, thus avoiding tedious resolution procedures. Carbohydrates, together with aminoacids, are the most prominent members of the "chiral pool". Carbohydrates have many advantages: they are readily available,

highly functionalised and contain several stereogenic centers. Carbohydrates have been mainly used as chiral templates for the synthesis of enantiomerically pure organic compounds by using stereoselective transformations (the "chiron" approach).[3] The presence of hydroxyl functions in carbohydrate derivates facilitates the synthesis of series of chiral phosphorus ligands such as phosphines, phosphinites, phosphonites and phosphites. Furthermore, the possibility to introduce easy modification in the carbohydrate contributes to the rational design of ligands in the search for high activities and selectivities for each particular reaction.

In addition, most carbohydrates, and in particular the most commonly used pentoses and hexoses (Figure 1), can be easily and selectively obtained in the pyranose or the furanose form.

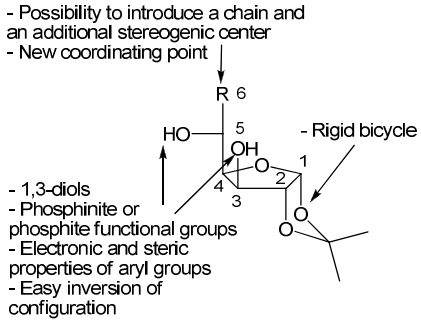

Figure 1.1. Diol carbohydrate backbone in the furanose form.

Ligands with a furanoside backbone are usually prepared from xylose or glucose[4].The main structural features of furanoside ligands are the following (Figure 1.1): a) The anomeric position is usually blocked with a 1,2-*O*-isopropylidene group to give a bicycle, which restricts the conformational freedom; b) phosphorus functions can be attached to 3,5-OH (xylose and glucose derivates) and 5,6-OH (glucose derivates) to give their corresponding 1,2 or 1,3-phosphorus derivatives.

One of the main limitations of using natural products as precursors for ligands is that often only one for the enantiomers (in the case of carbohydrates, the *D* series) is readily available. However, this limitation can be overcome by using pseudo-enantiomer ligands or by suitable ligand tuning of the 1,3-diol furanoside carbohydrate backbone.[4]

UNIVERSITAT ROVIRA I VIRGILI
1,3- DIPHOSPHITE LIGANDS WITH FURANOSIDE BACKBONE: A POWERFUL TOOL IN ASYMMETRIC CATALYSIS
Aitor Gual Gozalbo
DL: T-1535-2009/ISBN: 978-84-692-4554-5

Ligands derived with a 1,2-*O*-isopropylidene-α-*D*-furanoside backbone derived from xylose and glucose have been successfully used in several transition metal catalysed processes[4,5]. These ligands were prepared from *D*-xylose and *D*-glcuose. Xylose (**1**) was treated with acetone in acid medium afforded the 1,2;3,5-*O*-di-isopropylidene-α-*D*-xylofuranoside, and its selective hydrolysis of 3,5-*O*-isopropylidene group gave the 1,2-O-isopropylidene-α-*D*-xylofuranoside (**2**) (Scheme 1.1).

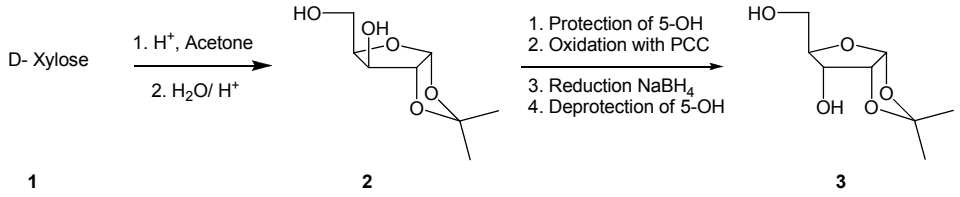

1 **2** **3**

Scheme 1.1. Synthesis of 1,3-diol furanose backbones **2** and **3**.

The inversion of the C-3 stereogenic center afforded the 1,2-*O*-isopropylidene-α-*D*-ribofuranoside **3** (Scheme 1.1). Thus, compound **3** was synthesized from **2** by selective protection of OH-5, oxidation of OH-3 to ketone with PCC (pyridinium chlorochromate). Further reduction with $NaBH_4$ and deprotection of the 5-OH yielded the diol **3**, as a result of the attack of the hydride by the *exo* face of the ketone.

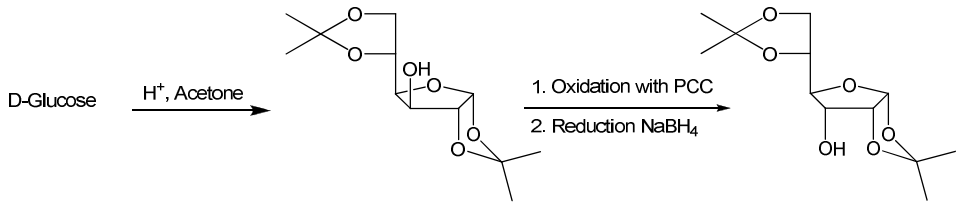

4 **5** **6**

Scheme 1.2. Synthesis of compounds **5** and **6**.

Compounds **13, 14** (Scheme 1.3) are related to **2** and **3**, respectively, in which both hydroxyl groups are bonded to stereogenic centers. These compounds can be obtained from *D*-glucose but require more steps than for the synthesis of **2** and **3** (Scheme 1.2). The synthesis of those compounds starts from the 1,2;3,5-di-*O*-isopropylidene-α-*D*-glucofuranoside **5**

UNIVERSITAT ROVIRA I VIRGILI
1,3- DIPHOSPHITE LIGANDS WITH FURANOSIDE BACKBONE: A POWERFUL TOOL IN ASYMMETRIC CATALYSIS
Aitor Gual Gozalbo
DL: T-1535-2009/ISBN: 978-84-692-4554-5

backbone, which is commercially available, although it can be easily prepared from *D*-glucose **4** by reaction with acetone in acidic medium (Scheme 1.2). Similarly to the synthesis of **3**, compound **5** was converted into 1,2;5,6-*O*-di-isopropylidene-α-*D*-allofuranoside **6** by oxidation with PCC and reduction with $NaBH_4$ (Scheme 1.2).

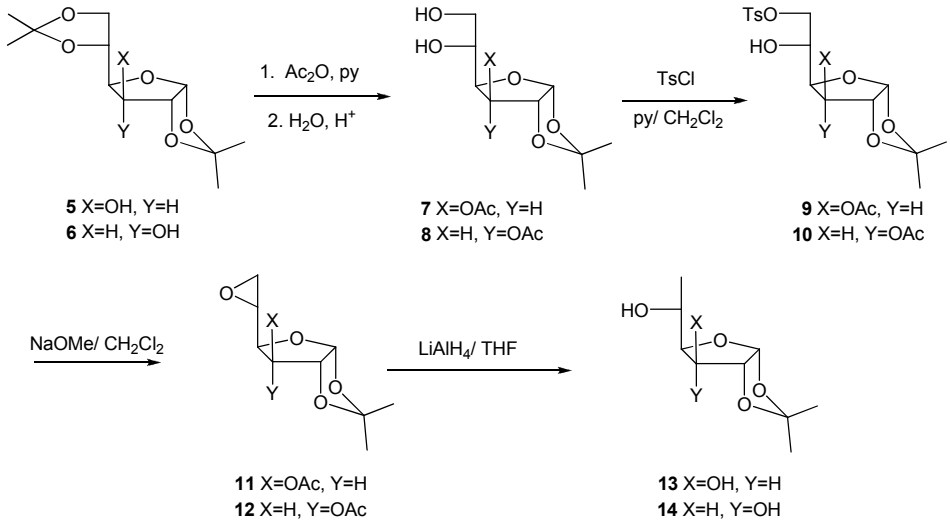

Scheme 1.3. Synthesis of 1,3-diol furanose backbones **13** and **14**.

A five step procedure was required to obtain the 6-*O*-deoxy-1,2-*O*-isopropylidene-α-*D*-furanose derivates **13**,**14** from **5**,**6**, respectively, (Scheme 1.3). The synthesis of both compounds is identical and starts by the acetylation and selective hydrolysis of the 5,6-*O*-isopropylidene acetal to afford **7**,**8**. Deoxygenation of position 6 is carried out by selective tosylation of OH-6 of **7,8** to give **9**,**10**, treatment with NaOMe to afford the 5,6-anhydrosugar (epoxide) derivates **11**,**12**, by an intramolecular nucleophilic attack and deprotection of OH-3 group, and, finally, opening of the 5,6-anhydrosugar by reaction with $LiAlH_4$ afford 6-*O*-deoxy-1,2-O-isopropylidene-α-*D*-glucofuranose **13** and 6-*O*-deoxy-1,2-*O*-isopropylidene-α-*D*-allofuranose **14**.

UNIVERSITAT ROVIRA I VIRGILI
1,3- DIPHOSPHITE LIGANDS WITH FURANOSIDE BACKBONE: A POWERFUL TOOL IN ASYMMETRIC CATALYSIS
Aitor Gual Gozalbo
DL: T-1535-2009/ISBN: 978-84-692-4554-5

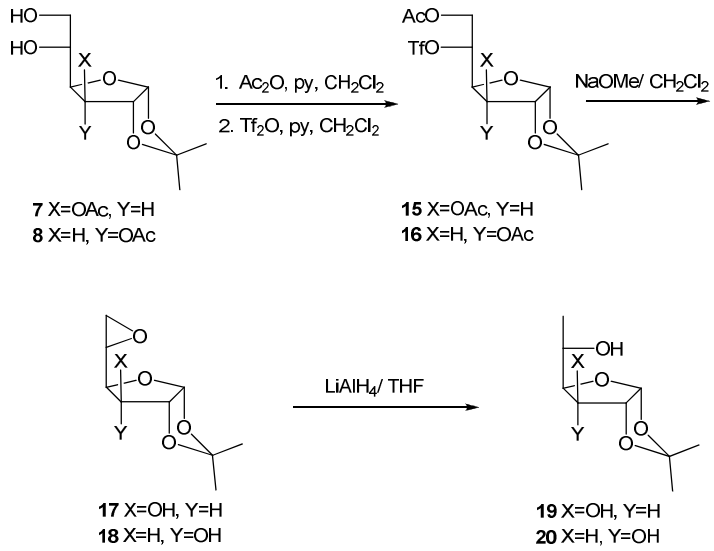

7 X=OAc, Y=H
8 X=H, Y=OAc

15 X=OAc, Y=H
16 X=H, Y=OAc

17 X=OH, Y=H
18 X=H, Y=OH

19 X=OH, Y=H
20 X=H, Y=OH

Scheme 1.4. Synthesis of 1,3-diol furanose backbones **19** and **20**.

Diols **19** and **20** can be considered as pseudo enantiomers of **14** and **13**, respectively, since the C-3 and C-5 have the opposite configuration (Scheme 1.3 vs. Scheme 1.4). The synthesis of **19** and **20** is carried out from **7**,**8** by selective acetylation of 6-OH and triflation of 5-OH to give **15**, **16**. Treatment of the compounds **15**-**16** with NaOMe afforded the corresponding 5,6-anhydrosugars **17, 18** with inversion of the configuration at C-5. Epoxide opening with $LiAlH_4$ afforded the 6-*O*-deoxy-1,2-*O*-isopropylidene-*β*-*L*-idofuranose (**19**) and 6-*O*-deoxy-1,2-*O*-isopropylidene-*β*-*L*-talofuranose (**20**).

1.2. 1,3-Phosphorus based ligands containing furanose carbohydrate backbone in metal-catalysed asymmetric processes.

Series of 1,3-diphosphites ligands with a furanoside backbone (Figure 1.2) derived from 1,2-O-isopropyliden-*α*-*D*-xylofuranose (**21**,**22**) and 6-deoxy-1,2-O-isopropyliden-*α*-*D*-glucofuranose (**23**-**26**) were previously synthesised.[5] The modular construction of these ligands means that there is enough flexibility to fine-tune (a) the various configurations of the

carbohydrate backbone and (b) the steric and electronic properties of the diphosphite substitutuents.

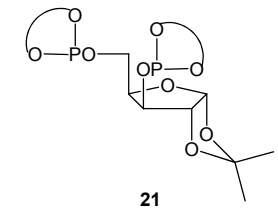

21

Hydroformylation [Rh] 53% (*S*)
Allylic alkylation [Pd] 90% *ee*
Allylic amination [Pd] 97% *ee*
1,4-Addition [Cu] 81% *ee*
Hydrogenation [Ir] 46% *ee*

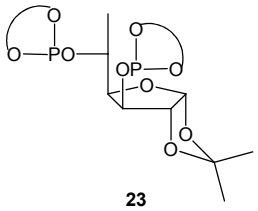

23

Hydroformylation [Rh] 93% (*S*)
Allylic alkylation [Pd] 95% *ee*
1,4-Addition [Cu] 84% *ee*

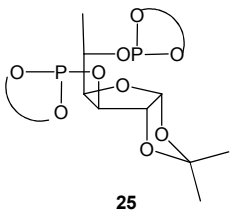

25

Hydroformylation [Rh] 64% (*S*)
Hydrogenation [Rh] 99% *ee*

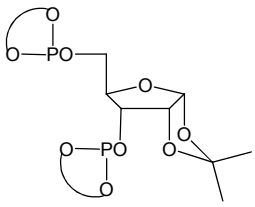

22

Hydroformylation [Rh] 53% (*R*)

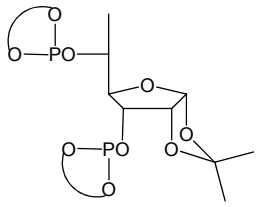

24

Hydroformylation [Rh] 58% (*R*)
Hydrogenation [Rh] 92% *ee*

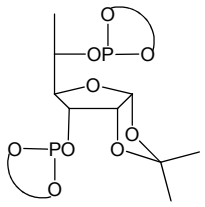

26

Hydroformylation [Rh] 89% (*R*)

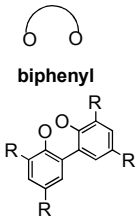

biphenyl

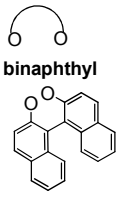

binaphthyl

Figure 1.2. 1,3-Diphosphite ligands **21-26**.

Phosphite ligands **21**-**26** directly prepared from diols **2**, **3**, **13**, **14**, **19** and **20** by reaction with the corresponding phosphorochloridites, were successfully applied in the Rh-asymmetric hydroformylation of monosubstituted vinyl arenes,[5] Rh-catalysed asymmetric hydrogenation of dehydroamino acid derivates,[6] Pd-catalysed asymmetric allylic substitution reactions [7] and in the Cu-catalysed 1,4-addition.[8] The ligand **21** was also tested in the Ir-catalysed hydrogenation of imines producing moderate enantioselectivities (*ee* up to 46%).[9]

UNIVERSITAT ROVIRA I VIRGILI
1,3- DIPHOSPHITE LIGANDS WITH FURANOSIDE BACKBONE: A POWERFUL TOOL IN ASYMMETRIC CATALYSIS
Aitor Gual Gozalbo
DL: T-1535-2009/ISBN: 978-84-692-4554-5

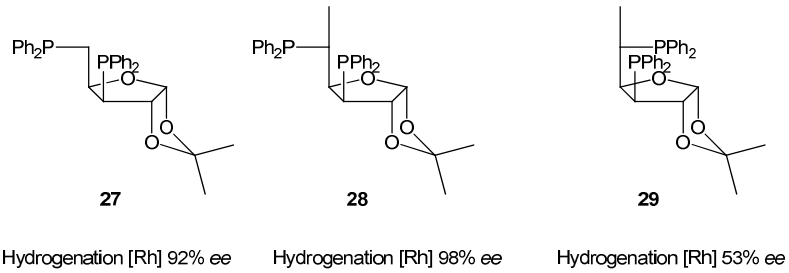

Figure 1.3. 1,3-Diphosphine ligands **27**-**29**.

The diphosphine ligands **27**-**29** (Figure 1.3) with sugar furanose backbone were also synthesised starting from diols **3**, **14** and **20**. These ligands were applied in the Rh-asymmetric hydrogenation.[10] Ligands **27** and **28** provided excellent enantioselectivities in the Rh-catalysed hydrogenation of α,β-unsaturated carboxylic acid derivates. However, results were more modest when diphosphine ligands **27**-**29** were applied in the Rh-catalysed asymmetric hydroformylation of styrene derivates [11] and in the Pd-catalysed asymmetric allylic substitution [12].

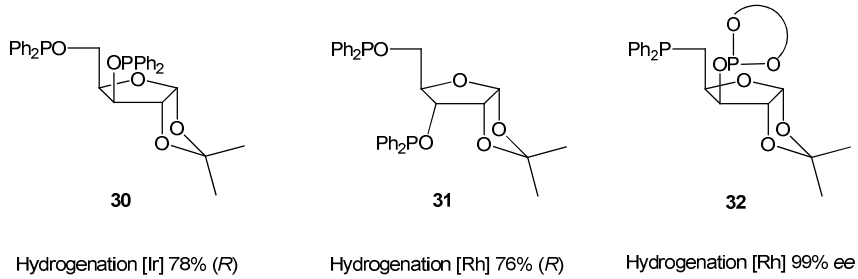

Figure 1.4. 1,3-Diphosphinite ligands **30,31** and 1,3-phosphine-phosphite ligand **32**.

Diphosphinite ligands with furanoside backbone **30-31** were synthesised starting from the 1,2-*O*-isopropyliden-α-*D*-xylofuranose derivates **2**-**3** (Figure 1.4). Diphophinite **30** was applied in the Rh-catalysed asymmetric hydrogenation of α-acetamidocinnamic acid, obtaining low to moderate enantioselectivity. This ligand afforded an ee of 78% (*R*) in the Ir-catalysed hydrogenation of methyl α-acetamidoacrylate,[13] and 57% in the hydrogenation of imines.[9] Comparable enantiomeric excess (76% (*R*))

was obtained in the hydrogenation of methyl α-acetamidoacrylate by using the Rh/**31** catalytic system.[13] Curiously, the catalytic systems Rh/**30** and Ir/**31** gave very low *ee*´s in the hydrogenation of methyl α-acetamidoacrylate.

The phosphine-phosphite ligand **32** was tested in Rh-catalysed asymmetric hydrogenation,[14] Rh-catalysed hydroformylation,[15] Pd-allylic alkylation[7a] and in the Cu-catalysed 1,4-addition reaction[16] (Figure 1.4). High enantioselectivities (*ee* up to 99%) were obtained in the Rh-asymmetric hydrogenation of α,β-unsaturated carboxylic acid derivates, and low to moderate enantioselectivities in the Rh-asymmetric hydroformylation of styrene (*ee* up to 49%), in Pd-catalysed allylic alkylation (*ee* up to 42%) and in the Cu-catalysed 1,4-addition of diethyl zinc to 2-cyclohexenoen (*ee* up to 19%).

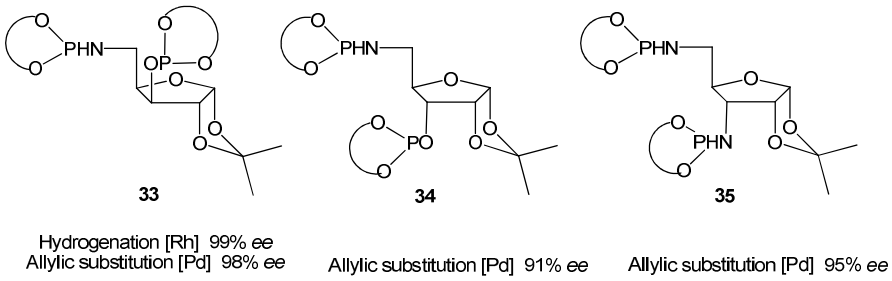

Figure 1.5. Phosphite-phosphoramidite ligands **33**, **34** and diphosphoramidite ligand **35**.

The ligands **33**-**35** were developed because of the higher π-acceptor capacity of the phosphoramidite moiety than the phosphite moiety diphosphite (Figure 1.5). The phosphite-phosphoramidite ligands **33** and **34** were applied in the Rh-catalysed asymmetric hydrogenation of α,β-unsaturated carboxylic acid derivates,[17] in the Rh-catalysed asymmetric hydroformylation of styrene,[18] in Cu-catalysed 1,4-addition reaction[19] and in Pd-allylic substitution reactions.[20]

The enantioselectivities were moderate in the Rh-catalysed asymmetric hydroformylation of styrene and in Cu-catalysed 1,4-addition reactions. However, the ligand **33** provided high enantioselectivities (*ee* up to 99%) in the Rh-catalysed asymmetric hydrogenation of α,β-unsaturated carboxylic

acid derivates, and in the Pd-allylic substitution of hindered disubstituted linear substrates (*ee* up to 98%). Ligand **34** also provided high enantioselectivities in the Pd-allylic substitution of hindered monosubstituted linear substrates (*ee* up to 90%), unhindered linear substrates (*ee* up to 89%) and cyclic substrates (*ee* up to 91%). Furthermore, the bis-phosphoramidite ligand **35** provided excellent enantioselectivities (*ee* up to 95%) in Pd-allylic alkylation of several di- and monosubstituted linear and cyclic substrates.[21]

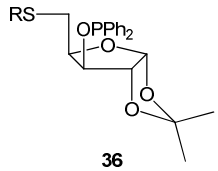

36

R= Ph, Me, iPr, tBu, 4-Me-C_6H_4, 4-CF_3-C_6H_4, 2,6-di-Me-C_6H_3.

Allylic substitution [Pd]	95% *ee*
Hydrogenation [Rh]	96% *ee*
1,4-Addition [Cu]	72% *ee*

Figure 1.6. 1,3-thioether-phosphinite ligand **36**.

Finally, a series of thioether-phosphinite ligands **36** (Figure 1.6) were successfully applied in Pd-allylic substitution of mono- and disubstituted linear and cyclic substrates (*ee* up to 95%),[22] Rh-catalysed hydrogenation of dehydroamino acids and itaconates (*ee* up to 96%)[23] and Cu-catalysed 1,4-additions to cyclohexenones (*ee* up to 72%)[24].

1.3. Scope and objectives

This thesis focus on the development and application in asymmetric catalysis of new 1,3-diphosphite with furanoside backbone. As mentioned in the section 1.1, the synthesis of series 1,3-diols with 1,2-O-isopropylidene-α-*D*-furanose backbone by varying the configuration of the stereocenters directly bonded to the phosphorus function is a crucial step in the design of most efficient bidentate ligands.

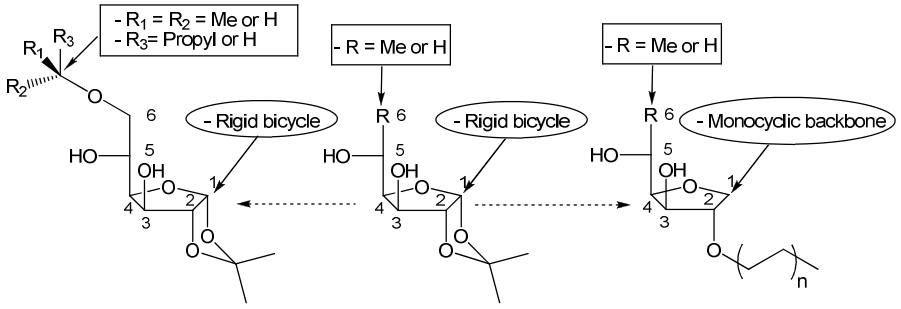

Figure 1.7. Design of new 1,3-diols with furanose backbone.

Our first objective was to design and synthesize new 1,3-diol with furanoside bicyclic backbone related to the well-known 1,2-*O*-isopropylidene-α-*D*-xylofuranose and 6-*O*-deoxy-1,2-*O*-isopropylidene-α-*D*-glucofuranose backbones. The modifications of these 1,3-diol backbones were carried out in two directions (Figure 1.7): a) Introduction of *O*-alkyl substituents in the positions C-6 of the furanoside bicyclic backbone, and b) reduction of the 1,2-*O*-isopropylidene ring in order to obtain 1,3-diol with furanoside monocyclic backbones and introduction of *O*-alkyl substituent in the C-2 position. The synthetic work carried out to achieve these new diol backbones was introduced in chapter 2.

Our second objective was the synthesis of new 1,3-diphosphite ligands with the biphenyl moieties **a** and **b** starting from the new 1,3-diols with furanoside backbone (Figure 1.8). The phosphite moieties **a** and **b** were selected because their versatility in several asymmetric processes.[5-9] Additionally, the use of biphenyl moiety **w** was also tested. Recently, this biphenyl moiety was probed to be efficient in the Ir-catalysed

hydrogenation of ketimines by using 1,2-phosphinite-phosphite ligands with manitol derived backbone.[25] The synthesis of these new 1,3-diphosphite ligands were placed in chapter 2.

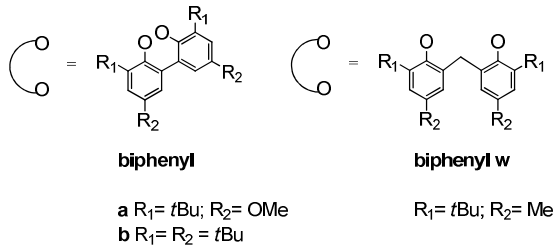

Figure 1.8. Biphenyl moieties used in the synthesis of new 1,3-diphosphite ligands.

Our third objective was the application of the new 1,3-diphosphite ligands series in the Rh-asymmetric hydroformylation of monosubstituted alkenes, such as styrene and vinyl acetate, and disubstituted internal alkenes, 2,5-dihydrofuran and 2,3-dihydrofuran. Additionally, in collaboration with the Prof. Dr. Dieter Vogt these ligands were applied in the Rh-asymmetric hydroformylation of 1,1-disubstituted alkenes, such as methyl methacrylate and α-methylstyrene. The effect of the structural modifications of these 1,3-diphosphite ligands on the catalytic results was studied and the results were introduced in chapter 2.

Our fourth objective was the study of the effect of the structural modification of these 1,3-diphosphite ligands on the catalytic results of the Pd-allylic alkylation of phenyl-allyl compounds. In this section was studied the Pd-allylic alkylation of *rac*-1,3-diphenyl-3-acetoxy-propene using dimethyl malonate as nucleophile and the Pd-allylic alkylation of 1-phenyl-3-acetoxy-propene using dimethyl malonate and α-(ethoxycarbonyl)-cyclohexanone as nucleophiles. The results of this study were placed in chapter 3.

The last objective is the stabilization of metal nanoparticles and their use as nanocatalysts. The metal nanoparticles are active in processes in which the homogeneous catalysts are not active. Therefore, we decided to apply the series of 1,3-diphosphites to stabilize metal nanoparticles (ruthenium, rhodium and iridium nanoparticles) and to study the effect of their selective structural modification in the size, shape and dispersion of the

nanoparticles. The synthesised nanocatalysts were tested in the hydrogenation of pro-chiral monocyclic arenes, such as *o*-methylanisole and *m*-methylanisole. These results were placed in chapter 4.

DL: T-1535-2009/ISBN: 978-84-692-4554-5

[1] P. W. N. M. van Leeuwen, in *Homogeneous Catalysis: Understanding the Art*, Kluwer, Dordrecht, **2004**.

[2] A. Börner, *Phosphorous Ligands in Asymmetric Catalysis*, Wiley VCH, Weinheim, **2008**.

[3] a) S. Hanessian, *Total Synthesis of Natural Products. The Chiron Approach*. Pergamon Press, Oxford, **1983**; b) K. Totami, K.-i. Tabao and K.-i. Tadano, *Synlett*, **2004**, 2006.

[4] a) S. Castillón, C. Claver, Y. Díaz, *Chem. Soc. Rev.* **2005**, *34*, 702; b) M. Diéguez, O. Pàmies, A. Ruiz, Y. Díaz, S. Castillón, C. Claver, *Coord. Chem. Rev.* **2004**, *248*, 2165; c) M. Diéguez, O. Pàmies, C. Claver, *Chem. Rev.* **2004**, *104*, 3189; d) M. Diéguez, C. Claver, O. Pàmies, *Eur. J. Org. Chem.* **2007**, 4621.

[5] a) G.J.H. Buisman, M.E. Martin, E.J. Vos, A. Klootwijk, P.C.J. Kamer, P.W.N.M. van Leeuwen, *Tetrahedron: Asymmetry*. **1995**, *6*, 719; b) O. Pàmies, G. Net, A. Ruiz, C. Claver, *Tetrahedron: Asymmetry*. **2000**, *11*, 1097; c) M. Diéguez, O. Pàmies, A. Ruiz, S. Castillón, C. Claver, *Chem. Eur. J.* **2001**, *7*, 3086; d) M. Diéguez, O. Pàmies, A. Ruiz, C. Claver, *New. J. Chem.* **2002**, *26*, 827.

[6] a) M. Diéguez, A. Ruiz, C. Claver*, J. Org. Chem*. **2002**, *67*, 3796; b) O. Pàmies, G. Net, A. Ruiz, C. Claver, *Eur. J. Inorg. Chem.* **2000**, 1287.

[7] a) O. Pàmies, G.P.F Van Strijdonck, M. Diéguez, S. Deerenberg, G. Net, A. Ruiz, C. Claver, P.C.J. Kamer, P.W.N.M. Van Leeuwen, *J. Org. Chem.* **2001**, *66*, 8867; b) M. Diéguez, S. Jansat, M. Gómez, A. Ruiz, G. Muller, C. Claver, *Chem. Commun.* **2001**, 1132.

[8] a) M. Diéguez, A. Ruiz, C. Claver, *Tetrahedron: Asymmetry*. **2001**, *12*, 2895; b) O. Pàmies, M. Diéguez, G. Net, A. Ruiz, C. Claver, *Tetrahedron: Asymmetry*. **2000**, *11*, 4377; c) O. Pàmies, G. Net, A. Ruiz, C. Claver, *Tetrahedron: Asymmetry*. **1999**, *10*, 2007.

[9] E. Guiu, B. Muñoz, S. Castillón, C. Claver, *Adv. Synth. Catal.* **2003**, *345*, 169.

[10] a) O. Pàmies, G. Net, A. Ruiz, C. Claver, *Eur. J. Inorg. Chem.* **2000**, 2011; b) M. Diéguez, O. Pàmies, A. Ruiz, S. Castillón, C. Claver, *Tetrahedron: Asymmetry*, **2000**, *11*, 4701.

[11] M. Diéguez, O. Pàmies, G. Net, A. Ruiz, C. Claver, *Tetrahedron: Asymmetry*, **2001**, *12*, 651.

[12] M. Diéguez, S. Jansat, M. Gomez, A. Ruiz, G. Muller, C. Claver, *Chem. Commun.* **2001**,1132.

[13] E. Guimet, M. Diéguez, A. Ruiz, C. Claver, *Tetrahedron: Asymmetry*. **2004**, *15*, 2247.

[14] a) O. Pàmies, M. Diéguez, G. Net, A. Ruiz, C. Claver, *Chem. Commun.* **2000**, 2383; b) O. Pàmies, M. Diéguez, G. Net, A. Ruiz, C. Claver, *J. Org. Chem.* **2001**, *66*, 8364.

DL: T-1535-2009/ISBN: 978-84-692-4554-5

[15] O. Pàmies, G. Net, A. Ruiz, C. Claver, *Tetrahedron: Asymmetry*. **2001**, *12*, 3441.

[16] M. Diéguez, O. Pàmies, G. Net, A. Ruiz, C. Claver, *J. Mol. Catal. A: Chem.* **2002**, *185*, 11.

[17] M.Diéguez, A. Ruiz, C. Claver, *Chem. Commun.* **2001**, 2702.

[18] M. Diéguez, A. Ruiz, C. Claver, *Tetrahedron: Asymmetry*. **2001**, *12*, 2827.

[19] M. Diéguez, A. Ruiz, C. Claver, *Tetrahedron: Asymmetry*. **2001**, *12*, 2861.

[20] E. Raluy, C. Claver, O. Pàmies, M. Diéguez, *Org. Lett.* **2007**, *9*, 49.

[21] E. Raluy, M. Diéguez, O. Pàmies, *J. Org. Chem.* **2007**, *72*, 2842.

[22] a) E. Guimet, M. Diéguez, A. Ruiz, C. Claver, *Tetrahedron: Asymmetry*. **2005**, *16*, 959; b) M. Diéguez, O. Pàmies, C. Claver. *J. Organomet. Chem*. **2006**, *691*, 2257.

[23] E. Guimet, M. Diéguez, A. Ruiz, C. Claver, *Dalton Trans*. **2005**, 2557.

[24] E. Guimet, M. Diéguez, A. Ruiz, C. Claver, *Tetrahedron: Asymmetry*. **2005**, *16*, 2161.

[25] E. Guiu, M. Aghmiz, Y. Díaz, C. Claver, B. Meseguer, C. Militzer, S. Castillón, *Eur. J. Org. Chem.* **2006**, 627.

Chapter 2

Synthesis of novel 1,3-diphosphite ligands with furanoside backbone and their application in Rh-catalysed asymmetric hydrofomylation

2.4 Results and Discussion.

2.4.1. C1-Symmetry diphosphite ligands derived from carbohydrates. Influence of structural modifications on the Rh-catalysed asymmetric hydroformylation of styrene.

2.4.2. Highly enantioselective Rh-catalysts for the asymmetric hydroformylation of vinyl- and allylethers using C1-Symmetry diphosphite ligands.

2.4.3. Highly enantioselective Rh-catalysts for the asymmetric hydroformylation of α-methylstyrene and methyl-methacrylate using C1-Symmetry diphosphite ligands.

2.5 Conclusions.

2.6 Experimental Section.

2.1 Introduction to Rh-catalysed hydroformylation reaction

The hydroformylation of alkenes, which was originally discovered by Otto Roelen in 1938 [1], has developed into one of the most important applications of homogeneous catalysis in industry (Scheme 2.1) [2,3]. Today, more than 9 millions tons of so-called oxo-products are produced per year, a number which is still rising continuously. The majority of these oxo-products stem from hydroformylation of propene, which is a fraction of the steam-cracking process. The resulting products *n*butanal and isobutyraldehyde are important intermediates for the production of esters and acrylates. [2].

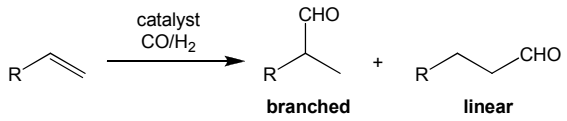

Scheme 2.1. Hydroformylation of alkenes.

From a synthetic point of view the reaction is one-carbon chain elongation caused by the addition of carbon monoxide and hydrogen across the π system of a C=C double bond [4-5]. As a pure addition reaction, the hydroformylation reaction meets all requirements of an atom economic process [6]. Furthermore, the synthetically valuable aldehyde function is introduced which allows subsequent skeleton expansion that may even be achieved in one-pot sequential transformations [7,8].

In 1968, Wilkinson discovered that phosphine-modified rhodium complexes display a significantly higher activity and selectivity compared to the first generation of cobalt catalyst [9]. Since this time, ligand modification of the rhodium catalyst has been the method of choice in order to influence the catalyst activity and selectivity [10].

Despite significant research efforts in the past, one of the remaining problems to be solved in industry is the chemoselective (and simultaneously regioselective) in the low-pressure hydroformylation of internal alkenes. The problem originates from the exponential drop of alkene reactivity with increasing the number of alkene substitutents. The known hydroformylation catalysts for internal alkene hydroformylation operating under low-pressure conditions rely on the use of strong π-

acceptor ligands, such as bulky phosphites and phosphabenzene systems [11,12,13]. However, the high activity of the corresponding rhodium catalysts is always associated with a high tendency towards alkene isomerisation, which renders a position-selective hydroformylation of an internal alkene so far impossible.

The regioselectivity of the hydroformylation of alkenes is a function of many factors. These include inherent substrate preferences, directing effects exerted by functional groups as part of the substrate, as well as catalyst effects. In order to appreciate substrate inherent regioselectivity trends, alkenes have to be classified according to the number and nature of their substituent pattern (Scheme 2.2) [4,5].

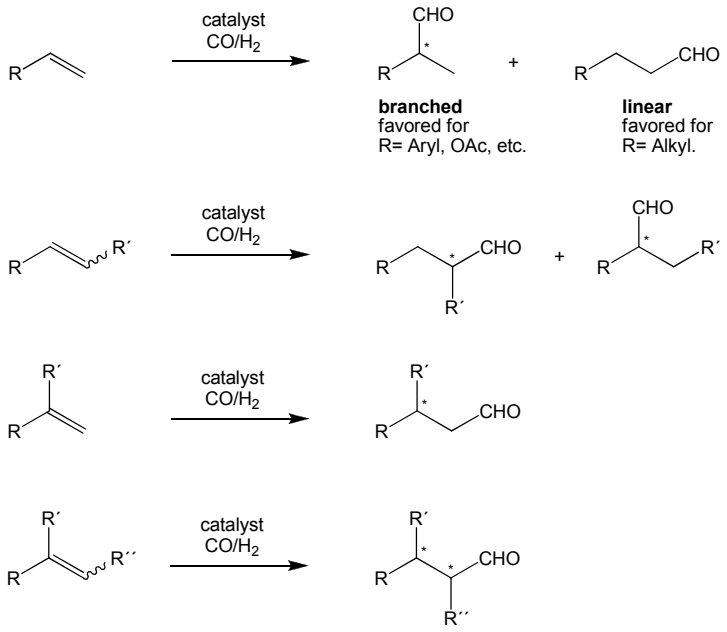

Scheme 2.2. Regioselective trends on hydroformylation of different alkenes.

The problem of regioselectivity arises in general only for terminal and 1,2-disubstituted alkenes. For alkyl-substituted terminal alkenes there is a slight preference for the linear product. For terminal alkene functions attached to an inductively electron-withdrawing substituent the branched regioisomer is preferred, and sometimes is the exclusive product. This tendency is more or less unaffected by the catalyst structure. Both 1,1-

disubstituted and trisubstituted alkenes generally provide only one regioisomer based on Keuleman´s rule, which states that the formyl group is attached such as to avoid the formation of a quaternary carbon centre [14].

Asymmetric hydroformylation is a very promising catalytic reaction that produces chiral aldehydes from inexpensive feedstock (alkenes, *syngas*) in a single step under essentially neutral reaction conditions. Since the aldehyde is one of the most versatile functional groups, a variety of useful chiral chemicals such as amines, imines, alcohols, and acids can be easily prepared from chiral aldehydes. Even though asymmetric hydroformylation offers great promise to the fine chemical industry, this reaction has not yet been utilized on an industrial scale due to several technical challenges. [2] Among the most significant are (a) low reaction rates at low temperature where good selectivitities are usually observed, (b) difficulty in controlling the regio- and enantioselectivities concurrently, and (c) limited substrate scope for any single ligand.

2.2 Rh-catalysed hydroformylation mechanism

In Scheme 2.3 the well-known mechanism is depicted the Rh-catalysed hydroformylation mechanism proposed by Heck [15]. It corresponds to Wilkinson's so-called dissociative mechanism. [9] The associative mechanism involving 20-electron intermediates for ligand/substrate exchange will not be considered. For bidentate ligands (**L**-**L**) a common starting complex is [RhH(**L**-**L**)$(CO)_2$], complexes **37eq-eq** and **37eq-ax**, containing the phosphite functions in equatorial positions (denoted **eq-eq** throughout the Scheme) or one in an apical position and the other ligand in an equatorial position (complexes denoted **eq-ax**).

Dissociation of equatorial CO from **37** leads to the square-planar intermediate **38**, which have **L** in *cis* configuration. Complex **38** associates with ethene to give complexes **39**, again in two isomeric forms **eq-ax** and **eq-eq**, having a hydride in an apical position and ethene coordinated in the equatorial plane.

It has not been established experimentally whether alkene complexation is reversible or not; we have drawn in the Scheme 2.3 all steps as reversible except the final hydrogenolysis. Experiments with the use of deuterated

substrates suggest that alkene coordination and insertion into the Rh-H bond can be reversible, certainly when the pressures are low. Complexes **39** undergo migratory insertion to give the square-planar alkyl complex **40**. Complex **40** can undergo β-hydride elimination, thus leading to isomerisation, or can react with CO to form the trigonal bipyramidal (TBP) complexes **41**. Thus, under low pressure of CO more isomerisation may be expected. At low temperatures (< 70ºC) and a sufficiently high pressure of CO (> 10bar) the insertion reaction is usually irreversible and thus the regioselectivity and the enantioselectivity in the hydroformylation of alkenes is determined at this point.

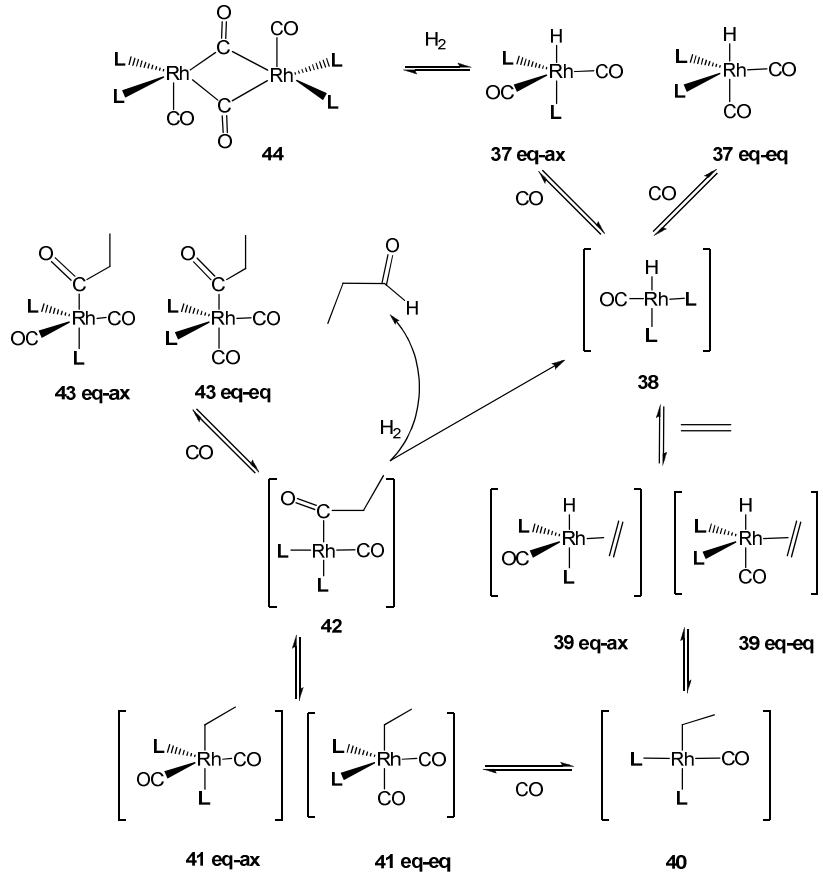

Scheme 2.3. Mechanism of the Rh-asymmetric hydroformylation in presence of bidentate ligand (**L**-**L**).

Complexes **41** undergo the second migratory insertion (see Scheme 2.3) to form the acyl complex **42**. Complex **42** can react with CO to give the saturated acyl intermediates **43** or with H_2 to give the aldehyde product

and the unsaturated intermediate **38**. The reaction with H_2 involves presumably oxidative addition and reductive elimination, but for rhodium no trivalent intermediates have been observed. [16]
At low hydrogen pressures and high rhodium concentrations, the formation of dirhodium dormant species such as **44** becomes significant.

2.3 Rh-catalysed asymmetric hydroformylation

As it was mentioned above, the catalytic hydroformylation of alkenes is one of the largest applications of homogeneous organotransition metal catalysis today. The robustness of the process and the wide availability of alkene substrates, enantioselective hydroformylation provided high possibilities to obtain a great variety of chiral-enantiomerically pure aldehydes.

2.3.1 Rh-catalysed asymmetric hydroformylation of monosubstituted alkenes

The hydroformylation of monosubstituted alkenes (Scheme 2.4) was extensively studied because their interest in the synthesis of linear substrates (non-chiral) or the enantioselective synthesis of 2-substituted branched aldehydes.[2-5]

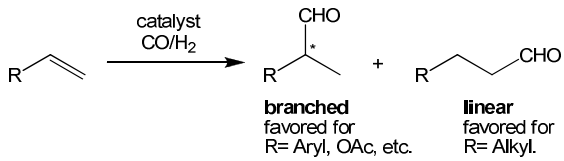

Scheme 2.4. Asymmetric hydroformylation of monosubstituted alkenes.

For example, the 2-aryl propanaldehydes obtained through the hydroformylation of vinylarenes (R= Aryl) are used as intermediates in the synthesis of 2-aryl propionic acids, the profen class of non-stereoidal drugs. Nowadays, the application of the Rh-asymmetric hydroformylation to obtain enantiomerically pure chiral aldehydes is growing. The Rh-asymmetric hydroformylation of several other monosubstituted alkenes was successfully carried out, such as allyl cyanide and vinyl acetate. [3-5] In general, 1,3-diphosphite and phosphine-phosphite ligands provided the

best results in these processes. However the use of bisphophacyclic ligands has recently emerged as an efficient alternative.

1,3-Diphosphites

The initial success in the rhodium-catalysed asymmetric hydroformylation of vinylarenes came from Union Carbide with the discovery of the diphosphite ligand (2*R*, 4*R*)-pentane-2,4-diol **45** (Figure 2.5) (Scheme 2.5).[17]

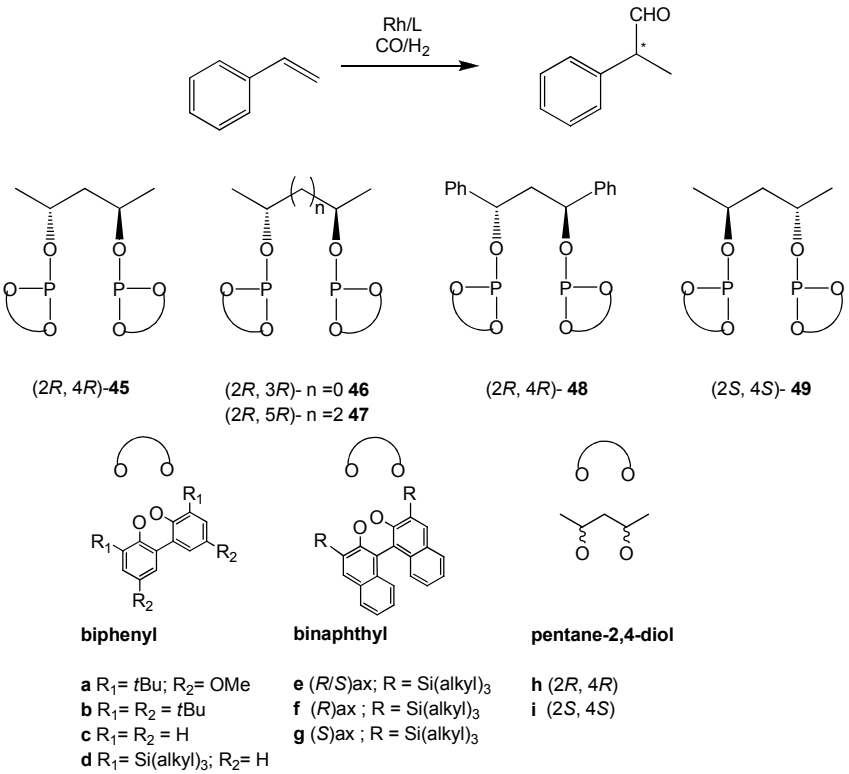

Scheme 2.5. Rh-asymmetric hydroformylation of styrene using ligands **45**-**49**.

Good chemo-, regio- and enantioselectivities (*ee* up to 90%) were obtained with (2*R*,4*R*)-pentane-2,4-diol (**45a**-**c**) but only when the reaction was performed around room temperature. Inspired by these excellent results, other research groups synthesised the series of diphosphite ligands

46-**49** in order to study the effect of several modifications on the Rh-asymmetric hydroformylation of vinylarenes (Scheme 2.5).[18,19, 20]

The influence of the bridge length was studied with diphosphite ligands (2*R*, 4*R*)-pentane-2,4-diol **45**, (2*R*, 4*R*)-butane-2,4-diol **46** and (2*R*, 4*R*)-hexane-2,4-diol **47**. [18b] In general, ligand **45**, which contains three carbon atoms in the bridge, provided higher enantioselectivities than ligands **46** and **47**, which have two and four carbon atoms in the bridge.

The effect of different phosphite moieties was studied with ligands **45a**-**g**.[18] In general, sterically hindered phosphite moieties are necessary to achieve high enantioselectivities. The results indicated that varying the *ortho* and *para* substituents on the biphenyl and binaphthyl moieties has also a great effect on the asymmetric induction. The highest enantioselectivity (*ee* up to 90% at 20 bar of syngas and 25ºC) in the Rh-asymmetric hydroformylation of styrene was obtained by using ligands **45b** and **45d**.

The influence of the backbone was studied by comparing ligands **45** and **48**.[18] Surprisingly, ligand **48**, which have a more sterically hindered phenyl group, provided lower enantioselectivity than ligand **45**.

A possible cooperative effect between the different chiral centres of the phosphite ligands **45f**-**i** and **49f**-**i** was also studied. Initially, van Leeuwen and co-workers studied the cooperative effect between the chiral ligand bridge and the axially chiral binaphthyl phosphite moieties by comparing ligands **45f**,**g** and **49f**,**g**. The hydroformylation results indicated a cooperative effect that leads to a matched combination for ligand **45g** (*ee´*s up to 86%).[18] Later, Bakos and co-workers found a similar cooperative effect between the chiral ligand bridge and the chiral phosphite moiety of the ligands **45h**,**i** and **49h**,**i**.[19] Interestingly, the hydroformylation results obtained with ligands **45b** and **45d**, which have conformationally flexible axially chiral biphenyl moieties, are similar to those obtained with ligand **45g**. This indicated that diphosphite ligands containing the conformationally flexible axially chiral biphenyl moieties predominantly exist as a single atropoisomer in the hydridorhodium diphosphite complexes [$RhH(CO)_2$(diphosphite)] when the right bulky substituents in the *ortho* positions are presented.[18] It is therefore not necessary to use expensive conformationally rigid binaphthyl moieties to reduce the degrees of freedom of the system.

To investigate whether a relationship exists between the solution structures of the [$RhH(CO)_2$(diphosphite)] species and catalytic performance. van Leeuwen and co-workers extensively studied the [$RhH(CO)_2$(diphosphite)] (diphosphite= **45**, **49**) species formed under hydroformylation conditions by high pressure NMR techniques (HP-NMR).[5,10] It is well known that these complexes have a trigonal bipyramidal (TBP) structure. Two isomeric structures of these complexes, one containing the diphosphite coordinated in a bis-equatorial (**eq-eq**) fashion and one containing the diphosphite in an equatorial-axial (**eq-ax**) fashion, are possible (See Scheme 2.3). The results indicated that the stability and catalytic performance of the [$RhH(CO)_2$(diphosphite)] (diphosphite = **45**, **49**) species strongly depended on the configuration of the pentane-2,4-diol ligand backbone and on the chiral biaryl phosphite moieties. Thus, ligands **45b**, **45d** and **45g**, which form a well-defined stable bis-equatorial (**eq-eq**) complexes, lead to good enantiomeric excesses, whereas enantioselectivities were low with ligand **45i** and **49g**, which form unidentified mixtures of complexes.[18,21]

1,3-Diphosphite ligands derived from 1,2-*O*-isopropyliden-α-*D*-xylofuranose (**21**,**22**) and 6-deoxy**-**1,2-*O*-isopropyliden-α-*D*-glucofuranose (**23**, **26**) were successfully applied in the Rh-asymmetric hydroformylation of vinylarenes (Scheme 2.6).[22]

The use of diphosphite ligands **23a**,**d** and **26a**,**d** in the Rh-asymmetric hydroformylation of styrene provided the *S*- and *R*- enatiomer of the product in high enantioselectivies (*ee* up to 93%) and excellent regioselectivity (Scheme 2.6).[22c-d]

The results in the Rh-asymmetric hydroformylation suggest: a) the absolute configuration of the product is governed by the configuration at the stereogenic centre C-3; b) the level of enantioselectivity is influenced by the cooperative effect between the chiral sugar backbone stereocentres directly bonded to the phosphorus function (C-3 and C-5); c) as previously observed for the ligand **48**, bulky substituents in the *ortho* positions of the biaryl phosphite moieties are necessary to achieve high levels of enantioselectivity.

UNIVERSITAT ROVIRA I VIRGILI
1,3- DIPHOSPHITE LIGANDS WITH FURANOSIDE BACKBONE: A POWERFUL TOOL IN ASYMMETRIC CATALYSIS
Aitor Gual Gozalbo
DL: T-1535-2009/ISBN: 978-84-692-4554-5

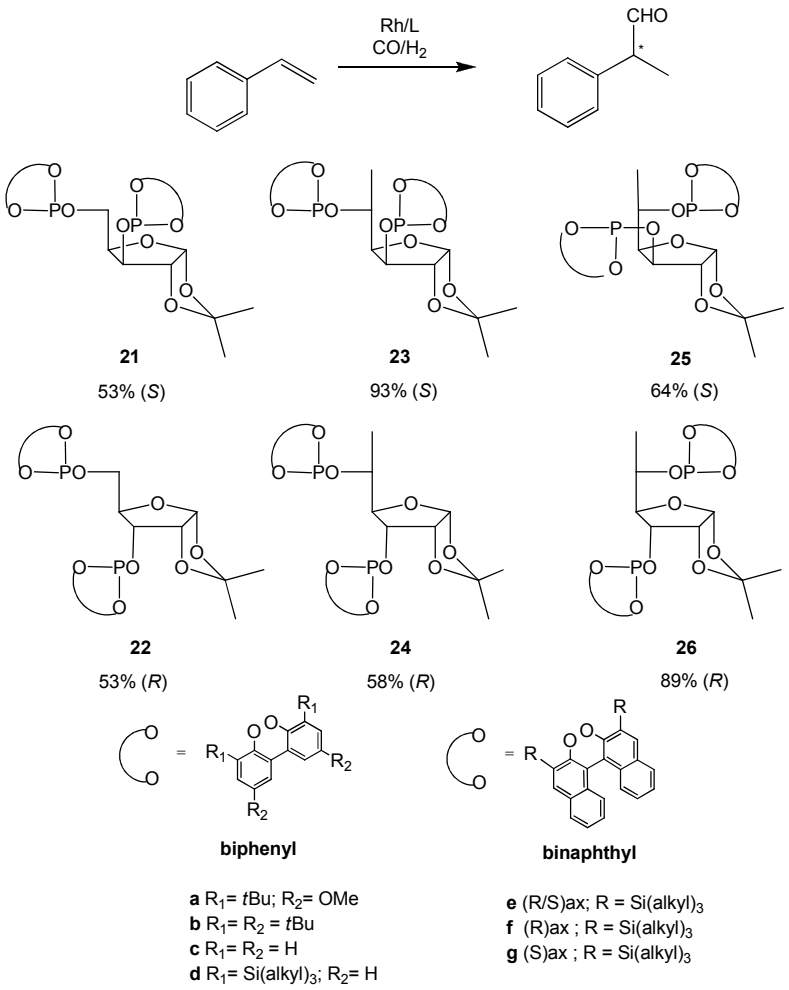

Scheme 2.6. Rh-asymmetric hydroformylation of styrene using ligands **21**-**26**.

Interestingly, the ligands **23** and **26**, for which only [$RhH(CO)_2$(L)] species with **eq-eq** coordination were observed by HP-NMR techniques, provided higher enantioselectivity (*ee* up to 93%) than the related ligands **24** and **25** (*ee* up to 64%), for which the presence of equilibrium between **eq-eq** and **eq-ax** [$RhH(CO)_2$(L)] species was confirmed by HP-NMR and HP-IR techniques. Therefore, the characterization of the [$RhH(CO)_2$(diphosphite)] (diphosphite= **23**, **26**) species confirmed that there is a relationship between the high preference for the equatorial-equatorial (**eq-eq**) coordination of the ligand and the high levels of enantioselectivity achieved in the Rh-asymmetric hydroformylation of styrene.[22c-d]

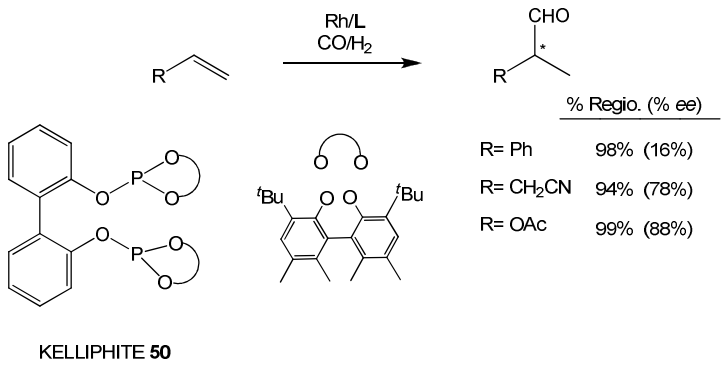

Scheme 2.7. Rh-asymmetric hydroformylation of monosubstituted alkenes using ligand KELLIPHITE **50**.

Recently, the ligand KELLIPHITE **50** was tested by Dow Chemical Company in the Rh-asymmetric hydroformylation of styrene, allyl cyanide and vinyl acetate (Scheme 2.7). The results with styrene were rather moderate, however high regio- and enantioselectivities were achieved in the reaction with vinyl acetate and allyl cyanide.[23]

Phosphine-Phosphite

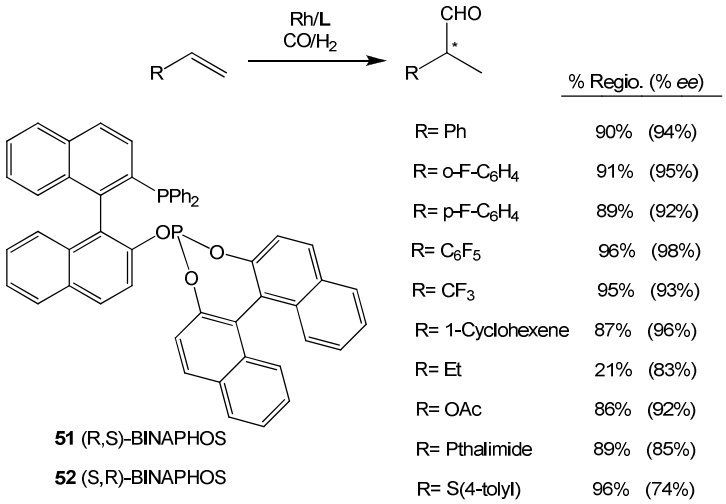

Scheme 2.8. Rh-asymmetric hydroformylation of monosubstituted alkenes using (*R*,*S*)-BINAPHOS **51** and (*S*,*R*)-BINAPHOS **52** ligands.

In 1993, the discovery of the (*R*,*S*)-BINAPHOS **51** and (*S*,*R*)-BINAPHOS **52** ligands by Takaya and Nozaki produced a real breakthrough in the Rh-catalysed asymmetric hydroformylation (Scheme 2.8).[24]

These ligands provided high enantioselectivity in the Rh-asymmetric hydroformylation of several classes of monosubstituted alkenes, such as aryl alkenes, 1-heteroatom-functionalized alkenes, and substituted 1,3-dienes, and is still a benchmark in this area. Furthermore, the use of the (*R*,*S*)-BINAPHOS **51** or the (*S*,*R*)-BINAPHOS **52** ligands allowed to obtain the two enantiomer of the product with similar enantioselectivity.[25,26] But still the remaining problem in this field is the simultaneous control of enantio- and regioselectivity, which significantly limits the structural variety of suitable alkenes for this reaction.

A second generation BINAPHOS-type ligands **53** (Scheme 2.9) has been recently developed. The introduction of 3-methoxy substituents on the aryl phosphine units yields a catalyst which increased the regio- and enantioselectivity of the Rh-asymmetric hydroformylation of styrene and produced high enantioselectivity Rh-asymmetric hydroformylation of vinylfurans and thiophenes.[27]

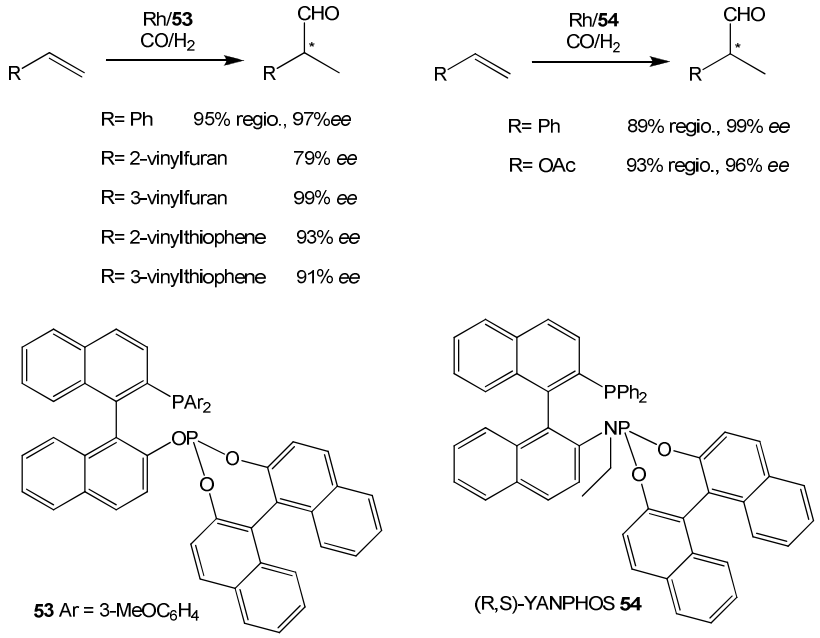

Scheme 2.9. Rh-asymmetric hydroformylation of monosubstituted alkenes using ligands **53** and **54**.

A new structural feature is obtained by replacement of the phosphite donor within BINAPHOS **51** by a phosphoramidite system within YANPHOS **54** (Scheme 2.9). This ligand provided higher enantioselectivity (*ee* up to 99%) with similar regioselectivity in the Rh-asymmetric hydroformylation of styrene and vinyl acetate.[28]

Bisphospholane

Several series of bisphospholane chiral ligands, which are known as efficient ligands for asymmetric hydrogenation, were evaluated in asymmetric hydroformylation (Scheme 2.10). Two ligands, (*S*)-BINAPINE **55** and (*S*,*S*,*R*,*R*)-TANGPHOS **56**, were found to give excellent enantioselectivities for the hydroformylation of styrene, allyl cyanide, and vinyl acetate (Scheme 2.10). The enantioselectivities achieved for the allyl cyanide product with these ligands are the highest ever reported for this substrate.[29]

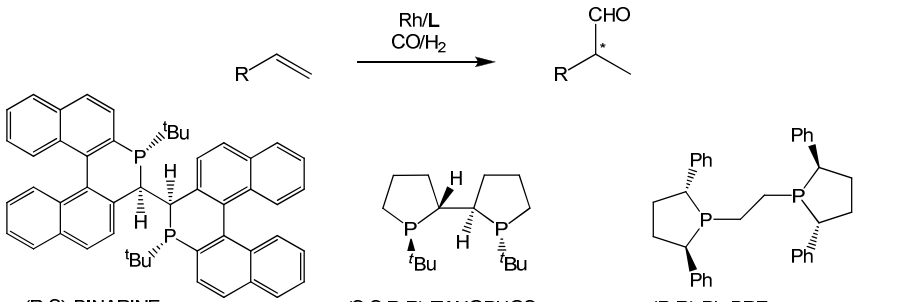

55	% Regio. (% *ee*)	**56**	% Regio. (% *ee*)	**57**	% Regio. (% *ee*)
R= Ph	90% (94%)	R= Ph	93% (90%)	R= Ph	98% (94%)
R= CH_2CN	87% (94%)	R= CH_2CN	88% (93%)	R= CH_2CN	88% (90%)
R= OAc	97% (87%)	R= OAc	97% (83%)	R= OAc	99.7% (82%)

Scheme 2.10. Rh-asymmetric hydroformylation of monosubstituted alkenes using ligands **55**-**57**.

The discovery of the biphospholane scaffold as a new privileged structure for asymmetric induction in alkene hydroformylation has triggered research for new and improved bisphospholane type ligands. In this context (*R*,*R*)-

UNIVERSITAT ROVIRA I VIRGILI
1,3- DIPHOSPHITE LIGANDS WITH FURANOSIDE BACKBONE: A POWERFUL TOOL IN ASYMMETRIC CATALYSIS
Aitor Gual Gozalbo
DL: T-1535-2009/ISBN: 978-84-692-4554-5

Ph-BPE **57** (Scheme 2.10) has been identified as an excellent ligand for asymmetric hydroformylation, which gives state of the art regio and enantioselectivities for styrene, allyl cyanide, and vinyl acetate.[30]

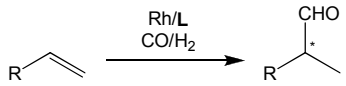

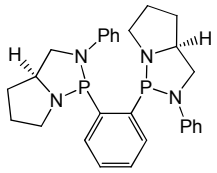

Esphos **58**	% Regio. (% *ee*)
R= OAc	94% (89%)

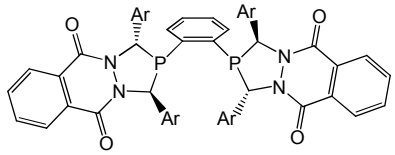

Bis-3,4-diazaphospholane **59**	% Regio. (% *ee*)
R= Ph	97% (89%)
R= CH_2CN	83% (87%)
R= OAc	98% (96%)

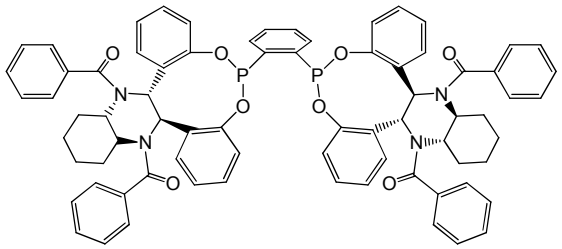

Bis-phosphonite **60**	% Regio. (% *ee*)
R= Ph	92% (79%)
R= CH_2CN	82% (79%)
R= OAc	98% (91%)

Scheme 2.11. Rh-asymmetric hydroformylation of monosubstituted alkenes with ligands **58**, **59** and **60**.

Some related systems are the bis-diazaphospholane ligands of which ESPHOS **58** has proved optimal. The best results were obtained in the hydroformylation of vinyl acetate (*ee* up to 89%) (Scheme 2.11).[31] The bis 3,4-diazaphospholane ligands **59** also provided excellent regio- and enantioselectivity (*ee* up to 96%) in this reaction (Scheme 2.11).[32] Finally, the bis-phosphonite ligand **60**, related to **59**, provided promising

results in the Rh-asymmetric hydroformylation of monosubstituted alkenes.[33]

Monodentate Phosphorus ligands

Nowadays, the successful application of monodentate phosphorus ligands in Rh-asymmetric hydroformylation is still a challenge due to the problem of the selectivity.

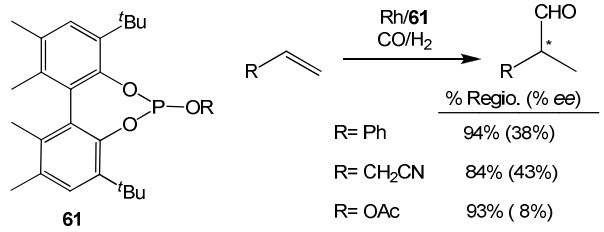

Scheme 2.12. Rh-asymmetric hydroformylation of monosubstituted alkenes using ligand **61**.

However, the use of monodentate phosphorus provided higher catalytic activity than their counterpart bidentate phosphorus ligand. Only a few examples are in the literature and moderate enantioselectivities were reported (Scheme 2.12). The ligand **61**, related to KELLIPHITE **50**, was tested in the Rh-asymmetric hydroformylation of several monosubstituted alkenes. Moderate enantioselectivities were achieved in the Rh-asymmetric hydroformylation of styrene and allyl cyanide.[23]

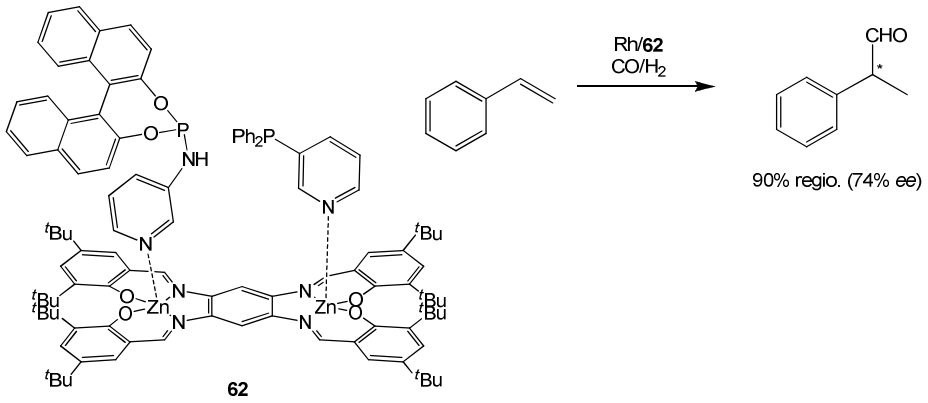

Scheme 2.13. Rh-asymmetric hydroformylation of styrene using the ligand **62**.

Recently van Leeuwen and Reek reported the template-induced formation of chelating heterobidentate ligands by the self-assembly of two different monodentate ligands on a rigid bis-zinc(II)-salphen template with two identical binding sites (Scheme 2.13).[34]

The templated heterobidentate ligand **62** induced much higher enantioselectivities (*ee* up to 72%) in the Rh-asymmetric hydroformylation of styrene than any of the corresponding homobidentate ligands or non-templated mixed ligand combinations (*ee* up to 13%).

2.3.1 Rh-asymmetric hydroformylation of disubstituted alkenes

The Rh-asymmetric hydroformylation of disubstituted alkenes has received little attention. As far as we know, only a few examples in the Rh-asymmetric hydroformylation of disubstituted alkeneic compounds, such as 1,2-disubstituted and 1,1-disubstituted alkenes, were reported (Scheme 2.14). [35-41]

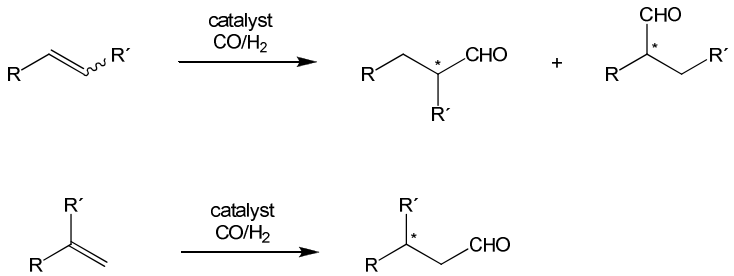

Scheme 2.14. Asymmetric hydroformylation of disubstituted alkenes.

1,2-Disubstituted alkenes

The asymmetric hydroformylation of propenylbenzenes was studied by Kollár using $PtCl_2$(bdpp)/$SnCl_2$ as catalysts.

The reaction was performed using *trans*-anethole and estragole as substrate in order to synthesise the branched chiral aldehydes (Scheme 2.15), however the isomerisation of the alkene to the terminal monosubstituted alkene, leads to the formation of the linear aldehydes. The $PtCl_2$(bdpp)/$SnCl_2$ system produced low regioseletivity to the branched product and moderate to low enantioselectivities (*ee* up to 27%). Recently,

the use of the 1,3-diphosphite ligand **21** in the Rh-asymmetric hydroformylation of *trans*-anethole and estragole was reported (Scheme 2.15).[35]

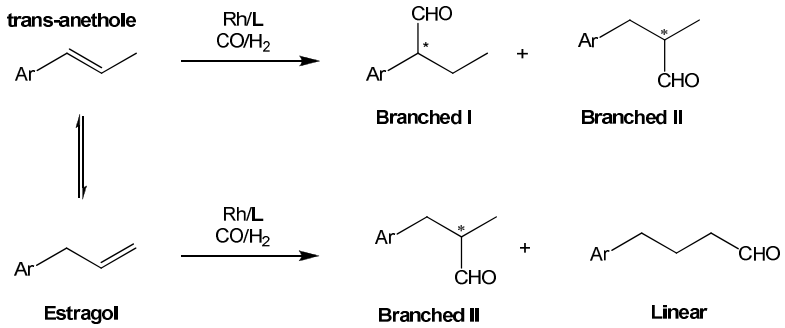

Scheme 2.15. Isomerisation processes and asymmetric hydroformylation of tran-anethole and estragol.

The catalytic system Rh/**21** improved the regioselectivity obtained by the use of the Pt based catalytic system; however low enantioselectivities were achieved (*ee* up to 15%).

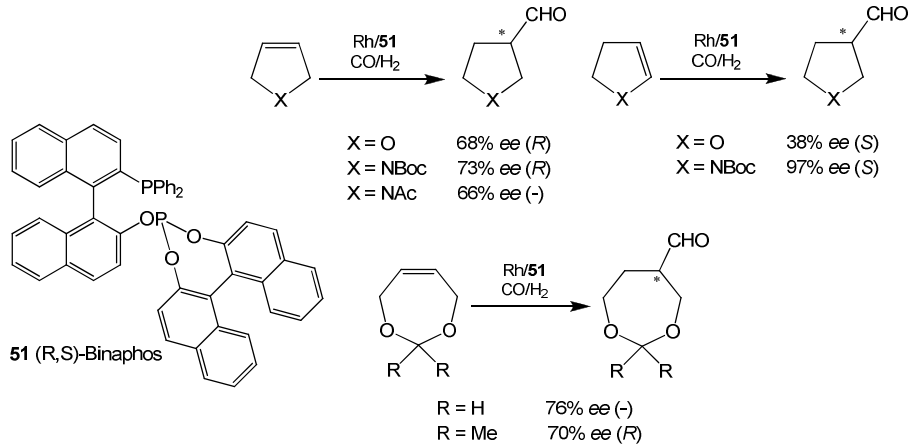

Scheme 2.16. Rh-asymmetric hydroformylation of cyclic alkenes using (*R*,*S*)-BINAPHOS ligand **51**.

The first successful results in the Rh-asymmetric hydroformylation of 1,2-disubstituted alkenes were obtained by using cyclic compounds as substrates, such as dihydrofuran, 3-pyrroline derivates and 4,7-dihydro-

1,3-dioxepin derivates, and the phosphine-phosphite (*R,S*)-BINAPHOS ligand **51** (Scheme 2.16). [36]

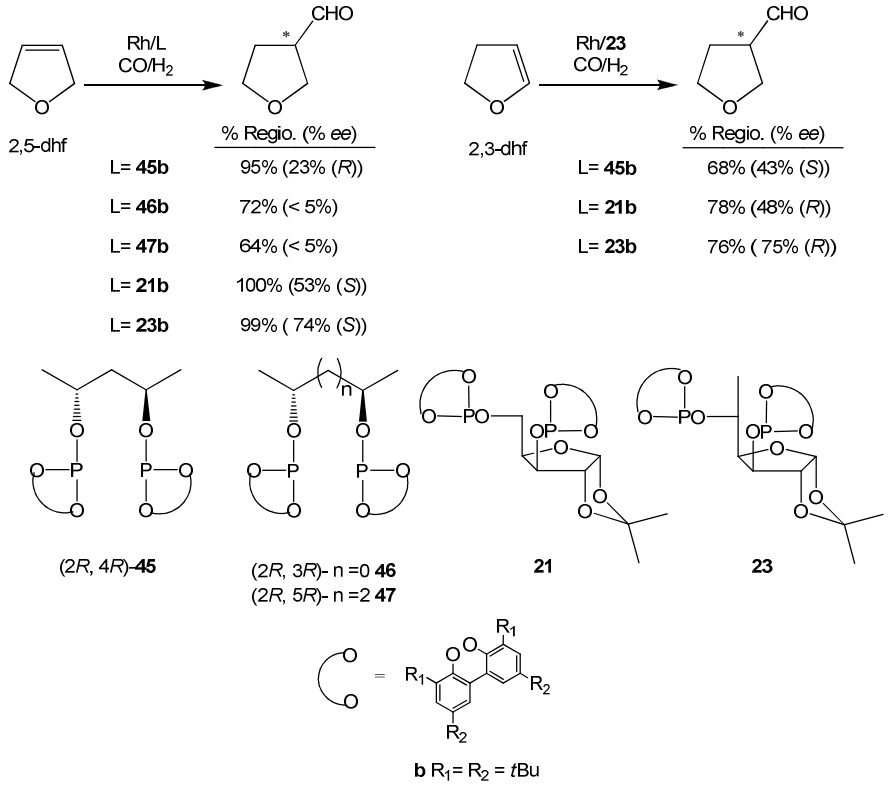

Scheme 2.17. Rh-asymmetric hydroformylation of 2,5- and 2,3-dihydrofuran using the ligand **21b**, **23b**, **45**, **46b** and **47b**.

Recently, the previously mentioned 1,3-diphosphites **21**, **23**, **45**, **46** and **47** were successfully applied in the Rh-catalysed hydroformylation of 2,3- and 2,5-dihydrofuran (Scheme 2.17). The results indicated that the backbone of the ligand is crucial to suppress isomerisation and obtaining high enantioselectivities. The diphosphite ligand **23b** provided de highest enantioselectivities (*ee* up to 74%) reported in the literature for these substrates. Note that 2,5- and 2,3-dihydrofurans afforded the two enantiomers of tetrahydrofuran-3-carbaldehyde using the same ligand **23b**.[37]

UNIVERSITAT ROVIRA I VIRGILI
1,3- DIPHOSPHITE LIGANDS WITH FURANOSIDE BACKBONE: A POWERFUL TOOL IN ASYMMETRIC CATALYSIS
Aitor Gual Gozalbo
DL: T-1535-2009/ISBN: 978-84-692-4554-5

The regioselectivity is also a problem in the Rh-asymmetric hydroformylation of cyclic compounds, such as 2,5-dihydrofuran, because isomerisation processes take place under hydroformylation conditions.
The effect reaction conditions and the electronic and steric properties of the ligand moieties on the regioselectivity of the non-asymmetric Rh-catalysed hydroformylation of 2,5-dihydrofuran and 2,3-dihydrofuran were studied by our group [38] (Scheme 2.18).

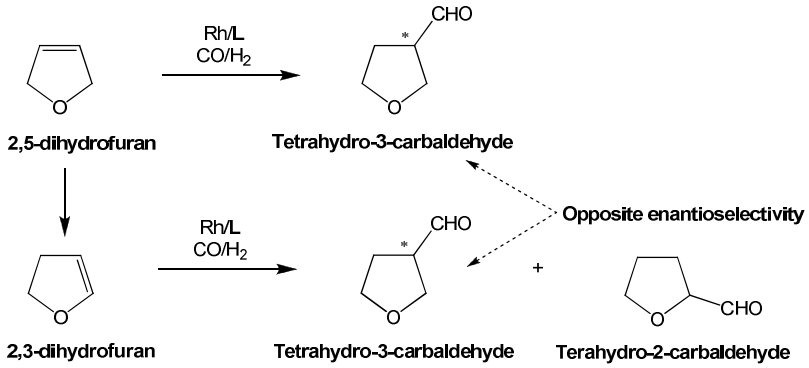

Scheme 2.18. Isomerisation processes and asymmetric hydroformylation of 2,3- and 2,5-dihydrofurans.

It was reported that the isomerisation processes in the Rh-asymmetric hydroformylation of 2,5-dihydrofuran produced the 2,3-dihydrofuran, and after that the two alkeneic compounds were hydroformylated producing mixtures of the tetrahydro-3-carbaldehyde and tetrahydro-2-carbaldehyde (Scheme 2.18). Furthermore, the isomerisation of the dihydrofuran compounds reduces the enantioselectivity of the hydroformylation reaction because the opposite enantiomer of the tetrahydro-3-carbaldehyde was preferently obtained starting from the two different dihydrofuranes.

UNIVERSITAT ROVIRA I VIRGILI
1,3- DIPHOSPHITE LIGANDS WITH FURANOSIDE BACKBONE: A POWERFUL TOOL IN ASYMMETRIC CATALYSIS
Aitor Gual Gozalbo
DL: T-1535-2009/ISBN: 978-84-692-4554-5

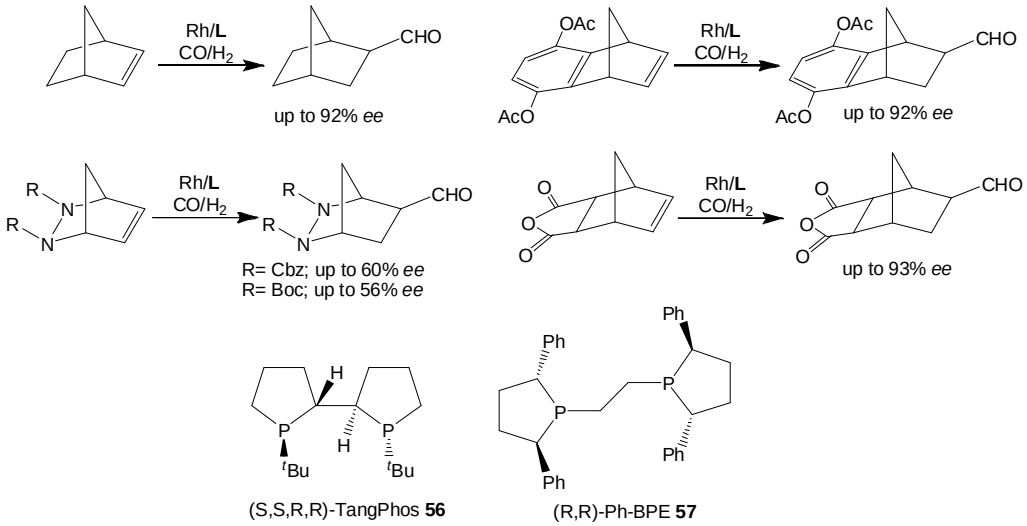

Scheme 2.19. Rh-asymmetric hydroformylation of bicylic alkenes using ligands **56** and **57**.

Recently, the first successful Rh-asymmetric hydroformylation of [2,2,1] bicyclic alkenes was reported using phospholane type ligands **56** and **57** (Scheme 2.19). Comparable enantioselectivities were reported by using ligands **56** and **57**, however the (*S*,*S*,*R*,*R*)-TangPhos **56** produced slightly higher enantioselectivities than (*R*,*R*)-Ph-BPE ligand **57**.[39]

1,1´-Disubstituted alkene

The asymmetric hydroformylation of 1,1´-disubstituted alkenes differs from the classical asymmetric hydroformylation of monosubstituted terminal alkenes because in this case the interest focus in the regio- and enantioselective synthesis of the chiral linear aldehydes (Scheme 2.20).

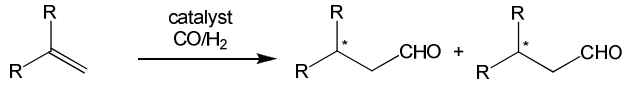

Scheme 2.20. Asymmetric hydroformylation of 1,1´-disubstituted alkenes.

As far as we know, only a few of the successful asymmetric hydroformylation of 1,1´-disubstituted substrates are reported to date.[40,41]

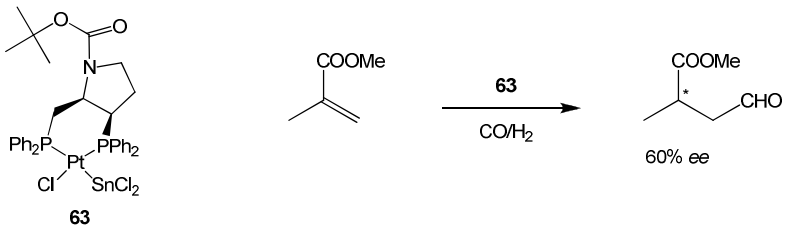

Scheme 2.21. Asymmetric hydroformylation of methyl-methacrylate using **63** as catalyst.

In 1987, Stille et al. reported the first successful asymmetric hydroformylation of methyl methacrylate using **63** as catalyst (Scheme 2.21).[40] Moderate enantioselectivity (*ee* up to 60%) was obtained, but this is the highest enantioselectivity ever reported for this reaction.

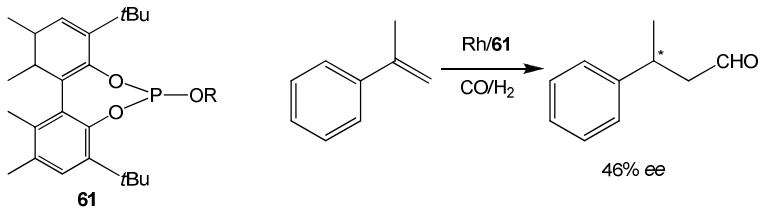

Scheme 2.22. Rh-asymmetric hydroformylation of α-methyl-styrene using ligands **61**.

Finally, the Rh-asymmetric hydroformylation of 1,1-methylstyrene using monophosphite ligand **61**, related to KELLIPHITE **50**, was recently patented (Scheme 2.22).[41] Although the enantioselectivity was moderate (*ee* up to 46%) this is the highest enantioselectivity ever reported for this reaction.

2.4. Results and Discussion.

As previously mentioned in the introduction, the use of 1,3-diphosphite ligands derived from carbohydrates gives excellent results in the Rh-asymmetric hydroformylation of styrene. Our group was interested in studying the effect of the carbon stereocentres non-directly bonded to the phosphite function and a new biphenyl moiety which possesses a carbon bridge between the phenyl functions (See scheme 2.23 in section 2.4.1). With this aim, a new series of 1,3-diphosphite ligands were designed and their synthesis is described in this chapter. The ligands series were applied in the Rh-asymmetric hydroformylation of monosusbtituted substrates, such as styrene (Section 2.4.1) and vinyl acetate (Section 2.4.2), and disubstituted internal substrates, such as 2,5-dihydrofurane and 2,3-dihydrofurane (Section 2.4.2). The application of these series of ligands in the Rh-asymmetric hydroformylation of norbonene is being developed and it will be described in a next doctoral thesis from this group, the Ph-D thesis of Carolina Blanco.

Additionally, in collaboration with Dr Leandra Cornelissen, Dr. Christian Muller and Prof. Dr. Dieter Vogt, from the Technical University of Eindhoven, the designed diphosphite ligands were successfully applied in the Rh-asymmetric hydroformylation of 1,1´-disubstituted substrates, as α-methyl-styrene and methyl-methacrylate. These results were described in the Ph-D thesis of Dr. Leandra Cornelissen and are collected in a joint publication in preparation. The best results and the reaction conditions were collected in the section 2.4.3.

2.4.1. C1-Symmetry diphosphite ligands derived from carbohydrates. Influence of structural modifications on the Rh-catalysed asymmetric hydroformylation of styrene.

A. Gual, C. Godard, C. Claver, and S. Castillón, *Eur. J. Org. Chem.* **2009**, 1191.

Summary

New 3,5-diphosphite-xylofuranoside (**21w**, **86a**,**w** and **87a**,**w**) and -glucofuranoside (**64a**, **65a**, **66a** and **67a**,**w**) ligands with C_1-symmetry were prepared and applied in the Rh-catalysed asymmetric hydroformylation of styrene. The main structural features of these ligands are: a) the presence of a 6-*O*-alkyl group (*n*Bu, *iso*-propyl and *sec*-hexyl) in ligands of *gluco* configuration, b) the absence of 1,2-*O*-isopropylidene, a common group in many ligands with a furanoside skeleton, c) the presence of an alkyl chain bound to the 2-OH, and d) the modification of the diol in the phosphite moiety. The modification of the carbohydrate backbone and diphosphite bridge affects the activity and selectivity of the reaction. Catalytic systems with ligands **21w** and **67w** were not active at 40 ºC, although the formation of the expected hydride species [RhH(CO)$_2$(**21w**)] was demonstrated by NMR spectroscopy. The highest enantioselectivity (83%) was obtained with the catalytic system Rh/**67a**. The complex [RhH(CO)$_2$(**67a**)] was characterized by NMR spectroscopy using high pressure techniques, and was shown to exist in solution as two isomers in equilibrium, with both presenting an equatorial-equatorial (**eq-eq**) configuration.

Synthesis of new diphosphite ligands with carbohydrate backbone

In view of the interesting results with ligands obtained modifying the stereocentres directly bonded to the phosphorus function of the 1,2-O-isoporpyliden-α-*D*-xylofuranoside backbone (effect of C-3 stereocentre, see section 1.1 and 1.2) and of the 1,2-O-isoporpyliden-α-*D*-glucofuranoside backbone (effect of C-3 and C-5 stereocentres, see section 1.1 and 1.2),

UNIVERSITAT ROVIRA I VIRGILI
1,3- DIPHOSPHITE LIGANDS WITH FURANOSIDE BACKBONE: A POWERFUL TOOL IN ASYMMETRIC CATALYSIS
Aitor Gual Gozalbo
DL: T-1535-2009/ISBN: 978-84-692-4554-5

we decided to explore the selective modification of the stereocentres non-directly bonded to the phosphorus function. We report here the synthesis of new C_1-symmetrical diphosphite ligands with xylofuranoside backbone (**86**-**87**, Scheme 2.27) and glucofuranoside backbone (**64**-**67**, Scheme 2.23) and their use in the rhodium-catalysed hydroformylation of styrene. The main structural features of these new ligands are the following (see Scheme 2.23): a) higher substitution at position C-6 of the sugar to increase the steric hindrance of the coordinating phosphorus atom, b) absence of 1,2-*O*-isopropylidene ring in order to increase the conformational freedom, and c) new diol skeleton in the diphosphite moieties (see diol **w** in Scheme 2.27) that will provide a different environment around the rhodium centre.

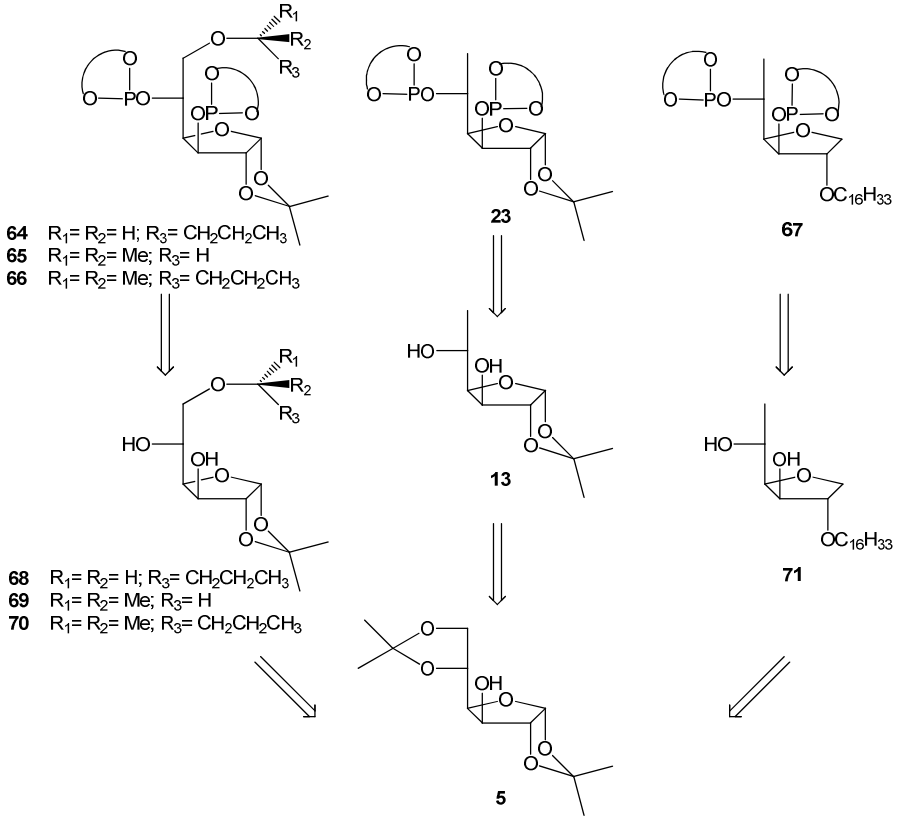

Scheme 2.23. Retrosynthesis of the ligands **23**, **64**, **65**, **66** and **67**.

The general synthetic strategies to obtain the ligands **23**, **64**, **65**, **66** and **67** from the commercially available compound **5** are shown in Scheme

2.23. Ligands **64**, **65** and **66** were prepared from diol **68**, **69** and **70**, which in turn can be easily prepared from **5**. Ligands **67** were prepared from diol **71** which was obtained from **5** by removal of the 5,6- and the 1,2-*O*-isopropylidene groups, which can be carried out by controlled hydrolysis and by reduction of the acetal function, respectively.

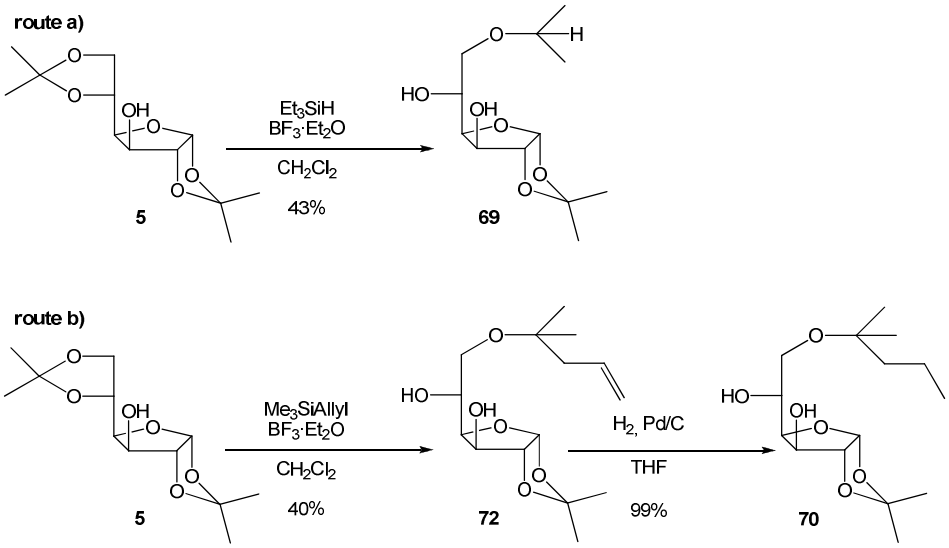

Scheme 2.24. Synthesis of the diols **69** and **70**.

The diol **69** was synthesized in a straightforward manner by selective reductive opening of the 5,6-*O*-isopropylidene group of **5** by reaction with BF_3•Et_2O and using triethylsilane (Et_3SiH) as hydride source (route a, Scheme 2.24).[42] The diol **70** was synthesized by selective reductive opening of the 5,6-*O*-isopropylidene group of **5** by reaction with BF_3•Et_2O and using trimethylallylsilane ($Me_3SiAllyl$) as nucleophile source to obtain **72** in moderate yield (route b, Scheme 2.24).[42] The double bond of the diol **72** was reduced using Pd/C as catalyst under 1 atm. of H_2 affording the diol **70** in high yield.

UNIVERSITAT ROVIRA I VIRGILI
1,3- DIPHOSPHITE LIGANDS WITH FURANOSIDE BACKBONE: A POWERFUL TOOL IN ASYMMETRIC CATALYSIS
Aitor Gual Gozalbo
DL: T-1535-2009/ISBN: 978-84-692-4554-5

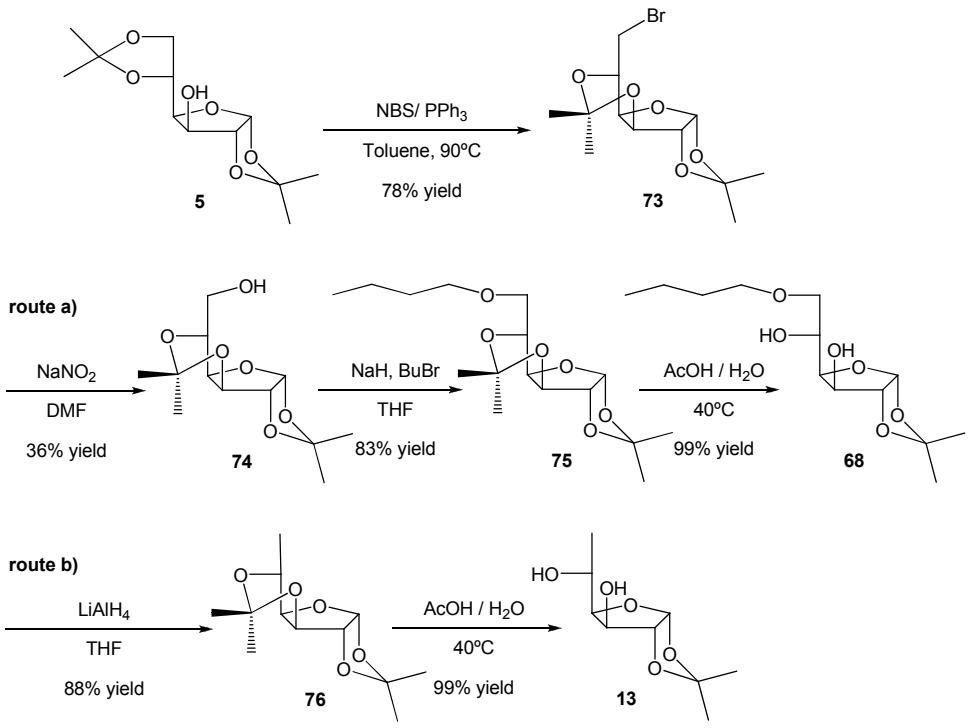

Scheme 2.25. Synthesis of the diols **13** and **68**.

In order to explore new routes to introduce bulky substituents at the C-6 position¸ compound **5** was treated with *N*-bromosuccinimide (NBS) /PPh_3 to obtain the 6-bromo derivative **73**, which was isolated in 78% yield (Scheme 2.25).[43,44] This reaction involves the migration of the 5,6-*O*-isopropylidene group to 3,5-*O*-isopropylidene with concomitant entry of bromide at C-6 position. Various substitution reactions of the bromide in **73** were attempted but were all unsuccessful. In all cases the major product was the elimination product. Therefore, the compound **73** was treated with $NaNO_2$ to afford the alcohol **74** in moderate yield (route a, Scheme 2.25). The alcohol function in **74** allowed the introduction of a great variety of moieties by etherification. The compound **74** reacted with NaH and n-butyl bromide to give compound **75**, from which the selective hydrolysis of the 3,5-O-isopropylidene acetal afforded **68** (route a, Scheme 2.25).

Furthermore, the reaction of **73** with $LiAlH_4$ afforded **76**, from which the selective hydrolysis of the 3,5-*O*-isopropylidene acetal afforded **13**, thus

completing a new and shorter synthetic route to the diol **13**, which is the precursor of the diphosphite **23** (route b, Scheme 2.25).

The syntheses of diols **71**, **84** and **85** (Scheme 2.26) were carried out from compounds **2** and **13**, respectively. [45]

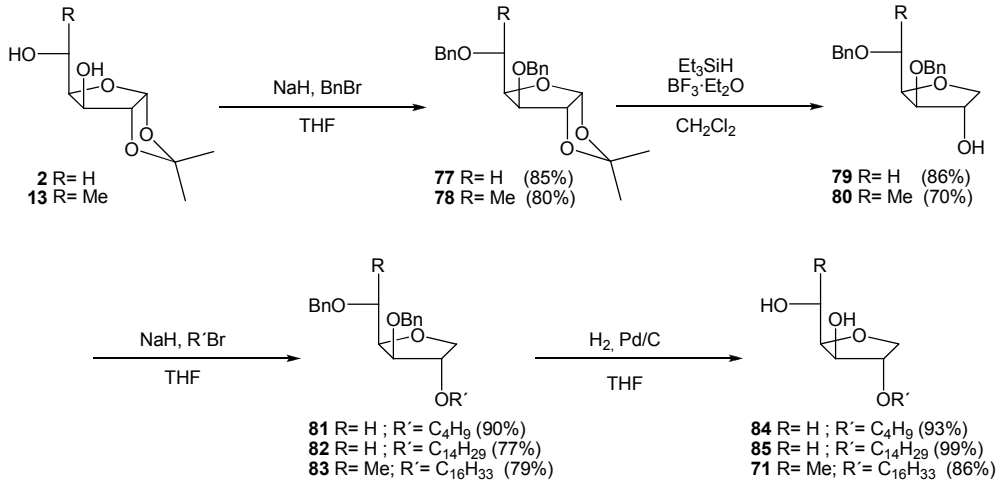

Scheme 2.26. Synthesis of the diols **71**, **84** and **85**.

Initially, the 3,5-hydroxyl groups in compounds **2** and **13** were protected as benzyl ether by reaction with BnBr to give compounds **77** and **78** in 85% and 60% yield, respectively.[45] Treatment of **77** and **78** with $Et_3SiH/BF_3{\bullet}Et_2O$ afforded the alcohols **79** and **80** in high yields (86% and 70%, respectively) by selective reductive opening of the 1,2-*O*-isopropylidene acetal.[46] The replacement of $BF_3{\bullet}Et_2O$ by trimethylsilyl triflate resulted in the formation of 2-*O*-isopropyl derivatives (10-20%) as by-products. *p*MeO-benzyl ether derivatives of **2** and **13** were also prepared in order to have alternative procedures for deprotection.[45] However, when these compounds were treated with $Et_3SiH/BF_3{\bullet}Et_2O$ deprotection of the *p*MeO-benzyl ether groups was achieved.

The compounds **79** and **80** were reacted with NaH and $n$$C_4H_9$-, $n$$C_{14}H_{29}$-, and $n$$C_{16}H_{33}$-bromide to give compounds **81**-**83** in high yields (90%, 77% and 70%, respectively). Benzyl groups were removed by hydrogenolysis using Pd/C as catalyst under 1 atm. of H_2 affording the diols **71**, **84** and **85** in high yields (93%, 99% and 86%, respectively) (Scheme 2.26).

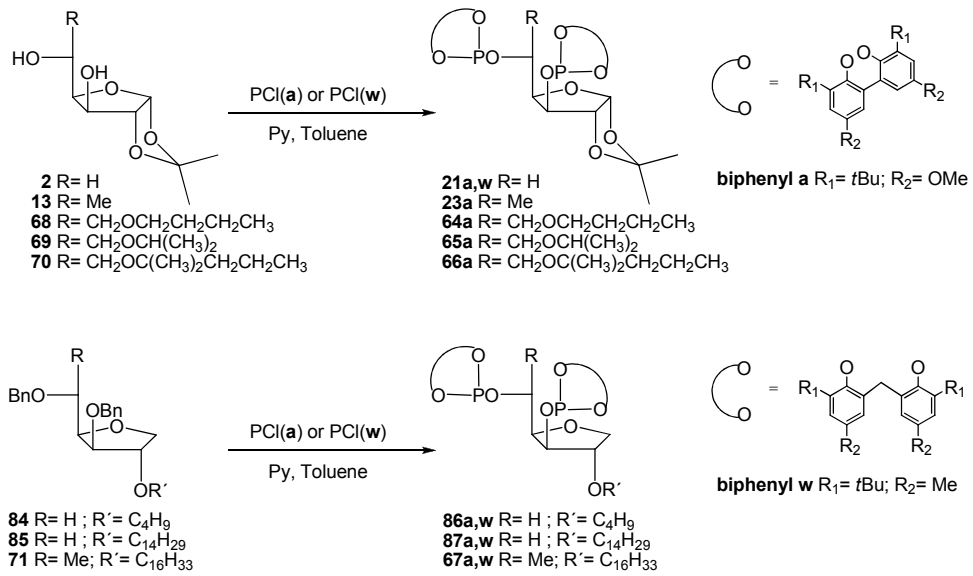

Scheme 2.27. Synthesis of 1,3-diphosphite ligands.

Finally, the diols **2**, **13**, **68**, **69**, **70**, **71**, **84** and **85** were treated with phosphorochloridites derived from bis-phenols **a** and **w** (Scheme 2.27), that were previously synthesized in situ by standard procedures to yield the corresponding diphosphite ligands **21a**,**w**, **23a**, **64a**, **65a**, **66a**, **67a**,**w**, **86a**,**w** and **87a**,**w** in moderate to good yields (20-70%).[47] All these ligands were characterized by NMR spectroscopy and elemental analysis (See Experimental Section for spectroscopic details).

Rh-catalysed asymmetric hydroformylation of styrene

The results obtained using the ligands **21a**-**26a** in the Rh-asymmetric hydroformylation of styrene were introduced in section 2.3.1. These series of ligands differ by the configuration of the C-3 and C-5 stereocentres, and the presence or not of the stereocentre in C-5 positions (See Scheme 2.6).
In 1995, van Leeuwen and co-workers achieved excellent regioselectivity to the branched aldehyde with enantioselectivity up to 53% for the S product through the use of a catalytic system containing ligand **21a**.[22a] Later, modifications of the ligand structure were used to provide insights into the role of the different moieties contained in these ligands on the activity and/or selectivity of the catalytic system. The use of ligand **22a** afforded

53% ee of the R product, demonstrating that the configuration of the catalysis product is determined by the configuration of the C-3 stereocentre.[22b] The introduction of a new stereocentre at C-5 position established that the value of the enantiomeric excess of the product is the result of the cooperative effect between both C-3 and C-5 stereocentres.[22c,d] Within these ligand series, the highest selectivity was achieved using the Rh/**23a**,**d** and Rh/**26a**,**d** systems in the asymmetric hydroformylation of vinylarenes, with regioselectivity to the branched aldehyde up to 98% and excellent enantioselectivity (up to 93% *S* and 89% *R*, respectively).[22c,d] In these studies, the nature of the group contained in the phosphite moiety was also investigated and revealed to play an important role in the activity and enantioselectivity of the catalysts in this reaction.[22] Thus, the introduction of bulky substituents in *ortho* position and electron donating groups in *para* position revealed to be the most appropriate combination in terms of activity and selectivity.

Therefore the use of the new chiral 1,3-diphosphites, L= **21a**,**w**, **23a**, **64a**, **65a**, **66a**, **67a**,**w**, **86a**,**w** and **87a**,**w**, related to **21a** and **23a**, in the rhodium-asymmetric hydroformylation of styrene offers the possibility to study the effect of the structural modification of the backbone and the biphenyl moiety on the catalytic results.

The catalytic systems were formed in situ by addition of the 1,3-diphosphite ligands to a toluene solution of $[Rh(acac)(CO)_2]$ (acac = acetylacetonate). The substrate was then added and the solution was introduced into an autoclave. Finally, the autoclave was pressurized (CO/H_2 ratio 1:1) and heated at the desired temperature. The results are summarized in Tables 2.1-2.3.

In Table 2.1, the results obtained for the rhodium-catalysed hydroformylation of styrene using the xylofuranoside derived ligands **21a**,**w**, **86a**,**w**, and **87a**,**w** are described.

When the reaction was performed in the presence of ligand **21a**, the conversion was measured to be 41% with a regioselectivity to the branched product of 96% and an *ee* of 50% (Entry 1). This result was in agreement with that previously reported for this system.[22a] Surprisingly, using the catalytic system containing ligand **21w**, where the biphenyl moiety was modified, no conversion was observed at 40 ºC (Entry 2). An incubation period to promote the formation of the active species [21,22] did not

UNIVERSITAT ROVIRA I VIRGILI
1,3- DIPHOSPHITE LIGANDS WITH FURANOSIDE BACKBONE: A POWERFUL TOOL IN ASYMMETRIC CATALYSIS
Aitor Gual Gozalbo
DL: T-1535-2009/ISBN: 978-84-692-4554-5

provide activity (Entry 3). It was found that a temperature of 80 °C (Entry 4) was required to obtain significant conversion (56%), although the regio- and enantioselectivity were low (58 and 27 %, respectively). Further investigations into this system were performed in situ using High Pressure NMR techniques and will be presented later.

Table 2.1. Rhodium-catalysed hydroformylation of styrene using diphosphites **21a**,**w**, **86a**,**w**, and **87a**,**w**.

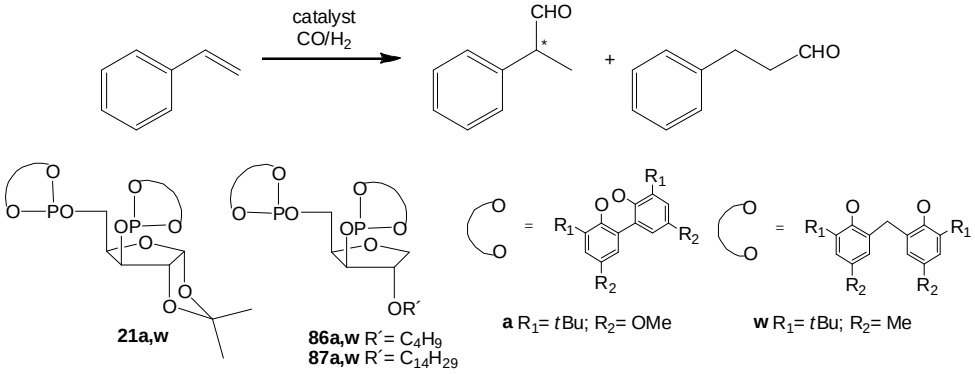

Entry[a] [b]	Ligand	Conversion(%)	Regio.(%)[c]	ee (%)
1	**21a**	41	96	50(*S*)
2	**21w**	0	-	-
3 [d]	**21w**	0	-	-
4 [e]	**21w**	56	58	27(*S*)
5	**86a**	11	97	61(*S*)
6	**86w**	30	96	60(*S*)
7	**87a**	23	96	60(*S*)
8	**87w**	33	94	61(*S*)

[a] Substrate/Rh =1000, styrene 13 mmol, Rh/L = 1/1.1, $[Rh(acac)(CO)_2]$ = 0.0135 mmol, P = 25 bar, P_{CO/H_2}= 1, 15 mL toluene, t = 15h, T = 40 ºC. [b] Conversion of styrene, regioselectivity and enantiomeric excess determined by GC. [c] 2-phenylpropanal. [d] Incubation: 16 hours at 40 ºC. [e] T = 80ºC.

When ligands **86a**,**w** and **87a**,**w** were used (Entries 5-8) the resulting catalytic systems were moderately active with conversions up to 33%. All systems yielded high regioselectivity to the branched product (up to 97%) and moderate enantioselectivity (up to 61 %). These results indicated that the use of ligands containing a monocyclic backbone **86** and **87** provided

higher ee's than when the bicyclic ligand **21a** was used. However, conversions were slightly lower and no effect was observed on the regioselectivity of the reaction.

Table 2.2. Rhodium-catalysed hydroformylation of styrene using diphosphites **23a**, **64a**, **65a**, **66a** and **67a**,**w**.

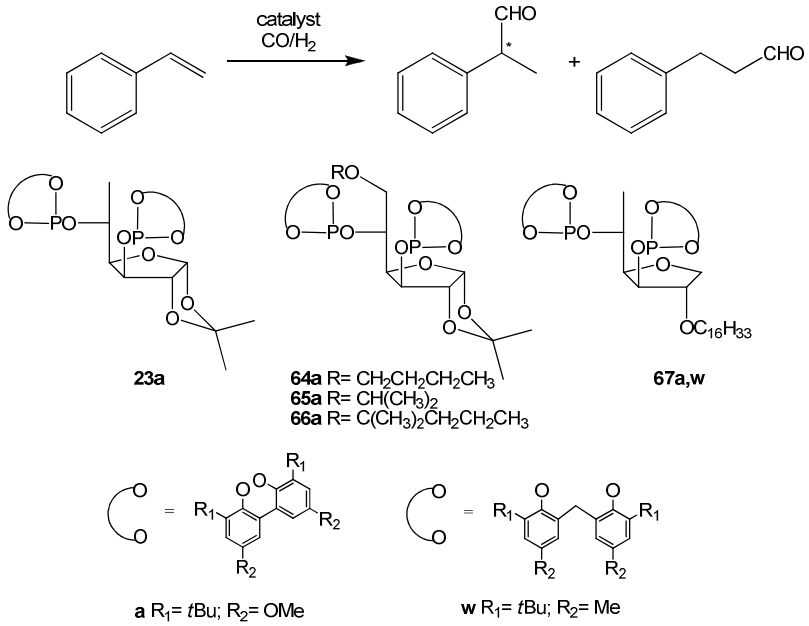

Entry[a] [b]	Ligand	Conversion(%)	Regio.(%)[c]	ee (%)
1	**23a**	30	96	73(*S*)
2	**64a**	33	96	70(*S*)
3	**65a**	48	97	68(*S*)
4	**66a**	99	85	62(*S*)
5	**67a**	50	97	75(*S*)
6	**67w**	0	-	-
7[d]	**67w**	97	54	-

[a] Substrate/Rh =1000, styrene 13 mmol, Rh/L = 1/1.1, $[Rh(acac)(CO)_2]$ = 0.0135 mmol, P = 25 bar, P_{CO/H_2}= 1, 15 mL toluene, t = 15 h, T = 40 ºC. [b] Conversion of styrene, regioselectivity and enantiomeric excess determined by GC. [c] 2-phenylpropanal. [d] T = 80ºC.

Previously, the introduction of a new stereogenic centre in C-5 (glucofuranoside derivatives) was shown to improve the catalytic results in this reaction.[22] Therefore, we considered of interest to synthesize ligands

23a, **64a**, **65a**, **66a** and **67a**,**w** containing substituents at the C-5 position.

The 6-*O*-deoxy-1,2-*O*-isopropylidene-glucofuranose ligand **23a**, which contains a bicyclic backbone and a methyl group at C-5, provided 30% of conversion with 96% of regioselectivity to the branched product and 73% of *ee* (Entry 1, Table 2.2). The Rh/**64a** catalytic system, where the ligand contains a bicyclic backbone with an O-*n*Bu substituent at C-6 position, afforded 33% of conversion, 96% of regioselectivity and 70% of enantioselectivity (Entry 2). The Rh/**65a** catalytic system, where the ligand contains a bicyclic backbone with an $OCH(CH_3)_2$ substituent at C-6 position, afforded higher conversion with 97% of regioselectivity and 68% of enantioselectivity (Entry 3). Interestingly, the catalytic system bearing the ligand **66a**, where the ligand contains a bicyclic backbone with an $OC(CH_3)_2CH_2CH_2CH_3$ substituent at C-6 position, afforded total conversion with moderate regioselectivity and 62% of enantioselectivity (Entry 4). The catalytic system containing the ligand **67a**, which has a monocyclic backbone, provided similar conversion and regioselectivity as ligand **65a**, but the *ee* increased to 75% (Entry 5). The effect of the diphosphite bridge in **67a**,**w** (Entries 5-7) is similar to that described for ligands **21a**,**w** (Entries 1, 2, Table 2.1). Again, a temperature of 80 ºC was required to obtain significant conversions, but the results of selectivity suggested the presence of the unmodified $[RhH(CO)_4]$ as active species under these conditions (Entry 5).[5,10] As previously observed, the *ee* values obtained with the ligands with glucofuranoside backbone **23a**, **64a, 65a**, **66a** and **67a** (up to 75%) were higher than those obtained with ligands with a xylofuranoside backbone **21a**, **86a** and **87a** (up to 61 %).

In Table 2.3, the optimization of the reaction conditions performed with the catalytic systems containing ligands **65a** and **67a** is presented.

Interestingly, when the total pressure was decreased from 25 to 10 bar, an increase of the catalytic activity was observed without affecting the regio- and enantioselectivity of the reaction (Entries 1, 2). Furthermore, lowering the CO to H_2 ratio again increased the conversion (83%) while the regio- and enantioselectivity remained unchanged (Entry 3). These results can be attributed to the presence of inactive carbonyl dinuclear or clusters species at high CO pressure.[48] When the temperature was decreased to 20 °C, an increase of the enantiomeric excess to 73% was observed (Entry 4).

However, no noticeable effect on the *ee* value was observed when the ligand-to-rhodium ratio was increased from 1.1 to 2 (Entry 5). The catalytic system containing ligand **67a** under these conditions provided low conversions and the enantioselectivity slightly increased to 79%. Using a lower ligand-to-metal ratio, the activity was found to increase (29%) without affecting the regio- (98%) and enantioselectivity (83%) (Entry 7).

Table 2.3. Rhodium-catalysed hydroformylation of styrene using diphosphites **65a** and **67a**.

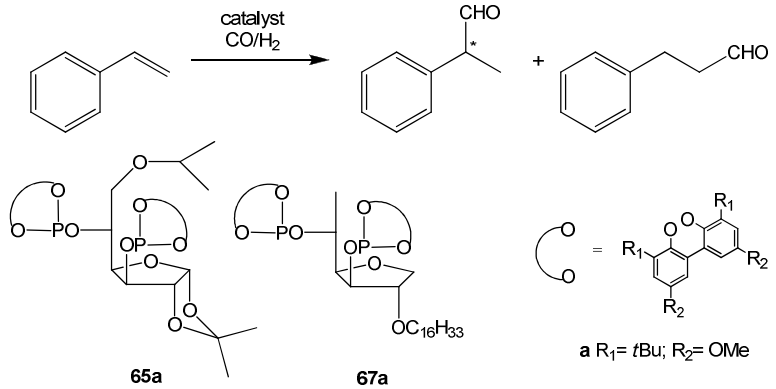

65a 67a

Entry [a],[b]	L	P (bar)	P_{CO/H_2}	Rh/L	T (ºC)	Conv.(%) [time]	Regio. (%)[c]	ee(%)
1	**65a**	25	1	1:1.1	40	48(15h)	97.4	68(*S*)
2	**65a**	10	1	1:1.1	40	66(15h)	97.0	67(*S*)
3	**65a**	10	0.5	1:1.1	40	83(15h)	97.4	67(*S*)
4[d]	**65a**	10	0.5	1:1.1	20	78(48h)	98.5	73(*S*)
5[d]	**65a**	10	0.5	1:2.0	20	38(48h)	96.4	76(*S*)
6[d]	**67a**	10	0.5	1:1.1	20	29(48h)	98.3	81(*S*)
7[d]	**67a**	10	0.5	1:2.0	20	10(48h)	96.5	79(*S*)

[a] Substrate/Rh =1000, styrene 13 mmol, Rh/L = 1/1.1, $[Rh(acac)(CO)_2]$ = 0.0135 mmol, 15 mL toluene. [b] Conversion of styrene, regioselectivity and enantiomeric excess determined by GC. [c] 2-phenylpropanal. [d] t = 48 h. Incubation: 16h at 40ºC.

The enantiomeric excesses obtained with ligands **65a** and **67a** in the rhodium-catalysed hydroformylation of styrene were both rather high (76 and 83%, respectively) although they do not overcome that previously reported for ligand **23a** (ee up to 90%).[22b-d]

High-pressure NMR study

In order to gain information into the effect of the modifications in the diphosphite moiety as well as in the sugar backbone, high pressure NMR experiments of the systems containing **67a**, which provided the best enantioselectivity, and **21w**, which was not active in the standard conditions, were performed (Scheme 2.28).

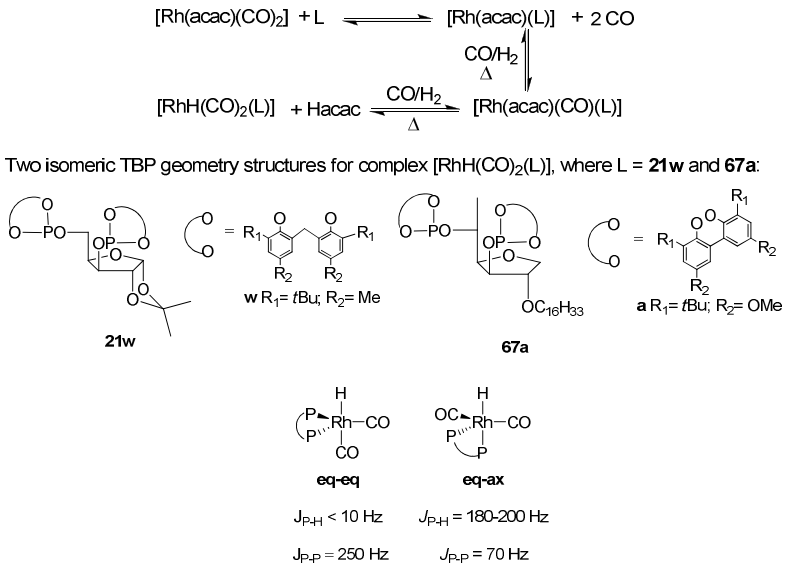

Scheme 2.28. General mechanism for the formation of the $[RhH(CO)_2(L)]$ (L = **21w** and **67a**) species.

One equivalent of the diphosphite ligand (**67a** or **21w**) was added to a 2 mM solution of $[Rh(acac)(CO)_2]$ in toluene-d_8 at room temperature within a 10 mm NMR tube. In both cases, a rapid change of colour was observed at this stage from colourless to yellow. The NMR tube was shaken under hydroformylation conditions for 16 h at 40ºC, placed into the spectrometer and the NMR spectra were recorded at various temperatures. Under these conditions, signals corresponding to the rhodium hydride species $[RhH(CO)_2(L)]$ (L = **67a** or **21w**) were readily detected as the only organometallic product. The general mechanism for the formation of these species is described in Scheme 2.28.[10,21,22,25,49] The hydridorhodium

diphosphite complexes [RhH(CO)$_2$(L)] (L: bidentate ligand) are often observed as resting states in the hydroformylation reaction. Two isomeric TBP geometry structures can be formed with a coordinated bidentate ligand (See Scheme 2.28). The complexes with **eq-eq** (equatorial-equatorial) configuration are expected to exhibit a $J_{P\text{-}H}$ < 10 Hz and a $J_{P\text{-}P}$ ≈ 250 Hz, whereas for the **eq-ax** (equatorial-axial) configuration, $J_{P\text{-}H}$ ≈ 180-200 Hz and $J_{P\text{-}P}$ ≈ 70 Hz are usually observed.[10,21,22,25,49]

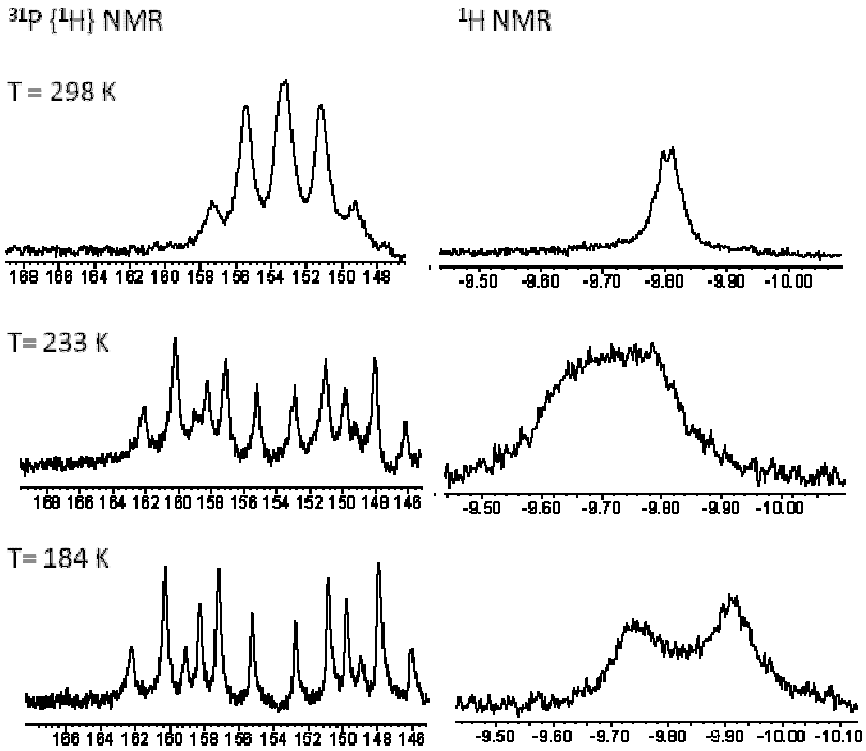

Figure 2.1. Selected regions of ^{1}H and ^{31}P{^{1}H} NMR spectra of complex [RhH(CO)$_2$(**67a**)] in toluene-d$_8$ recorded at variable temperature.

The ^{31}P{^{1}H} NMR spectra of the solution containing [Rh(acac)(CO)$_2$]/**67a** under 10 bar of syngas at room temperature showed four doublets exhibiting a characteristic $^1J_{Rh\text{-}P}$ ≈ 300 Hz and $^2J_{P\text{-}P}$ ≈ 100 Hz that were readily attributed to the [Rh(acac)(CO)(**67a**)] complex, together with a broad multiplet assigned to [RhH(CO)$_2$(**67a**)] (See Figure 2.1). [22b-d] The ^{1}H NMR spectrum of the solution containing [Rh(acac)(CO)$_2$]/**67a** at room

UNIVERSITAT ROVIRA I VIRGILI
1,3- DIPHOSPHITE LIGANDS WITH FURANOSIDE BACKBONE: A POWERFUL TOOL IN ASYMMETRIC CATALYSIS
Aitor Gual Gozalbo
DL: T-1535-2009/ISBN: 978-84-692-4554-5

temperature showed the hydride peak as a doublet signal (J = 3.9 Hz). The broad signals detected in the $^{31}P\{^{1}H\}$ NMR spectra suggested that a rapid exchange on the NMR timescale was occurring at room temperature. Therefore, ^{1}H and $^{31}P\{^{1}H\}$ NMR spectra were recorded at variable temperatures (Figure 2.1). Broadening of the signal was observed when the temperature was decreased to 233K, which split in two broad peaks when the temperature was decreased to 184K. In the $^{31}P\{^{1}H\}$ NMR spectrum two second order groups of signals were detected at 233K, which become better resolved at 184K.

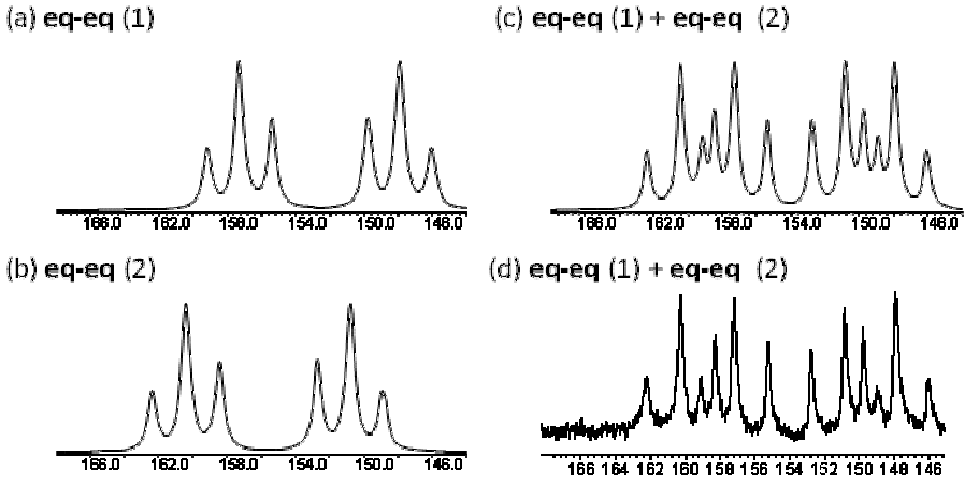

Figure 2.2. Simulated $^{31}P\{^{1}H\}$ NMR spectra corresponding to two isomers (traces a and b) of complex [$RhH(CO)_2$(**67a**)] with the ligand in eq-eq configuration; c) Overlay of simulated spectra a)+b); d) recorded $^{31}P\{^{1}H\}$ NMR spectra of the complex [$RhH(CO)_2$(**67a**)] in toluene-d_8. Spectrum recorded at 184 K.

To determine the identity of these two species, simulations of the $^{31}P\{^{1}H\}$ NMR spectra were performed using the *gNMR V4.0 software*. The results obtained by these simulations were described in Figure 2.2, and the calculated coupling constants were placed in table 2.4.

The results obtained by these simulations indicated that the spectrum obtained experimentally (Figure 2.2, trace d) corresponded to the sum of the signals (Figure 2.2, trace c) arising from two distinct species and exhibiting coupling constants $J_{Rh\text{-}P}$=250-231Hz and $J_{P\text{-}P}$ = 247-227Hz, which

is in agreement with **eq-eq** structures for both species. The simulated spectra corresponding to each species separately are shown in traces a and b of Figure 2.2. It was therefore concluded that two isomeric complexes of formula [(**eq-eq**)-RhH(CO)$_2$(**67a**)] were coexisting in solution. The spectral features of the complex [RhH(CO)$_2$(**67a**)] at temperatures between 184 and 298 K are summarized in Table 2.4.

Table 2.4. Selected ^{1}H and ^{31}P{^{1}H} NMR data for [RhH(CO)$_2$(**67a**)] complex.[a][b]

T (K)	δ(P1) [c]	δ(P2) [c]	J_{Rh-P1} [d]	J_{Rh-P2} [d]	J_{P1-P2} [d]	δ(H) [c]
298	153.3(m)	153.3(m)	-	-	-	-9.8
233	Broad	Broad	-	-	-	-9.8
193	160.3	151.0	241	229	235	-9.8
	157.1	148.0	231	225	228	-9.8
184	160.3	150.9	241	229	235	-9.7
	157.2	148.0	234	224	229	-9.9

[a] Rh/L = 1/1.1, solvent= toluene-d$_8$, P = 10 bar, P_{CO/H_2}= 0.5. Incubation: 16h at 40ºC. [b] ^{31}P and ^{1}H NMR spectra recorded using a 10 mm high-pressure NMR tube. [c] Chemical shifts in ppm. [d] Coupling constants in Hz.

Interestingly, in a previous report on [RhH(CO)$_2$(L)] using the bicyclic 1,3-diphosphite ligand **23a**, only one species containing the ligand coordinated in an **eq-eq** fashion was detected.[22b-d] The flexibility of the monocyclic structure of the ligand **67a** could explain the formation of two species with different conformation of the tetrahydrofuran ring.

In the ^{31}P{^{1}H} NMR spectrum of [RhH(CO)$_2$(**21w**)] under 25 bar of syngas at room temperature, two broad doublets arising from Rh-P coupling ($^1J_{Rh-P}$ = 232.08 Hz and $^1J_{Rh-P}$ = 233.90 Hz) were observed without discernible J_{P-P} coupling (Figure 2.3). The hydride signal was observed in the ^{1}H NMR spectrum as a broad multiplet ($\Delta\omega_{1/2} \leq$ 36Hz). Broad signals were again observed when ^{1}H and ^{31}P{^{1}H} NMR spectra were recorded at lower temperatures. In a previous work on the system containing the diphosphite ligand **21a**, only one ^{31}P doublet resonance was reported for the corresponding complex with a $^1J_{Rh-P}$ coupling constant close to 236 Hz without discernible $^2J_{P-P}$ coupling constant. An **eq-eq** configuration was then attributed for this complex.[22a] It was therefore concluded that, although

no conversion was obtained with this system (see Table 2.1, Entry 3-4), the formation of the hydride species was occurring under these conditions. Thus, as the modification of the phosphite moiety does not affect the formation of the hydride complex, the cause of the inactivity of this system must be located at a later stage of the catalytic cycle.

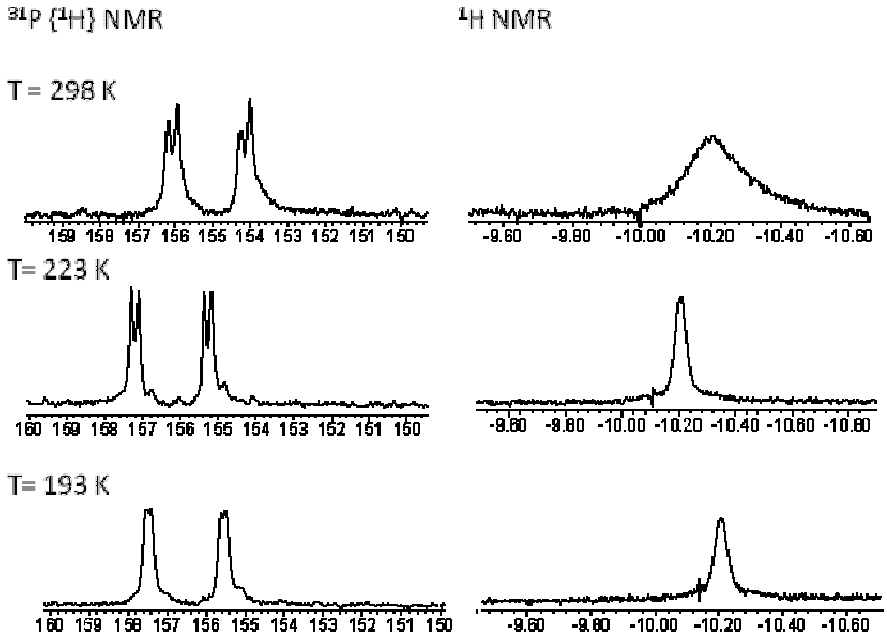

Figure 2.3. Selected regions of ^{1}H and $^{31}P\{^{1}H\}$ NMR spectra of complex [$RhH(CO)_2$(**21w**)] in d_8-toluene recorded at variable temperature.

The steric bulk induced by this moiety could hinder the coordination of the substrate, thus hampering the reaction to proceed. At higher temperature (80 ºC) the results obtained support the formation of the unmodified rhodium hydride carbonyl system, which would explain that no enantioselectivity was achieved.

Conclusions

A new series of diphosphite ligands **21w**, **64a**, **65a**, **66a**, **67a**,**w**, **84a**,**w** and **85a**,**w** with C_1-symmetry were prepared through modifications of the 1,2-*O*-isopropylidene-furanoside backbone and the substituent at C-6 and the diphosphite moiety. New synthetic routes have been developed for these ligands and a shorter route for the reference ligand **23a** has been established. These new diphosphite ligands were applied in the Rh-catalysed asymmetric hydroformylation of styrene. The introduction of a new phosphite bridge (ligands **21w**, **84w**, **85w** and **67w**) leads to a decrease or a lack of activity, depending on the substituents in the backbone. In spite of this lack of activity, the intermediate $[RhH(CO)_2(L)]$ (L=**21w**) has been observed by high pressure NMR techniques, demonstrating that the formation of this species is not a limiting step of the reaction. Enantioselectivities up to 83% *ee* were obtained for ligand **67a**. The high pressure NMR study provided a possible explanation for the lower *ee* value obtained with ligand **67a** when compared to that obtained with ligand **23a**. Two $[RhH(CO)_2(PP)]$ **eq-eq** isomers where detected for the ligand **67a**, whereas in the case of ligand **23a** only one specie was formed.

2.4.2. Highly enantioselective Rh-catalysts for the asymmetric hydroformylation of vinyl- and allylethers using C1-Symmetry diphosphite ligands.

A. Gual, C. Godard, C. Claver, and S. Castillón, *Chem. Eur. J.* **2009**, Submitted.

Summary

Novel glucofuranose derived 1,3-diphosphites (**64-67b**) were successfully applied in the Rh-asymmetric hydroformylation of vinyl acetate, 2,5-dihydrofuran and 2,3-dihydrofuran. Excellent regioselectivity (up to 99.9%) and high ee (up to 73%) were obtained in the hydroformylation of vinyl acetate. Cyclic unsaturated ethers, such as 2,3- and 2,5-dihydrofuran, were hydroformylated with excellent chemo- and regioselectivity (up to 99.9%) and ee's up to 88%. To date, these results correspond to the highest ee values reported in the asymmetric hydroformylation of these substrates. We also describe the HP-NMR studies of the [$RhH(CO)_2(L)$] species (L= **65b** and **67b**), demonstrating that both ligands coordinate to the Rh centre in an **eq-eq** fashion in these hydride complexes. The complex [$RhH(CO)_2$(**65b**)] was detected as a single isomer with characteristic features of **eq-eq** coordination. However, the broadening of the corresponding signals indicated that two isomeric forms species were rapidly interchanging in solution. Even more, the complex [$RhH(CO)_2$(**67b**)] was detected as a mixture of two conformational isomers at low temperature due to the greater flexibility of the monocyclic backbone of this ligand.

Synthesis of diphosphite ligands with carbohydrate backbone

The ligands **21b**, **23b**, **64b**, **65b**, **66b**, **67b, 87b** and **88b** (Scheme 2.31) were synthesized from the commercially available 1,2;5,6-O-di-isopropyliden-glucofuranose. These ligands were prepared from the corresponding diols, which were prepared following the procedures previously described in section 2.4.1.

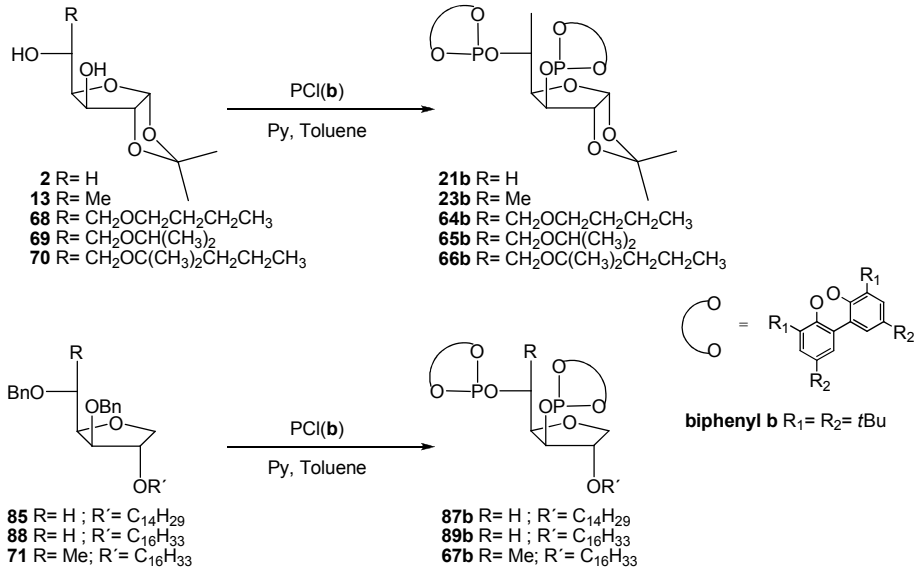

Scheme 2.29. Synthesis of 1,3-diphosphite ligands.

The diols **2**, **13**, **68**, **69**, **70**, **71**, **85** and **88** were treated with phosphorochloridites derived from bis-phenol **b** (Scheme 2.29), that were previously synthesized in situ by standard procedures to yield the corresponding diphosphite ligands **21b**, **23b**, **64b**, **65b**, **66b**, **67b**, **87b** and **89b** in moderate to good yields (50-70%). [47] All these ligands were characterized by NMR spectroscopy and elemental analysis (See Experimental Section for spectroscopic details).

Rh-catalysed asymmetric hydroformylation

The synthesis of enantiomerically pure aldehydes derived from vinyl- and allylethers such as vinyl acetate and dihydrofuran derivatives is of great interest in organic chemistry as building blocks for the synthesis of natural products and pharmaceuticals (Scheme 2.30).[2,4] In this context, the asymmetric hydroformylation reaction offers an ideal synthetic method for the production of such compounds.

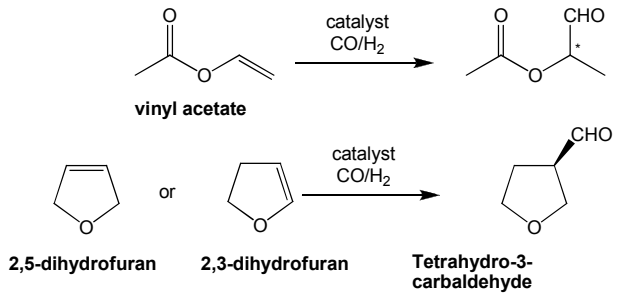

Scheme 2.30. Rh-asymmetric hydroformylation of vinyl- and allyl-ethers such as vinyl acetate and dihydrofuran derivates.

The use of chiral phosphite ligands in the Rh-catalysed asymmetric hydroformylation provide excellent results in the synthesis of chiral enantiopure aldehydes from terminal alkenes.[3] However, the only diphosphite ligand that was found to be efficient in this reaction is the KELLIPHITE ligand **50**, which yielded excellent regioselectivity (99%) with 88% *ee* (See Scheme 2.7).[23]

In the Rh-asymmetric hydroformylation of internal heterocyclic alkenes such as tetrahydrofuran, the simultaneous control of the chemo-, regio- and enantioselectivity is often a problem. [36- 38] For example, the regioselective hydroformylation of cyclic vinyl ethers can be modified by the optimisation of the reaction conditions and the properties of the catalyst,[38] while with acyclic vinyl ethers, the branched aldehydes are usually formed with high selectivity.[3] Furthermore, with cyclic allyl ethers such as 2,5-dihydrofurans, high degrees of isomerisation into the corresponding vinyl ethers were reported.[38] This competing isomerisation process has a great impact on the enantioselectivity of the hydroformylation reaction since each isomer yields the opposite enantiomer of the same aldehyde. Thus, a high degree of isomerisation results in low *ee* values.

The proposed mechanism for the Rh-catalysed hydroformylation of 2,5-dihydrofuran and 2,3-dihydrofurn is presented in Scheme 2.30.[36-38] First, the alkene coordinates to rhodium hydride species, and the 2- or 3-alkyl complexes are formed by subsequent migratory insertion. Carbonylation of these species yields acyl complexes which react with H_2 to reductively eliminate the aldehyde product(s) and regenerates the initial hydride species. The previously mentioned isomerisation between allyl and

vinyl ethers is governed by the equilibrium between the two rhodium hydride alkene species (Scheme 2.31) that occurs through insertion/β-elimination. It is noteworthy that the formation of the 3-alkyl intermediate was shown to be thermodynamically favoured although carbonylation of the 2-alkyl species was shown to be faster than that of the 3-alkyl species.[36-38]

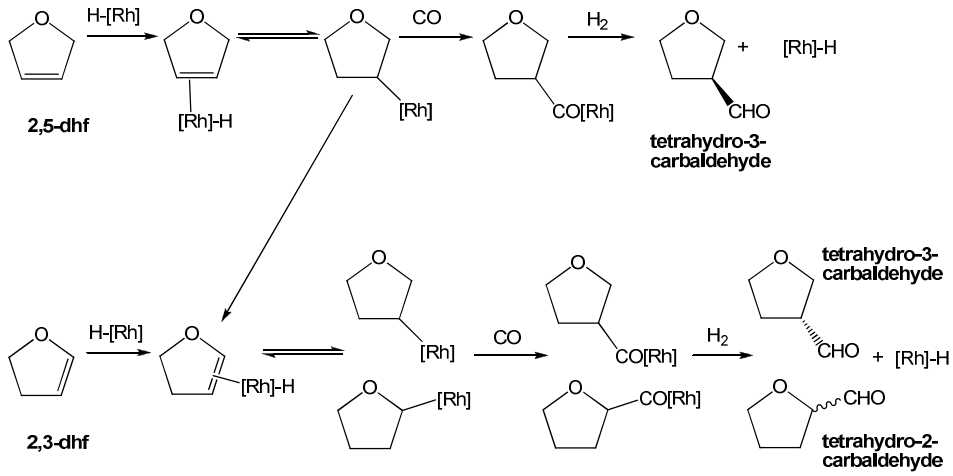

Scheme 2.31. Rh-catalysed asymmetric hydroformylation of 2,5-dihydrofuran (2,5-dhf) and 2,3-dihydrofuran (2,3-dhf).

The highest enantioselectivities in the asymmetric Rh-hydroformylation of 2,5-dihydrofuran and 2,3-dihydrofuran (*ee* up to 74% S and R, respectively) were reported using the 1,3-diphosphite with 6-O-deoxy-1,2-O-isopropylidene-glucofuranose **23b** (See Scheme 2.17).Here, we report the application of 1,3-diphosphite ligands with a glucofuranose derived backbone and containing the phosphite moiety **b** in the asymmetric hydroformylation of vinyl-and allyl-ethers, such as vinyl acetate and 2,3- and 2,5-dihydrofurans.

Therefore, the catalytic systems containing the chiral 1,3-diphosphites were used in the rhodium-catalysed asymmetric hydroformylation of vinyl acetate, 2,5-dihydrofuran and 2,3-dihydrofuran in order to gain information about the effect of the structural modifications on the catalytic results.

UNIVERSITAT ROVIRA I VIRGILI
1,3- DIPHOSPHITE LIGANDS WITH FURANOSIDE BACKBONE: A POWERFUL TOOL IN ASYMMETRIC CATALYSIS
Aitor Gual Gozalbo
DL: T-1535-2009/ISBN: 978-84-692-4554-5

The catalytic systems were formed in situ by addition of the diphosphite ligands (L= **23b**, **64b**, **65b**, **66b** and **67b**) to a toluene solution of $[Rh(acac)(CO)_2]$ (acac = acetylacetonate). The substrate was then added and the solution was introduced into an autoclave. Finally, the autoclave was pressurized with 18 bar of CO/H_2 mixture (ratio 1:1) and heated at the desired temperature. The results are summarized in Tables 2.5-2.7.

Table 2.5. Rhodium-catalysed hydroformylation of vinyl acetate using diphosphites **23b** and **64b**-**67b**.

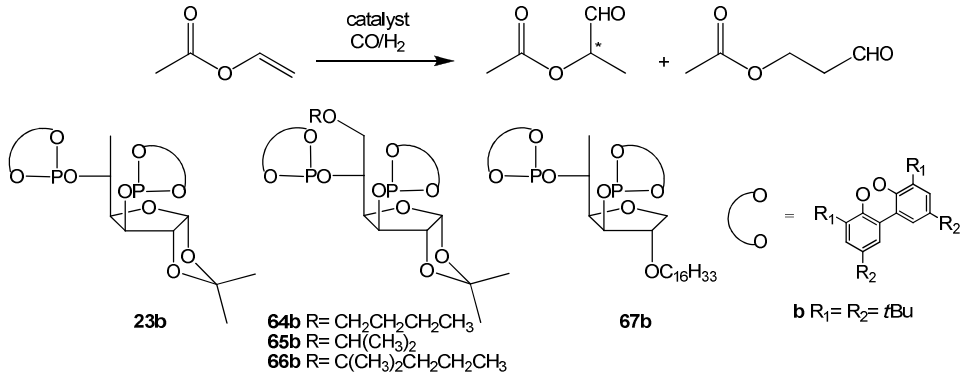

23b

64b R= $CH_2CH_2CH_2CH_3$
65b R= $CH(CH_3)_2$
66b R= $C(CH_3)_2CH_2CH_2CH_3$

67b

b $R_1 = R_2 = t$Bu

Entry[a]	Ligand	Conv.(%)[b]	Regio.(%)[c]	*ee* (%)[d]
1	**23b**	100	99	65
2[e]	**23b**	47	99.9	70
3[e],[f]	**23b**	43	99.9	73
4	**64b**	100	99	41
5	**65b**	100	99	60
6[e]	**65b**	20	99.9	66
7[e],[f]	**65b**	18	99.9	68
8	**66b**	100	99	48
9	**67b**	100	99	51

[a] P= 18 bar, P_{CO/H_2}= 1, $[Rh(acac)(CO)_2]$ = 0.012 mmol, Substrate / Rh = 400, vinyl acetate 4.8 mmol, toluene = 5 mL, Ligand/ Rh = 1, T= 45 ºC, t = 24h . [b] Conversion and regioselectivity determined by GC analysis. [c] % branched product. [d] Enantioselectivity measured by GC analysis. [e] T= 20ºC. Incubation: 24h at 45ºC under hydroformylation condtions. [f] Ligand/ Rh = 2.

In Table 2.5, the results obtained for the rhodium-catalysed hydroformylation of vinyl acetate in 24 h under standard conditions using the 1,3-diphosphites **23b**, **64b**, **65b**, **66b** and **67b** are presented. When the reaction was carried out with ligand **23b** at 45ºC with a ligand to Rh ratio of 1, total conversion was achieved with excellent regioselectivity to the branched product (up to 99%) and enantioselectivity of 65% (Entry 1). Using the ligand **65b**, lower enantioselectivity (41%) was obtained although conversion and regioselectivity remained unaltered (Entry 4). The use of ligand **65**-**67b** provided comparable activities and regioselectivities to those obtained with ligand **23b**, although the enantioselectivities were slightly lower (*ee* between 48 and 60%) (Entries 5, 8 and 9). Next, the reaction conditions were optimised with the catalytic systems Rh/**23b** and Rh/**65b**, which provided the highest enantioselectivity in the previous experiments. When the temperature was decreased to 20ºC (Entries 2 and 6), lower conversions were achieved with improved regioselectivity (up to 99.9%) and higher enantioselectivity (*ee* up to 70% and 66%, respectively) (Entry 1 vs. 2 and 5 vs. 6). Furthermore, when the ligand to rhodium ratio was increased to 2, the results were very similar although slightly higher enantioselectivity (*ee* up to 73% and 68%, respectively) (Entry 2 vs. 3 and 6 vs. 7) were obtained.

The ligand **23b** provided the highest regioselectivity (99.9%) and enantioselectivity (73%) of this series of ligands in the Rh-asymmetric hydroformylation of vinyl acetate. Ligand **65b** afforded lower conversion and enantioselectivity than ligand **23b**. These results suggested that an increase in steric hindrance at C-6 position was not beneficial in order to improve the activity and selectivity of this reaction.

In Table 2.6, the results obtained for the rhodium-catalysed hydroformylation of 2,5-dihydrofuran using the 1,3-diphosphites **64b**, **65b**, **66b** and **67b** are collected. The reaction conditions were 18 bar of CO/H_2 (ratio 1:1) at 45ºC with a ligand to rhodium ratio of 2.

When the reaction was performed using the ligand **64b**, total conversion of the substrate was achieved with a chemoselectivity to aldehydes of 79%. The regioselectivity to tetrahydro-3-carbaldehydes was 81% and a moderate *ee* (51%) was achieved (Entry 1). The diphosphite ligand **65b** provided lower conversion and chemoselectivity than ligand **64b**. However, this ligand furnished higher regioselectivity to tetrahydro-3-carbaldehydes

with a higher enantioselectivity (*ee* = 64%) (Entry 1 vs. 2). The catalytic system Rh/**66b** provided total conversion of the substrate, but with a low chemo- and regioselectivity and poor enantioselectivity (36%).

Table 2.6. Rhodium-catalysed hydroformylation of 2,5-dihydrofuran using diphosphites **64b**-**67b**.

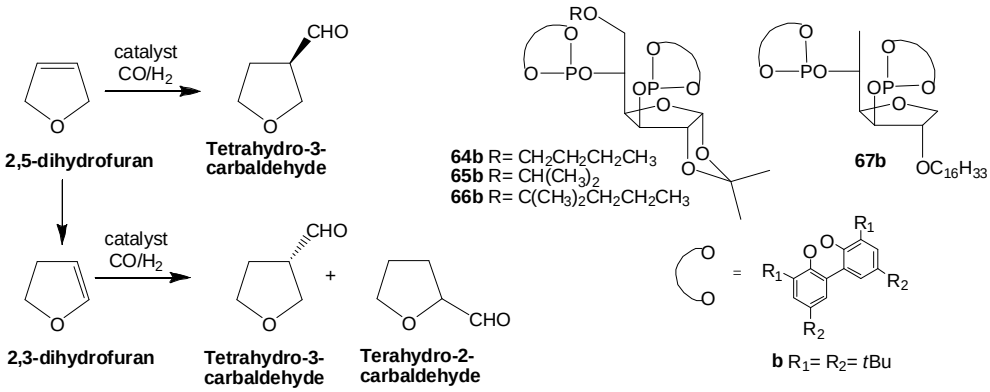

Entry[a]	Ligand	Conv.(%)[b]	Chemio.(%) [Regio.(%)][c]	% 2,3-dhf[d]	*ee* (%) [e]
1	**64b**	100	79[81/19]	21	51(*S*)
2	**65b**	85	71[87/13]	29	64(*S*)
3[g]	**65b**	100	55[80/20]	45	25(*S*)
4[h]	**65b**	100	98[86/14]	2	10(*S*)
5	**66b**	100	66[66/34]	34	36(*S*)
6	**67b**	100	96[96/ 4]	4	72 (*S*)
7[f]	**67b**	25	100[100/0]	-	88(*S*)

[a] P= 18 bar, P_{CO/H_2}= 1, [Rh(acac)$(CO)_2$] = 0.012 mmol, Substrate / Rh = 400, 2,5-dihydrofuran (dhf) 4.8 mmol, toluene = 5 mL, Ligand/ Rh = 2, T= 45 ºC, t = 24h . [b] Total conversion measured by ^{1}H NMR. [c] Conversion into aldehydes and regioselectivity to tetrahydro-3-carbaldehydes determined by ^{1}H NMR. [d] Isomerisation product 2,3-dihydrofuran measured by ^{1}H NMR. [e] Enantioselectivity of tetrahydro-3-carbaldehydes measured by ^{1}H NMR using Eu(hcf)$_3$. [f] T = 20 ºC. Incubation: 24h at 45ºC under hydroformylation conditions. [g] P_{CO/H_2}= 2. [h] P= 36 bar.

The larger amount of isomerised product 2,3-dihydrofuran and tetrahydro-2-carbaldehydes formed during the catalysis suggested that the isomerisation process was favoured with the catalytic system Rh/**66b** when compared to Rh/**65b** and Rh/**64b**. When the Rh/**67b** system was used

(Entry 6), total conversion was achieved with 96% chemoselectivity and 96% of regioselectivity to tetrahydro-3-carbaldehydes. Furthermore, the enantioselectivity was 72%, which is similar to the best results reported for this reaction with ligand **23b**.[37]

It is noteworthy that the highest chemo- and regioselectivities reported for this reaction were obtained with ligands **23b** and **67b**, which contain a methyl group at C-5 position. The results obtained with ligands **64**-**66b** thus indicate that the increase in steric hindrance at C-6 position (and therefore at the Rh centre) favours the *β*-elimination from Rh-alkyl intermediates and consequently, leads to a higher degree of isomerisation.

This effect is of importance since in this reaction, the chemoselectivity and enantioselectivity of product tetrahydro-3-carbaldehyde are linked as the hydroformylation of the isomerisation product 2,5-dihydrofuran yields the aldehyde tetrahydro-3-carbaldehyde with the opposite enantioselectivity than when tetrahydro-3-carbaldehyde is produced by direct hydroformylation of 2,3-dihydrofuran (Scheme 2.32).

In Scheme 2.32, an attempt for rationalizing this fact is described. Since the determining step for the regio- and enantioselectivity of this reaction is the insertion of the alkene into the Rh-H bond, only the RhH(alkene) species and subsequent insertion products are represented.

When the C2-symmetry 2,5-dihydrofuran is the substrate, there are two possible coordination modes of this molecule to the Rh-hydride complex (**Ia**-*R* and **Ia**-*S*, Scheme 2.32). Insertion of the double bond into the Rh-H can therefore yield two diastereoisomeric Rh-3-alkyls (**IIa**-*R* and **IIa**-*S*), which after further carbolynation and hydrogenolysis, lead to the formation of the two enantiomers of tetrahydro-3-carbaldehyde (Scheme 2.32). The chiral nature of the C1-symmetry diphosphite ligands leads to the discrimination of one of the two pro-chiral faces of the substrate [Rh-H(2,5-dhf)(PP)(CO)] (**Ia**-*R* vs. **Ia**-*S*) and therefore, the formation of one enantiomer of the hydroformylation products is favoured. In order to match the results obtained in this article (the *S*-enantiomer of tetrahydro-3-carbaldehyde is mainly produced), the spatial arrangement around the Rh centre requires the formation of the Rh-alkyl where the alkyl substituent is pointing forward, probably corresponding to the less sterically hindered area of the ligand (represented in white in the Scheme 2.32).

However, when 2,3-dihydrofurane is the substrate, the lower symmetry of this molecule leads to the formation of four possible [Rh-hydride(2,3- dhf)] complexes **Ib**-*R*, **Ib**-*S*, **Ic**-*R* and **Ic**-*S* (Scheme 2.32). Two sets of diastereoisomeric Rh-alkyls species can therefore be formed: the two Rh-2-alkyl species **Ic**-*R* and **Ic**-*S*, which after further reaction yield two enantiomers of tetrahydro-2-carbaldehyde and two Rh-3-alkyl complexes **Ib**-*R* and **Ib**-*S* which yield the two enantiomers of tetrahydro-3-carbaldehyde. As in the case of 2,5-dihydrofuran, the chiral discrimination produced by the disphosphite ligands favour the formation of one of the enantiomers formed by hydroformylation for each set of diastereoisomeric Rh-alkyl.

As this discrimination depends on the structural features of the ligand used, the preferred arrangement of the Rh-alkyl must be identical than in the case of the 2,5-dhf, with the alkyl substituent pointing forward (Scheme 2.32).In this case, the formation of the *R*-enantiomer is therefore favoured. This analysis explains the formation of the opposite enantiomers of tetrahydro-3-carbaldehyde when the hydroformylation reaction occurs from 2,3- or 2,5-dihydrofuran. This schematic representation is in agreement with the results obtained in the Rh-asymmetric hydroformylation of 2,5-dihydrofuran and 2,3-dihydrofuran described here.

When 2,3-dihydrofurane was used as substrate, there are four possible coordination modes of this molecule to the Rh-hydride complex which is active specie in the hydroformylation process. Insertion of the double bond into the Rh-H can therefore yield two enantiomeric Rh-3-alkyl species and two enantiomeric Rh-2-alkyl species. As in the case of 2,5-dihydrofuran, the steric interactions produced by the spatial arrangement of the C1-symmetry disphosphite ligands and the substrate favour the discrimination between the two pro-chiral faces in the coordination step, and therefore one of the enantiomers was preferment formed by hydroformylation, in this case the *R*-enantiomer (see Scheme 2.32).

This schematic representation is in agreement with the results obtained in the Rh-asymmetric hydroformylation of 2,5-dihydrofuran and 2,3-dihydrofuran using C-1 symmetry ligands, and confirmed the great importance of the spatial arrangements of the C-1 symmetry ligands and the steric properties of the ligand moieties.

UNIVERSITAT ROVIRA I VIRGILI
1,3- DIPHOSPHITE LIGANDS WITH FURANOSIDE BACKBONE: A POWERFUL TOOL IN ASYMMETRIC CATALYSIS
Aitor Gual Gozalbo
DL: T-1535-2009/ISBN: 978-84-692-4554-5

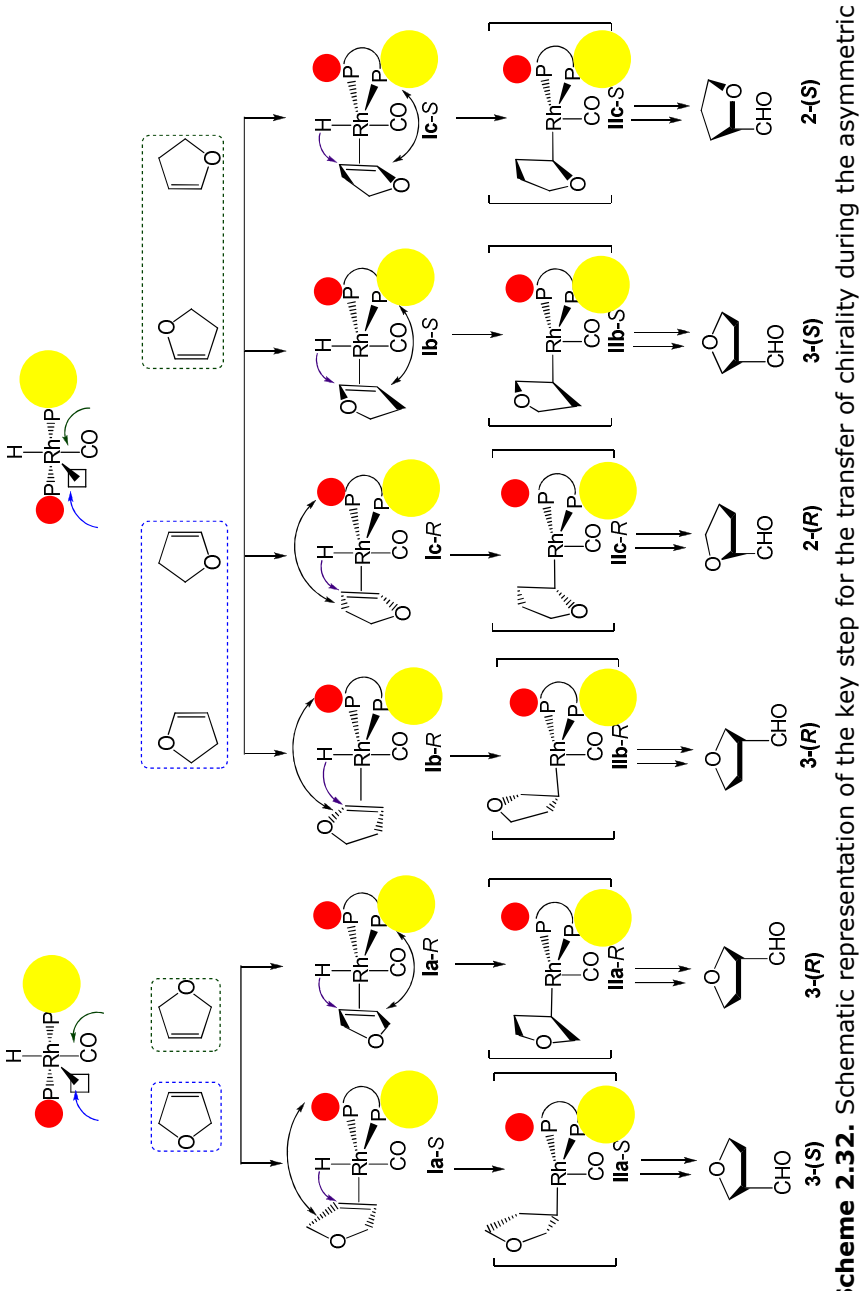

Scheme 2.32. Schematic representation of the key step for the transfer of chirality during the asymmetric hydroformylation of 2,5-dihydrofuran (2,5-dhf) and 2,3-dihydrofuran (2,3-dhf) using C1-symmetry ligands.

To further improve the enantioselectivity, the reaction with the Rh/**67b** catalytic system was performed at 20ºC (Entry 7). Under these conditions, moderate conversion (25%) was obtained with total chemo- and regioselectivity to the tetrahydro-3-carbaldehyde. Furthermore, the enantioselectivity of the reaction increased to 88%. To the best of our knowledge, the Rh/**67b** system provides the highest selectivity reported for this substrate.

Next, the Rh/**65b** catalytic system was tested under higher CO/H_2 ratio and higher total pressure. When the CO/H_2 ratio was increased to 2 (Entry 3), lower chemoselectivity to aldehydes and lower enantioselectivity were achieved, although the regioselectivity to tetrahydro-3-carbaldehydes remained comparable (80%). However, when the total pressure was increased to 36 bar (Entry 4), total conversion of the substrate was achieved with a clear increase in chemoselectivity to aldehydes. In contrast, the enantioselectivity was found to decrease to 10%. The displacement of the ligand due to the increase in pressure to form the unselective $[RhH(CO)_4]$ species could explain this result.

These results obtained in the asymmetric hydroformylation of 2,5-dihydrofuran using ligands **64b**-**67b** show that that the use of ligands with monocyclic carbohydrate backbone improves the performance of the catalyst since ligand **67b** yielded the best results reported to date in this reaction. However, the introduction of bulky groups at C-6 led to a higher degree of isomerisation and consequently, lower regio- and enantioselectivity were obtained.

As previously mentioned, the production of the opposite enantiomer of tetrahydro-3-carbaldehyde can be achieved through the asymmetric hydroformylation of the 2,3-dihydrofuran using the same catalytic Rh systems bearing ligands **64b**-**67b**. The results obtained in the asymmetric hydroformylation of 2,3-dihydrofuran are listed in Table 2.7.[36,37]

The use of the catalytic system Rh/**64b** resulted in 45% of conversion, 78% of regioselectivity to tetrahydro-3-carbaldehyde and enantioselectivity of 83% (Entry 1). When the catalytic system Rh/**65b** was used, lower conversion (25%) was obtained while the regioselectivity to tetrahydro-3-carbaldehyde and the enantioselectivity (84%) remained unchanged (Entry 2). Using the catalytic system Rh/**66b**, 28% conversion was achieved, with 62% of regioselectivity to tetrahydro-3-carbaldehyde and 61% *ee* (Entry

UNIVERSITAT ROVIRA I VIRGILI
1,3- DIPHOSPHITE LIGANDS WITH FURANOSIDE BACKBONE: A POWERFUL TOOL IN ASYMMETRIC CATALYSIS
Aitor Gual Gozalbo
DL: T-1535-2009/ISBN: 978-84-692-4554-5

3). These results confirmed that the activity, the regioselectivity and the enantioselectivity were highly affected by the presence of steric bulky substituents around the coordination sphere of the rhodium catalyst (Entry 1-3). It is noteworthy that the catalytic systems Rh/**64b** and Rh/**65b** provided the highest enantioselectivity (up to 84%) reported in the Rh-asymmetric hydroformylation of 2,3-dihydrofuran (Entry 1 and 2). Using the catalytic system Rh/**67b** (Entry 4), only 10% of conversion was obtained with poor regioselectivity to tetrahydro-3-carbaldehyde (50%) and no enantioselectivity.

Table 2.7. Rhodium-catalysed hydroformylation of 2,5-dihydrofuran using diphosphites **64b**-**67b**.

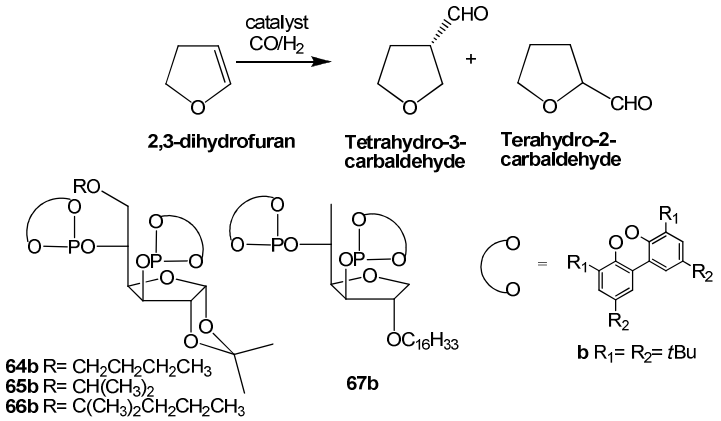

Entry[a]	Ligand	Conv.(%)[b]	Chemio.(%)[Regio.(%)][c]	*ee*(%)[d]
1	**64b**	45	100 [78/22]	83 (*R*)
2	**65b**	25	100 [78/22]	84 (*R*)
3	**66b**	28	100 [62/38]	61 (*R*)
4	**67b**	10	100 [50/50]	-

[a] P= 18 bar, P_{CO/H_2}= 1, [Rh(acac)$(CO)_2$] = 0.012 mmol, Substrate / Rh = 400, 2,3-dihydrofuran (dhf) 4.8 mmol, toluene = 5 mL, Ligand/ Rh = 2, T= 45 ºC, t = 48h . [b] Total conversion measured by ^{1}H NMR. [c] Conversion into aldehydes and regioselectivity to tetrahydro-3-carbaldehydes determined by ^{1}H NMR. [d] Enantioselectivity of tetrahydro-3-carbaldehydes measured by ^{1}H NMR using Eu(hcf)$_3$.

The best results in the hydroformylation of 2,3-dihydrofuran were thus obtained with Rh/**64b** and Rh/**65b** systems and the less selective system was Rh/**67b**. This is a striking difference with the results obtained in the

hydroformylation of 2,5-dihydrofuran for which the best catalytic system was Rh/**67b** and Rh/**64b** and Rh/**65b** revealed to be less selective.

High-pressure NMR study

To investigate the coordination mode of the ligands **65b** and **67b**, which provided the best catalytic results using 2,3-dihydrofuran and 2,5-dihydrofuran as substrates, respectively, the $[RhH(CO)_2(L)]$,with L= **65b** and **67b**, were studied by HP-NMR techniques (Scheme 2.33).

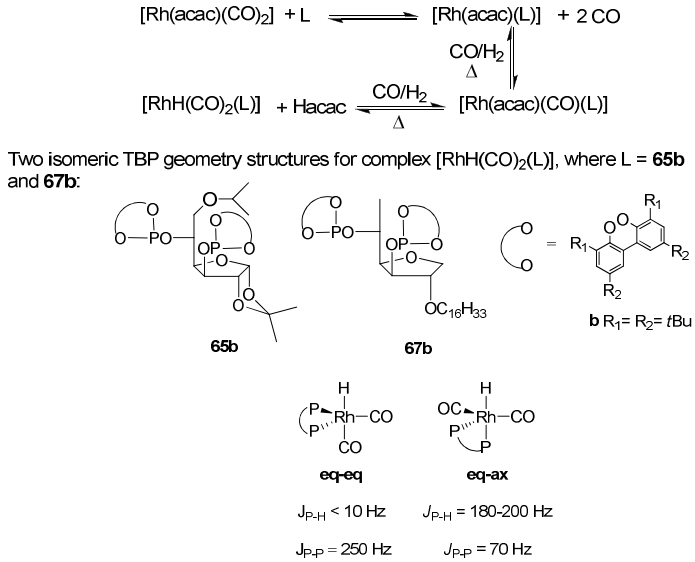

Scheme 2.33. General mechanism for the formation of the $[RhH(CO)_2(L)]$ (L = **65b** and **67b**) species.

One equivalent of the diphosphite ligand (**65b** or **67b**) was added to a 2 mM solution of $[Rh(acac)(CO)_2]$ in toluene-d_8 at room temperature within a 10 mm NMR tube. In both cases, a rapid change of colour was observed at this stage from colourless to yellow. The NMR tube was shaken under hydroformylation conditions for 24 h at 45ºC, placed into the spectrometer and the NMR spectra were recorded at various temperatures. Under these conditions, signals corresponding to the rhodium hydride species $[RhH(CO)_2(L)]$ (L = **67a** or **21w**) were readily detected as the only

organometallic product. The general mechanism for the formation of these species is described in Scheme 2.33.[10,21,22,25,49]

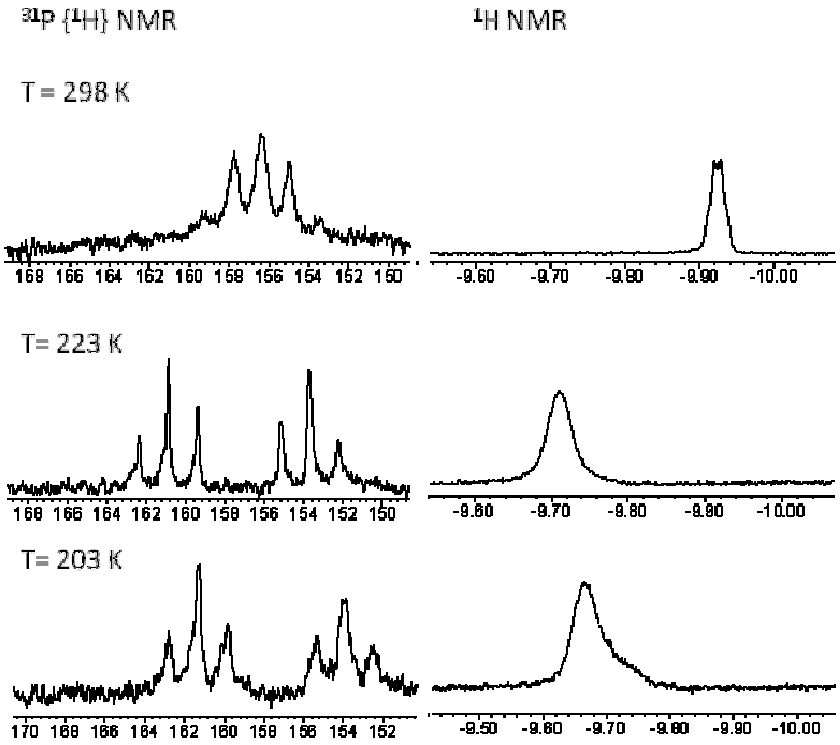

Figure 2.4. Selected regions of ^{1}H and $^{31}P\{^{1}H\}$ NMR spectra of complex $[RhH(CO)_2(\mathbf{65b})]$ in d8-toluene recorded at variable temperature.

In the ^{1}H NMR spectrum of a solution containing $[RhH(CO)_2(\mathbf{65b})]$ at room temperature, a broad doublet at -9.92 ppm (J= 3.2 Hz) was observed. The small coupling constant $J_{P\text{-}H}$ suggested an **eq-eq** coordination of the ligand. In the $^{31}P\{^{1}H\}$ NMR spectrum, a broad signal at 156.30 ppm was detected, suggesting that a fluxional process was occurring on the NMR timescale was occurring at room temperature. Therefore, ^{1}H and $^{31}P\{^{1}H\}$ NMR spectra were recorded at variable temperatures (Figure 2.4). At low temperatures, the ^{1}H NMR signal of the hydride remained broad whereas at 223 K, the corresponding ^{31}P signals were resolved as two mutually coupled doublets of doublets at 153.7 ppm and 161.2 ppm that were assigned to the two inequivalent phosphorus atoms bonded to rhodium. The broadness of these two signals at temperature above 243 K was interpreted as a very fast interchange of the coordinated phosphorus atom positions.

To determine the preferred coordination mode of ligand **65b** in [RhH(CO)$_2$(**65b**)], simulations of the $^{31}P\{^1H\}$NMR spectrum were performed using the *gNMR V4.0* software. The coupling constants obtained by simulation of the recorded $^{31}P\{^1H\}$ NMR spectra at 233, 223 and 203 K are listed in Table 2.8. These coupling constants obtained are $J_{P\text{-}P}\approx$ 239 Hz and $J_{Rh\text{-}P}\approx$ 240 Hz and are in agreement with an **eq-eq** coordination of the ligands in the TBP [RhH(CO)$_2$(**65b**)] species.

In previous studies of analogous complexes bearing diphosphite ligands derived from carbohydrates, rapid exchange at room temperature between **eq-eq** and **eq-ax** coordination of the ligands was reported based on NMR and IR analysis.[22b-d] Due to the similarity of the spectroscopic data, it was concluded that rapid exchange between **eq-eq** and **eq-ax** coordination of the [RhH(CO)$_2$(**65b**)] species was occurring at room temperature. However, the interchange between the two diastereoisomers **eq-eq**-[RhH(CO)$_2$(**65b**)] previously proposed for analogous species, cannot be discarded.

Table 2.8. Selected ^1H and $^{31}P\{^1H\}$ NMR data for [RhH(CO)$_2$(**65b**)] complex.[a][b]

T (K)	δ(P1) [c]	δ(P2) [c]	$J_{Rh\text{-}P1}$[d]	$J_{Rh\text{-}P2}$[d]	$J_{P1\text{-}P2}$[d]	δ(H) [c]
298	157.0(m)	157.0(m)	-	-	-	-9.92
233	153.7	160.6	239.7	240.0	239.7	-9.75
223	153.8	160.8	238.9	239.0	238.9	-9.72
203	154.1	161.2	239.0	239.1	239.1	-9.68

[a] Rh/L = 1/1.1, solvent= toluene-d_8, P = 18 bar, P_{CO/H_2}= 1. Incubation: 24h at 45ºC. [b] ^{31}P and ^1H NMR spectra recorded using a 10 mm high-pressure NMR tube. [c] Chemical shifts in ppm. [d] Coupling constants in Hz.

The complex [RhH(CO)$_2$(**67b**)] was also synthesised under the same conditions and characterised by multinuclear NMR techniques.

In the ^1H NMR spectrum at room temperature, an hydride peak was observed as a broad quadruplet at -9.93 ppm with $J_{H\text{-}P1} = J_{H\text{-}P2} = J_{H\text{-}Rh} \approx$ 4.4 Hz This coupling constant is in agreement with an **eq-eq** disposition of the phosphorus atoms in the [RhH(CO)$_2$(**67b**)]. In the $^{31}P\{^1H\}$NMR a broad signal at 156.2 ppm was detected. This observation suggested the presence

of a rapid exchange on the NMR timescale. The spectra were therefore recorded at lower temperatures and at 213 K, two broad hydride signals were detected at -9.62 ppm ($\Delta\omega_{1/2}\approx$ 40Hz) and -9.75 ppm ($\Delta\omega_{1/2}\approx$ 60Hz) with a ratio of intensity of 1:0.6. In the $^{31}P\{^{1}H\}$NMR spectrum, 2 sets of complex multiplets were observed at 159.5 ppm and 150.5 ppm. Variable temperature experiments showed that these signals were best resolved at 233 K (Figure 2.5) and at this temperature, it became evident that each set of signal corresponded to two pseudo-triplet ^{31}P signals in the ratio of intensity 1:0.5. Based on these observations, these signals were assigned to two isomeric forms of [$RhH(CO)_2$(**67b**)].

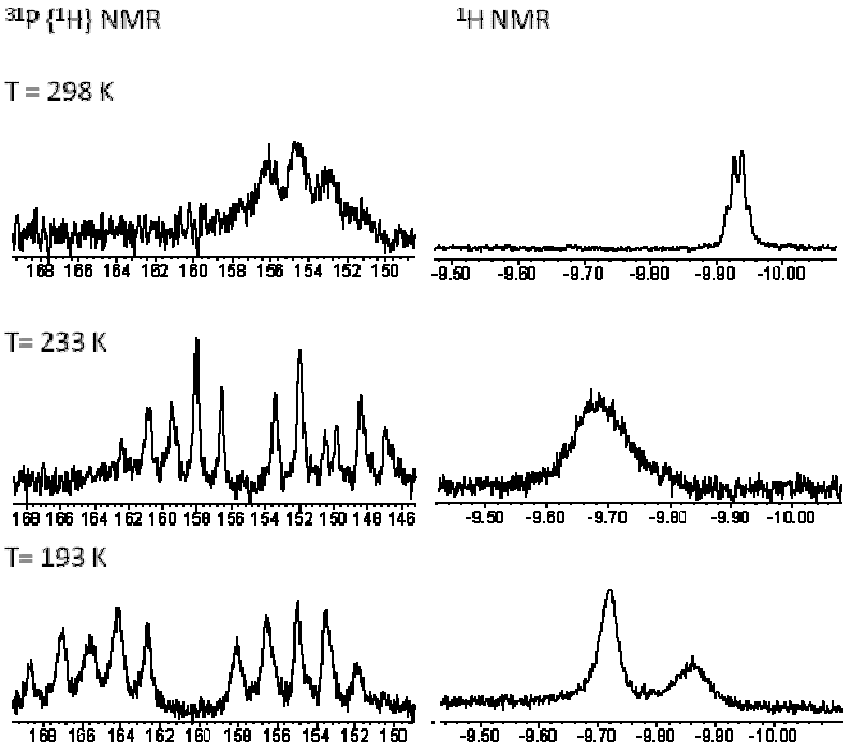

Figure 2.5. Selected regions of ^{1}H and $^{31}P\{^{1}H\}$ NMR spectra of complex [$RhH(CO)_2$(**67b**)] in d8-toluene recorded at variable temperature.

To confirm the identity of these species, simulations of the $^{31}P\{^{1}H\}$NMR spectra were performed using the *gNMR V4.0 software*. The coupling constants obtained by simulation and the chemical shifts recorded at 233 K, 213K and 193 K are listed in Table 2.9. Comparing the calculated coupling

constants (J_{Rh-P}=J_{P-P}≈ 235-240 Hz) with the literature data, the recorded NMR signals were attributed to two isomers of the complex [RhH(CO)$_2$(**67b**)], which both contain the diphosphite ligand in **eq-eq** position and rapidly interchange on the NMR timescale. [22]

Table 2.9. Selected ^{1}H and ^{31}P{^{1}H} NMR data for [RhH(CO)$_2$(**67b**)] complex.[a][b]

T (K)	δ(P1) [c]	δ(P2) [c]	J_{Rh-P1}[d]	J_{Rh-P2}[d]	J_{P1-P2}[d]	δ(H) [c]
298	156.2(m)	156.2(m)	-	-	-	-9.93
233	152.0	157.9	236.3	239.0	237.6	-9.70
	148.5	160.8	237.0	236.3	238.6	-9.70
223	157.0	163.4	236.7	243.3	240.0	-9.70
	153.5	166.4	236.7	243.2	240.0	-9.70
193	156.6	164.1	250.8	239.9	245.3	-9.70
	153.6	167.1	237.8	245.4	241.6	-9.85

[a] Rh/L = 1/1.1, solvent= toluene-d_8, P = 10 bar, P_{CO/H_2}= 0.5. Incubation: 16h at 40ºC. [b] ^{31}P and ^{1}H NMR spectra recorded using a 10 mm high-pressure NMR tube. [c] Chemical shifts in ppm. [d] Coupling constants in Hz.

In the work described in the section 2.4.1 with analogous ligand **67a**, such isomers were also detected by HP-NMR techniques. The presence of the less rigid monocyclic backbone in these ligands could explain the coexistence of these isomers. Indeed, the increased flexibility of monocyclic tetrahydrofurans when compared to bicyclic structures is well known and documented.[50] These structural features were shown to lead to the formation of various conformational isomers which interconvert in solution.
The signals observed in this study were therefore assigned to two conformational isomers of the **eq-eq**-[RhH(CO)$_2$(**67b**)] complex. It is thought that upon coordination to the Rh centre, two conformations of the furan backbone are preferred.

Conclusions

The syntheses of the new chiral diphosphite ligands **64b**, **65b**, **66b**, **67b**, **87b** and **89b** containing a furanoside backbone were successfully completed. These ligands are shown to be very selective in the Rh-asymmetric hydroformylation of vinyl acetate and dihydrofurans. When vinyl acetate was the substrate, excellent regioselectivities (up to 99.9%) and good enantioselectivities were achieved using ligands **23b** (73%) and **65b** (68%). In the hydroformylation of 2,5-dihydrofurane, the ligand **67b** provided excellent chemoselectivity (100%) and regioselectivity to tetrahydro-3-carbaldehydes (100%) together with the highest enantioselectivity (88%) reported to date for this reaction. When 2,3-dihydrofurane was the substrate, the use of ligands **64b** and **65b** provided excellent chemoselectivity (100%), good regioselectivity to tetrahydro-3-carbaldehydes (78%) and the highest enantioselectivity reported to date (84%).

This study was completed with the NMR characterization of the $[RhH(CO)_2(L)]$, where L= **65b** and **67b**, demonstrating that both ligands **65b** and **67b** coordinate to the Rh centre in an **eq-eq** fashion in these hydride complexes. The complex $[RhH(CO)_2($**65b**$)]$ was detected as a single isomer with characteristic features of **eq-eq** coordination. However, the broadening of the corresponding signals indicated that this species is rapidly interchanging in solution. The absence of signals for the second species involved did not permit to undoubtedly determine the nature of this exchange process, although an equilibrium between **eq-eq** and **eq-ax** coordinations is likely. In contrast, complex $[RhH(CO)_2($**67b**$)]$ was detected as a mixture of two isomers at low temperature, and that both contained the diphosphite ligand in an **eq-eq** fashion. In this case, the increased flexibility of ligand **67b** monocyclic backbone is thought to be responsible for the formation of two conformational isomers of this complex.

2.4.3. Highly enantioselective Rh-catalysts for the asymmetric hydroformylation of α-methylstyrene and methyl-methacrylate using C1-Symmetry diphosphite ligands.

L. Cornelissen, A. Gual, C. Müller, S. Castillón, C. Claver, D. Vogt, manuscript in preparation.

Rh-asymmetric hydroformylation of α-methylstyrene and methyl-methacrylate

Additionally, in collaboration with Dr Leandra Cornelissen, Dr. Christian Muller and Prof. Dieter Vogt, from the Technical University of Eindhoven, the designed diphosphite ligands (see Figure 2.6) were successfully applied in the Rh-asymmetric hydroformylation of 1,1´-disubstituted substrates, as α-methyl-styrene and methyl-methacrylate. These results are described in the Ph-D thesis of Dr. Leandra Cornelissen and are collected in a joint publication in preparation. The best results and the reaction conditions are summarized in this section.

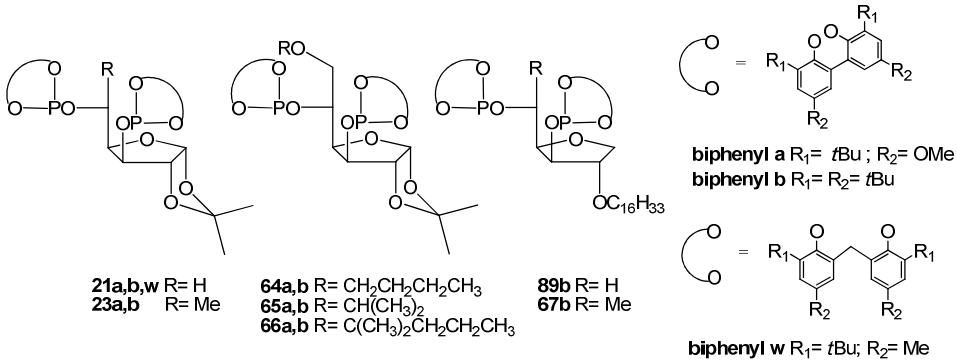

Figure 2.6. Rh-asymmetric hydroformylation of α-methylstyrene and methyl-methacrylate using the series of 1,3-diphosphite ligands with furanoside backbone.

In general, the size and nature of the C-6 substituent of the furanose backbone have an effect on conversion, the regio- and the enantioselectivity. The conversion increases in the order **21b** < **23b** <

65b. The conversion does not increase further when the more bulky ligand **66b** was used. The regio- and enantioselectivity were higher with the ligands containing substituents at C-6, but little difference is observed between catalysts based on ligands **64a,b**, **65a,b** and **66a,b**. The effect of the biphenyl moiety was studied by comparing the ligands **23a**,**b**, **64a**,**b**, **65a**,**b** and **66a**,**b**. The ligands with biphenyl moiety **a** produce lower conversion with higher l/b ratio and similar enantioselectivity than for their counterparts containing the biphenyl moiety **b**.

Interestingly, the ligands **67b** and **89b** with the the monocyclic furanose backbones produced lower conversion and regioselectivity with slightly higher enantioselectivities. This behaviour is in agreement with the previously observed in section 2.4.1 in the Rh-asymmetric hydroformylation of styrene. Additionally, also in agreement to the Rh-asymmetric hydroformylation of styrene the use of the phosphite moiety **w** produced much lower conversions (**21b** vs. **21w**).

The reaction conditions were optimised and the best results in terms of activity, regio-and enantio-selectivity are shown in figure 2.34.

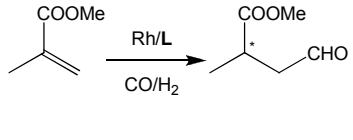

	T(ºC)	%conv	% l/b	% *ee*
L= **64a**	100	87%	34.4%	52%
L= **65a**	100	77%	33.9%	56%
L= **65a**	60	9%	4.8%	71%
L= **66a**	100	86%	33.6%	55%

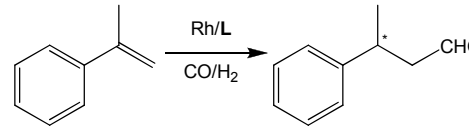

	T(ºC)	%conv	% l/b	% *ee*
L= **64a**	100	14%	38.2%	30%
L= **65a**	100	11%	32.9%	33%
L= **65a**	80	7%	18.8%	36%
L= **66a**	100	11%	29.9%	31%

Scheme 2.34. Rh-asymmetric hydroformylation of α-methylstyrene and methyl-methacrylate using the series of 1,3-diphosphite ligands with furanoside backbone. Reaction conditions: L/Rh=2, Substrate/Rh=1000, P=10bar, CO:H_2= 1:1, t=16h [Rh] = 1 mM. Preformation: P=10bar, T=60ºC, t=1h.

In conclusion, the ligand **64a** provided the highest enantioselectivity ever reported in the Rh-asymmetric hydroformylation of methyl methacrylate (*ee* up to 71%), and slighltly lower enantioselectivity to the highest reported in the Rh-asymmetric hydroformylation of α-methylstyrene.

UNIVERSITAT ROVIRA I VIRGILI
1,3- DIPHOSPHITE LIGANDS WITH FURANOSIDE BACKBONE: A POWERFUL TOOL IN ASYMMETRIC CATALYSIS
Aitor Gual Gozalbo
DL: T-1535-2009/ISBN: 978-84-692-4554-5

2. 5. Conclusions

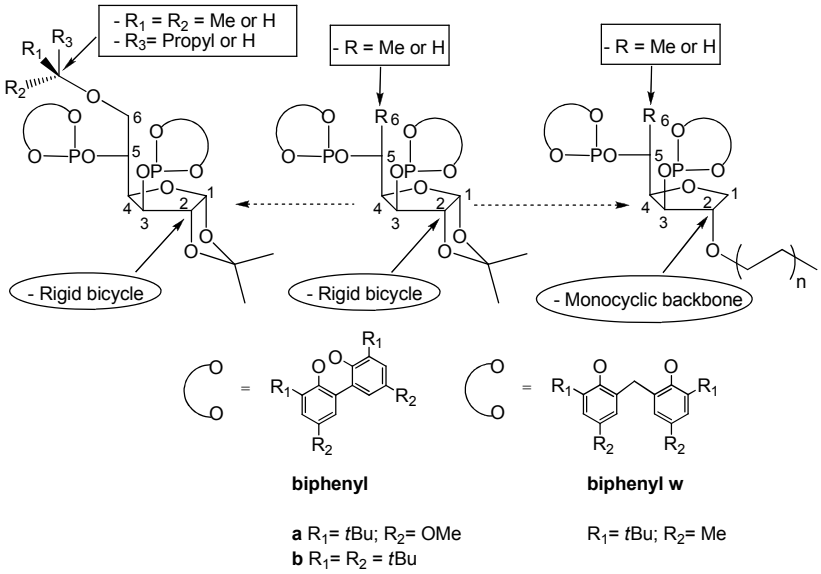

Figure 2.6. Structural diversity in 1,3-diphosphite ligands derived from carbohydrates with a furanoside (tetrahydrofuran) backbone prepared in this chapter.

New 1,3-Diphosphite ligands (**21aw**, **64a**,**b**, **65a**,**b**, **66a**,**b**, **67a**,**b**,**w**, **86a**,**w**, **87a**,**b**,**w**, and **89b**) with a furanoside (tetrahydrofuran) backbone were successfully prepared from common carbohydrates through new synthetic strategies. The phosphite moiety of these ligands incorporate different biphenyl units such as **a**, **b** and **w**.

This small library of diphosphite was applied in Rh-catalysed hydroformylation of styrene, vinyl acetate, 2,3- and 2,5-dihydrofuran.

In the frame of collaboration with the group of Prof. Dr. Vogt and Dr. Christian Muller these ligands were applied in the Rh-asymmetric hydroformylation of α-methylstyrene and methyl-methacrylate.

In the case of styrene, the best results were obtained using the catalytic system Rh/**67a**. Moderate conversion with excellent regio-and enantioselectivity (*ee* up to 83%) was achieved. However, higher activities with slightly higher enantiomeric excesses (*ee* up to 90%) were reported using the ligand **23a**. These differences in activity and selectivity could be

explained by the presence of two **eq**-**eq** [$RhH(CO)_2(L)$] species in equilibrium in the case of ligand **67a**, suggesting that the suppression of the 1,2-isopropylidene group reduces the rigidity of the carbohydrate backbone facilitating the presence of two conformers in solution. In the case of glucofuranose ligand **23a** only one [$RhH(CO)_2(L)$] specie in **eq**-**eq** conformation was detected.

Additionally, the results using the ligands **21a**,**w** and **67a**,**w** suggested that the biphenyl moiety produced a high steric hindrance around the coordination sphere of the [$RhH(CO)_2(L)$] species avoiding the hydroformylation of the substrate under standard reaction conditions. The formation of the [$RhH(CO)_2(L)$], where L= **21w**, was confirmed by HP-NMR.

In the Rh-asymmetric hydroformylation of vinyl acetate moderate conversion with excellent regioselectivity and *ee* up to 73% were achieved using the diphosphite ligand **23b**.

In the Rh-asymmetric hydroformylation of 2,5-dihydrofuran the best results were achieved using the monocyclic ligand **67b**. The only product formed was the tetrahydro-3-carbaldehyde with moderate conversion and enantioselectivity of 88% (*S*). Interestingly, it was found that increasing the steric bulk in the position C-6 of the ligand carbohydrate backbone favour the isomerisation processes. As described for the ligand **67a**, two **eq**-**eq** [$RhH(CO)_2$(**67b**)] species in equilibrium were detected by HP-NMR variable temperature studies.

In the Rh-asymmetric hydroformylation of 2,3-dihydrofuran the best results were achieved using the bicyclic ligands **64b** and **65b**. Comparable results in terms of selectivity were achieved by using both catalytic systems (regio. up to 78% and *ee* up to 84% (*S*)). However, the ligand **64b** produced higher activities than ligand **65b**. The [$RhH(CO)_2(L)$], where L= **65b**, structure was also characterized. The $^{31}P\ \{^1H\}$ NMR spectra at room temperature revealed the presence of a fluxional equilibrium on the NMR-time scale. Only one **eq-eq** [$RhH(CO)_2(L)$], where L= **65b**, specie was detected by HP-NMR variable temperature studies. The absence of signals for the second species involved did not permit to undoubtedly determine the nature of this exchange process, although an equilibrium between **eq-eq** and **eq-ax** coordinations is likely.

It is noteworthy that the results obtained in the Rh-asymmetric hydroformylation of 2,5-dihydrofuran, 2,3-dihydrofuran and methyl

methacrylate are the best ever reported in terms of enantioselectivity for each substrate.

2.6. Experimental Section

General methods. All syntheses were performed using standard Schlenk techniques under N_2 atmosphere. Solvents were purified by standard procedures. All other reagents were used as received. Elemental analyses were performed on a Carlo Erba EA-1108 instrument. Optical rotations were measured at room temperature in 10 cm cell. ^{1}H, $^{13}C\{^{1}H\}$ and $^{31}P\{^{1}H\}$ NMR spectra were recorded on a Varian Gemini 400 MHz spectrometer. Chemical shifts are relative to $SiMe_4$ (^{1}H and ^{13}C) as internal standard or H_3PO_4 (^{31}P) as external standard. All NMR spectral assignments were determined by COSY and HSQC spectra. Hydroformylation reactions were carried out in a Berghof 100 mL stainless steel autoclave.

Synthesis of the ligands

6-*O*-Isopropyl-1,2-*O*-isopropylidene-*α*-*D*-glucofuranoside (69). To a solution of **5** (1.76 g, 6.63 mmol) in CH_2Cl_2 (250 mL) cooled at -10 ºC Et_3SiH (4.26 mL, 26.7 mmol) and $BF_3{\bullet}Et_2O$ (1.51 mL, 11.9 mmol) were added. The reaction mixture was stirred at -10 ºC for 2h, and was later quenched by careful addition to saturated $NaHCO_3/H_2O$ (50mL). The aqueous layer was extracted with CH_2Cl_2 (3×50 mL), and the combined organic phases were washed with brine and dried over $MgSO_4$. Purification by flash chromatography (EtOAc, Rf= 0.42) gave compound **69** as colorless oil (748 mg, 43%). $[\alpha]^{D}_{25} = -1.13$ cm^3 g^{-1} dm^{-1}(c = 1.0 g cm^{-3}, CH_2Cl_2). **^{1}H NMR** (400 MHz, $CDCl_3$) δ: 1.19 (d, *J*= 5.6Hz, 6H, $(OCH(CH_3)_2)$), 1.32 (s, 3H, $O_2C(CH_3)_2$), 1.49 (s, 3H, $O_2C(CH_3)_2$), 3.54 (dd, *J*= 10, 5.6 Hz, 1H, 6-H), 3.67 (m, 1H, $OCH(CH_3)_2$), 3.74 (dd, *J*= 10, 3.2 Hz, 1H, 6´-H), 4.08 (dd, *J*= 5.8, 2.7 Hz, 1H, 4-H), 4.15 (m, 1H, 5-H), 4.35(b, 1H, 3-H), 4.55 (d, *J*= 3.2 Hz, 1 H, 2-H), 5.97 (d, *J*= 3.6Hz, 1 H, 1-H); **^{13}C NMR** (100.6 MHz, $CDCl_3$) δ: 22.1 $(OCH(CH_3)_2)$, 26.3 $(O_2C(CH_3)_2)$, 26.9 $(O_2C(CH_3)_2)$, 68.9 (C-6), 69.7 (C-5), 72.7 $(OCH(CH_3)_2)$, 76.0 (C-4), 80.2 (C-3), 85.2 (C-2)), 105.0 (C-1), 111.7 $(O_2C(CH_3)_2)$. Anal. calcd for $C_{12}H_{22}O_6$ (262.30): C, 54.95; H, 8.45. Found: C, 54.59; H, 8.70.

1,2-*O*-isopropylidene-6-*O*-(1,1-dimethyl-3-butene)-*α*-*D*-glucofuranoside (72). To a solution of **5** (1.76 g, 6.63 mmol) in CH_2Cl_2

(250 mL) cooled at -10 ºC $Me_3SiAllyl$ (4.24 mL, 26.5 mmol) and $BF_3•Et_2O$ (1.51 mL, 11.9 mmol) were added. The reaction mixture was stirred at -10 ºC for 2h, and was later quenched by careful addition to saturated $NaHCO_3/H_2O$ (50mL). The aqueous layer was extracted with CH_2Cl_2 (3 × 50 mL), and the combined organic phases were washed (brine) and dried ($MgSO_4$). Purification by flash chromatography (EtOAc, Rf= 0.42) gave compound **72** as a colorless oil (802 mg, 40%).$[\alpha]^D_{25}$ = + 0.24 $cm^3\ g^{-1}\ dm^{-1}$ (c = 1.0 g cm^{-3}, CH_2Cl_2). **^{1}H NMR** (400 MHz, $CDCl_3$) δ: 1.18 (d, *J*= 5.6Hz, 6H, $OC(CH_3)_2CH_2CH=CH_2$), 1.31 (s, 3H, $O_2C(CH_3)_2$), 1.48 (s, 3H, $O_2C(CH_3)_2$), 2.25 (d, *J*= 7.2 Hz, 2H, $CH_2CH=CH_2$), 3.47 (dd, *J*= 9.5, 5.2 Hz, 1H, 6-H), 3.66 (dd, *J*= 9.3, 3.0 Hz, 1H, 6-H) , 4.08 (d, *J*= 4.2 Hz, 1H, 4-H), 4.35 (d, *J*= 2.4Hz, 1H, 3-H), 4.53 (d, *J*= 3.6 Hz, 1H, 2-H), 5.05 (m, 1H, 5-H), 5.08 (m, 2H, CH2CH=CH2), 5.82 (m, 1H, CH2CH=CH2), 5.95 (d, J= 3.6Hz, 1H, 1-H); **^{13}C NMR** (100.6 MHz, $CDCl_3$) δ: 25.3 ($OC(CH_3)_2CH_2CH=CH_2$), 25.4 ($OC(CH_3)_2CH_2CH=CH_2$), 26.3 ($O_2C(CH_3)_2$), 27.0 ($O_2C(CH_3)_2$), 45.1 ($CH_2CH=CH_2$), 62.6 (C-6), 69.7 (C-5), 75.5 ($OC(CH_3)_2CH_2CH=CH_2$), 76.0 (C-4), 80.3 (C-3), 85.2 (C-2)), 105.0 (C-1), 111.7 ($O_2C(CH_3)_2$), 117.9 ($CH_2CH=CH_2$). 134.3 ($CH_2CH=CH_2$). Anal. calcd for $C_{15}H_{26}O_6$ (302.36): C, 59.58; H, 8.67. Found: C, 59.50; H, 8.70.

1,2-*O*-isopropylidene-6-*O*-(1,1-dimethyl-3-butyl)-*α*-*D*-glucofuranoside (70). To a solution of **72** (802 mg, 2.65 mmol) in THF (4 mL) a catalytic amount of Pd/C (0.1 mmol) was added. The reaction mixture was stirred for 12 h under 1 atm. H_2 pressure. The H_2 pressure was removed. The mixture was filtered through celite to obtain the corresponding diol **70** as a white powder (800 mg, 99%). $[\alpha]^D_{25}$ = + 11.50 $cm^3\ g^{-1}\ dm^{-1}$ (c = 1.0 g cm^{-3}, CH_2Cl_2). **^{1}H NMR** (400 MHz, $CDCl_3$) δ: 0.91 (t, *J*= 7.2Hz, 3H, $CH_2CH_2CH_3$), 1.18 (m, 6H, $OC(CH_3)_2CH_2CH_2CH_3$), 1.32 (s, 3H, $O_2C(CH_3)_2$), 1.44 (m, 4H, $CH_2CH_2CH_3$), 1.49 (s, 3H, $O_2C(CH_3)_2$), 3.45 (dd, *J*= 9.2, 4.8 Hz, 1H, 6´-H), 3.64 (dd, *J*= 9.4, 2.6 Hz, 1H, 6-H) , 4.09 (d, *J*= 2.0 Hz, 1H, 4-H), 4.35 (d, *J*= 2.0Hz, 1H, 3-H), 4.55 (d, *J*= 3.6 Hz, 1H, 2-H), 5.96 (d, *J*= 3.6Hz, 1H, 1-H); **^{13}C NMR** (100.6 MHz, $CDCl_3$) δ: 14.5 ($CH_2CH_2CH_3$), 17.0 ($CH_2CH_2CH_3$), 25.2 ($OC(CH_3)_2CH_2CH_2CH_3$), 25.3 ($OC(CH_3)_2CH_2CH_2CH_3$), 26.0 ($O_2C(CH_3)_2$), 26.7 ($O_2C(CH_3)_2$), 42.6 ($CH_2CH_2CH_3$), 62.0 (C-6), 69.5 (C-5), 75.6 ($OC(CH_3)_2CH_2CH_2CH_3$), 75.8 (C-

4), 80.1 (C-3), 85.0 (C-2)), 104.8 (C-1), 111.5 ($O_2C(CH_3)_2$). Anal. calcd for $C_{15}H_{28}O_6$ (304.38): C, 59.19; H, 9.27. Found: C, 59.10; H, 9.30.

6-Bromo-6-deoxy-1,2:3,5-di-*O*-isopropylidene-*α*-*D*-glucofuranoside (73). Compound **5** (5g, 19.2 mmol), Ph_3P (8.31g, 31.7 mmol), and *N*-bromosuccinimide (5.13g, 28.8 mmol) were dissolved in toluene (50 mL). The resulting solution was heated at 90 ºC for 2 h, then cooled, washed with 5% $NaHCO_3/H_2O$ and dried ($MgSO_4$). Purification by flash chromatography (EtOAc/Hexane = 1/16, Rf= 0.25) gave **73** as a colorless oil (4.84 g, 78 %). $[\alpha]^D_{25}$ = +31.82 $cm^3\ g^{-1}\ dm^{-1}$ (c = 1.0 g cm^{-3}, CH_2Cl_2). **^{1}H NMR** (400 MHz, $CDCl_3$) δ: 1.32 (s, 3H, ($O_2C(CH_3)_2$), 1.36 (s, 3H, $O_2C(CH_3)_2$), 1.37 (s, 3H, $O_2C(CH_3)_2$), 1.48 (s, 3H, $O_2C(CH_3)_2$), 3.43 (dd, *J*= 11.2, 7.6 Hz, 1H, 6-H), 3.60 (dd, *J*= 11.0, 3.4Hz, 1H, 6´-H), 3.73 (td, *J*= 7.2, 3.2Hz, 1H, 5-H), 4.22 (d, *J*= 4.4 Hz, 1H, 3-H), 4.31 (dd, *J*= 7.2, 4.0Hz, 1H, 4-H), 4.58 (d, *J*= 3.6 Hz, 1H, 2-H), 5.98 (d, *J*= 3.6 Hz, 1H, 1-H); **^{13}C NMR** (100.6 MHz, $CDCl_3$) δ: 23.9 ($O_2C(CH_3)_2$), 24.0 ($O_2C(CH_3)_2$), 26.6 ($O_2C(CH_3)_2$), 27.3 ($O_2C(CH_3)_2$), 33.1 (C-6), 72.0 (C-5), 75.2 (C-3), 81.7 (C-4), 84.0 (C-2), 101.5($O_2C(CH_3)_2$), 106.5 (C-1), 112.5 ($O_2C(CH_3)_2$). Anal. calcd for $C_{12}H_{19}BrO_5$ (323.18): C, 44.60; H, 5.93. Found: C, 44.28; H, 6.12.

6-hydroxy-1,2:3,5-di-*O*-isopropylidene-*α*-*D*-glucofuranoside (74). $NaNO_2$ (0.84g, 12.4 mmol) was added to a solution of compound **73** (2g, 6.2 mmol) in DMF (20 mL), and the mixture was stirred at 70ºC for 4h. The reaction was monitorized by TLC (1:1 hexane-EtOAc). The reaction was stopped and the residue was evaporated to dryness. Purification by flash chromatography (EtOAc/Hexane = 1/1, Rf= 0.40) gave **74** as a colorless oil (580mg, 36%). $[\alpha]^D_{25}$ = +29.49 $cm^3\ g^{-1}\ dm^{-1}$ (c = 1.0 g cm^{-3}, CH_2Cl_2). **^{1}H NMR** (400 MHz, $CDCl_3$) δ: 1.29 (s, 3H, $O_2C(CH_3)_2$), 1.33 (s, 6H, $O_2C(CH_3)_2$), 1.45 (s, 3H, $O_2C(CH_3)_2$), 3.63 (m, 2H, 5-H, 6´-H), 3.79 (dd, *J*= 11.6, 2.8Hz, 1H, 6-H), 4.15 (d, *J*= 3.6 Hz, 1H, 3-H), 4.33 (dd, *J*= 6.8, 3.6 Hz, 1H, 4-H), 4.54 (d, *J*= 4.0 Hz, 1H, 2-H), 5.95 (d, *J*= 4.0 Hz, 1H, 1-H); **^{13}C NMR** (100.6 MHz, $CDCl_3$) δ: 24.1($O_2C(CH_3)_2$), 24.2($O_2C(CH_3)_2$), 26.6($O_2C(CH_3)_2$), 27.2($O_2C(CH_3)_2$), 63.4(C-6), 72.6(C-5), 75.1(C-3), 79.1(C-4), 84.0(C-2), 101.0($O_2C(CH_3)_2$), 106.5 (C-1), 112.3 ($O_2C(CH_3)_2$).

Anal. calcd for $C_{12}H_{20}O_6$ (260.28): C, 55.37; H, 7.74. Found: C, 55.32; H, 7.80.

1,2:3,5-di-*O*-isopropylidene-6-O-butyl-*α*-*D*-glucofuranoside (75). NaH (320mg, 8.0 mmol) was added to a solution of **75** (520 mg, 2.0 mmol) in THF (15 mL) at room temperature. The reaction mixture was stirred at room temperature for 1h and butyl-bromide (308mg, 2.2 mmol) was added together with catalytic quantities of 18-crown-6 ether. The reaction mixture was stirred overnight at room temperature. The reaction was quenched by careful addition of H_2O. The aqueous layer was extracted with CH_2Cl_2 (3 × 50 mL). The combined organic phases were washed with brine and dried ($MgSO_4$) and evaporated to dryness. Purification by flash chromatography (EtOAc/Hexane = 1/3, Rf= 0.70) gave **75** as colorless oil (525 mg, 83 %). $[\alpha]^D_{25}$ = +18.68 $cm^3\ g^{-1}\ dm^{-1}$ (c = 1.0 g cm^{-3} , CH_2Cl_2). **^{1}H NMR** (400 MHz, $CDCl_3$) δ: 0.88 (t, *J*= 7.6Hz, 3H, $O(CH_2)_3CH_3$), 1.29 (s, 3H, $O_2C(CH_3)_2$), 1.33 (s, 3H, $O_2C(CH_3)_2$), 1.34 (m, 5H, $O_2C(CH_3)_2$, $O(CH_2)_3CH_3$), 1.45 (s, 3H, $O_2C(CH_3)_2$), 1.53 (m, 2H, $O(CH_2)_3CH_3$), 3.58 (m, 2H, $O(CH_2)_3CH_3$), 3.58 (m, 2H, 6-H, 6´-H), 3.68 (td, *J*= 6.8, 3.2Hz, 1H, 5-H), 4.17 (d, *J*= 3.6 Hz, 1H, 3-H), 4.30 (dd, *J*= 6.8, 3.6 Hz, 1H, 4-H), 4.54 (d, *J*= 3.6 Hz, 1H, 2-H), 5.95 (d, *J*= 3.6 Hz, 1H, 1-H); **^{13}C NMR** (100.6 MHz, $CDCl_3$) δ: 14.0($O(CH_2)_3CH_3$), 19.3($O(CH_2)_3CH_3$), 24.0($O_2C(CH_3)_2$), 24.1($O_2C(CH_3)_2$), 26.6($O_2C(CH_3)_2$), 27.2($O_2C(CH_3)_2$), 31.7($O(CH_2)_3CH_3$), 71.2(C-6), 71.4(C-5), 71.5($O(CH_2)_3CH_3$), 75.0(C-3), 79.6(C-4), 84.1(C-2), 101.0($O_2C(CH_3)_2$), 106.4 (C-1), 112.2 ($O_2C(CH_3)_2$). Anal. calcd for $C_{16}H_{28}O_6$ (316.39): C, 60.74; H, 8.92. Found: C, 60.68; H, 9.00.

1,2-*O*-isopropylidene-6-*O*-butyl-*α*-*D*-glucofuranoside (68). Compound **75** (700 mg, 2.2 mmol) was dissolved in AcOH/H_2O (65%, 10 mL), and the mixture was stirred at 40ºC for 10h. After cooling to room temperature, the solution was co-evaporated with EtOH and toluene at reduced pressure to afford **68** as a white powder (446 mg, 73 % yield). $[\alpha]^D_{25}$ = + 1.32 $cm^3\ g^{-1}\ dm^{-1}$ (c = 1.0 g cm^{-3}, CH_2Cl_2). **^{1}H NMR** (400 MHz, $CDCl_3$) δ: 0.91 (t, *J*= 7.4Hz, 3H, $O(CH_2)_3CH_3$), 1.30 (s, 3H, $O_2C(CH_3)_2$), 1.36 (s, 2H, $O(CH_2)_3CH_3$), 1.47 (s, 3H, $O_2C(CH_3)_2$), 1.56 (m, 2H, $O(CH_2)_3CH_3$), 3.50 (m, 2H, $O(CH_2)_3CH_3$), 3.55 (dd, *J*= 10.4, 4.4Hz, 1H, 6-H), 3.69 (dd, *J*= 10, 3.6Hz, 1H, 6´-H), 4.05 (dd, *J*= 6.8, 3.2Hz, 1H, 3-H),

4.15 (m, 1H, 5-H), 4.32 (d, *J*= 3.2Hz, 1H, 4-H), 4.52 (d, *J*= 3.6 Hz, 1H, 2-H), 5.95 (d, *J*= 4.0 Hz, 1H, 1-H); **^{13}C NMR** (100.6 MHz, $CDCl_3$) δ: 14.0($O(CH_2)_3CH_3$), 19.3($O(CH_2)_3CH_3$), 26.3($O_2C(CH_3)_2$), 26.9($O_2C(CH_3)_2$), 31.7($O(CH_2)_3CH_3$), 69.3(C-5), 71.6(C-6), 71.7($O(CH_2)_3CH_3$), 75.7(C-3), 80.0(C-4), 85.2(C-2), 105.0 (C-1), 111.8 ($O_2C(CH_3)_2$). Anal. calcd for $C_{13}H_{24}O_6$ (276.32): C, 56.51; H, 8.75. Found: C, 56.47; H, 8.80.

6-Deoxy-1,2:3,5-di-*O*-isopropylidene-*α*-*D*-glucofuranoside (76). To a solution of **73** (900 mg, 2.7 mmol) in THF (30 mL) $LiAlH_4$ (275mg, 7.0 mmol) was added. The mixture was stirred for 16 h at room temperature. The reaction was quenched by careful addition of EtOAc and NaOH 2.5 M (5 mL). The precipitated formed was removed by filtration. The aqueous layer was extracted with CH_2Cl_2 (3 × 50 mL), and the combined organic phases were washed with brine and dried over $MgSO_4$. Purification by flash chromatography (EtOAc/Hexane = 1/14, Rf= 0.25) gave **76** as a colorless oil (581 mg, 88 %). $[\alpha]^D_{25}$ = +34.43 $cm^3\ g^{-1}\ dm^{-1}$ (c = 1.0 g cm^{-3}, CH_2Cl_2). **^{1}H NMR** (400 MHz, $CDCl_3$) δ: 1.28 (s, 3H, $O_2C(CH_3)_2$), 1.30 (s, 6H, $O_2C(CH_3)_2$), 1.31 (d, $_J$= 4.0Hz, 3H, 6-H), 1.46 (s, 3H, $O_2C(CH_3)_2$), 3.61 (m, 1 H, 5-H), 4.18 (dd, *J*= 7.2, 3.6Hz, 1H, 3-H), 4.17 (d, *J*= 3.6Hz, 1H, 4-H), 4.55 (d, *J*= 4.0Hz, 1H, 2-H), 5.96 (d, *J*= 3.6Hz, 1H, 1-H); **^{13}C NMR** (100.6 MHz, $CDCl_3$) δ: 19.7 (C-6), 24.2 ($O_2C(CH_3)_2$), 24.3 ($O_2C(CH_3)_2$), 26.7 ($O_2C(CH_3)_2$), 27.3 ($O_2C(CH_3)_2$), 68.0 (C-5), 74.9 (C-3), 84.3 (C-4), 85.0 (C-2), 100.7($O_2C(CH_3)_2$), 106.4 (C-1), 112.2 ($O_2C(CH_3)_2$) Anal. calcd for $C_{12}H_{20}O_5$ (244.28): C, 59.00; H, 8.25. Found: C, 58.76; H, 8.50.

6-Deoxy-1,2-O-isopropylidene-*α*-*D*-glucofuranoside (13). Compound **76** (1.0 g, 4.1 mmol) was dissolved in AcOH/H_2O (65%, 5 mL), and the mixture was stirred at 40 ºC for 10h. After cooling to room temperature, the solution was co-evaporated with EtOH and toluene at reduced pressure, and the residue was purified by flash chromatography (EtOAc/hexane = 1/1, Rf= 0.1) to afford **13** as a colorless oil (829 mg, 99 % yield). $[\alpha]^D_{25}$ = −10.43 $cm^3\ g^{-1}\ dm^{-1}$ (c = 1.0 g cm^{-3}, CH_2Cl_2). **^{1}H NMR** (400 MHz, $CDCl_3$) δ: 1.31 (s, 3H, $O_2C(CH_3)_2$), 1.37 (d, *J*= 6.0Hz, 3H, 6-H), 1.48 (s, 3H, $O_2C(CH_3)_2$), 3.93 (m, 1 H, 5-H), 4.31 (m, 1H, 3-H), 4.36 (d, *J*= 2.0Hz, 1H, 4-H), 4.52 (d, *J*= 3.6Hz, 1H, 2-H), 5.97 (d, 1H, *J*= 3.6 Hz, H-1); **^{13}C NMR** (100.6 MHz, $CDCl_3$) δ: 18.7 (C-6), 26.3 ($O_2C(CH_3)_2$), 26.9 ($O_2C(CH_3)_2$),

67.4 (C-5), 75.6 (C-3), 82.0 (C-4), 85.4 (C-2), 105.0 (C-1), 111.9 ($O_2C(CH_3)_2$). Anal. calcd for $C_9H_{16}O_5$ (204.22) C, 52.90; H, 7.90. Found: C, 52.70; H, 8.02.

General procedure for the benzylation of 2 and 13. NaH (653 mg, 16.0 mmol) was added to a solution of diol **2**, **13** (4.0 mmol) in THF (30 mL) at room temperature. After, the reaction was stirred for 1h at room temperature. Benzyl bromide (1.94 mL, 16 mmol) was then added and the reaction mixture was stirred for 16 h at room temperature. The reaction was quenched by careful addition of H_2O. The aqueous layer was extracted with CH_2Cl_2 (3 × 50 mL), and the combined organic phases was washed with brine and dried over $MgSO_4$. Purification by flash chromatography gave the corresponding benzylated products **77**, **78**.

3,5-Di-*O*-benzyl-1,2-isopropylidene-α-*D*-xylofuranoside (77). The synthesis of compound **77** was completed according to the general procedure previously described. The product was isolated as a colorless oil in 85% yield (1.26g) after purification using the eluent system EtOAc/Hexane = 1/8 (Rf = 0.34). $[\alpha]^D_{25}$ = − 4.45 $cm^3\ g^{-1}\ dm^{-1}$ (c = 1.0 g cm^{-3}, CH_2Cl_2). **^{1}H NMR** (400 MHz, $CDCl_3$) δ: 1.33 (s, 3H, $O_2C(CH_3)_2$), 1.50 (s, 3H, $O_2C(CH_3)_2$), 3.77 (m, 2H, 5,5´-H), 3.99 (d, *J*= 3.2 Hz, 1H, 3-H), 4.41 (dt, *J*= 6.8, 2.8Hz, 1H, 4-H), 4.52 (m, 2H, OCH_2Ph), 4.62 (m, 3H, 2-H, OCH_2Ph), 5.95 (d, J= 3.6 Hz, 1H, 1-H), 7.32 (m, 10H, Aromatic); **^{13}C NMR** (100.6 MHz, $CDCl_3$) δ: 26.5 ($O_2C(CH_3)_2$), 27.0 ($O_2C(CH_3)_2$), 67.7 (C-5), 72.2 (OCH_2Ph), 73.7 (OCH_2Ph), 79.4 (C-4), 81.9 (C-3), 82.6 (C-2), 105.3 (C-1), 111.9 ($O_2C(CH_3)_2$), 127.8-128.6 (Aromatic), 137.7 (Aromatic), 138.2 (Aromatic). Anal. calcd for $C_{22}H_{26}O_5$ (370.44): C, 71.33; H, 7.07. Found: C, 70.98; H, 7.25.

3,5-Di-*O*-benzyl-6-deoxy-1,2-isopropylidene-α-*D*-glucofuranoside (78). The synthesis of compound **78** was completed according to the general procedure previously described. The product was isolated as a colorless oil in 60% yield (923 mg, 2.4 mmol) after purification using the eluent system EtOAc/Hexane = 1/8 (Rf = 0.30). $[\alpha]^D_{25}$ = − 26.83 $cm^3\ g^{-1}\ dm^{-1}$ (c = 1.0 g cm^{-3}, CH_2Cl_2). **^{1}H NMR** (400 MHz, $CDCl_3$) δ: 1.35 (s, 3H, $O_2C(CH_3)_2$), 1.41 (d, *J* = 6.0 Hz, 3H, 6-H), 1.53 (s, 3H, $O_2C(CH_3)_2$), 4.02

(m, 1H, 5-H), 4.10 (dd, *J* = 9.0, 3.0 Hz, 1H, 3-H), 4.15 (d, *J*= 2.8Hz, 1H, 4-H), 4.48 (m, 2H, OCH_2Ph), 4.66 (b, 3H, 2-H, OCH_2Ph), 5.95 (d, *J*= 3.6 Hz, 1H, 1-H), 7.30 (m, 10H, Aromatic); **^{13}C NMR** (100.6 MHz, $CDCl_3$) δ: 17.4 (C-6), 26.4 ($O_2C(CH_3)_2$), 26.9 ($O_2C(CH_3)_2$), 70.9 (C-5), 72.1 (OCH_2Ph), 72.2 (OCH_2Ph), 81.6 (C-4), 82.3 (C-2), 83.4 (C-3), 105.0 (C-1), 111.7 ($O_2C(CH_3)_2$), 127.6-128.5 (Aromatic), 137.8 (Aromatic), 138.7 (Aromatic). Anal. calcd for $C_{23}H_{28}O_5$ (384.47): C, 71.85; H, 7.34. Found: C, 71.58; H, 7.47.

General procedure for deprotection/reduction of 1,2-O-isopropylidene-furanosides. To a solution of starting material **77**, **78** (2.0 mmol) in CH_2Cl2 (15 mL) cooled at 0ºC Et_3SiH (1.5 mL, 9.2 mmol) and BF_3•Et_2O (1.2 mL, 9.4 mmol) were added. The reaction mixture was stirred at room temperature for 2h. The reaction was quenched by careful addition of saturated $NaHCO_3$/H2O (15 mL) and CH_2Cl_2 (40 mL). The aqueous layer was extracted with CH_2Cl_2 (3 × 50 mL), and the combined organic phases were washed with brine and dried over $MgSO_4$. Purification by flash chromatography gave the corresponding alcohols **79**, **80**.

1,4-Anhydro-3,5-di-*O*-benzyl-*D*-xylitol (79). The synthesis of compound **79** was completed according to the general procedure previously described. The product was isolated as a white solid in 86% yield (541 mg, 1.72 mmol) after purification using the eluent system EtOAc/Hexane = 1/4, (Rf = 0.30). $[\alpha]^D_{25}$ = − 11.09 cm^3 g^{-1} dm^{-1} (c = 1.0 g cm^{-3}, CH_2Cl_2). **^{1}H NMR** (400 MHz, $CDCl_3$) δ: 3.74 (m, 3H, 1´-H, 5,5´-H), 3.94 (d, *J* = 4.0Hz, 1H, 2-H), 4.19 (dd, *J* = 9.6, 4.4Hz, 1H, 1-H), 4.32 (m, 1H, 4-H), 4.37 (m, 1H, 3-H), 4.55 (m, 2H, OCH_2Ph), 4.64 (m, 2H, OCH_2Ph), 7.30 (m, 10H, Aromatic); **^{13}C NMR** (100.6 MHz, $CDCl_3$) δ: 69.0 (C-5), 72.8 (C-1), 74.0 (OCH_2Ph), 74.1 (OCH_2Ph), 75.6 (C-3), 79.7 (C-4), 84.8 (C-2), 129.0-128.0 (Aromatic), 138.1 (Aromatic), 138.5 (Aromatic). Anal. calcd for $C_{19}H_{22}O_4$ (314.38): C, 72.59; H, 7.05. Found: C, 72.42; H, 7.40.

1,4-Anhydro-3,5-di-*O*-benzyl-6-deoxy-*D*-glucitol (80). The synthesis of compound **80** was completed according to the general procedure previously described. The product was isolated as a white solid in 70% yield (460 mg, 1.40 mmol) after purification using the eluent system

EtOAc/Hexane = 1/3, (Rf = 0.20). $[\alpha]^{D}_{25}$ = − 19.04 $cm^3\ g^{-1}\ dm^{-1}$ (c = 1.0 g cm^{-3}, CH_2Cl_2). **^{1}H NMR** (400 MHz, $CDCl_3$) δ: 1.62 (d, *J* = 4.8 Hz, 3H, 6-H), 3.95 (m, 1H, 5-H), 4.19 (m, 2H, 1,1´-H), 4.34 (dd, J = 6.6, 3.9 Hz, 1H, 4-H), 4.48 (d, J = 3.6 Hz, 1H, 3-H), 4.63 (m, 2H, OCH_2Ph), 4.75 (m, 1H, 2-H), 4.85 (m, 2H, OCH_2Ph), 7.54 (m, 10H, Ph); **^{13}C NMR** (100.6 MHz, $CDCl_3$) δ: 17.4 (C-6), 70.9 (C-5), 72.1 (OCH_2Ph), 72.9 (OCH_2Ph), 73.9 (C-1), 74.3 (C-3), 83.3 (C-4), 83.8 (C-2), 127.5-128.5 (Aromatic), 138.2 (Aromatic), 138.7 (Aromatic). Anal. calcd for $C_{20}H_{28}O_4$ (332.43): C, 73.15; H, 7.37. Found: C, 72.89; H, 7.70.

General procedure of etherification of 1,4-anhydro-3,5-di-O-benzyl-alditols. To a solution of starting material **79**, **80** (2.0 mmol) in THF (15 mL) at room temperature NaH (320mg, 8.0 mmol) was added. The reaction mixture was stirred at room temperature for 1h and the corresponding alkyl-bromide (2.2 mmol) was added together with catalytic quantities of 18-crown-6 ether. The reaction mixture was stirred overnight at room temperature. The reaction was quenched by careful addition of H_2O. The aqueous layer was extracted with CH_2Cl_2 (3 × 50 mL), and the combined organic phases were washed with brine and dried with $MgSO_4$. Purification by flash chromatography gave the corresponding products **81**, **82** and **83**.

1,4-Anhydro-2-*O*-butyl-3,5-di-*O*-benzyl-*D*-xylitol (81). The synthesis of compound **81** was completed according to the general procedure previously described. The product was isolated as a colorless syrup in 90% yield (667 mg, 1.80 mmol) after purification using the eluent system EtOAc/Hexane = 1/8 (Rf = 0.30). $[\alpha]^{D}_{25}$ = − 2.55 $cm^3\ g^{-1}\ dm^{-1}$ (c = 1.0 g cm^{-3}, CH_2Cl_2). **^{1}H NMR** (400 MHz, $CDCl_3$) δ: 0.98(t, *J*= 7.2Hz, 3H, $O(CH_2)_3CH_3$), 1.40(m, 2H, $O(CH_2)_3CH_3$), 1.58 (m, 2H, $O(CH_2)_3CH_3$), 3.43(t, *J* = 6.6 Hz, 2H, $O(CH_2)_3CH3$), 3.81(m, 3H, 1´-H, 5,5´-H), 4.01(m, 2H, 2-H, 3-H), 4.23 (m, 2H, 1-H, 4-H), 4.57(m, 2H, OCH_2Ph), 4.67(m, 1H, OCH_2Ph), 7.35(m, 10H, Aromatic); **^{13}C NMR** (100.6 MHz, $CDCl_3$) δ: 13.1 ($O(CH_2)_3CH_3$), 19.4 ($O(CH_2)_3CH_3$), 32.0 ($O(CH_2)_3CH_3$), 68.7 (C-5), 69.6 ($O(CH_2)_3CH_3$), 71.9 (C-1), 74.0(OCH_2Ph), 74.1(OCH_2Ph), 75.6(C-3), 79.7(C-4), 82.9(C-2), 128.7-127.8(Aromatic), 138.1 (Aromatic), 138.5 (Aromatic). Anal. calcd for $C_{23}H_{30}O_4$ (370.48): C, 74.56; H, 8.16. Found: C, 74.31; H, 8.35.

1,4-Anhydro-3,5-di-*O*-benzyl-2-*O*-tetradecyl-*D*-xylitol (82). The synthesis of compound **82** was completed according to the general procedure previously described. The product was isolated as a colorless syrup in 77% yield (812 mg, 1.54 mmol) after purification using the eluent system EtOAc/Hexane = 1/8 (Rf = 0.37). $[\alpha]^{D}_{25}$ = − 0.94 $cm^3\ g^{-1}\ dm^{-1}$ (c = 1.0 g cm^{-3}, CH_2Cl_2). **^{1}H NMR** (400 MHz, $CDCl_3$) δ: 0.91 (t, J= 9.2Hz, 3H, O(CH2)13CH3), 1.29 (s, 22H, $O(CH_2)_{13}CH_3$), 1.54 (m, 2H, $O(CH_2)_{13}CH_3$), 3.43 (t, *J* = 6.6 Hz, 2H, $O(CH_2)_{13}CH_3$), 3.80 (m, 3H, 1´-H, 5,5´-H), 4.01 (m, 2H, 2-H, 3-H), 4.23 (m, 2H, 1-H, 4-H), 4.59 (m, 2H, OCH_2Ph), 4.69 (m, 2H, OCH_2Ph), 7.37 (m, 10H, Aromatic); **^{13}C NMR** (100.6 MHz, $CDCl_3$) δ: 14.3 ($O(CH_2)_{13}CH_3$), 22.9 ($O(CH_2)_{13}CH_3$), 26.3 ($O(CH_2)_{13}CH_3$), 30.0-29.6 (9×CH_2, $O(CH_2)_{13}CH_3$), 32.1 ($O(CH_2)_{13}CH_3$), 68.7 (C-5), 69.9 ($O(CH_2)_{13}CH_3$), 71.9 (C-1), 74.0(OCH_2Ph), 74.1(OCH_2Ph), 79.7(C-3), 82.2(C-4), 82.9(C-2), 128.6-127.8(Aromatic), 138.2 (Aromatic), 138.5 (Aromatic). Anal. calcd for $C_{33}H_{50}O_4$ (510.75): C, 77.60; H, 9.81. Found: C, 77.2; H, 10.9.

1,4-Anhydro-3,5-di-*O*-benzyl-2-*O*-hexadecyl-*D*-glucitol (83). The synthesis of compound **83** was completed according to the general procedure previously described. The product was isolated as a colorless syrup in 79% yield (797 mg, 1.40 mmol) after purification using the eluent system EtOAc/Hexane = 1/14 (Rf = 0.40). $[\alpha]^{D}_{25}$ = − 12.79 $cm^3\ g^{-1}\ dm^{-1}$ (c = 1.0 g cm^{-3}, CH_2Cl_2). **^{1}H NMR** (400 MHz, $CDCl_3$) δ: 0.89 (t, *J*= 6.8Hz, 3H, O(CH2)15CH3), 1.27 (s, 26H, $O(CH_2)_{15}CH_3$), 1.36 (d, *J*= 6.0Hz, 3H, 6-H), 1.52 (m, 2H, $O(CH_2)_{15}CH_3$), 3.36 (m, 2H, $O(CH_2)_{15}CH_3$), 3.75 (dd, *J*= 10, 1.6Hz, 1H, 5-H), 3.82 (dd, *J*= 8.6, 3.4Hz, 1H, 1´-H), 3.93 (m, 2H, 2-H, 1-H), 4.07 (d, *J*= 3.6Hz, 1H, 3-H), 4.13 (dd, *J*= 9.8, 4.6Hz, 1H, 4-H), 4.42 (m, 2H, OCH_2Ph), 4.60 (m, 2H, OCH_2Ph), 7.30(m, 10H, Ph); **^{13}C NMR** (100.6 MHz, $CDCl_3$) δ: 14.7 ($O(CH_2)_{15}CH_3$), 17.8 (C-6), 23.2($O(CH_2)_{15}CH_3$), 26.6($O(CH_2)_{15}CH_3$), 30.2-29.9 (11×CH_2, $O(CH_2)_{13}CH_3$), 32.4($O(CH_2)_{13}CH_3$), 70.1 (C-5), 71.1 ($O(CH_2)_{15}CH_3$), 72.4 (C-1), 72.5(OCH_2Ph), 73.0(OCH_2Ph), 81.7(C-3), 82.9(C-4), 84.3(C-2), 128.8-127.8(Aromatic), 138.6 (Aromatic), 139.3 (Aromatic). Anal. calcd for $C_{37}H_{60}O_4$ (568.87): C, 78.12; H, 10.63. Found: C, 77.88; H, 10.50.

General procedure for removing benzyl groups of the 1,4-anhydro-3,5-di-O-benzyl-2-alkyl-alditols. To a solution of **81**, **82**, **83** (5 mmol) in THF (15 mL) was added a catalytic amount of Pd/C (0.5 mmol). The reaction mixture was stirred for 12 h over 1 atm. H_2 pressure. The H_2 pressure was removed. The mixture was filtered though celite to obtain the corresponding diols **84**, **85**, **71**.

1,4-Anhydro-2-*O*-butyl-*D*-xylitol (84). The synthesis of compound **84** was completed according to the general procedure previously described. The product was isolated as a white solid in 93% yield (885 mg, 4.65 mmol). $[\alpha]^{D}_{25}$ = − 8.74 cm^3 g^{-1} dm^{-1} (c = 1.0 g cm^{-3}, CH_2Cl_2). **^{1}H NMR** (400 MHz, $CDCl_3$) δ: 0.89(t, *J*= 6.0Hz, 3H, $O(CH_2)_3CH_3$), 1.40 (m, 2H, $O(CH_2)_3CH_3$), 1.55 (m, 2H, $O(CH_2)_3CH_3$), 3.48 (m, 2H, $O(CH_2)_3CH_3$), 3.79 (dd, *J*= 10.0, 2.4 Hz, 1H, 1´-H), 3.88 (dd, *J*= 4.4, 2.0 Hz, 1H, 2-H), 3.95 (d, *J*= 2.8 Hz, 1H, 4-H), 4.00 (m, 1H, 5´-H), 4.05 (m, 1H, 5-H), 4.19 (dd, *J*= 10, 2.4 Hz, 1H, 1-H), 4.29 (m, 1H, 3-H); **^{13}C NMR** (100.6 MHz, $CDCl_3$) δ: 13.1 ($O(CH_2)_3CH_3$), 19.4 ($O(CH_2)_3CH_3$), 32.0 ($O(CH_2)3CH_3$), 60.5 (C-5), 70.5 ($O(CH_2)_3CH_3$), 72.3 (C-1), 77.7(C-3), 79.4(C-4), 86.3(C-2). Anal. calcd for $C_9H_{18}O_4$ (190.24): C, 56.82; H, 9.54. Found: C, 56.57; H, 9.80.

1,4-Anhydro-2-O-tetradecyl-D-xylitol (85). The synthesis of compound **85** was completed according to the general procedure previously described. The product was isolated as a white solid in 99% yield (1.64 g, 4.95 mmol). $[\alpha]^{D}_{25}$ = − 2.07 cm^3 g^{-1} dm^{-1} (c = 1.0 g cm^{-3}, CH_2Cl_2). **^{1}H NMR** (400 MHz, $CDCl_3$) δ: 0.89 (t, *J*= 6.0Hz, 3H, O(CH2)13CH3), 1.25 (s, 22H, $O(CH_2)_{13}CH_3$), 1.58(m, 2H, $O(CH_2)_{13}CH_3$), 3.48 (m, 2H, , $O(CH_2)_{13}CH_3$), 3.79 (dd, *J*= 9.2, 2.0Hz, 1H, 1´-H), 3.90 (m, 1H, 2-H), 3.98 (m, 1H, 4-H), 4.02 (m, 1H, 5-H), 4.10 (m, 1H, 5´-H), 4.20 (dd, *J*= 10.0, 4.8 Hz, 1H, 1-H), 4.31 (m, 1H, 3-H); **^{13}C NMR** (100.6 MHz, $CDCl_3$) δ: 14.7 ($O(CH_2)_{13}CH_3$), 23.2 ($O(CH_2)_{13}CH_3$), 26.6 ($O(CH_2)_{13}CH_3$), 30.3-29.9 (9×CH_2, $O(CH_2)_{13}CH_3$), 32.5 ($O(CH_2)_{13}CH_3$), 62.3 (C-5), 70.5 ($O(CH_2)_{13}CH_3$), 72.3 (C-1), 77.7(C-3), 79.4(C-4), 86.2(C-2). Anal. calcd for $C_{19}H_{38}O_4$ (330.50): C, 69.05; H, 11.59. Found: C, 68.78; H, 11.78.

1,4-Anhydro-2-O-hexadecyl-D-glucitol (71). The synthesis of compound **71** was completed according to the general procedure previously

described. The product was isolated as a white powder in 86% yield (1.60 g, 4.30 mmol). $[\alpha]^{D}_{25}$ = − 16.59 $cm^3\ g^{-1}\ dm^{-1}$ (c = 1.0 g cm^{-3}, CH_2Cl_2). **^{1}H NMR** (400 MHz, $CDCl_3$) δ: 0.88(t, J= 6.8Hz, 3H, $O(CH_2)_{15}CH_3$), 1.26 (s, 26H, $O(CH_2)_{15}CH_3$) 1.39(d, *J*= 6.4Hz, 3H, 6-H), 1.55 (m, 2H, $O(CH_2)_{15}CH_3$), 3.48 (m, 2H, $O(CH_2)_{15}CH_3$), 3.75(dd, *J*= 3.8Hz, 1H, 4-H), 3.82(dd, *J*= 9.4, 1.4Hz, 1H, 1´-H), 3.89(d, *J*= 4.4Hz, 1H, 2-H), 4.23(dd, *J*= 9.6, 4Hz, 1H, 1-H), 4.28(dd, *J*= 7.0, 4.2Hz, 1H, 5-H), 4.33(d, *J*= 2.4Hz, 1H, 3-H); **^{13}C NMR** (100.6 MHz, $CDCl_3$) δ: 14.7 ($O(CH_2)_{15}CH_3$), 18.3 (C-6), 22.3($O(CH_2)_{15}CH_3$), 26.0 ($O(CH_2)_{15}CH_3$), 30.2-29.7 (11×CH_2, $O(CH_2)_{15}CH_3$), 31.8, 67.8 (C-5), 69.7 ($O(CH_2)_{15}CH_3$), 71.9 (C-1), 75.1 (C-3), 82.3(C-4), 85.1(C-2). Anal. calcd for $C_{22}H_{44}O_4$ (372.58): C, 70.92; H, 11.90. Found: C, 70.65; H, 12.03.

General procedure for synthesizing diphosphite ligands. A solution of the diol **2**, **13**, **68**, **69**, **70**, **71**, **84** and **85** (1.0 mmol), previously azeotropically dried with toluene (3 × 1 mL), in dry and degassed toluene (10 mL) and cooled to 0 ºC, was slowly added to a solution of phosphorochloridites **a**, **b** or **w**(2.1 mmol), synthesized in situ by standard procedures, in dry and degassed pyridine (1.5 mL). The mixture was allowed to rise to room temperature and stirred for 16 h. The mixture was then filtered to remove the pyridine salts, and the filtrate was concentrated to dryness. The white foam obtained was purified by flash chromatography under nitrogen atmosphere.

3,5-Bis-*O*-[(3,3'-di-tert-butyl-5,5'-dimethoxy-1,1'-biphenyl-2,2'-diyl)phosphite]-1,2-*O*-isopropyliden-*α*-*D*-xylofuranose (21a). The synthesis of diphosphite **21a** was completed according to the general procedure previously described. The product was purified by flash column chromatography (toluene/THF= 98/2, Rf= 0.35) to afford **21a** as a white solid, 20 % yield (193 mg, 0.2 mmol). $[\alpha]^{D}_{25}$ = + 77.88 $cm^3\ g^{-1}\ dm^{-1}$ (c = 1.0 g cm^{-3}, CH_2Cl_2). **^{1}H NMR** (400 MHz, $CDCl_3$) δ: 1.14 (s, 3H, $O_2C(CH_3)_2$), 1.16 (s, 3H, $O_2C(CH_3)_2$), 1.44 (4xs, 36H, *o*$C(CH_3)_3$), 3.82-3.80 (2xs, 16H, *p*OCH_3), 3.94 (m, 1H, 2-H), 4.07 (m, 2H, 5,5´-H), 4.31 (dt, *J*= 6.8, 2.4 Hz, 1H, 4-H), 4.77 (dd, *J*= 8.4, 2.4 Hz, 1H, 3-H), 5.60 (d, *J*= 3.6 Hz, 1H, 1-H), 7.30-6.70 (m, 8H, Aromatic). **^{13}C NMR** (100.6 MHz, $CDCl_3$) δ: 26.1 ($O_2C(CH_3)_2$), 26.8 ($O_2C(CH_3)_2$), 31.2 (*o*$C(CH_3)_3$), 35.6 (*o*$C(CH_3)_3$), 55.8

(*p*OCH_3), 61.8 (C-5), 79.0 (C-3), 81.4 (C-4), 84.2 (C-2), 105.0 (C-1), 111.9 ($O_2C(CH_3)_2$), 156.0-113.0 (aromatic). **^{31}P NMR** (161.97 MHz, $CDCl_3$) δ: 134.8 (s), 143.4 (s). Anal. calcd for $C_{52}H_{68}O_{13}P_2$ (963.04): C, 64.85; H, 7.12. Found: C, 64.4; H, 7.3.

3,5-Bis-*O*-[(3,3'-5,5´-tetra-tert-butyl-1,1'-biphenyl-2,2'-diyl)phosphite]-1,2-*O*-isopropyliden-α-*D*-xylofuranose (21b). The synthesis of diphosphite **21b** was completed according to the general procedure previously described. The product was isolated as a white solid in 75 % yield (800 mg, 0.75 mmol) after purification by flash column chromatography (toluene, Rf= 0.70). $[\alpha]^D_{25}$ = + 78.33 $cm^3\ g^{-1}\ dm^{-1}$ (c = 1.0 g cm^{-3}, CH_2Cl_2). **^{1}H NMR** (400 MHz, $CDCl_3$) δ: 1.10 (s, 6H, $O_2C(CH_3)_2$), 1.48-1.35 (m, 72H, $C(CH_3)_3$), 3.95 (m, 1H, 2-H), 4.01 (m, 2H, 5,5´-H), 4.27 (dt, *J*= 5.6, 2.4 Hz, 1H, 4-H), 4.77 (dd, *J*= 7.2, 2.4 Hz, 1H, 3-H), 5.60 (d, *J*= 3.6 Hz, 1H, 1-H), 7.30-6.70 (m, 8H, Aromatic). **^{13}C NMR** (100.6 MHz, $CDCl_3$) δ : 27.0 ($O_2C(CH_3)_2$), 27.2 ($O_2C(CH_3)_2$), 32.1-31.6 ($C(CH_3)_3$), 36.0-35.2 ($C(CH_3)_3$), 62.8 (C-5), 77.0 (C-3), 79.5 (C-4), 84.8 (C-2), 106.0 (C-1), 112.3 ($O_2C(CH_3)_2$), 148.0-124.0 (Aromatic). **^{31}P NMR** (161.97 MHz, $CDCl_3$) δ: 134.8 (s), 143.3 (s). Anal. calcd for $C_{64}H_{92}O_9P_2$ (1067.35): C, 72.02; H, 8.69. Found: C, 70.9; H, 9.3.

3,5-Bis-*O*-[4,8-di-tert-butyl-2,10-di-metyl-12H-dibenzo[δ,γ][1,2,3]dioxa- phosphorcine]-1,2-*O*-isopropyliden-α-*D*-xylofuranose (21w). The synthesis of diphosphite **21w** was completed according to the general procedure previously described. The product was isolated as a white solid in 65 % yield (603 mg, 0.65 mmol) after purification by flash column chromatography (toluene, Rf= 0.60). $[\alpha]^D_{25}$ = − 2.08 $cm^3\ g^{-1}\ dm^{-1}$ (c = 1.0 g cm^{-3}, CH_2Cl_2). **^{1}H NMR** (400 MHz, $CDCl_3$) δ: 1.50 (s, 3H, $O_2C(CH_3)_2$), 1.58 (4xs, 36H, *o*C(CH3)3), 1.73 (s, 3H, $O_2C(CH_3)_2$), 2.45 (2xs, 12H, *p*CH_3), 3.53 (dd, *J*= 12.8, 5.6Hz, 2H, $PhCH_2Ph$), 4.53 (m, 2H, $PhCH_2Ph$), 5.04 (m, 3H, 4-H, 5,5´-H), 5.63 (d, *J*=2.4Hz, 1H, 2-H), 5.79 (d, *J*= 6.0Hz, 1H, 3-H), 6.31 (d, *J*= 3.6 Hz, 1H, 1-H), 7.41-7.16 (m, 8H, Aromatic). **^{13}C NMR** (100.6 MHz, $CDCl_3$) δ: 21.4 (*p*CH_3), 26.6 ($O_2C(CH_3)_2$), 27.0 ($O_2C(CH_3)_2$), 31.1 (*o*$C(CH_3)_3$), 34.9 ($PhCH_2Ph$), 61.6 (C-5), 77.3 (C-3), 80.4 (C-4), 84.3 (C-2), 105.3 (C-1), 112.3 ($O_2C(CH_3)_2$), 146.0-125.4 (Aromatic). **^{31}P NMR** (161.97 MHz, $CDCl_3$)

δ: 129.2 (s), 132.1 (s). Anal. calcd for $C_{54}H_{72}O_9P_2$ (927.09): C, 69.96; H, 7.83. Found: C, 69.67; H, 8.01.

3,5-Bis-*O*-[(3,3'-di-tert-butyl-5,5'-dimethoxy-1,1'-biphenyl-2,2'-diyl)phosphite]-6-deoxy-1,2-*O*-isopropyliden-*α*-*D*-glucofuranoside (23a). The synthesis of diphosphite **23a** was completed according to the general procedure previously described. The product was isolated as a white solid in 50 % yield (489 mg, 0.5 mmol) after purification by flash column chromatography (toluene/THF= 99/1, Rf= 0.25). $[\alpha]^D_{25}$ = + 110.12 $cm^3\ g^{-1}\ dm^{-1}$ (c = 1.0 g cm^{-3}, CH_2Cl_2). **^{1}H NMR** (400 MHz, $CDCl_3$) δ: 1.13 (s, 3H, $O_2C(CH_3)_2$), 1.30 (d, *J*= 6.4Hz, 3H, 6-H), 1.47-1.42 (s, 39H, *o*$C(CH_3)_3$, $O_2C(CH_3)_2$), 3.80 (s, 12H, *p*OCH_3), 3.97 (d, *J*= 3.6Hz, 1H, 2-H), 4.05 (dd, *J*= 8.2, 2.6Hz, 1H, 4-H), 4.73 (m, 1H, 5-H), 4.82 (d, *J*= 2.8Hz, 1H, 3-H), 5.59 (d, *J*= 3.2Hz, 1H, 1-H), 6.99-6.70 (m, 8H, Aromatic). **^{13}C NMR** (100.6 MHz, $CDCl_3$) δ: 20.1 (C-6), 26.0 ($O_2C(CH_3)_2$), 26.7 ($O_2C(CH_3)_2$), 31.3-29.7 (*o*$C(CH_3)_3$), 35.6-35.4 (*o*$C(CH_3)_3$), 55.8 (*p*OCH_3), 68.9 (C-5), 76.3 (C-3), 83.2 (C-4), 84.2 (C-2), 104.9 (C-1), 111.7($O_2C(CH_3)_2$), 156.3-113.2 (Aromatic). **^{31}P NMR** (161.97 MHz, $CDCl_3$) δ: 144.8 (s, 2P) (**^{31}P NMR** (161.97 MHz, toluene-d_8) δ:144.8 (d, *J*= 35.3 Hz), 145.3 (d, *J*= 35.3 Hz)). Anal. calcd for $C_{53}H_{70}O_{13}P_2$ (977.06): C, 65.15; H, 7.22. Found: C, 64.95; H, 7.45.

3,5-Bis-*O*-[(3,3'-5,5´-tetra-tert-butyl-1,1'-biphenyl-2,2'-diyl)phosphite]-6-deoxy-1,2-*O*-isopropyliden-*α*-*D*-glucofuranose (23b). The synthesis of diphosphite **23b** was completed according to the general procedure previously described. The product was isolated as a white solid in 58 % yield (628 mg, 0.58 mmol) after purification by flash column chromatography (toluene, Rf= 0.63). $[\alpha]^D_{25}$ = + 117.36 $cm^3\ g^{-1}\ dm^{-1}$ (c = 1.0 g cm^{-3}, CH_2Cl_2). **^{1}H NMR** (400 MHz, $CDCl_3$) δ: 1.10 (s, 3H, $O_2C(CH_3)_2$), 1.18 (d, *J*= 6.0Hz, 3H, 6-H), 1.48-1.32 (s, 75H, $C(CH_3)_3$, $O_2C(CH_3)_2$), 4.07 (m, 1H, 2-H), 4.75 (dd, *J*= 8.2, 2.6Hz, 1H, 4-H), 4.73 (m, 1H, 5-H), 4.81 (dd, *J*= 6.4, 2.4 Hz, 1H, 3-H), 5.48(d, *J*= 3.6Hz, 1H, 1-H), 7.45-7.16 (m, 8H, Aromatic). **^{13}C NMR** (100.6 MHz, $CDCl_3$) δ : 19.4 (C-6), 26.3 ($O_2C(CH_3)_2$), 26.7 ($O_2C(CH_3)_2$), 31.5-31.2 ($C(CH_3)_3$), 35.4-34.6 ($C(CH_3)_3$), 68.9 (C-5), 76.2 (C-3), 83.0 (C-4), 84.2 (C-2), 104.7 (C-1), 111.6($O_2C(CH_3)_2$), 146.8-124.0 (Aromatic). **^{31}P NMR** (161.97 MHz, $CDCl_3$)

δ: 144.4(d, *J*= 34.0 Hz), 145.6 (d, *J*= 35.3 Hz). Anal. calcd for $C_{65}H_{94}O_9P_2$ (1081.39): C, 72.19; H, 8.76. Found: C, 72.00; H, 8.95.

3,5-Bis-*O*-[(3,3'-5,5´-tetra-tert-butyl-1,1'-biphenyl-2,2'-diyl)phosphite]-6-deoxy-1,2-*O*-isopropyliden-*α*-*D*-glucofuranose (23b). The synthesis of diphosphite **23b** was completed according to the general procedure previously described. The product was isolated as a white solid in 58 % yield (628 mg, 0.58 mmol) after purification by flash column chromatography (toluene, Rf= 0.63). $[\alpha]^D_{25}$ = + 117.36 $cm^3\ g^{-1}\ dm^{-1}$ (c = 1.0 g cm^{-3}, CH_2Cl_2). **^{1}H NMR** (400 MHz, $CDCl_3$) δ: 1.10 (s, 3H, $O_2C(CH_3)_2$), 1.18 (d, *J*= 6.0Hz, 3H, 6-H), 1.48-1.32 (s, 75H, $C(CH_3)_3$, $O_2C(CH_3)_2$), 4.07 (m, 1H, 2-H), 4.75 (dd, *J*= 8.2, 2.6Hz, 1H, 4-H), 4.73 (m, 1H, 5-H), 4.81 (dd, *J*= 6.4, 2.4 Hz, 1H, 3-H), 5.48(d, *J*= 3.6Hz, 1H, 1-H), 7.45-7.16 (m, 8H, Aromatic). **^{13}C NMR** (100.6 MHz, $CDCl_3$) δ : 19.4 (C-6), 26.3 ($O_2C(CH_3)_2$), 26.7 ($O_2C(CH_3)_2$), 31.5-31.2 ($C(CH_3)_3$), 35.4-34.6 ($C(CH_3)_3$), 68.9 (C-5), 76.2 (C-3), 83.0 (C-4), 84.2 (C-2), 104.7 (C-1), 111.6($O_2C(CH_3)_2$), 146.8-124.0 (Aromatic). **^{31}P NMR** (161.97 MHz, $CDCl_3$) δ: 144.4(d, *J*= 34.0 Hz), 145.6 (d, *J*= 35.3 Hz). Anal. calcd for $C_{65}H_{94}O_9P_2$ (1081.39): C, 72.19; H, 8.76. Found: C, 72.00; H, 8.95.

3,5-Bis-*O*-[(3,3'-di-tert-butyl-5,5'-dimethoxy-1,1'-biphenyl-2,2'-diyl)phosphite]-6-*O*-butyl-1,2-*O*-isopropyliden-*α*-*D*-glucofuranoside (64a). The synthesis of diphosphite **64a** was completed according to the general procedure previously described. The product was isolated as a white solid in 42% yield (441 mg, 0.42 mmol) after purification by flash column chromatography (toluene/THF= 95/5, Rf= 0.25). $[\alpha]^D_{25}$ = + 97.21 $cm^3\ g^{-1}\ dm^{-1}$ (c = 1.0 g cm^{-3}, CH_2Cl_2). **^{1}H NMR** (400 MHz, $CDCl_3$) δ: 0.88 (t, *J*= 7.4Hz, 3H, $O(CH_2)_3CH_3$), 1.15 (s, 3H, $O_2C(CH_3)_2$), 1.47 (m, 43H, $O_2C(CH_3)_2$, $O(CH_2)_3CH_3$, *o*$C(CH_3)_3$), 3.32 (m, 2H, $O(CH_2)_3CH_3$), 3.74 (m, 1H, 6´-H), 3.86-3.79 (m, 13H, 6-H, *p*OCH_3), 3.92(m, 1H, 2-H) 4.37 (d, *J*= 8.4 Hz, 1H, 4-H), 4.70 (m, 1H, 5-H), 4.83 (m, 1H, 3-H), 5.62 (d, *J*= 3.2 Hz, 1H, 1-H), 7.30-6.66 (m, 8H, Aromatic). **^{13}C NMR** (100.6 MHz, $CDCl_3$) δ: 14.1 ($O(CH_2)_3CH_3$), 19.4 ($O(CH_2)_3CH_3$), 26.1 ($O_2C(CH_3)_2$), 26.6 ($O_2C(CH_3)_2$), 31.2 (*o*$C(CH_3)_3$), 31.9 ($O(CH_2)_3CH_3$), 35.5 (*o*$C(CH_3)_3$), 55.7 (*p*OCH_3), 70.7 (C-6), 71.3 (C-5), 72.2 ($O(CH_2)_3CH_3$), 76.7 (C-3), 79.2 (C-4), 83.8 (C-2), 105.0 (C-1), 111.9 ($O_2C(CH_3)_2$), 156.0-112.8 (Aromatic).

^{31}P NMR (161.97 MHz, $CDCl_3$) δ: 144.6 (d, J= 30.9Hz), 146.1 (d, J= 30.9Hz). Anal. calcd for $C_{57}H_{78}O_{14}P_2$ (1049.17): C, 65.25; H, 7.49. Found: C, 65.10; H, 7.59.

3,5-Bis-*O*-[(3,3'-di-tert-butyl-5,5'-dimethoxy-1,1'-biphenyl-2,2'-diyl)phosphite]-6-*O*-butyl-1,2-*O*-isopropyliden-α-*D*-glucofuranose (64b). The synthesis of diphosphite **64b** was completed according to the general procedure previously described. The product was isolated as a white solid in 65 % yield (749 mg, 0.65 mmol) after purification by flash column chromatography (toluene, Rf= 0.60). $[\alpha]^D_{25}$ = + 98.78 $cm^3\ g^{-1}\ dm^{-1}$ (c = 1.0 g cm^{-3}, CH_2Cl_2). **^{1}H NMR** (400 MHz, $CDCl_3$) δ: 0.94 (m, 3H, $O(CH_2)_3CH_3$), 1.17 (s, 3H, $O_2C(CH3)_2$), 1.26 (m, 41H, $O_2C(CH_3)_2$, $O(CH_2)_3CH_3$, $C(CH_3)_3$), 1.38 (m, 38H, $O(CH_2)_3CH_3$, $C(CH_3)_3$), 3.14 (m, 2H, $O(CH_2)_3CH_3$), 3.64 (d, *J*= 11.2 Hz, 1H, 6-H), 3.61 (dd, *J*= 11.2, 4.8 Hz, 1H, 6´-H), 4.02 (m, 1H, 2-H), 4.31 (m, 1H, 4-H), 4.57 (m, 1H, 5-H), 4.74 (m, 1H, 3-H), 5.37 (d, *J*= 3.2 Hz, 1H, 1-H), 7.36-7.03 (m, 8H, Aromatic). **^{13}C NMR** (100.6 MHz, $CDCl_3$) δ : 14.2 ($O(CH_2)_3CH_3$), 19.5 ($O(CH_2)_3CH_3$), 21.7 ($O(CH_2)_3CH_3$), 26.7 ($O_2C(CH_3)_2$), 26.9 ($O_2C(CH_3)_2$), 32.0-31.5 ($C(CH_3)_3$), 35.6-34.8 ($C(CH_3)_3$), 70.7 (C-6), 71.3 ($O(CH_2)_3CH_3$), 72.2 (C-5), 77.4 (C-4), 78.9 (C-3), 84.3 (C-2), 105.0 (C-1), 112.0 ($O_2C(CH_3)_2$), 146.9-124.2 (Aromatic). **^{31}P NMR** (161.97 MHz, $CDCl_3$) δ: 145.1 (d, *J*= 43.7Hz), 146.1 (d, *J*= 43.7Hz). Anal. calcd for $C_{69}H_{102}O_{10}P_2$ (1153.49): C, 71.85; H, 8.91. Found: C, 71.75; H, 9.05.

3,5-Bis-*O*-[(3,3'-di-tert-butyl-5,5'-dimethoxy-1,1'-biphenyl-2,2'-diyl)phosphite]-6-*O*-isopropyl-1,2-*O*-isopropyliden-α-*D*-glucofuranoside (65a). The synthesis of diphosphite 7a was completed according to the general procedure previously described. The product was isolated as a white solid in 54% yield (559 mg, 0.54 mmol) after purification by flash column chromatography (toluene/THF= 95/5, Rf= 0.35). $[\alpha]^D_{25}$ = + 129.49 $cm^3\ g^{-1}\ dm^{-1}$ (c = 1.0 g cm^{-3}, CH_2Cl_2). **^{1}H NMR** (400 MHz, $CDCl_3$) δ: 1.14 (dd, *J*= 6.4Hz, 6H, $OCH(CH_3)_2$), 1.20 (s, 3H, $O_2C(CH_3)_2$), 1.50 (4xs, 39H, $O_2C(CH_3)_2$, *o*$C(CH_3)_3$), 3.54 (m, 1H, $OCH(CH_3)_2$), 3.80 (dd, *J*= 11.0, 5.4Hz, 1H, 6-H), 3.85-3.89 (m, 14H, 2-H, 6-H, *p*OCH_3), 4.41 (d, *J*= 6.4 Hz, 1H, 4-H), 4.71 (m, 1H, 5-H), 4.89 (d, *J*= 4.4 Hz, 1H, 3-H), 5.67 (d, *J*= 3.6 Hz, 1H, 1-H), 7.30-6.70 (m, 8H,

Aromatic). **^{13}C NMR** (100.6 MHz, $CDCl_3$) δ: 22.1 ($OCH(CH_3)_2$), 26.1 ($O_2C(CH_3)_2$), 26.8 ($O_2C(CH_3)_2$), 31.2 (*o*$C(CH_3)_3$), 35.6 (*o*$C(CH_3)_3$), 55.8 (*p*OCH_3), 68.0 (C-6), 72.2 ($OCH(CH_3)_2$), 72.4 (C-5), 76.7 (C-3), 79.2 (C-4), 83.8 (C-2), 105.0 (C-1), 111.8 ($O_2C(CH_3)_2$), 156.0-112.7 (Aromatic). **^{31}P NMR** (161.97 MHz, $CDCl_3$) δ: 144.5 (d, *J*= 30.9Hz), 145.8 (d, *J*= 30.9Hz). Anal. calcd for $C_{56}H_{76}O_{14}P_2$ (1035.14): C, 64.98; H, 7.40. Found: C, 64.76; H, 7.59.

3,5-Bis-*O*-[(3,3'-di-tert-butyl-5,5'-dimethoxy-1,1'-biphenyl-2,2'-diyl)phosphite]-6-*O*-isopropyl-1,2-*O*-isopropyliden-*α*-*D*-glucofuranose (65b). The synthesis of diphosphite **65b** was completed according to the general procedure previously described. The product was isolated as a white solid in 50 % yield (569 mg, 0.50 mmol) after purification by flash column chromatography (toluene, Rf= 0.60). $[\alpha]^D_{25}$ = + 138.54 $cm^3\ g^{-1}\ dm^{-1}$ (c = 1.0 g cm^{-3}, CH_2Cl_2). **^{1}H NMR** (400 MHz, $CDCl_3$) δ: 0.94 (dd, *J*= 6.4, 9.4Hz, 6H, $OCH(CH_3)_2$), 1.09 (s, 3H, $O_2C(CH_3)_2$), 1.34 (s, 39H, $O_2C(CH_3)_2$, $C(CH_3)_3$), 1.48 (s, 36H, $C(CH_3)_3$), 3.40 (m, 1H, $OCH(CH_3)_2$), 3.71 (m, 2H, 6-H), 4.00 (d, *J*= 3.2Hz, 1H, 2-H), 4.41 (dd, *J*= 2.4, 8.4 Hz, 1H, 5-H), 4.60 (m, 1H, 3-H), 4.81 (dd, *J*= 6.0, 2.4 Hz, 1H, 4-H), 5.46 (d, *J*= 3.2 Hz, 1H, 1-H), 7.45-7.13 (m, 8H, Aromatic). **^{13}C NMR** (100.6 MHz, $CDCl_3$) δ : 22.0 ($OCH(CH_3)_2$), 22.3 ($OCH(CH_3)_2$), 26.8 ($O_2C(CH_3)_2$), 26.9 ($O_2C(CH_3)_2$), 31.6 ($C(CH_3)_3$), 31.8 ($C(CH_3)_3$), 34.7 ($C(CH_3)_3$), 35.6 ($C(CH_3)_3$), 67.9 (C-6), 72.0 ($OCH(CH_3)_2$), 72.3 (C-5), 77.5 (C-4), 78.9 (C-3), 84.3 (C-2), 105.0 (C-1), 112.0 ($O_2C(CH_3)_2$), 146.9-124.2 (Aromatic). **^{31}P NMR** (161.97 MHz, $CDCl_3$) δ: 145.2 (d, *J*= 47.9Hz), 146.3 (d, *J*= 48.1Hz). Anal. calcd for $C_{68}H_{100}O_{10}P_2$ (1139.47): C, 71.68; H, 8.85. Found: C, 71.45; H, 9.00.

3,5-Bis-*O*-[(3,3'-di-tert-butyl-5,5'-dimethoxy-1,1'-biphenyl-2,2'-diyl)phosphite]-6-*O*-(1,1´-dimethyl-3-butyl)-1,2-*O*-isopropyliden-*α*-*D*-glucofuranoside (66a). The synthesis of diphosphite **66a** was completed according to the general procedure previously described. The product was isolated as a white solid in 58% yield (623 mg, 0.58 mmol) after purification by flash column chromatography (toluene/THF= 95/5, Rf= 0.40). $[\alpha]^D_{25}$ = + 111.74 $cm^3\ g^{-1}\ dm^{-1}$ (c = 1.0 g cm^{-3}, CH_2Cl_2). **^{1}H NMR** (400 MHz, $CDCl_3$) δ: 0.93 (t, *J*= 6.8Hz, 3H, $CH_2CH_2CH_3$), 1.18 (m, 6H,

$OC(CH_3)_2CH_2CH_2CH_3$), 1.40 (s, 3H, $O_2C(CH_3)_2$), 1.50 (4xs, 43H, $O_2C(CH_3)_2$, $CH_2CH_2CH_3$, *o*$C(CH_3)_3$), 3.76 (m, 1H, 6-H), 3.85-3.89 (s, 14H, 2-H, 6-H, *p*OCH_3), 4.47 (d, *J*= 8.4 Hz, 1H, 4-H), 4.69 (m, 1H, 5-H), 4.90 (m, 1H, 3-H), 5.67 (d, *J*= 4.0 Hz, 1H, 1-H), 7.36-6.78 (m, 8H, Aromatic). **^{13}C NMR** (100.6 MHz, $CDCl_3$) δ: 14.9 ($CH_2CH_2CH_3$), 17.2 ($CH_2CH_2CH_3$), 25.2 ($OC(CH_3)_2CH_2CH_2CH_3$), 25.3 ($OC(CH_3)_2CH_2CH_2CH_3$), 26.0 ($O_2C(CH_3)_2$), 26.6 ($O_2C(CH_3)_2$), 31.2 (*o*$C(CH_3)_3$), 35.5 (*o*$C(CH_3)_3$), 43.6 ($CH_2CH_2CH_3$), 55.8 (*p*OCH_3), 61.5 (C-6), 72.4 (C-5), 75.0 ($OC(CH_3)_2CH_2CH_2CH_3$) 76.6 (C-3), 78.9 (C-4), 83.8 (C-2), 105.1 (C-1), 111.7 ($O_2C(CH_3)_2$), 156.0-111.9 (Aromatic). **^{31}P NMR** (161.97 MHz, $CDCl_3$) δ: 144.7 (d, *J*= 32.1Hz), 145.7 (d, *J*= 32.1Hz). Anal. calcd for $C_{59}H_{82}O_{14}P_2$ (1077.22): C, 65.78; H, 7.67. Found: C, 65.70; H, 7.72.

3,5-Bis-*O*-[(3,3'-di-tert-butyl-5,5'-dimethoxy-1,1'-biphenyl-2,2'-diyl)phosphite]-6-*O*-(1,1-dimethyl-3-butane)-1,2-*O*-isopropyliden-*α*-*D*-glucofuranose (66b). The synthesis of diphosphite **66b** was completed according to the general procedure previously described. The product was isolated as a white solid in 50 % yield (590 mg, 0.50 mmol) after purification by flash column chromatography (toluene, Rf= 0.60). $[\alpha]^{D}_{25}$ = + 112.18 $cm^3\ g^{-1}\ dm^{-1}$ (c = 1.0 g cm^{-3}, CH_2Cl_2). **^{1}H NMR** (400 MHz, $CDCl_3$) δ: 0.94 (t, *J*= 6.8Hz, 3H, $CH_2CH_2CH_3$), 1.12 (s, 3H, $O_2C(CH_3)_2$), 1.40 (s, 41H, $O_2C(CH_3)_2$, $CH_2CH_2CH_3$, $C(CH_3)_3$), 1.53 (s, 38H, $CH_2CH_2CH_3$, $C(CH_3)_3$), 3.64 (dd, *J*= 10.4, 4.0Hz, 1H, 6-H), 3.73 (d, *J*= 10.4 Hz, 1H, 6´-H), 4.02 (d, *J*= 3.2Hz, 1H, 2-H), 4.49 (dd, *J*= 8.4, 2.4 Hz, 1H, 4-H), 4.59 (m, 1H, 5-H), 4.83 (d, *J*= 3.2 Hz, 1H, 3-H), 5.46 (d, *J*= 3.6 Hz, 1H, 1-H), 7.48-7.17 (m, 8H, Aromatic). **^{13}C NMR** (100.6 MHz, $CDCl_3$) δ : 14.8 ($CH_2CH_2CH_3$), 17.1 ($CH_2CH_2CH_3$), 21.7 ($CH_2CH_2CH_3$), 26.2 ($O_2C(CH_3)_2$), 26.9 ($O_2C(CH_3)_2$), 31.8-31.2 ($C(CH_3)_3$), 35.7-34.7 ($C(CH_3)_3$), 43.9 ($CH_2CH_2CH_3$), 61.5 (C-6), 71.7 ($OC(CH_3)_2CH_2CH_2CH_3$), 74.8 (C-5), 76.9 (C-4), 78.6 (C-3), 84.4 (C-2), 105.1 (C-1), 112.0 ($O_2C(CH_3)_2$), 146.9-124.1 (Aromatic). **^{31}P NMR** (161.97 MHz, $CDCl_3$,) δ: 145.8 (d, *J*= 45.8Hz), 146.7 (d, *J*= 50.2Hz). Anal. calcd for $C_{71}H_{106}O_{10}P_2$ (1181.54): C, 72,17; H, 9,04. Found: C, 72.05; H, 9.20.

1,4-Anhydro-3,5-Bis-*O*-[(3,3'-di-tert-butyl-5,5'-dimethoxy-1,1'-biphenyl-2,2'-diyl)phosphite]-2-*O*-butyl-*D*-xylitol (86a). The

synthesis of diphosphite **86a** was completed according to the general procedure previously described. The product was isolated as a white solid in 71 % yield (684 mg, 0.71 mmol) after purification by flash column chromatography (toluene/THF= 98/2, Rf= 0.35). $[\alpha]^{D}_{25}$ = − 3.30 $cm^3\ g^{-1}\ dm^{-1}$ (c = 1.0 g cm^{-3}, CH_2Cl_2). **^{1}H NMR** (400 MHz, $CDCl_3$) δ: 0.81 (t, *J*= 6.4Hz, 3H, $O(CH_2)_3CH_3$), 1.40 (m, 40H, *o*$C(CH_3)_3$, $O(CH_2)_3CH_3$), 3.14 (m, 2H, $O(CH_2)_3CH_3$), 3.60 (m, 2H, 1´-H, 4-H), 3.80 (2xs, 12H, *p*OCH_3), 3.90 (dd, *J*= 9.6, 4.4Hz,1H, 1-H), 4.00 (m, 2H, 5,5´-H), 4.08 (m, 1H, 2-H), 4.70 (dd, *J*= 8.0, 2.0Hz, 1H, 3-H), 6.97-6.67 (m, 8H, Aromatic). **^{13}C NMR** (100.6 MHz, $CDCl_3$) δ: 14.3 ($O(CH_2)_3CH_3$), 19.3 ($O(CH_2)_3CH_3$), 31.2 (*o*$C(CH_3)_3$), 31.9 ($O(CH_2)_3CH_3$), 35.6 (*o*$C(CH_3)_3$), 55.8 (*p*OCH_3), 62.8 (C-5), 69.6 ($O(CH_2)_3CH_3$), 71.9 (C-1), 76.5 (C-3), 79.4 (C-4), 84.2 (C-2), 156.0-113.0 (Aromatic). **^{31}P NMR** (161.97 MHz, $CDCl_3$) δ: 136.3 (s), 143.2 (s). Anal. calcd for $C_{53}H_{72}O_{12}P_2$ (963.08): C, 66.10; H, 7.54. Found: C, 65.90; H, 7.67.

1,4-Anhydro-3,5-Bis-O-[4,8-di-tert-butyl-2,10-di-metyl-12H-dibenzo[*δ,γ*][1,2,3]di-oxaphosphocine]-2-O-butyl-D-xylitol (86w). The synthesis of diphosphite **86w** was completed according to the general procedure previously described. The product was isolated as a white solid in 55% yield (510 mg, 0.55 mmol) after purification by flash column chromatography (toluene, Rf= 0.60). $[\alpha]^{D}_{25}$ = − 2.15 $cm^3\ g^{-1}\ dm^{-1}$ (c = 1.0 g cm^{-3}, CH_2Cl_2). **^{1}H NMR** (400 MHz, $CDCl_3$) δ: 1.03 (*t*, J= 10.0Hz, 3H, $O(CH_2)_3CH_3$), 1.41 (m, 2H, $O(CH_2)_3CH_3$), 1.55 (s, 36H, *o*$C(CH_3)_3$), 1.71 (m, 2H, $O(CH_2)_3CH_3$), 2.45 (2xs, 12H, *p*CH_3), 3.54 (dd, *J*= 11.2, 5.6Hz, 2H, $PhCH_2Ph$), 3.77 (m, 1H, $O(CH_2)_3CH_3$), 3.87 (m, 1H, $O(CH_2)_3CH_3$), 4.12 (d, *J*= 13.2, 1H, 1´-H), 4.50 (m, 2H, $PhCH_2Ph$), 4.57 (dd, *J*= 13.2, 5.6Hz, 1H, H-1), 4.77 (m, 1-H, 4-H), 4.90 (m, 1H, 5´-H), 5.00 (d, *J*= 5.2Hz, 1H, 2-H), 5.08 (m, 1H, 5-H), 5.75 (dd, *J*= 8.4, 4.4Hz, 1H, 3-H), 7.21-7.17 (m, 8H, Aromatic). **^{13}C NMR** (100.6 MHz, $CDCl_3$) δ: 14.2 ($O(CH_2)_3CH_3$), 19.5 ($O(CH_2)_3CH_3$), 21.3 (*p*CH_3), 31.3 (*o*$C(CH_3)_3$), 32.1 ($O(CH_2)_3CH_3$), 34.9 ($PhCH_2Ph$), 62.5 (C-5), 69.9 ($O(CH_2)_3CH_3$), 72.3 (C-1), 77.4 (C-3), 80.3 (C-4), 84.3 (C-2), 142.3-125.5 (Aromatic). **^{31}P NMR** (161.97 MHz, $CDCl_3$) δ: 129.3 (s), 131.6 (s). Anal. calcd for $C_{55}H_{76}O_8P_2$ (927.13): C, 71.25; H, 8.26. Found: C, 70.95; H, 8.40.

1,4-Anhydro-3,5-Bis-*O*-[(3,3'-di-tert-butyl-5,5'-dimethoxy-1,1'-biphenyl-2,2'-diyl)phosphite]-2-*O*-tetradecyl-*D*-xylitol (87a). The synthesis of diphosphite **87a** was completed according to the general procedure previously described. The product was isolated as a white solid in 27% yield (298 mg, 0.27 mmol) after purification by flash column chromatography (toluene/THF= 98/2, Rf= 0.35). $[\alpha]^{D}_{25}$ = − 0.60 $cm^3\ g^{-1}\ dm^{-1}$ (c = 1.0 g cm^{-3}, CH_2Cl_2). **^{1}H NMR** (400 MHz, $CDCl_3$) δ: 0.81 (t, *J*= 6.4Hz, 3H, $O(CH_2)_{13}CH_3$), 1.40 (m, 60H, *o*$C(CH_3)_3$, $O(CH_2)_{13}CH_3$), 3.14 (m, 2H, $O(CH_2)_{13}CH_3$), 3.60 (m, 2H, 1´-H, 4-H), 3.82-3.80 (s, 12H, *p*OCH_3), 3.92 (dd, *J*= 10.0, 4.4Hz, 1H, 1-H), 4.01 (m, 2H, 5,5´-H), 4.09 (m, 1H, 2-H), 4.71 (dd, *J*= 8.8, 3.2Hz, 1H, 3-H), 6.97-6.67 (m, 8H, Aromatic). **^{13}C NMR** (100.6 MHz, $CDCl_3$) δ: 14.3 ($O(CH_2)_{13}CH_3$), 26.2 ($O(CH_2)_{13}CH_3$), 29.2 ($O(CH2)_{13}CH_3$), 29.8 ($O(CH_2)_{13}CH_3$), 31.2 (*o*$C(CH_3)_3$), 32.1 ($O(CH_2)_{13}CH_3$), 35.6 (*o*$C(CH_3)_3$), 55.8 (*p*OCH_3), 62.8 (C-5), 70.0 ($O(CH_2)_{13}CH_3$), 71.9 (C-1), 76.5 (C-3), 79.3 (C-4), 84.2 (C-2), 156.0-113.0 (Aromatic). **^{31}P NMR** (161.97 MHz, $CDCl_3$) δ: 136.3 (s), 143.2 (s). Anal. calcd for $C_{63}H_{92}O_{12}P_2$ (1103.34): C, 68.58; H, 8.40. Found: C, 68.27; H, 8.57.

1,4-Anhydro-3,5-Bis-*O*-[(3,3'-5,5´-tetra-tert-butyl-1,1'-biphenyl-2,2'-diyl) phosphite]-2-*O*-tetradecyl-*D*-xylitol (87b). The synthesis of diphosphite **87b** was completed according to the general procedure previously described. The product was isolated as a white solid in 75 % yield (906 mg, 0.75 mmol) after purification by flash column chromatography (toluene, Rf= 0.75). $[\alpha]^{D}_{25}$ = − 2.00 $cm^3\ g^{-1}\ dm^{-1}$ (c = 1.0 g cm^{-3}, CH_2Cl_2). **^{1}H NMR** (400 MHz , $CDCl_3$) δ: 0.89 (t, *J*= 6.8Hz, 3H, $O(CH_2)_{13}CH_3$), 1.27 (m, 22H, $O(CH_2)_{13}CH_3$), 1.35 (m, 36H, $C(CH_3)_3$), 1.45 (m, 36H, $C(CH_3)_3$), 3.12 (m, 2H, $O(CH_2)_{13}CH_3$), 3.51 (m, 1H, 1´-H), 3.54 (d, 1H, *J*= 9.2Hz, 4-H), 3.79 (dd, *J*= 10.0, 4.4Hz, 1H, 1-H), 4.00 (m, 2H, 5,5´-H), 4.07 (m, 1H, 2-H), 4.69 (dd, *J*= 7.6, 2.0Hz, 1H, 3-H), 7.42-7.13 (m, 8H, Aromatic). **^{13}C NMR** (100.6 MHz, $CDCl_3$) δ : 14.3 ($O(CH_2)_{13}CH_3$), 26.3 ($O(CH_2)_{13}CH_3$), 29.6 ($O(CH_2)_{13}CH_3$), 29.8 ($O(CH_2)_{13}CH_3$), 29.8 ($O(CH_2)_{13}CH_3$), 31.8-31.2 ($C(CH_3)_3$), 32.1 ($O(CH_2)_{13}CH_3$), 35.6-34.8 ($C(CH_3)_3$), 62.8 (C-5), 70.1 ($O(CH_2)_{13}CH_3$), 71.9 (C-1), 76.5 (C-3), 79.4 (C-4), 84.1 (C-2), 146.8-124.3 (Aromatic). **^{31}P NMR** (161.97 MHz, $CDCl_3$) δ: 135.9 (s), 143.6 (s). Anal. calcd for $C_{75}H_{116}O_8P_2$ (1207.67): C, 74.59; H, 9.68. Found: C, 74.40; H, 9.95.

1,4-Anhydro-3,5-Bis-*O*-[4,8-di-tert-butyl-2,10-di-metyl-12H-dibenzo[*δ,γ*][1,2,3]di-oxaphosphocine]-2-*O*-tetradecyl-*D*-xylitol (87w). The synthesis of diphosphite **87w** was completed according to the general procedure previously described. The product was isolated as a white solid in 50 % yield (534 mg, 0.50 mmol) after purification by flash column chromatography (toluene, Rf= 0.60). $[\alpha]^{D}_{25}$ = – 0.82 $cm^3\ g^{-1}\ dm^{-1}$ (c = 1.0 g cm^{-3}, CH_2Cl_2). **^{1}H NMR** (400 MHz, $CDCl_3$) δ: 0.90 (t, *J*= 10.0Hz, 3H, $O(CH_2)_{13}CH_3$), 1.28 (m, 22H, $O(CH_2)_{13}CH_3$), 1.43 (s, 36H, *o*$C(CH_3)_3$), 1.61 (m, 2H, $O(CH_2)_{13}CH_3$), 2.31 (2xs, 12H, *p*CH_3), 3.40 (dd, *J*= 12.8, 8.4Hz, 2H, $PhCH_2Ph$), 3.64 (m, 1H, $O(CH_2)_{13}CH_3$), 3.70 (m, 1H, $O(CH_2)_{13}CH_3$), 3.99 (d, *J*= 10.0, 1H, 1´-H), 4.36 (m, 2H, $PhCH_2Ph$), 4.42 (dd, *J*= 9.6, 4.4Hz, 1H, 1-H), 4.63 (m, 1H, 4-H), 4.78 (m, 1H, 5´-H), 4.86 (d, *J*= 4.0Hz, 1H, 2-H), 4.94 (m, 1H, 5-H), 5.60 (dd, *J*= 6.0, 3.2Hz, 1H, 3-H), 7.14-7.01 (m, 8H, Aromatic). **^{13}C NMR** (100.6 MHz, $CDCl_3$) δ: 14.6 ($O(CH_2)_{13}CH_3$), 21.5 (*p*CH_3), 23.1 ($O(CH_2)_{13}CH_3$), 26.6 ($O(CH_2)_{13}CH_3$), 29.9 ($O(CH_2)_{13}CH_3$), 30.1 (*o*C(CH3)3), 31.4 ($O(CH_2)_{13}CH_3$), 35.2 ($PhCH_2Ph$), 62.7 (C-5), 70.5 ($O(CH_2)_{13}CH_3$), 72.5 (C-1), 77.4 (C-3), 80.5 (C-4), 84.5 (C-2), 136.6-127.2 (Aromatic). **^{31}P NMR** (161.97 MHz, $CDCl_3$) δ: 129.7 (s), 132.1 (s). Anal. calcd for $C_{65}H_{96}O_8P_2$ (1067.40): C, 73.14; H, 9.07. Found: C, 73.00; H, 9.24.

1,4-Anhydro-3,5-Bis-*O*-[(3,3'-5,5´-tetra-tert-butyl-1,1'-biphenyl-2,2'-diyl) phosphite]-2-*O*-hexadecyl-*D*-xylitol (89b). The synthesis of diphosphite **89b** was completed according to the general procedure previously described. The product was isolated as a white solid in 75 % yield (927 mg, 0.75 mmol) after purification by flash column chromatography (toluene, Rf= 0.75). $[\alpha]^{D}_{25}$ = −2.11 $cm^3\ g^{-1}\ dm^{-1}$ (c = 1.0 g cm^{-3}, CH_2Cl_2). **^{1}H NMR** (400 MHz , $CDCl_3$) δ: 0.88 (t, *J*= 6.8Hz, 3H, $O(CH_2)_{15}CH_3$), 1.26 (m, 26H, $O(CH_2)_{15}CH_3$), 1.34 (m, 36H, $C(CH_3)_3$), 1.46 (m, 36H, $C(CH_3)_3$), 3.10 (m, 2H, $O(CH_2)_{15}CH_3$), 3.51 (m, 1H, 1´-H), 3.54 (d, 1H, *J*= 9.2Hz, 4-H), 3.79 (dd, *J*= 10.0, 4.4Hz, 1H, 1-H), 4.00 (m, 2H, 5,5´-H), 4.07 (m, 1H, 2-H), 4.69 (dd, *J*= 7.6, 2.0Hz, 1H, 3-H), 7.42-7.13 (m, 8H, Aromatic). **^{13}C NMR** (100.6 MHz, $CDCl_3$) δ : 14.3 ($O(CH_2)_{15}CH_3$), 21.7 ($O(CH_2)_{15}CH_3$), 22.9 ($O(CH_2)_{15}CH_3$), 26.3 ($O(CH_2)_{15}CH_3$), 29.6 ($O(CH_2)_{15}CH_3$), 29.8 ($O(CH_2)_{15}CH_3$), 29.8 ($O(CH_2)_{15}CH_3$), 31.8-31.2 ($C(CH_3)_3$), 32.1 ($O(CH_2)_{15}CH_3$), 35.6-34.8 ($C(CH_3)_3$), 62.8 (C-5), 69.8

($O(CH_2)_{15}CH_3$), 71.9 (C-1), 76.5 (C-3), 79.4 (C-4), 84.1 (C-2), 146.8-124.3 (Aromatic). **^{31}P NMR** (161.97 MHz, $CDCl_3$) δ: 135.8 (s), 143.5 (s). Anal. calcd for $C_{77}H_{120}O_8P_2$ (1265.72): C, 74.84; H, 9.79. Found: C, 74.74; H, 9.92.

1,4-Anhydro-3,5-Bis-O-[(3,3'-di-tert-butyl-5,5'-dimethoxy-1,1'-biphenyl-2,2'-diyl)- phosphite]-6-deoxy-2-O-hexadecyl-D-glucitol (67a). The synthesis of diphosphite **67a** was completed according to the general procedure previously described. The product was isolated as a white solid in 50 % yield (573 mg, 0.5 mmol) after purification by flash column chromatography (toluene/THF= 99/1, Rf= 0.25). $[\alpha]^D_{25}$ = − 0.34 $cm^3\ g^{-1}\ dm^{-1}$ (c = 1.0 g cm^{-3}, CH_2Cl_2). **^{1}H NMR** (400 MHz, $CDCl_3$) δ: 0.89 (t, *J*= 6.4Hz, 3H, $O(CH_2)_{15}CH_3$), 1.27 (s, 26H, $O(CH_2)_{15}CH_3$), 1.33 (d, *J*= 6.4Hz, 3H, 6-H), 1.46 (m, 36H, *o*$C(CH_3)_3$), 1.40 (m, 2H, $O(CH_2)_{15}CH_3$), 3.23 (m, 1H, $O(CH_2)_{15}CH_3$), 3.35 (m, 1H, $O(CH_2)_{15}CH_3$), 3.60 (m, 1H, 1´-H), 3.65 (m, 1H, 4-H), 3.82-3.80 (s, 13H, 1-H, *p*OCH3), 3.87 (dd, *J*= 8.0, 2.8Hz, 1H, 2-H), 4.72 (m, 1H, 5-H), 4.82 (dd, *J*= 7.0, 2.6Hz, 1H, 3-H), 6.97-6.70 (m, 8H, Aromatic). **^{13}C NMR** (100.6 MHz, $CDCl_3$) δ: 14.3 ($O(CH_2)_{15}CH_3$), 20.3 (C-6), 23.3 ($O(CH_2)_{15}CH_3$), 26.7 ($O(CH_2)_{15}CH_3$), 29.9 ($O(CH_2)_{15}CH_3$), 30.4 ($O(CH_2)_{15}CH_3$), 31.7 (*o*$C(CH_3)_3$), 32.5 ($O(CH_2)_{15}CH_3$), 35.9 (*o*$C(CH_3)_3$), 56.1 (*p*OCH_3), 69.7 (C-5), 70.5 ($O(CH_2)_{15}CH_3$), 72.6 (C-1), 76.0 (C-3), 84.0 (C-4), 84.5 (C-2), 156.3-113.2 (Aromatic). **^{31}P NMR** (161.97 MHz, $CDCl_3$) δ: 144.0 (d, *J*= 43.9 Hz), 146.5 (d, *J*= 43.7 Hz). Anal. calcd for $C_{66}H_{98}O_{12}P_2$ (1105.42): C, 69.21; H, 8.62. Found: C, 69.02; H, 8.79.

1,4-Anhydro-3,5-Bis-*O*-[(3,3'-5,5´-tetra-tert-butyl-1,1'-biphenyl-2,2'-diyl) phosphite]-6-deoxy-2-*O*-hexadecyl-*D*-glucitol (67b). The synthesis of diphosphite **67b** was completed according to the general procedure previously described. The product was isolated as a white solid in 74 % yield (925 mg, 0.74 mmol) after purification by flash column chromatography (toluene, Rf= 0.73). $[\alpha]^D_{25}$ = + 92.90 $cm^3\ g^{-1}\ dm^{-1}$ (c = 1.0 g cm^{-3}, CH_2Cl_2). **^{1}H NMR** (400 MHz, $CDCl_3$) δ: 0.90 (t, *J*= 6.4Hz, 3H, $O(CH_2)_{15}CH_3$), 1.25 (d, 3H, *J*= 6.0Hz, 6-H), 1.29 (s, 26H, $O(CH_2)_{15}CH_3$), 1.36 (m, 36H, $C(CH_3)_3$), 1.46 (m, 36H, $C(CH_3)_3$), 3.23 (m, 1H, $O(CH_2)_{15}CH_3$), 3.35 (m, 1H, $O(CH_2)_{15}CH_3$), 3.55 (m, 2H, 1,1´-H), 3.70 (dd,

J= 10.0, 4.4Hz, 1H, 4-H), 3.90 (dd, *J*= 7.4, 2.2Hz, 1H, 2-H), 4.76 (m, 1H, 5-H), 4.84 (m, 1H, 3-H), 7.44-7.14 (m, 8H, Aromatic). **^{13}C NMR** (100.6 MHz, $CDCl_3$) δ : 14.3 ($O(CH_2)_{15}CH_3$), 19.7 (C-6), 22.9 ($O(CH_2)_{15}CH_3$), 26.3 ($O(CH_2)_{15}CH_3$), 29.6 ($O(CH_2)_{15}CH_3$), 29.8 ($O(CH_2)_{15}CH_3$), 31.6 ($C(CH_3)_3$), 31.8 ($O(CH_2)_{15}CH_3$), 35.6-34.9 ($C(CH_3)_3$), 69.7 (C-5), 70.0 ($O(CH_2)_{15}CH_3$), 72.1 (C-1), 75.7 (C-3), 83.7 (C-4), 84.2 (C-2), 146.8-124.2 (Aromatic). **^{31}P NMR** (161.97 MHz, $CDCl_3$) δ: 144.6 (d, *J*= 45.8 Hz), 147.5 (d, *J*= 46.9 Hz). Anal. calcd for $C_{78}H_{122}O_8P_2$ (1249.75): C, 74,96; H, 9,84. Found: C, 74.75; H, 10.00.

1,4-Anhydro-3,5-Bis-*O*-[4,8-di-tert-butyl-2,10-di-metyl-12H-dibenzo[*δ,γ*][1,2,3]di- oxaphosphocine]-6-deoxy-2-*O*-hexadecyl-*D*-glucitol (67w). The synthesis of diphosphite **67w** was completed according to the general procedure previously described. The product was isolated as a white solid in 51% yield (566 mg, 0.51 mmol) after purification by flash column chromatography (toluene, Rf= 0.64). $[\alpha]^D_{25}$ = − 20.04 $cm^3\ g^{-1}\ dm^{-1}$ (c = 1.0 g cm^{-3}, CH_2Cl_2). **^{1}H NMR** (400 MHz, $CDCl_3$) δ: 0.91 (t, *J*= 6.8Hz, 3H, $O(CH_2)_{15}CH_3$), 1.27 (s, 26H, $O(CH_2)_{15}CH_3$), 1.44 (s, 36H, *o*$C(CH_3)_3$), 1.60 (m, 2H, $O(CH_2)_{15}CH_3$), 1.88(d, *J*= 6.4 Hz, 3H, 6-H), 2.30 (s, 12H, *p*CH_3), 3.54 (dd, *J*= 12Hz, 2H, $PhCH_2Ph$), 3.65 (m, 1H, $O(CH_2)_{15}CH_3$), 3.75 (m, 1H, $O(CH_2)_{15}CH_3$), 3.99 (d, *J*= 9.6, 1H, 1´-H), 4.36 (ddd, *J*= 17.9, 12.7, 2.7Hz, 2H, PhCH2Ph), 4.45(dd, *J*= 9.8, 4.6Hz, 1H, 1-H), 4.62 (dd, *J*= 3.6Hz, 1H, H-4), 4.92 (d, *J*= 3.6 Hz, 1H, 2-H), 5.55 (m, 1H, 3-H), 5.58 (m, 1H, 5-H), 7.00-7.30 (m, 8H, Aromatic). **^{13}C NMR** (100.6 MHz, $CDCl_3$) δ: 14.0 ($O(CH_2)_{15}CH_3$), 19.3(C-6), 20.9 (*p*CH_3), 21.4 ($O(CH_2)_{15}CH_3$), 22.6 ($O(CH_2)_{15}CH_3$), 26.2 ($O(CH_2)_{15}CH_3$), 29.3 ($O(CH_2)_{15}CH_3$), 29.5 ($O(CH_2)_{15}CH_3$), 30.7 (oC(CH3)3), 31.8 ($O(CH_2)_{15}CH_3$), 34.6 ($PhCH_2Ph$), 70.0 ($O(CH_2)_{15}CH_3$), 71.9 (C-5), 72.2 (C-1), 78.0 (C-3), 83.8 (C-2, C-4), 142.1-125.1 (Aromatic). **^{31}P NMR** (161.97 MHz, $CDCl_3$) δ: 131.9 (s), 133.5 (s). Anal. calcd for $C_{68}H_{102}O_8P_2$ (1109.48): C, 73.61; H, 9.27. Found: C, 73.31; H, 9.42.

In situ HP-NMR experiments. In a typical experiment, a sapphire tube (ø= 10 mm) was filled under nitrogen atmosphere with a solution of $[Rh(acac)(CO)_2]$ (2.10-2 mM) and ligand (molar ratio PP/Rh = 1.1) in toluene-d_8 (2 ml). The HP-NMR tube was purged three times with CO and

pressurized to the appropriate pressure of CO/H_2. After 24h, during which the solution was shaken under hydroformylation conditions, the solution was analyzed.

[RhH(CO)$_2$(67a)].

^{1}H NMR (300 MHz, toluene-d_8) δ:-9.80 (d, *J*= 5.2Hz, 1H), 0.92 (m, 3H, $O(CH_2)_{15}CH_3$), 1.32 (s, 26H, $O(CH_2)_{15}CH_3$), 1.33 (d, *J*= 2.4Hz, 3H, 6-H), 1.40(m, 2H, $O(CH_2)_{15}CH_3$), 1.65 (m, 36H, *o*$C(CH_3)_3$), 3.20 (m, 2H, $O(CH_2)_{15}CH_3$) , 3.33 (s, 13H, 1-H, *p*OCH_3), 3.43 (m, 2H, 1´-H, 4-H), 3.87 (d, *J*= 9.3Hz, 1H, 2-H), 4.94 (m, 1H, 5-H), 5.05 (dd, *J*= 7.0, 2.6Hz, 1H, 3-H), 6.85-6.67 (m, 8H, Aromatic). **^{13}C NMR** (75.5 MHz, toluene-d_8) δ: 14.4 ($O(CH_2)_{15}CH_3$), 20.3 (C-6), 23.2 ($O(CH_2)_{15}CH_3$), 26.7 ($O(CH_2)_{15}CH_3$), 29.9 ($O(CH_2)_{15}CH_3$), 30.4 ($O(CH_2)_{15}CH_3$), 31.7 (*o*$C(CH_3)_3$), 32.5 ($O(CH_2)_{15}CH_3$), 35.9 (*o*$C(CH_3)_3$), 56.1 (*p*OCH_3), 69.2 (C-5), 69.9 ($O(CH_2)_{15}CH_3$), 72.6 (C-1), 75.0 (C-3), 83.4 (C-4), 83.8 (C-2), 156.3-113.7 (Aromatic). **^{31}P NMR** (121.48 MHz, toluene-d_8) δ: 157.4- 149.2 (m).

[RhH(CO)$_2$(21w)].

^{1}H NMR (300 MHz, toluene-d_8) δ: -10.20(m, 1H), 1.10 (s, 3H, $O_2C(CH_3)_2$), 1.58 (m, 36H, *o*$C(CH_3)_3$), 1.98 (s, 3H, $O_2C(CH_3)_2$), 2.08 (2×s, 12H, *p*CH_3), 3.37 (dd, *J*= 14.6, 8.0Hz, 2H, $PhCH_2Ph$), 4.69 (m, 2H, $PhCH_2Ph$), 4.88 (d, *J*= 3Hz, 1H, 4-H), 5.04 (m, 2H, 5,5´-H), 5.25 (m, 2 H, 2-H-2, 3-H), 6.05 (d, *J*= 3.3 Hz, 1H, 1-H), 6.80-6.68 (m, 8H, Aromatic). **^{13}C NMR** (75.5 MHz, toluene-d_8) δ: 21.5 (*p*CH_3), 26.6 ($O_2C(CH_3)_2$), 27.0 ($O_2C(CH_3)_2$), 31.2 (*o*$C(CH_3)_3$), 35.0 ($PhCH_2Ph$), 61.7 (C-5), 77.4 (C-3), 79.9 (C-4), 84.2 (C-2), 105.1 (C-1), 111.9 ($O_2C(CH_3)_2$), 146.0-125.2 (Aromatic). **^{31}P NMR** (121.48 MHz, toluene-d_8) δ: 155.76(d, J_{Rh-P}= 232.08Hz), 155.46 (d, J_{Rh-P}= 233.90 Hz).

[RhH(CO)$_2$(65b)].

^{1}H NMR (400 MHz, toluene-d_8) δ: -9.92 (dd, J=3.2 Hz, 1H), 0.94 (dd, *J*= 6.4, 11.6Hz, 6H, $OCH(CH_3)_2$), 1.05 (s, 3H, $O_2C(CH_3)_2$), 1.27 (s, 39H, $O_2C(CH_3)_2$, $C(CH_3)_3$), 1.70 (s, 36H, $C(CH_3)_3$), 3.29 (m, 1H, $OCH(CH_3)_2$), 3.83 (m, 2H, 6-H), 3.99 (m, 1H, 2-H), 4.37 (d, *J*= 4.0 Hz, 1H, 5-H), 4.69 (m, 1H, 3-H), 4.83 (m, 1H, 4-H), 5.58 (d, *J*= 4.0 Hz, 1H, 1-H), 7.63-7.29 (m, 8H, Aromatic). **^{13}C NMR** (100.6 MHz, toluene-d_8) δ : 21.8 ($OCH(CH_3)_2$),

22.0 ($OCH(CH_3)_2$), 26.4 ($O_2C(CH_3)_2$), 26.7 ($O_2C(CH_3)_2$), 31.6 ($C(CH_3)_3$), 31.8 ($C(CH_3)_3$), 34.7 ($C(CH_3)_3$), 35.8 ($C(CH_3)_3$), 68.3 (C-6), 71.9 ($OCH(CH_3)_2$), 73.0 (C-5), 76.9 (C-4), 78.4 (C-3), 84.8 (C-2), 105.8 (C-1), 112.8 ($O_2C(CH_3)_2$), 148.3-123.2 (Aromatic). **^{31}P NMR** (161.97 MHz, toluene-d_8) δ: 158.5-153.8 (m).

[RhH(CO)$_2$(67b)].

^{1}H NMR (400 MHz, toluene-d_8) δ: -9.93 (dd, J=4.4 Hz, 1H), 0.89 (t, *J*= 6.8Hz, 3H, $O(CH_2)_{15}CH_3$), 1.29 (s, 29H, 6-H, $O(CH_2)_{15}CH_3$), 1.30 (m, 36H, $C(CH_3)_3$), 1.65 (m, 36H, $C(CH_3)_3$), 3.10 (m, 1H, $O(CH_2)_{15}CH_3$), 3.37 (m, 1H, $O(CH_2)_{15}CH_3$), 3.43 (dd, *J*= 4.4, 9.2 Hz, 1H, 1-H), 3.48 (d, J= 4Hz, 1H, 1´-H), 3.61 (d, *J*= 9.6Hz, 1H, 4-H), 3.88 (dd, *J*= 9.2, 1.6Hz, 1H, 2-H), 4.83 (m, 1H, 5-H), 5.02 (m, 1H, 3-H), 7.56-7.15 (m, 8H, Aromatic). **^{13}C NMR** (100.6 MHz, toluene-d_8) δ : 14.0 ($O(CH_2)_{15}CH_3$), 19.5 (C-6), 22.8 ($O(CH_2)_{15}CH_3$), 25.9 ($O(CH_2)_{15}CH_3$), 29.2 ($O(CH_2)_{15}CH_3$), 29.5 ($O(CH_2)_{15}CH_3$), 30.9 ($C(CH_3)_3$), 31.2 ($O(CH_2)_{15}CH_3$), 35.8-34.6 ($C(CH_3)_3$), 68.1 (C-5), 69.7 ($O(CH_2)_{15}CH_3$), 71.5 (C-1), 74.7 (C-3), 81.9 (C-4), 82.2 (C-2), 149.2-125.2 (Aromatic). **^{31}P NMR** (161.97 MHz, toluene-d_8) δ: 158.0-150.5 (m).

Rh-asymmetric hydroformylation of styrene. In a typical experiment, the autoclave was purged three times with CO. The solution formed by [Rh(acac)$(CO)_2$] (0.013 mmol), diphosphite (0.015 mmol) and styrene (13 mmol) in toluene (15 ml) was then introduced into the autoclave. Then, the autoclave was pressurized to the desired pressure of CO/H_2. After the desired reaction time, the autoclave was cooled to room temperature and depressurized. Gas chromatography analyses were run on a Hewlett-Packard HP 5890A instrument (split/splitless injector, J&W Scientific, HP-5, 25 m column, internal diameter 0.25 mm, film thickness 0.33 mm, carrier gas: 150 kPa He, F.I.D. detector) equipped with a Hewlett-Packard HP3396 series II integrator. Enantiomeric excesses were measured after oxidation of the aldehydes to the corresponding 2-aryl propionic acids on a Hewlett-Packard HP 5890A gas chromatograph (split/splitless injector, J&W Scientific, FS-Cyclodex β-I/P 50 m column, internal diameter 0.2 mm, film thickness 0.33 mm, carrier gas: 100 kPa He, F.I.D. detector). Absolute configuration was determined by comparing of retention times with

optically pure (*S*)-(+)-2-phenylpropionic and (*R)*-(-)-2-phenylpropionic acids.

Rh-asymmetric hydroformylation of vinyl acetate and dihydrofuran. In a typical experiment, the autoclave was purged 3 times with CO. The solution was formed from [Rh(acac)$(CO)_2$] (3.1 mg, 0.012 mmol), the corresponding quantities of diphosphite and the substrate (4.8 mmol) in toluene (5 mL). The autoclave was pressurised to the appropriate pressure of CO/H_2. After the desired reaction time, the autoclave was cooled to room temperature and depressurized. Conversion and selectivity of the hydroformylation of vinyl acetate was determined by GC analysis on a Hewlett-Packard HP 5890A instrument (split/splitless injector, J&W Scientific, HP-5, 25 m column, internal diameter 0.25 mm, film thickness 0.33 mm, carrier gas: 150 kPa He, F.I.D. detector) equipped with a Hewlett-Packard HP3396 series II integrator. The enantiomeric excess of the aldehydes was measured by GC analysis in a Hewlett-Packard HP 5890A gas chromatograph (split/splitless injector, J&W Scientific, FS-Betadex 25 m column, internal diameter 0.2 mm, film thickness 0.33 mm, carrier gas: 100 kPa He, F.I.D. detector). Conversion and selectivity of the hydroformylation of dihydrofurans were determined immediately after catalysis by ^{1}H NMR analysis of the crude reaction without evaporation of the solvent. The determination of the enantiomeric excess and absolute configuration of the methyl tetrahydro-3-furoate derived from tetrahydro-3-carbaldehyde was measured by ^{1}H NMR using Eu(hcf)$_3$ by previously described procedures.[36,37]

Determination of the absolute configuration and enantiomeric excess of tetrahydro-3-carbaldehydes. The reaction mixture was diluted with acetone and cooled with an ice bath. To this mixture, the Jones reagent was slowly added, and the mixture was stirred at room temperature overnight. The reaction mixture was treated with $NaHSO_3$. After disappearance of the orange colour, the insoluble material was filtered off. Then the filtrate was concentrated and the residue was diluted with brine and extracted three times with diethylether. The combined organic layers were washed twice with brine, dried over $MgSO_4$, and then concentrated to give the corresponding tetrahydro-3-furoic acid. **^{1}H NMR**

(400 MHz, $CDCl_3$) δ: 2.15 (m, 2H, 4-H), 3.15 (m, 1H, 3-H), 3.85 (m, 1H, 5-H), 3.90 (m, 1H, 5´-H), 4.00 (d, *J* = 7.20Hz, 1H, 2-H), 10.34 (s, 1H). To a mixture of crude acid and silica chloride, dry methanol was added dropwise at 0ºC under nitrogen atmosphere.[51] The reaction mixture was stirred overnight. The crude mixture was filtered and solvent was evaporated under reduced pressure to afford the methyl tetrahydro-3-furoate derivative. **^{1}H NMR** (400 MHz, $CDCl_3$) δ: 2.14 (m, 2H, 4-H), 3.08 (m, 1H, 3-H), 3.67 (s, 3H, OCH_3), 3.71 (s, 3H), 3.83 (m, 1H, 5-H), 3.86 (m, 1H, 5´-H), 3.93 (d, *J* = 8.4Hz, 1H, 2-H). Enantiomeric excess was determined by ^{1}H NMR spectroscopy using $Eu(hcf)_3$ as the chiral shift reagent ((*R*)-methyl tetrahydro-3-furoate δ 4.52 ppm and (*S*)-methyl tetrahydro-3-furoate δ 4.55 ppm).

DL: T-1535-2009/ISBN: 978-84-692-4554-5

[1] O. Roelen, *Chem. Abstr.***1994**, *38*, 550 (Chemische Verwertungsgesellschaft, mBH Oberhausen, (1938/1952) DE Patent 849 584).

[2] K. Weissermel, H. J. Arpe, *Industrial organic chemistry*. VCH, Weinheim, p. 127, **2003**.

[3] a) J. Klosin, C. R. Landis, *Acc. Chem. Res.* **2007**, *40*, 1251; b) B. Breit, *Top. Curr. Chem.* **2007**, *279*, 139; c) F. Ungvári, *Coord. Chem. Rev.* **2007**, *251*, 2087; d) F. Ungvári, *Coord. Chem. Rev.* **2007**, *251*, 2072; e) K. D. Wiese, D. Obst, *Top. Organomet. Chem.* **2006**, *18*, 1.

[4] B. Breit, *Aldehydes: synthesis by hydroformylation of alkenes*. In *Science of synthesis*, R. Brückner vol. 25. Thieme, Stuttgart, p 277, **2007**.

[5] P. W. N. M. van Leeuwen, in *Homogeneous Catalysis: Understanding the Art*, Kluwer, Dordrecht, **2004**.

[6] B. M. Trost, *Science*, **1991**, *254*, 1471.

[7] B. Breit, *Acc. Chem. Res.* **2003**, *36*, 264.

[8] P. Eilbracht, A. M. Schmidt, *Top. Organomet. Chem.* **2006**, *18*, 65.

[9] a) D. A. Evans, J. A. Osborn, G. Wilkinson, *J. Chem. Soc. A* **1968**, 3133; b) D. Evans, G. Yagupsky, G. Wilkinson, *J. Chem. Soc. A.* **1968**, 2660; c) J. F. Young, J. A. Osborn, F. A. Jardine, G. Wilkinson, *J. Chem. Soc. Chem. Comm.* **1965**, 131.

[10] P. W. N. M. van Leeuwen, C. Claver, in *Rhodium catalysed hydroformylation*, Kluwer, Dordrecht, **2000**.

[11] T. Jongsma, G. Challa, P. W. N. M. van Leeuwen, *J. Organomet. Chem.* **1991**, *421*, 121.

[12] D. Selent, K. D. Wiese, D. Röttger, A. Börner, *Angew. Chem. Int. Ed.* **2000**, *39*, 1639.

[13] B. Breit, R. Winde, T. Mackewitz, R. Paciello, K. Harms, *Chem. Eur. J.* **2001**, *7*, 3106.

[14] A. I. M. Keulemans, A. Kwantes, T. van Bavel, *Rec. Trav. Chim. Pays Bas*. **1948**, *67*, 298.

[15] R. F. Heck, *Acc. Chem. Res.* **1969**, *2*, 10.

[16] P. P. Deutsch, R. Eisenberg, *Organometallics*. **1990**, *9*, 709.

[17] a) J. E. Babin, G. T. Whiteker, Asymmetric Synthesis, World Patent, WO 9303839, **1993**; b) G. T. Whiteker, J. R. Briggs, J. E. Babin, B. A. Barne, *Asymmetric Catalysis Using Biphosphite Ligands*. In *Chemical Industries*, Marcel Dekker, New York, vol. *89*, pp 359, **2003**.

[18] a) G. J. H. Buisman, E. J. Vos, P. C. J. Kamer, P. W. N. M. van Leeuwen, *J. Chem. Soc. Dalton Trans.* **1995**, 409; b) G. J. H. Buisman, L. A. van der Veen,

A. Klootwijk, W. G. J. de Lange, P. C. J. Kamer, P. W. N. M. van Leeuwen, *Organometallics*. **1997**, *16*, 2929.

[19] S. Cserépi-Szûcs, I. Tóth, L. Párkanyi, J. Bakos, *Tetrahedron: Asymmetry*, **1998**, *9*, 3135.

[20] R. Abdallah, J. A. J. Breuzard, M. C. Bonet, M. Lemaire, *J. Mol. Cat.: A Chem.* **2006**, *249*,218.

[21] G. J. H. Buisman, L. A. van der Veen, P. C. J. Kamer, P. W. N. M. van Leeuwen, *Organometallics*. **1997**, *16*, 5681.

[22] a) G.J.H. Buisman, M.E. Martin, E.J. Vos, A. Klootwijk, P.C.J. Kamer, P.W.N.M. van Leeuwen, *Tetrahedron: Asymmetry*. **1995**, *6*, 719; b) O. Pàmies, G. Net, A. Ruiz, C. Claver, *Tetrahedron: Asymmetry*. **2000**, *11*, 1097; c) M. Diéguez, O. Pàmies, A. Ruiz, S. Castillón, C. Claver, *Chem. Eur. J.* **2001**, *7*, 3086; d) M. Diéguez, O. Pàmies, A. Ruiz, C. Claver, *New. J. Chem.* **2002**, *26*, 827.

[23] a) C. J. Cobley, J. Klosin, C. Qin, G. T. Whiteker, *Org. Lett.* **2004**, *6*, 3277; b) C. J. Cobley, K. Gardner, J. Klosin, C. Praquin, C. Hill, G. T. Whiteker, A. Zanotti- Gerosa, *J. Org. Chem.* **2004**, *69*, 4031.

[24] N. Sakai, S. Mano, K. Nozaki, H. Takaya, *J. Am. Chem. Soc.* **1993**, *115*, 7033.

[25] K. Nozaki, N. Sakai, T. Nanno, T. Higashijima, S. Mano, T. Horiuchi, H. Takaya, *J. Am. Chem. Soc.* **1997**, *119*, 4413.

[26] K. Nozaki, Y. Ito, F. Shibahara, E. Shirakawa, T. Otha, H. Takaya, T. Hiyama, *J. Am. Chem. Soc.* **1998**, *120*, 4051.

[27] a) R. Tanaka, K. Nakano, K. Nozaki, *J. Org. Chem.* **2007**, *72*, 8671; b) K. Nakano, R. Tanaka, K. Nozaki, *Helv. Chim. Acta,* **2006**, *89*, 1681.

[28] Y. Yan, X. Zhang, *J. Am. Chem. Soc.* **2006**, *128*, 7198.

[29] A.T. Axtell, J. Klosin, K. A. Abboud, *Organometallics*, **2006**, *25*, 5003.

[30] A.T. Axtell, C. J. Colbey, J. Klosin, G. T. Whiteker, A. Zanotti-Gerosa, K. A. Abboud, *Angew. Chem. Int. Ed.* **2005**, *44*, 5834.

[31] G. J. Clarkson, J. R. Ansell, D. J. Cole-Hamilton, P. J. Pogorzelec, J. Whittell, M. Wills, *Tetrahedron: Asymmetry*, **2004**, *15*, 1787.

[32] T. P. Clark, C. R. Landis, S. L. Freed, J. Klosin, K. A. Abboud, *J. Am. Chem. Soc.* **2005**, *127*, 5040.

[33] B. Zhao, X. Peng, W. Wang, C. Xia, K. Ding, *Chem. Eur. J.* **2008**, *14*, 7847.

[34] a) M. Kuil, P. E. Goudriaan, P. W. N. M. van Leeuwen, J. N. H. Reek, *Chem. Commun.* **2006**, 4679; b) M. Kuil, P. E. Goudriaan, A. W. Kleij, D. M. Tooke, A. L. Spek, P. W. N. M. van Leeuwen, J. N. H. Reek, *Dalton Trans.* **2007**, 2311.

[35] M. R. Axet, S. Castillón, C. Claver, *Inorg. Chim. Acta*, **2006**, *359*, 2973.

[36] T. Horiuchi, T. Otha, E. Shirakawa, K. Nozaki, H. Takaya, *J. Org. Chem.* **1997**, *62*, 4285.

[37] M. Diéguez, O. Pamies, C. Claver. *Chem. Comm.* **2005**, 1121.

DL: T-1535-2009/ISBN: 978-84-692-4554-5

[38] a) A. Polo, C. Claver, S. Castillón, A. Ruiz, J. C. Bayón, J. Real, C. Mealli, D. Masi. *Organometallics*. **1992**, *11*, 3525; b) I. del Río, P. W. N. M. van Leeuwen, C. Claver. *Can. J. Chem.* **2001**, *79*, 560.

[39] J. Huang, E. Bunel, A. Allgeier, J. Tedrow, T. Storz, J. Preston, T. Correl, D. Manley, T. Soukup, R. Jensen, R. Syed, G. Moniz, R. Larsen, M. Martinelli, P. J. Reider, *Tetrahedron Letters*, **2005**, *46*, 7831.

[40] G. Parrinello, J.K. Stille, *J. Am. Chem. Soc,* **1987**, *109*, 7122-7127.

[41] I. Ojima, M. Takai, T. Takahashi, *Patent WO* **2004**-078766.

[42] S. Cruz-Gregorio, M. Sanchez, A. Clara-Sosa, S. Bèrnes, L. Quintero, F. Sartillo-Piscil, *J. Org. Chem.* **2005**, *70*, 7107.

[43] a) J.C. Lee, S.W. Chang, C.C. Liao, F.C. Chi, C.S. Chen, Y.S. Wen, C.C. Wang, S.S. Kulkarni, R. Puranik, Y.H. Liu, S.C. Hung, *Chem. Eur. J.* **2004**, *10*, 399; b) S.C. Hung, S.R. Thopate, R. Puranik, *Carbohydr. Res.* **2001**, *331*, 369.

[44] G. Hodosi, B. Podányi, J. Kuszmann, *Carbohydr. Res.* **1992**, *230*, 327.

[45] a) P.J. Kocienski, in *Protecting Groups*, Eds.: Thieme, Stuttgart, **2003**; b) T.W. Greene, P.G.M. Wuts, in *Protective Groups in Organic Synthesis*; Eds.: Wiley & Sons, New York, **1999**.

[46] a) J.E. Ewing, M.J. Robins, *Org. Lett.* **1999**, *4*, 635; b) A. Kakefuda, S. Shuto, T. Nagahata, J. Seki, T. Sasaki, A. Matsuda, *Tetrahedron* **1994**, *50*, 10167; c) J.A. Bennek, G.R. Gray, *J. Org. Chem.* **1987**, *52*, 892; d) D. Rolf, J.A. Bennek, G.R. Gray, *Carbohydr. Chem. Soc.* **1983**, *2*, 373; e) D. Rolf, G.R. Gray, *J. Am. Chem. Soc.* **1982**, *104*, 3539.

[47] Phosphorochloridites are easily prepared in one step from the corresponding bisphenol as described in a) G.J.H. Buisman, P.C.J. Kamer, P.W.N.M. van Leeuwen, *Tetrahedron: Asymmetry,* **1993**, *4*, 1625; b) E. Guiu, M. Aghmiz, Y. Díaz, C. Claver, B. Meseguer, C. Militzer, S. Castillón, *Eur. J. Org. Chem.* **2006**, 627.

[48] A. Castellanos-Páez, S. Castillón, C. Claver, P.W.N.M. van Leeuwen, W.G.J. de Lange, *Organometallics*, **1998**, *17*, 2543.

[49] G. Francio, W. Leitner, *Chem. Commun.* **1999**, 1663.

[50] a) J. B. Houseknecht, C. Altona, C. M. Hadad, T. L. Lowary, *J. Org. Chem.* **2002**, *67*, 4647; b) M. Seo, N. Castillo, R. Ganzynkowicz, C. R. Daniels, R. J. Woods, T. L. Lowary, P. N. Roy, *J. Chem. Theory Comput.* **2008**, *4*, 184.

[51] M. Sathe, M. P. Kaushik. *Catal. Comm.* **2006**, *7*, 644.

Chapter 3

Application of the novel 1,3-diphospihte ligands in the Pd-allylic alkylation of linear allyl compounds

3.1 Introduction to Pd-allylic substitution reaction.
3.2 Pd-allylic substitution mechanism.
3.3 Pd-asymmetric allylic substitution.
- **3.3.1** Pd-allylic substitution of 1,3-disubstituted substrates.
- **3.3.2** Pd-allylic substitution of monosubstituted substrates.

3.5 Results and Discussion: Pd-allylic alkylation provides easy access to chiral acyclic compounds. Searching the best C-1 symmetric furanoside diphosphite ligand for these reactions.
3.6 Conclusions.
3.7 Experimental Section.

UNIVERSITAT ROVIRA I VIRGILI
1,3- DIPHOSPHITE LIGANDS WITH FURANOSIDE BACKBONE: A POWERFUL TOOL IN ASYMMETRIC CATALYSIS
Aitor Gual Gozalbo
DL: T-1535-2009/ISBN: 978-84-692-4554-5

3.1. Introduction to Pd-allylic substitution reaction

Development of asymmetric metal-catalyzed reactions has played a significant role in allowing synthetic access to biologically important molecules. While the most widely utilized reactions involve hydrogenation, epoxidation, or dihydroxylation, these reactions form only one type of bond, either C-H or C-O bond, and normally involve only one mechanism for enantiodiscrimination, differentiating enantiotopic faces of a prochiral olefin or carbonyl group. [1, 2, 3] There are two important characteristics that distinguish asymmetric allylic alkylations from essentially all other methods of asymmetric induction: first, the number of mechanisms for enantiodiscrimination and, second, the diversity of bond types that can be formed. In the asymmetric allylic alkylation reaction, the chiral elements can be set a nucleophile, the electrophile, or both. [1-3] Furthermore, the ability to transform achiral or chiral racemic material to enantiopure material under similar conditions is unique to the asymmetric allylic alkylation reaction.[1-3]

3.2. Pd-allylic substitution mechanism

The general catalytic cycle of the Pd-allylic alkylation (Scheme 3.1) reaction offers at least five opportunities for enantiodiscrimination,[3] and in some instances more than one mechanism is operative when chiral elements at the electrophile and nucleophile are set in the same reaction.

The cycle starts with the complexation of the olefin by Pd(0)-complex **90**. Then, subsequent oxidative addition produced the Pd(II)-π-allyl complex **91** with elimination of a leaving group X^- . The Pd(II)-π-allyl complex **91** may be *syn-syn*, *syn-anti* or *anti-anti*. As shown in the catalytic cycle, the complexes that result from *E* olefins prefer the **91**-*syn-syn* configuration, while cyclic substrates are necessarily locked into the **91**-*anti-anti* geometry. The Pd(II)-π-allyl complex **91** can be a cationic complex, as shown in scheme 3.1, or a neutral complex if the resulting anion X^- coordinates with palladium. In presence of nucleophile, the Pd(II) center activates the π-allyl complex **91** towards the nucleophilic attack at the allyl termini. The addition of the nucleophile generates an unstable Pd(0)-olefin complex which readily releases the final product by decomplexation, and

undergoes coordination of a new molecule of substrate with subsequent oxidative addition to form the Pd(II)-allyl complex.

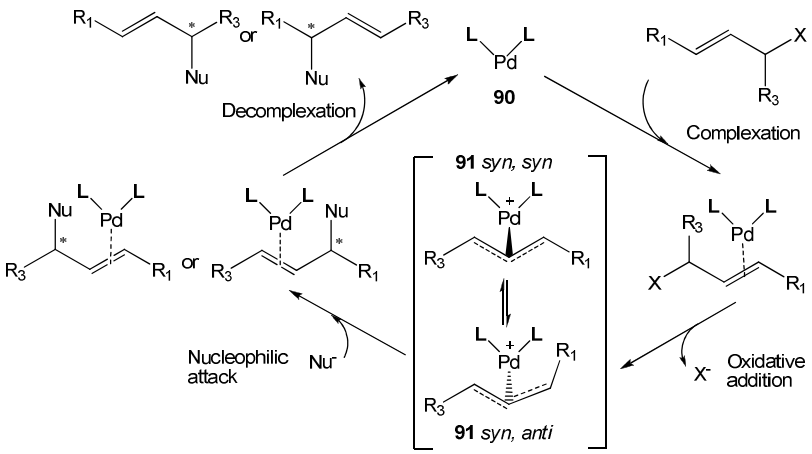

Scheme 3.1. Pd-asymmetric allylic substitution.

Except for decomplexation of the olefin from palladium-ligand system, where the chirality has already been set, each of these steps provides opportunity for enantioselection. If one Pd(0)-olefin complex leads to additive oxidation at a rate significantly faster than the other two diastereoisomeric Pd(II)-π-allyl complex **91**, and nucleophilic attack in that diastereoisomer is fast relative to π-σ-π equilibration, then enatiotopic olefin face oxidative addition becomes the enantiodiscriminating step.[2,3] In a case where there are two potential leaving groups on a *meso* or on an achiral *gem*-disubstituted Pd(0)-olefin complexes, enantiotopic oxidative addition of leaving groups to form the Pd(II)-π-allyl complex **91** is the enantiodetermining step.[2,3] If the starting olefin is a chiral racemic olefin but oxidative addition leads to *meso* Pd(II)-π-allyl complex **91**, the nucelophilic attack with differentiation of enantiotopic allyl termini is the enantioselection event.[2,3] If two diastereomeric Pd(II)-π-allyl complex **91** can be formed and these complexes can equilibrate through a π-σ-π equilibration step, where either the more abundant (assuming similar rates of nucleophilic attack step) or the more reactive diastereomeric complex leads the product. This type of selection, when the starting material is chiral racemic, constitutes a dynamic kinetic asymmetric transformation [2-4] Additionally, the chiral elements may be set at the nucleophile, and with

an achiral allyl complex, enantioface discrimination by prochiral nucleophiles is the enantiodetermining step.[2,3]

3.3 Pd-asymmetric allylic alkylation.

A wide variety of structurally very different substrates has been used for enantioselective allylic substitution. However, the synthesis of chiral linear allyl-phenyl compounds has a great importance in organic synthesis, because they are interesting building blocks in the synthesis of several compounds with biological and pharmaceutical properties.[1,5]

3.3.1 Pd-allylic substitution of 1,3-disubstituted linear substrates.

Allyl derivates with identical substituents at R_1 and R_3 are an important class of substrates for enantioselective allylic substitution (Scheme 3.2). Using this type of substrates, the first part of the catalytic cycle lead the same intermediate Pd(II)-π-allyl **91**, and therefore usually is irrelevant for the enantioselectivity of the overall reaction.

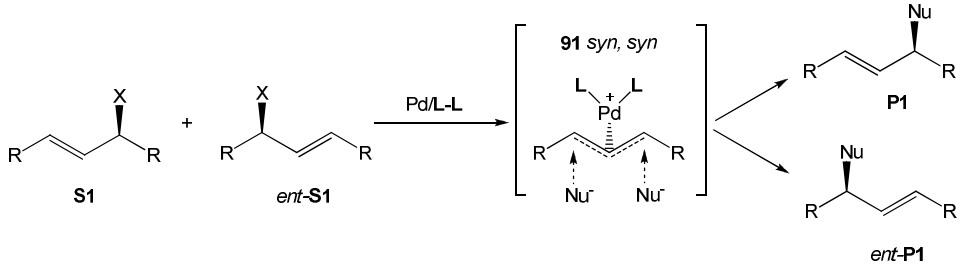

Scheme 3.2. Pd-asymmetric allylic substitution of racemic 1,3-disubstitued linear allyl derivates with identical substituents at R.

The two termini of the free allyl systems are enantiotopic. If the catalyst is chiral, they become diastereotopic in the Pd(II)-π-allyl **91** complex and, therefore, may exhibit different reactivities towards nucleophiles. Under the influence of a suitable chiral ligand, the nucleophilic attack can be rendered regioselective leading preferentially either one enatiomer of the product or the opposite enantiomer. And therefore, racemic allyl derivates with

identical substituents at R_1 and R_3 can be converted to enantiomerically enriched products.

The most widely studied reaction with this type of substrates is the Pd-allylic alkylation of *rac*-1,3-diphenyl-3-acetoxy-propen-1-ene *rac*-**S1** (R_1= R_3=Ph, X=OAc) using dimethyl malonate as nucleophile, which has become the standard test reaction for evaluating enantioselectivite catalysts (Scheme 3.3, 3.4 and 3.5) and therefore a great variety of ligands were tested in this reaction.

In the scheme 3.3 were introduced the ligands which provided the most successful results in this reaction. Although it is potentially a bidentate ligand, **92** behaves as a monodentate ligand in the Pd-allylic alkylation reaction.[6] *rac*-**S1** may be kinetically resolved to affort **P1** in 84% *ee* and the **S1** being recovered with greater than 99% *ee* using the chiral helical diphosphane ligand 2,15-bis(diphenylphosphanyl)hexahelicene **92** (Scheme 3.3).

Chiral imidazolium imine **93** has been used as a bidentate ligand in the presence of a base in this Pd-catalysed reaction to afford **P1** in greater than 99% yield and 92% *ee* (Scheme 3.3).[7] The use of other types of bidentate N,N ligands, such as optically active C_2-symmetric bisoxazoline ligand **94** [8]and diamine ligand **95** [9], was also described in this reaction to afford the **P1** in excellent enantioselectivity (*ee* up to 98% and 99%, respectively).

Bidentate N,P ligands, such as **96**,[10] **97**,[11] and **98**[12], were also applied in the Pd-allylic alkylation of *rac*-**S1** affording the **P1** in high enantioselectivity (*ee* up to 99%).

In a similar manner, the combination of the amide carbonyl group with a phosphite lead to the development of the bidentate P,O ligand **99** (Scheme 3.3), which provided the **P1** in excellent enantioselectivity (*ee* up to 97%) in the Pd-allylic alkylation of *rac*-**S1**.[13]

Bidentate phosphorus ligands (Scheme 3.3), such as the axially chiral biphenyl **100**[14], the ferrocene-diphosphine **101**[15], the C_2-symmetric bisphosphine with a cyclobutane backbone **102**[16], the bis-phospholane ligands **103**[17, 18] and **104**[17], the bis-(amidephosphine) **105**[19] and bis-(oxazolinephosphine) **106**[20], furnished also high the **P1** enantioselectivities (*ee* up to 99%) in the Pd-catalysed reaction *rac*-**S1**.

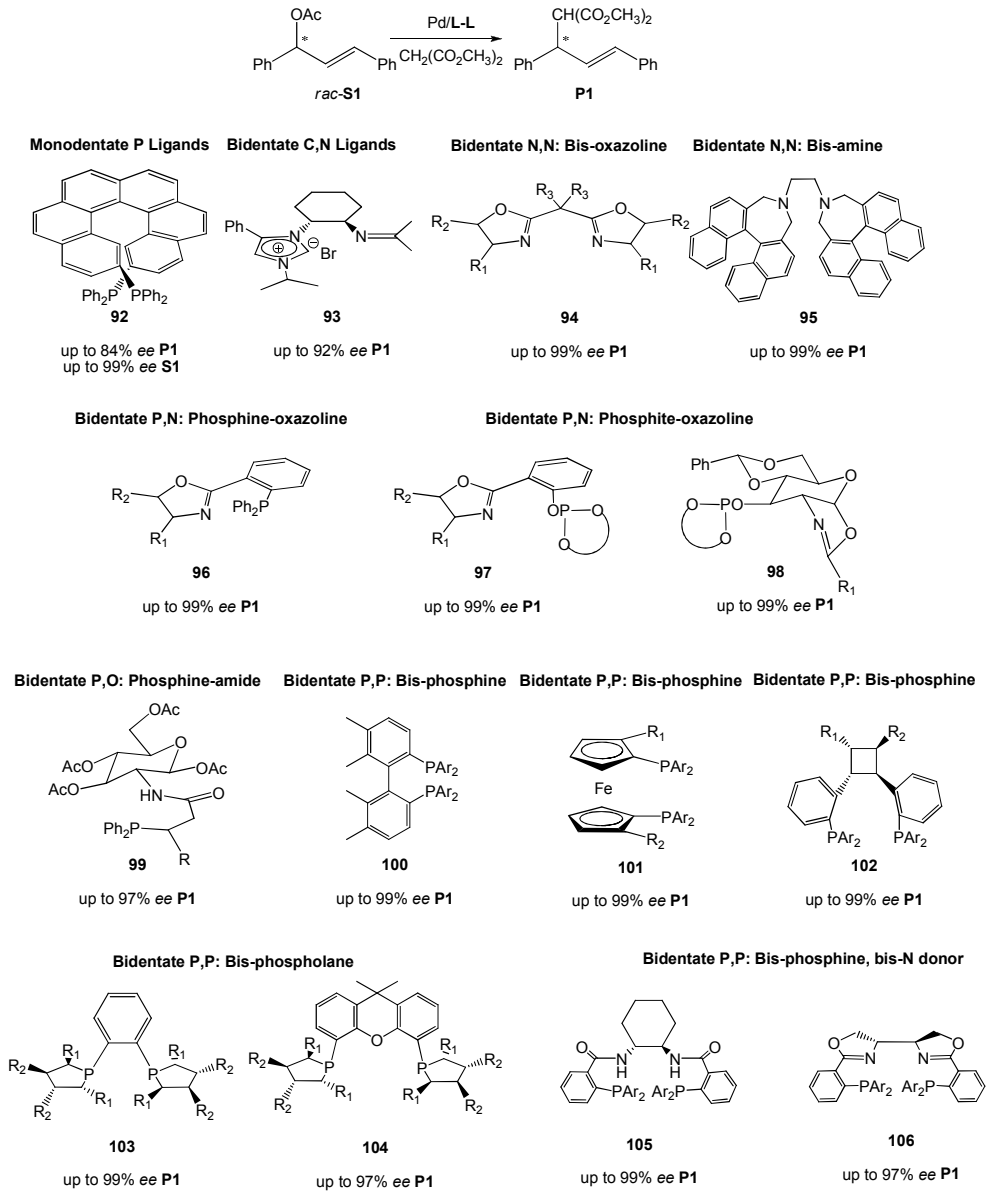

Scheme 3.3. Pd-asymmetric allylic substitution of *rac*-1,3-diphenyl-3-acetoxy-propen-1-ene (*rac*-**S1**) using dimethyl malonate as nucleophile and the ligand **92**-**106**.

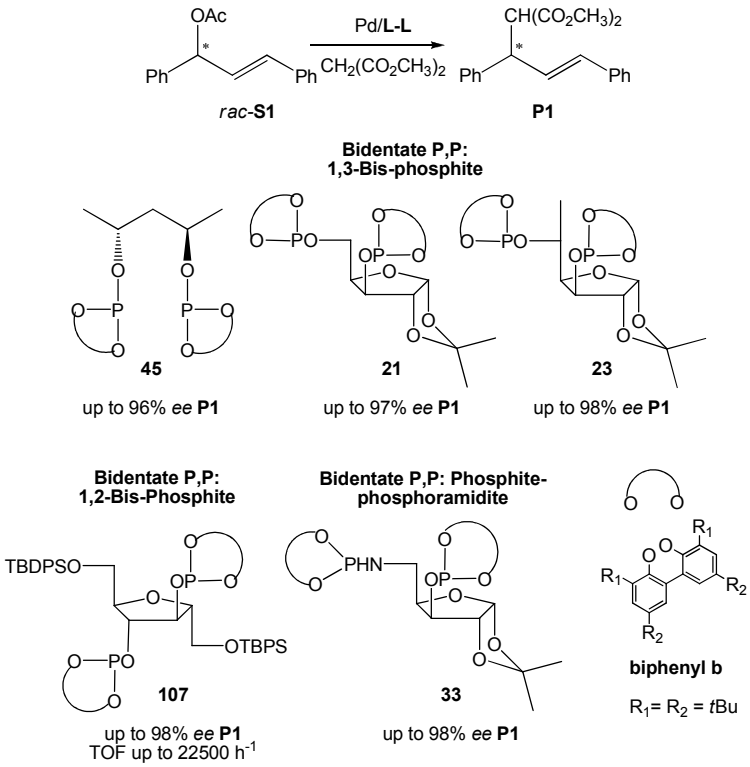

Scheme 3.4. Pd-asymmetric allylic substitution of *rac*-**S1** using dimethyl malonate as nucleophile and the diphosphite ligands **21b**, **23b**, **45b** and **107b**.

Diphosphite ligands, such as (*2R*,*4R*)-pentanediol derived ligand **45b**[21], C_1-symmetric carbohydrate derived ligands **21b**[22a] and **23b**[22b], and C_2-symmetric carbohydrate derived ligands **107b** [23], provided excellent enantioselectivities in Pd-asymmetric allylic substitution *rac*-**S1** using dimethyl malonate as nucleophile (*ee* up to 98%) (Scheme 3.4). Furthermore, the ligand **107b** provided the highest TOF value (up to 22500 h^{-1}) reported for this reaction.[23] Finally, the phosphite-phosphoramidite ligand **33** provided also excellent enantioselectivities in this reaction (Scheme 3.4).[24]

3.3.2 Pd-allylic substitution of monosubtituted linear substrates.

In allyl systems (Scheme 3.5) bearing two identical geminal substituents at one of the termini, such as substrates **S2** and **S3**, π-σ-π isomerisation can

results in a racemisation of the allyl-palladium intermediate. The relative rates of π-σ-π isomerisation and nucleophilic attack at the allyl system are of crucial importance for the stereochemical course of the allylic substitution with this type of substrates.

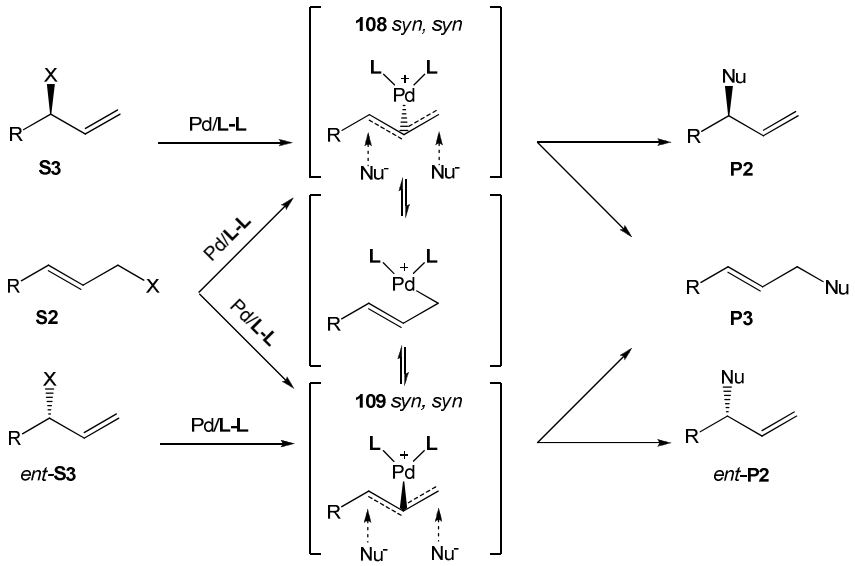

Scheme 3.5. Pd-asymmetric allylic substitution of racemic 3-substitued and achiral 1-substitued linear allyl derivates.

If π-σ-π isomerisation is fast compared to nucleophilic attack, the use of achiral **S2** or *rac*-**S3** compound gives the same equilibrium mixture of allyl intermediates **108** and **109**. [2,3] If a chiral palladium catalyst is used the intermediates **108** and **109** were diastereisomers , where either the more abundant (assuming similar rates of nucleophilic attack step) or the more reactive diastereisomeric complex leads the product (**P2**, *ent*-**P2** or **P3**). In this case, nucleophilic attack is the turnover-limiting and selectivity-determining step.

If the interconversion of the π-allyl intermediates **108** and **109** is much slower than nucleophilic attack, the product (**P2**, *ent*-**P2** and **P3**) distribution depends on the nature of the substrate. [2,3] In the case of the *rac*-**S3**, the two enantiomers of this chiral substrate are converted to the corresponding enantiomers with overall retention of configuration, and therefore the product was obtained as a racemic mixture (*rac*-**P2**).

However, the analogous reaction of the achiral **S2** can be rendered enantioselective if a chiral catalyst reacts preferentially to one of the enantiotopic faces of the substrate to give either complex **108** or **109**. In this case, the enantioselectivity is determined in the oxidative addition of the substrate to the catalyst while nucleophilic addition to the Pd(II)-π-allyl intermediate **108** or **109** is irrevelant for the enantiomeric excess of the overall reaction. The relative rates of π-σ-π isomerisation and the other processes shown in Scheme 3.5 strongly depend on the reaction conditions and, therefore, proper choice of the reaction parameters can be crucial for achieving satisfactory enantioselectivity.

In addition to enantiocontrol, the lack of regiocontrol is often a problem with these substrates; in general linear product rather than or together with the branched isomers. [1,25] There are various factors that influence the regioselectivity of allylic substitutions. Electronic effects exerted by the catalyst and the allylic substituents, steric interactions between the nucleophile, the allyl system and the catalyst, and the relative stabilities of the Pd(0)-π-olefin complexes formed after nucleophilic addition, can all play a role. The relative importance of these factors varies with the catalyst, the substrate, the nucleophile, the solvent and other reaction parameters and is difficult to predict.

Formation of Chiral-Branched Product

Although palladium catalyst usually favour the formation of the linear product, [26,27] several specially designed ligands have been tested for their ability to achieve the enantioselective formation of the chiral branched products **P2** or *ent*-**P2**.

Hayashi et al. described the selective modification of the sterically bulky monophosphine ligand **110** (Scheme 3.6), and the application of this ligand in the Pd-allylic alkylation of racemic mixtures of *rac*-**S3** derivates, where R= 4-MeO-C_4H_6, using dimethyl malonate as nucleophile to afford branched product as the mayor product and with high enantioselectivity (*ee* up to 87%).[28]

In addition, the chiral oxazoline ligand **97** provided good regio- and enantioselectivities in the Pd-allylic alkylation of *rac*-**S3** and achiral **S2** substituted linear derivates, where R= 1´-naphthyl, using dimethyl

malonate as nucleophile (Scheme 3.6 and 3.7, respectively). However, low regioselectivities were observed for other substrates with R= 2-naphthyl, phenyl, methyl, or $(CH_3)_3C$=CH. [11,29]

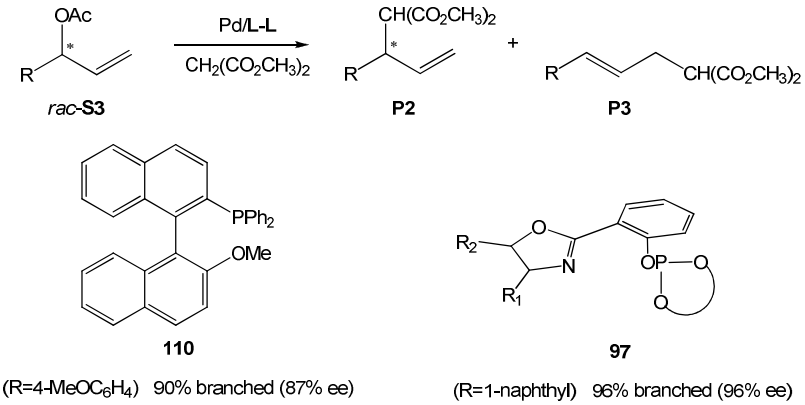

Scheme 3.6. Pd-asymmetric allylic substitution of *rac*-**S3** derivates using dimethyl malonate as a nucleophile and ligands **97**, **110**.

Finally, the ligand **111** produced high regio- and enantioselectivity in the in the Pd-allylic alkylation of achiral **S2** derivates, where R= 1´-naphthyl or methyl, using dimethyl malonate as a nucleophile (Scheme 3.7).[30]

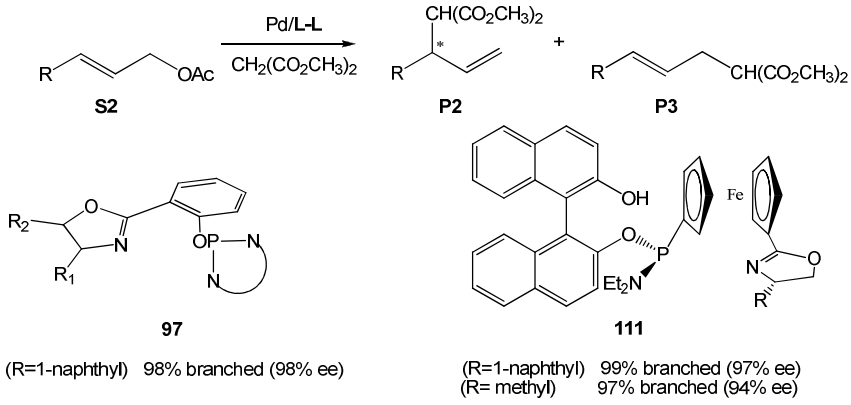

Scheme 3.7. Pd-asymmetric allylic substitution of achiral **S2** derivates using dimethyl malonate as a nucleophile and ligands **97**, **111**.

Although enantiocontrol combined with regiocontrol in favour of the chiral branched product is still a problem, recent progress in this area is encouraging. It has been shown that the regioselectivity in Pd-allylic alkylation of *rac*-**S3** and achiral **S1** derivates can be reversed by using of less electron-donating ligands, which render the palladium center more electrophilic.

Recently, new catalytic systems based on iridium and rhodium catalysts were tested in the allylic alkylation of these types of substrates (Scheme 3.8 and 3.9). The Ir-**112** catalytic system produced high enantioselectivity with total regioselectivity to **P2** in the allylic alkylation of *rac*-**S3** derivates, where R=CH_2CH_2Ph,[31] and the Ir-**97** provided total regioselectivity with excellent enantioselectivity in the allylic alkylation of achiral **S1** derivates, where R=4-$MeOC_6H_4$ (Scheme 3.8). [32]

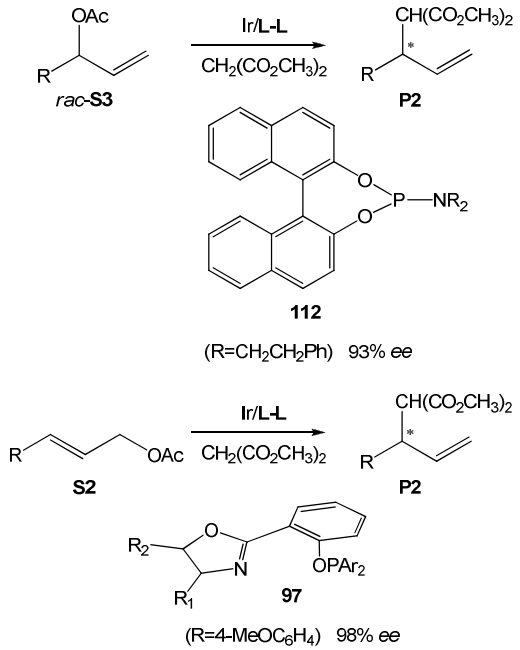

Scheme 3.8. Ir-asymmetric allylic substitution of *rac*-**S3** and achiral **S2** derivates using dimethyl malonate as a nucleophile and ligands **112** and **97**, respectively.

UNIVERSITAT ROVIRA I VIRGILI
1,3- DIPHOSPHITE LIGANDS WITH FURANOSIDE BACKBONE: A POWERFUL TOOL IN ASYMMETRIC CATALYSIS
Aitor Gual Gozalbo
DL: T-1535-2009/ISBN: 978-84-692-4554-5

The Rh-**113** catalytic system produced high regioselectivity and excellent enantioselectivity in the allylic alkylation of *rac*-**S3** derivates, where R=Ph, 4-$MeOC_6H_4$, 4-$CF_3C_6H_4$, 4-ClC_6H_4 (Scheme 3.9).[33]

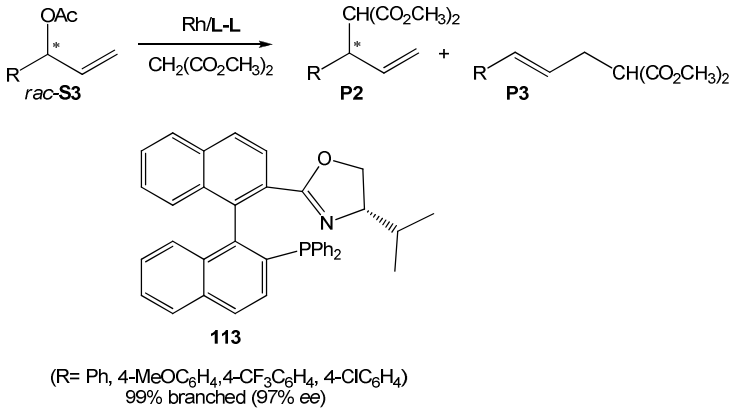

Scheme 3.9. Rh-asymmetric allylic substitution of *rac*-**S3** derivates using dimethyl malonate as a nucleophile and ligands **113**.

Formation of "Chiral"-Linear Product

The high selectivity of the Pd-catalyst towards the linear product is a disadvantage in order to obtain the chiral branched product, but is possible to form a "chiral" linear product with high regioselectivity by the use of the pro-chiral nucleophile or a racemic mixture.

Pd-allylic alkylation of **S2** derivates, where R= Ph, using racemic mixture of keto-steres compounds as nucleophiles in presence of ligand **114** afforded the chiral linear product derivate with high enantioselectivity (*ee* up to 92%) (Scheme 3.10).[34]

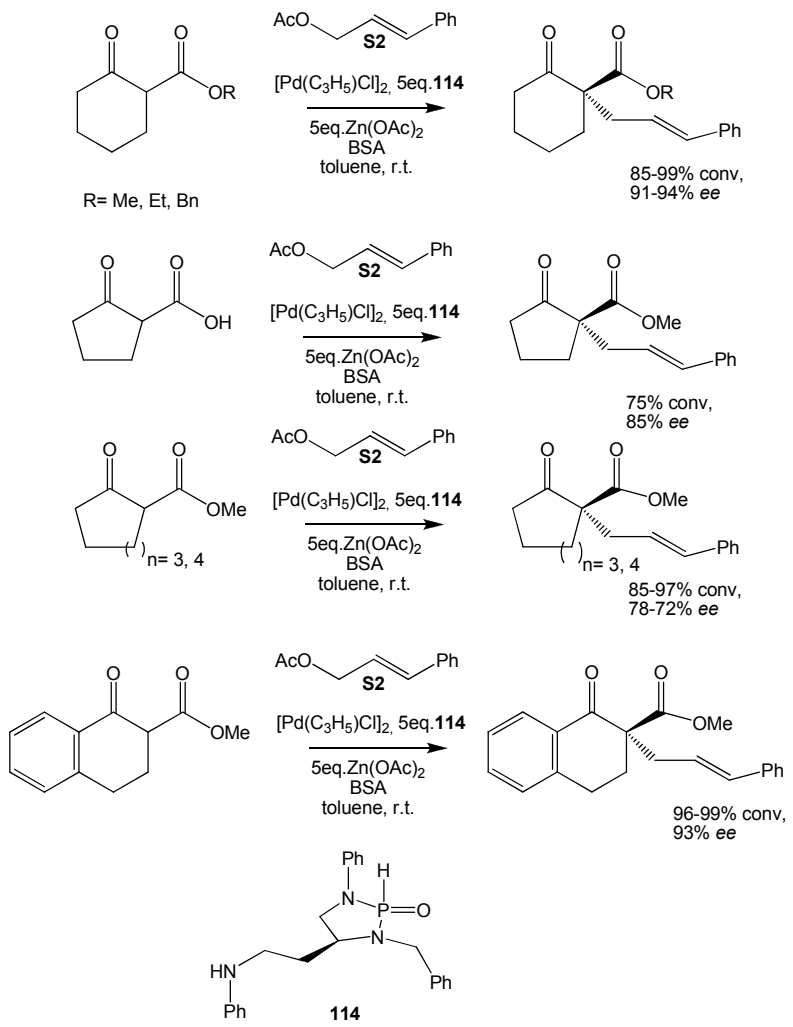

Scheme 3.10. Pd-asymmetric allylic substitution of achiral **S2** linear using β-keto ester as a nucleophile and ligand **114**.

Pd-allylic alkylation of **S2** derivates, where R= Ph, using racemic mixture of imine compounds as nucleophiles in presence of ligand **115** afforded the chiral linear product derivate with high enantioselectivity (*ee* up to 96%) (Scheme 3.11).[35]

The use of phosphorous ligands, such as (*R*)-BINAP **116**, was also reported in the Pd-allylic alkylation of **S2** derivates, where R= Ph, using racemic mixture of α-keto amines and using β-diketones as nucleophiles to afford

the chiral linear product derivate with high enantioselectivity (*ee* up to 88%) (Scheme 3.12) [36,37].

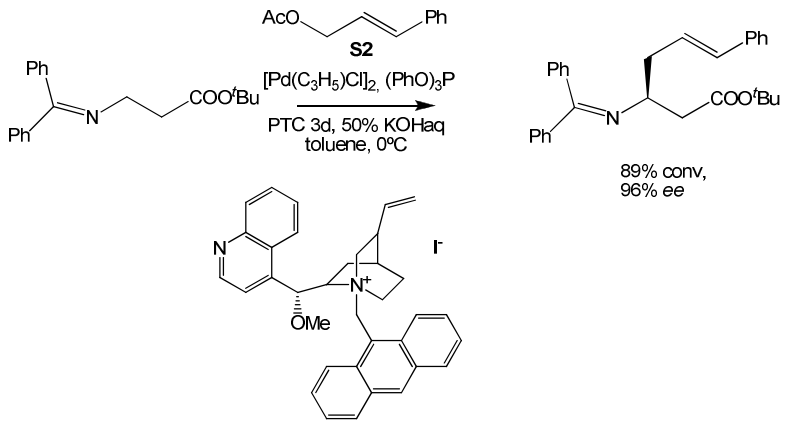

Scheme 3.11. Pd-asymmetric allylic substitution of achiral **S2** derivates using imine compounds as a nucleophile and ligand **115**.

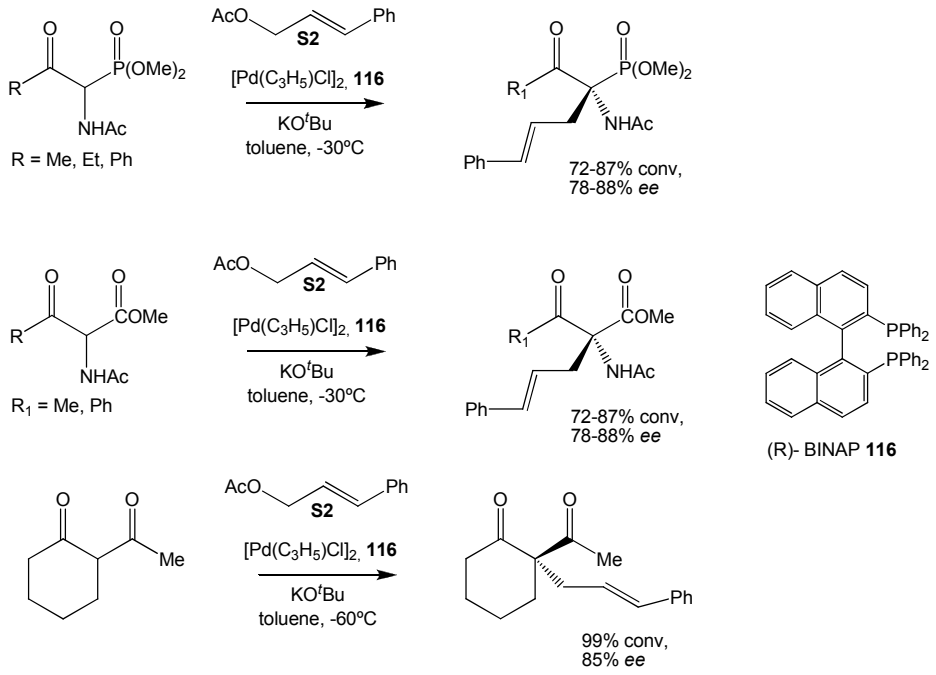

Scheme 3.12. Pd-asymmetric allylic substitution of achiral **S2** derivates using α-keto amines and β-diketones as a nucleophile and ligand **116**.

3.4. Results and Discussion.

As previously mentioned in the introduction, the use of 1,3-diphosphite ligands **21b** and **23b**, related to our new series of ligands, in the Pd-allylic alkylation of **S1** provided **P1** with high activities and with excellent enantioselectivity (See Scheme 3.4).

The new 1,3-diphosphite were applied in the Pd-allylic alkylation of **S1** using dimethyl malonate as a solvent in order to gain information about the effect of the structural modification of the ligand on the catalytic results. Futhermore, the ligands series were applied in the Pd-allylic alkylation of **S2** using dimethyl malonate as a nucleophile to obtain **P2** and using α-(ethoxycarbonyl)-cyclohexanone. The reaction conditions were optimized using the most promising catalytic system and varying the reaction parameters.

Pd-allylic alkylation provides easy access to chiral compounds. Searching the best C-1 symmetric furanoside diphosphite ligand for these reactions.

A. Gual, S. Castillón, O. Pàmies, M. Diéguez, C. Claver, manuscript in preparation.

Summary

C1-symmetrical diphosphite ligands derived from carbohydrates were applied in the Pd-allylic alkylation of mono-and di-substituted substrates. The catalytic results suggested that the use of monocyclic backbones, such as 6-deoxy-2-*O*-alkyl-glucofuranoside, the introduction of substitutes in the C-6 produced a great effect on the catalytic results. The reaction parameters were studied and optimised by varying the solvent, the Pd to substrate ratio and the Pd to ligand ratio. In the Pd-asymmetric allylic alkylation of *rac*-**S1**, the ligands **65a** and **67b** produced excellent enantioselectivities in **P2** (ee up to 98.4% and 95%, respectively) with excellent kinetic resolution of **S1** (ee 95% and 99.9%, respectively). In the case of the **S2** using dimethyl malonate as a substrate low regioselectivities with good enantioselectivities were obtained. For this reaction, the best results were obtained using ligands **21b**, **87b** and **89b**, obtaining regioselectivities up to 20% with good enantioselectivities (*ee* up to 83%). Even more, these ligands were tested in the Pd-allylic alkylation of **S2** using α-(ethoxycarbonyl)-cyclohexanone as a nucleophile obtaining high regioselectivities with moderate enantioselectivities (ee up to 38%). It is noteworthy, that in this reaction the enantioselectivity is induced in the nucleophile skeleton. Additionally, the use of a new phosphite moiety containing a carbon bridge between the two phenyl groups was revealed to be inefficient in the Pd-allylic alkylation of these two substrates. Finally, the complexes $[Pd(\eta^3\text{-}C_3H_5)(L)]PF_6$, L = **65b** and **67b**, were synthesised and characterised by NMR spectroscopy confirming the presence of a equilibrium between the *endo* and *exo* species.

Design and synthesis of series of 1,3-diphosphite ligands

The use of chiral 1,3-diphosphite ligands provided excellent results in the Pd-allylic alkylation of 1,3-diphenyl-3-acetoxy-propen-1-ene **S1** using dimethyl malonate as nucleophile (Scheme 3.13).[22]

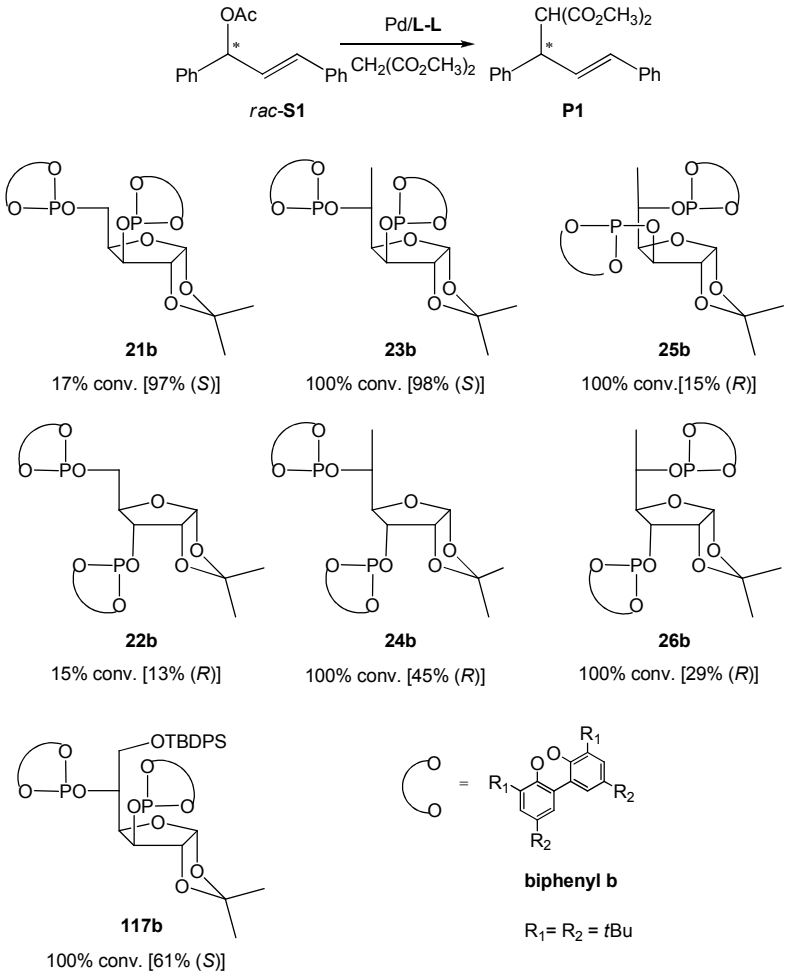

Scheme 3.13. Pd-asymmetric allylic substitution of *rac*-**S1** using dimethyl malonate as a nucleophile and ligand **21-26b** and **117b**. Reaction conditions: 0.5 mol % $[PdCl(\eta^3\text{-}C_3H_5)]_2$; Pd/L = 1: 1.1: CH_2Cl_2 as solvent; t= 5min.

Previously, the effect of the carbon stereocenters (C-3 and C-5) directly bonded to the phosphite function were studied and described. It was observed that the ligands with a *xylo*- (**21b** and **23b**) configuration

UNIVERSITAT ROVIRA I VIRGILI
1,3- DIPHOSPHITE LIGANDS WITH FURANOSIDE BACKBONE: A POWERFUL TOOL IN ASYMMETRIC CATALYSIS
Aitor Gual Gozalbo
DL: T-1535-2009/ISBN: 978-84-692-4554-5

provided the best results in terms of enantioselectivity (Scheme 3.13). [22] Furthermore, the ligand **23b** (methyl group in C-5) produced higher activities than ligand **21b**.

It is noteworthy that the ligand **117b**, related to **21b** and **23b**, which incorporates the bulky substituent OTBDPS (*t*butyl-di-phenyl-silylether) in the C-6 position of the carbohydrate backbone produced lower enantioselectivities with comparable activities to the ligand **23b**.

Therefore, new ligands 1,3-diphosphite ligands with furanoside backbone were designed and synthesised (Section 2.4.1. and 2.4.2). The main structural features of these new ligands are the following (Figure 3.1): a) higher substitution at position 6 of the sugar to increase the steric hindrance in the proximity of the coordinating phosphorus atom (**64**-**66**) to study more accurately the effect of this position on the catalytic results, b) absence of 1,2-*O*-isopropylidene ring in order to increase the conformational freedom (**67**, **87**, **89**) to understand the effect of the bicyclic backbone on the catalytic results, and c) new diol skeleton in the diphosphite moieties (see diol **w** in Figure 3.1) that will provide a different environment around the palladium center.

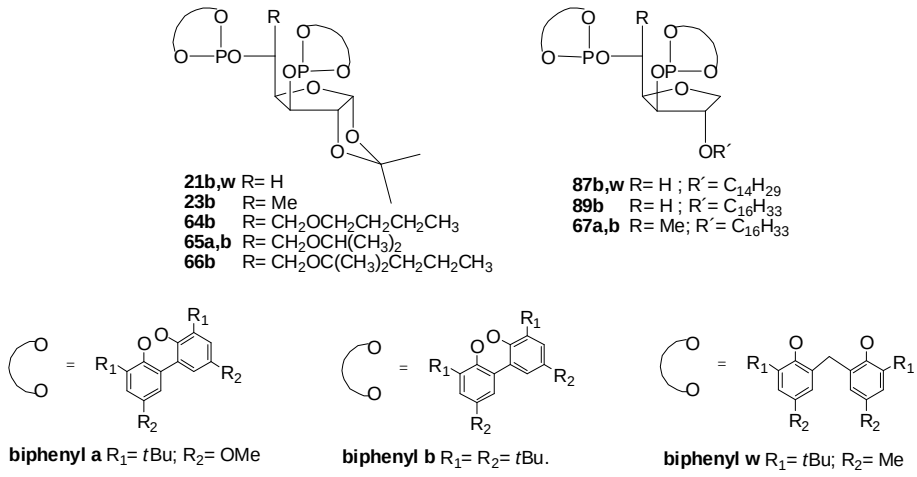

Figure 3.1. 1,3-diphosphite ligands applied in Pd-allylic alkylation.

The synthesised 1,3-diphosphite ligands were applied in the Pd-allylic alkylation of *rac*-1,3-diphenyl-3-acetoxy-propen-1-ene (*rac*-**S1**) and 1-phenyl-3-acetoxypropene (**S2**) using dimethyl malonate as a nucleophile.

UNIVERSITAT ROVIRA I VIRGILI
1,3- DIPHOSPHITE LIGANDS WITH FURANOSIDE BACKBONE: A POWERFUL TOOL IN ASYMMETRIC CATALYSIS
Aitor Gual Gozalbo
DL: T-1535-2009/ISBN: 978-84-692-4554-5

(Scheme 3.14a and b). The use of α-(ethoxycarbonyl)-cyclohexanone as a nucleophile was also tested because the achiral linear compound is the major product in the Pd-allylic alkylation of **S1**.

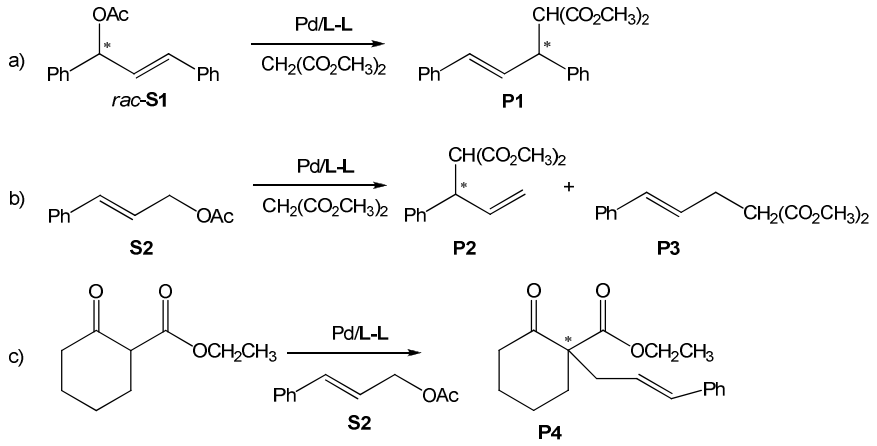

Scheme 3.14. Pd-asymmetric allylic substitution of: a) racemic 1,3-diphenyl-3-acetoxy-propen-1-ene (*rac*-**S1**) using dimethyl malonate as nucleophile, b) achiral 1-phenyl-3-acetoxy-propene (**S1**) using dimethyl malonate as nucleophile, c) achiral 1-phenyl-3-acetoxy-propene (**S1**) using α-(ethoxycarbonyl)-cyclohexanone.

Pd-allylic alkylation of 1,3-diphenyl-3-acetoxy-propen-1-ene

Chiral diphosphite ligands **21b**,**w**, **64b**, **65a,b**, **66b**, **67a**,**b**, **87b**,**w** and **89b** were used in the Pd-catalysed allylic alkylation of *rac*-**S1** using dimethyl manolate as nucleophile (Scheme 3.14a). In all the cases, the catalysts were generated in situ from π-allyl-palldium chloride dimmer $[PdCl(\eta^3\text{-}C_3H_5)]_2$ and the corresponding ligand. The results are summarized in table 3.1, 3.2 and 3.3.

The optimal reaction conditions by conducting a series of experiments using the ligands **65b** and **67b**, related to the most efficient ligand **23b**, in which the solvent, the ligand-to-palladium ratio and the substrate to metal ratio were varied.

Initially, the effect of the solvent was studied. Three solvents [tetrahydrofuran (THF), dichlorometane (DCM) and toluene] and the

catalysts Pd/**65b** and Pd/**67b** were tested at room temperature with a Pd to L ratio of 1:1.1 and substrate to Pd ratio of 100: 1 (Figure 3.2). The best combination of activity and enantioselectivity for both systems was achieved performing the reaction in dichloromethane (Figure 3.2). Interestingly, when Pd/**67b** was tested of toluene kinetic resolution of the substrate was achieved. This behaviour was not observed in the other solvents.

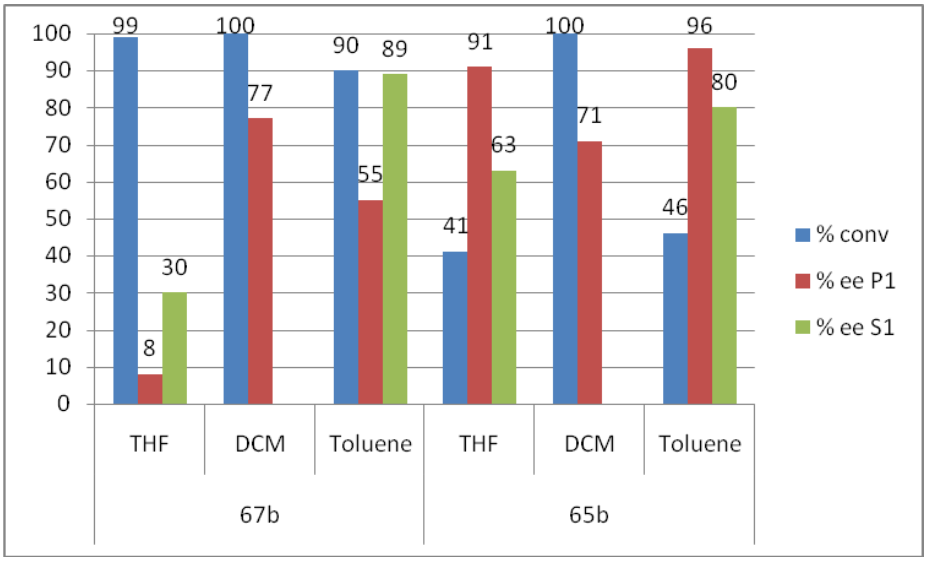

Figure 3.2. Effect of the solvent (THF, CH_2Cl_2 and Toluene) in the Pd-allylic alkylation of 1,3-diphenyl-3-acetoxy-propen-1-ene using dimethyl malonate as a nucleophile and the ligands **65b** and **67b**.

In the case of the catalyst system bearing the ligand **65b** different trends in terms of activity and selectivity were observed. The catalyst Pd/**65b** produced also higher activities when the reaction was performed in DCM than in THF or toluene. However, the enantioselectivity with toluene and THF was higher than in DCM. kinetic resolution of the substrate was observed with this catalytic system using THF or toluene.

These results indicated the great effect of the solvent on the catalytic results using Pd/**65b** and Pd/**67b** systems. According to these results, DCM and toluene were chosen as solvents to perform the optimization of the Pd to L ratio (Tables 3.1 and 3.2, respectively).

Table 3.1. Pd-allylic alkylation of *rac-S1* using dimethyl malonate as a nucleophile, dichloromethane (DCM) as a solvent and the ligands **64b**, **65a,b**, **66b**, **67a**,**b**, **87b**,**w** and **89b**.

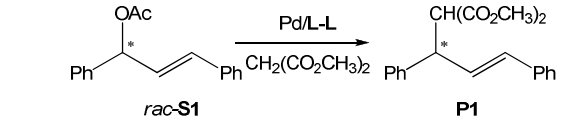

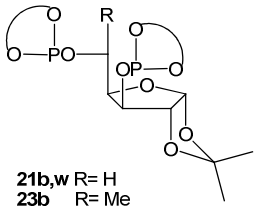

21b,w R= H
23b R= Me
64b R= $CH_2OCH_2CH_2CH_2CH_3$
65a,b R= $CH_2OCH(CH_3)_2$
66b R= $CH_2OC(CH_3)_2CH_2CH_2CH_3$

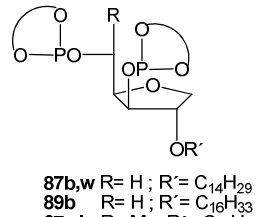

87b,w R= H ; R´= $C_{14}H_{29}$
89b R= H ; R´= $C_{16}H_{33}$
67a,b R= Me; R´= $C_{16}H_{33}$

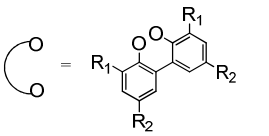

a R_1= t*Bu*; R_2= OMe
b R_1= R_2= *t*Bu.

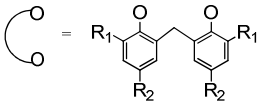

w R_1= *t*Bu; R_2= Me

Entry[a]	Ligand	Pd/L	Conv.(%)[b]	*ee* **P1** (%)[c]	*ee* **S1** (%)[c]
1	**64b**	1:1.1	100	54(*S*)	-
2	**65b**	1:1.1	100	71(*S*)	-
3	**65b**	1:2.0	100	77(*S*)	
4	**66b**	1:1.1	100	29(*S*)	-
5	**67b**	1:0.8	100	60(*S*)	-
6	**67b**	1:1.1	100	78(*S*)	-
7	**67b**	1:2.0	100	84(*S*)	-
8	**67a**	1:2.0	100	86(*S*)	-
9	**89b**	1:2.0	83	87(*S*)	99.9(*S*)
10	**87b**	1:2.0	100	77(*S*)	-
11[d]	**87w**	1:2.0	13	30(*R*)	5(*R*)

[a] All reactions were run at room temperature: 0.5 mol % $[PdCl(\eta^3\text{-}C_3H_5)]_2$; CH_2Cl_2 as solvent; t= 5min. [b] Conversion percentage of 1,3-diphenyl-3-acetoxy-propen-1-ene determined by ^{1}H-NMR. [c] Enantiomeric escesses determined by HPLC on a Chiralcel-OJ column. Absolute configuration given in parenthesis. [d] t = 300 min.

In Table 3.1 are introduced the results obtained in the Pd-allylic alkylation of *rac*-**S1** using the series of 1,3-diphosphite ligands, **64b**, **65a,b**, **66b**, **67a**,**b**, **87b**,**w** and **89b** in dichloromethane as the solvent. First of all, the Pd to L ratio was optimized (Entries 2-3 and 5-7). When the Pd to L ratio was 1:1.1 the ligands **67b** and **65b** provided total conversion with

enantioselectivities up to 78% and 71%, respectively (Entries 2 and 8). The enantioselectivities were improved using L to Pd ratio of 2 (ee up to 84% and 77%, respectively) (Entries 3 and 5). The ligands **64**-**66b** (*ee* 29-70%) substituents in the C-6 position of the glucofuranose backbone produced lower enantioselectivities to those previously reported using ligand **23b** (*ee* up to 98%) (Entries 1-4). [22b] However, the results with the ligand **65b** ($CH(CH_3)_2$) were similar to those reported using ligand **117b** (see scheme 3.13), while the **64b** ($CH_2CH_2CH_2CH_3$) and **66b** ($C(CH_3)_2CH_2CH_2CH_3$) produced lower enantioselectivities (ee up to 54% and 29%, respectively) (Entries 1-4) . These results clearly indicated that increasing the steric hindrance in the coordination sphere of the Pd(II)-π-allyl complex lower has a negative influence in the enantioselectivity.

Therefore, the related ligands **67a**, **87b** and **89b** were tested in the optimized conditions. The ligand **67a**, with MeO-substituents in the *para* positions of the biphenyl phosphite moiety, provided comparable results in terms of activity and enantioselectivity (*ee* up to 86%) than the ligand **67b**, which contains *t*Bu substituents in this positions (Entries 6 vs. 8). Thereafter, the ligand **87b** and **89b**, without substituents at the C5-positions, were tested (Entries 9 and 10). These ligands provided comparable activities and slightly lower enantioselectivities than the ligand **67b**. It has to be noted that the ligand **87w** produced much lower activities and enantioselectivities than ligand **87b**, but curiously the **P1**-enantiomer *R* is the major one (Entries 10 vs. 11). The decrease in the activity observed in the case of the catalytic system Pd/**87w** could be explained because the high steric hindrance caused by the biphenyl moiety **w**.

The behaviour of Pd/-**21b**,**w**, **64b**, **65a,b**, **66b** and **67b** using toluene as a solvent was then studied in order to know was how general was the previously observed kinetic resolution of *rac*-**S1** (Table 3.2).

As expected the catalytic activity was lower by using toluene as a solvent. Initially, the catalytic systems were tested for a Pd to L ratio of 1: 1.1 (Entries 1-3, 5 and 7-9). The ligands **21b** and **67b**, which contain H or Me in C-5, provided high activity with low enantioselectivity in **P1** (ee up 55%, 15% and 57%, respectively) (Entries 1 and 9). The ligand **21w** was tested in this reaction to confirm the behaviour caused by the biphenyl moiety **w** previously observed with the ligand **87w**. As previously observed with

87w, the ligand **21w** produced much lower activities with very low enantioselectivity (Entry 2).

The ligands **64b** provided low conversion (39%) with low enantioselectivity (*ee* up to 56%) (Entry 3). The ligand **66b**, which contain ($C(CH_3)_2CH_2CH_2CH_3$) in C-6, produced also high conversion with very low enantioselectivities (ee up to 15%) (Entry 8).

Table 3.2. Pd-allylic alkylation of *rac*-**S1** using dimethyl malonate as a nucleophile, toluene as a solvent and the ligands **21b**,**w**, **64b**, **65a,b**, **66b** and **67b**.

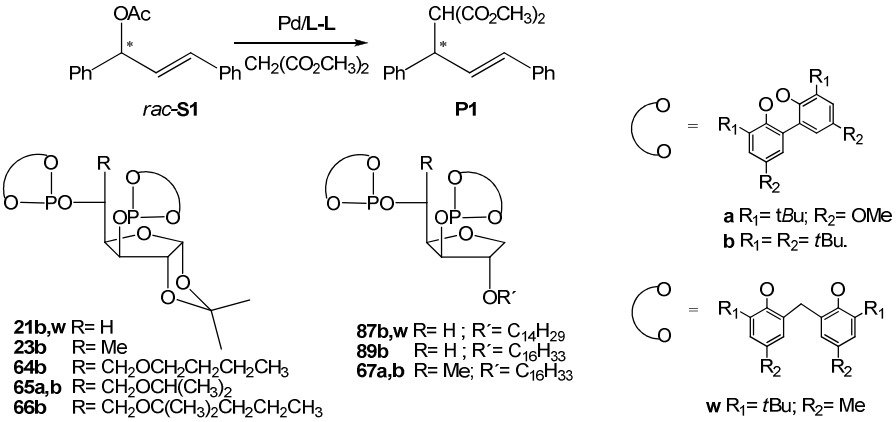

Entry[a]	Ligand	Pd/L	Conv.(%)[b]	*ee* **P1** (%)[c]	*ee* **S1** (%)[c]
1[d]	**21b**	1:1.1	100	57(*S*)	-
2[d]	**21w**	1:1.1	12	7(*R*)	0
3	**64b**	1:1.1	39	56(*S*)	36(*S*)
4	**65b**	1:0.8	33	97(*S*)	45(*S*)
5	**65b**	1:1.1	46	96(*S*)	80(*S*)
6	**65b**	1:2.0	56	94(*S*)	94(*S*)
7	**65a**	1:1.1	53	95(*S*)	99.9(*S*)
8	**66b**	1:1.1	91	15(*S*)	82(*S*)
9	**67b**	1:1.1	90	55(*S*)	89(*S*)

[a] All reactions were run at room temperature: 0.5 mol % $[PdCl(\eta^3\text{-}C_3H_5)]_2$; Toluene as solvent; t= 5min. [b] Conversion percentage of 1,3-diphenyl-3-acetoxy-propen-1-ene determined by ^{1}H-NMR. [c] Enantiomeric escesses determined by HPLC on a Chiralcel-OJ column. Absolute configuration given in parenthesis. [d] t = 300 min.

However, the catalytic systems Pd/**65b** afforded moderate conversion (35%) with comparable with *ee* up to 96% **P1** and unexpected good enantiomeric excess in **S1** (*ee* up to 80%) (Entry 5). These results suggested that the steric hindrance in the coordination sphere of the Pd(II)-π-allyl has a great importance in the activity and in the level of enantioselectivity achieved. Additionally, the Pd to L ratio was optimized in order to gain information about the catalytic active species which produced the enantiodiscrimination of the substrate (Entries 4-6). It was found that the use of the Pd to L ratio of 2 increased the activity with similar enantioselectivity in **P1** (*ee* up to 94%) and improved the enantiomeric excess of the **S1** (*ee* up to 94%). Furthermore, the ligand **65a** was tested in the same conditions than **65b** in order to test the effect of the electronic properties of the phosphorous ligands (Entries 4 vs. 6). By using ligand **65a** comparable conversion (up to 53%) and enantioselectivities in **P1** were achieved (*ee* up to 95%). Interestingly, the use of ligand **65a** improved the enantiomeric excess of **S1** (*ee* up to 99.9%).

In conclusion, the catalytic activity, the *ee* of **P1** and enantiodiscrimination of **S1** were highly affected by the steric and the electronic properties of the ligand, the palladium to ligand ratio and the solvent. Therefore, high dilution experiments were carried out to complete the study of the use of these series of diphosphite ligands in the Pd-allylic alkylation of *rac*-**S1** and to gain information about the enantiodiscrimination processes. These experiments were performed by using the ligand **65b** and **67b**, which provided the most promising results, in dichloromethane as a solvent with a Pd to L ratio of 2. The results of this study were shown in table 3.3.

In presence of 0.1% of catalyst Pd/**65b** a conversion of 43% was achieved with excellent enantioselectivity in **P1** (*ee* up to 97%) and low in **S1** (*ee* up to 30%) (Entry 1). Increasing the reaction time to 90 min, conversions and enantioselectitivities were not significantly improved (Entry 2). The catalytic system was still active when a 0.01% of catalyst was used. The enantioselectivity in **P1** (*ee* up to 99.9%) was excellent after 15 min but that in **S1** (*ee* up to 20%) was very low (Entry 3). After 90 min the conversion achieved was 43% with excellent enantioselectivity in **P1** (*ee* up to 95%) and moderate in **S1** (*ee* up to 80%) (Entry 4).

When the reaction was performed in presence of 0.1% of catalyst Pd/**67b** conversion was 51% after 90 minutes with an excellent enantioselectivity

of **S1** (*ee* up to 95%) and in **P1** (*ee* up to 98.4%) (Entries 5 and 6), as a consequence fo an highly efficient kinetic resolution. The reaction was also performed in presence of 0.01% of catalyst Pd/**67b** achieving similar results in terms of enantioselectivity in **S1** (*ee* up to 94%) and in **P1** (*ee* up to 90%) (Entries 7 and 8).

Table 3.3. Pd-allylic alkylation of *rac*-**S1** using dimethyl malonate as nucleophile and the ligands **65b** and **67b**. Pd to L ratio.

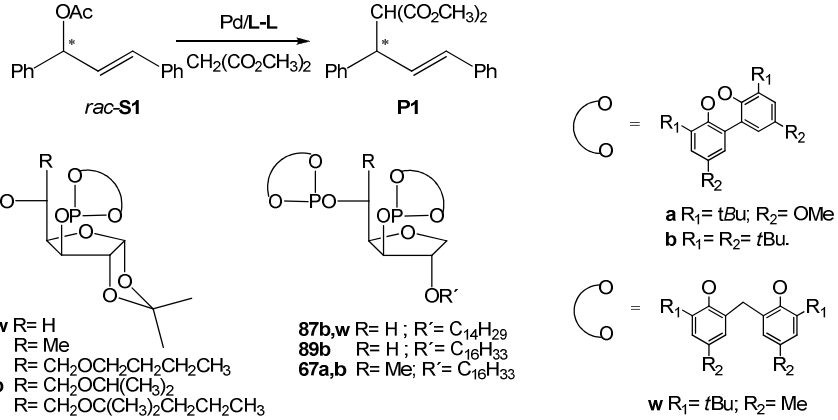

Entry[a]	Ligand	**S1**/Pd	t (min)	Conv. (%)[b]	*ee* **P1**(%)[c]	*ee* **S1**(%)[c]
1	**65b**	1000:1	15	43	97(*S*)	30(*S*)
2	**65b**	1000:1	90	45	93(*S*)	42(*S*)
3	**65b**	10000:1	15	31	99.9(*S*)	20(*S*)
4	**65b**	10000:1	90	43	95(*S*)	80 (*S*)
5	**67b**	1000:1	15	45	96(*S*)	73(*S*)
6	**67b**	1000:1	90	53	98.4(*S*)	95(*S*)
7	**67b**	10000:1	15	25	90(*S*)	16(*S*)
8	**67b**	10000:1	90	56	85(*S*)	94(*S*)

[a] All reactions were run at room temperature: Pd/L = 1: 2.0; CH_2Cl_2 as solvent. [b] Conversion percentage of 1,3-diphenyl-3-acetoxy-propen-1-ene **S1** determined by ^{1}H-NMR. [c] Enantiomeric escesses determined by HPLC on a Chiralcel-OJ column. Absolute configuration given in parenthesis.

In conclusion, .the systems Pd/**65b** (Table 3.2, Entry 6) and **67b** (Table 3.3, Entry 6) are excellent kinetic resolution catalyst for the Pd-alkylation of *rac*-**S1** using dimethyl malonate as nucleophile.

Pd-allylic alkylation of 1-phenyl-3-acetoxy-propen-1-ene

The chiral diphosphite ligands **21b**,**w**, **23b**, **64b**, **65a,b**, **66b**, **67a**,**b**, **87b**,**w** and **89b** were tested in the Pd-catalysed allylic alkylation of 1-phenyl-3-acetoxy-propen-1-ene **S2** using dimethyl manolate and α-(ethoxycarbonyl)-cyclohexanone as nucleophiles (Scheme 3.15b and 3.15c, respectively). In all the cases, the catalysts were generated in situ from π-allyl-palldium chloride dimmer $[PdCl(\eta^3\text{-}C_3H_5)]_2$ and the corresponding ligand. The results are summarized in tables 3.4 and 3.5.

We first studied the effect of the solvent in the Pd-allylic alkylation of **S2** using dimethyl malonate as nucleophile. The catalytic system Pd/**65b** and Pd/**67b** were tested to test three different solvents [tetrahydrofuran (THF), dichlorometane (DCM) and toluene] at room temperature with a Pd to L ratio of 1:1.1 and substrate to Pd ratio of 100: 1 (Figure 3.3). The reactions were monitorized and they were stopped at total conversion. As observed in the Pd-allylic alkylation of **S1**, also in this case the solvent has a high effect in the activity of the catalyst system. The Pd-catalyst provided lower selectivities to the chiral branched product in agreement with the reported for this reaction with palladium catalyst. In our case the higher regioselectivity to the branched product was 27% using ligand 65b in toluene as a. In general, the regioselectivity was better in DCM and toluene than in THF. However, much higher enantioselectivities were obtained by using THF as a solvent (*ee* up to 82%) than those obtained in DCM (*ee* up to 11%) or toluene (*ee* up to 7%).

In conclusion, the solvent highly affected the reaction parameters. When the reaction was carried out in toluene and DCM higher activities and regioselectivities were achieved, but enantioselectivities were higher driving the reaction in THF. Therefore, THF was selected as a solvent to test the reaction using diphosphite ligands **21b**,**w**, **23b**, **64b**, **65a,b**, **66b**, **67a**,**b**, **87b**,**w** and **89b**. The results are collected in Table 3.4.

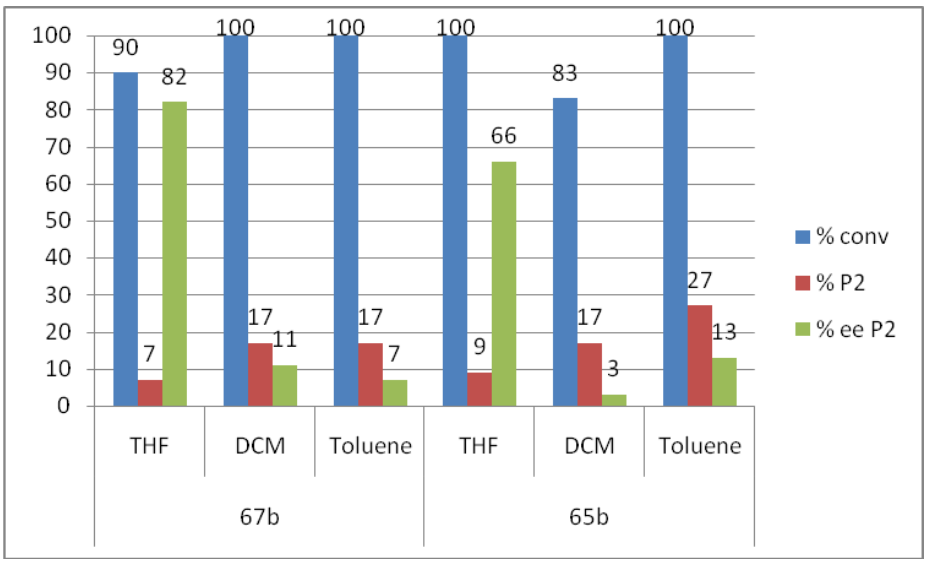

Figure 3.3. Pd-allylic substitution of 1-phenyl-3-acetoxy-propene **S2** using dimethyl malonate as a nucleophile and the Pd-catalyst bearing the ligands **65b** and **67b**. Effect of the solvent (THF, DCM and Toluene).

Two ligands, **21w** and **87w**, containing the diphosphite moiety **w** were tested in this case since it was expected that this bulky phosphite unit would worked better in this less hindered substrate. However, the behaviour was similar than for substrate **S1**, since very low conversions and enantioselectivities were obtained (Entries 2 and 11). Other wise the reaction was completed in 2-4 h with the other ligands. Curiously, ligands **65a** and **67a** (Entries 6, 9), containing the diphosphite moiety **a** produced moderate conversions.

Regioselectivities were low, ranging between 15-20% in the better cases. Concerning the effect of substituents at position C-6, more bulky ligands as **65b** and **66b** (Entries 5, 8) provided lower regioselectivities. Higher flexibility in the backbone had not a clear influence in the regioselectivity (Entries 8-11).

The enantioselectivity followed a similar trend than conversion. Ligands with diphosphite moiety **b** provided moderate enantioselectivities using ligands **23b** and **64b**, and moderate to high ee using ligands **21b**, **65b**, **66b**, **67b**, **87b** and **89b**(Entries 1, 3, 4, 5, 7, 8, 10 and 11). Curiously, the best *ee* was obtained with the less hindered ligand, **21b**. The influence of

other structural modifications was less significant. Thus. the more flexible ligands **67b**, **87b** and **89b** (Entries 8, 10 and 11), that have not the C-6 or is a methyl, provided enantioselectivities similar to **21b**.

Table 3.4. Pd-allylic alkylation of **S2** using dimethyl malonate as a nucleophile and the ligands **21b**,**w**, **64b**, **65a,b**, **66b**, **67a,b**, **87b**,**w** and **89b**.

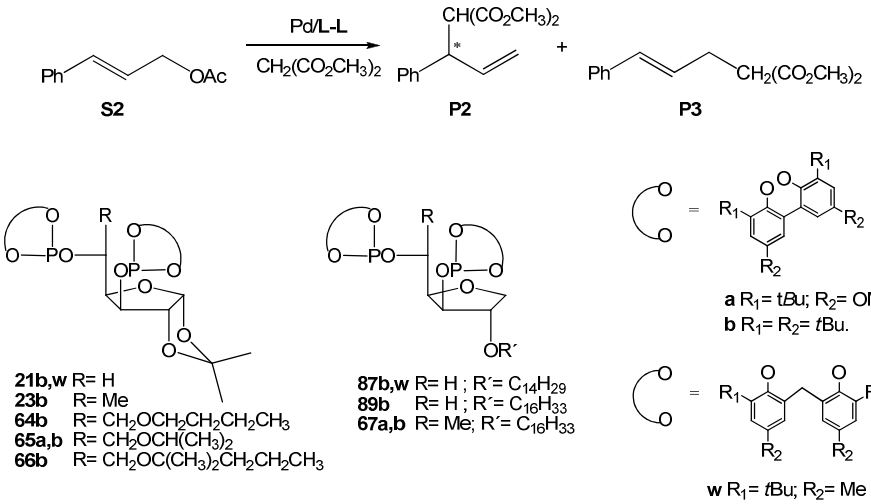

Entry[a]	Ligand	Time (h)	Conv.(%)[b]	**P2** (%)[c]	*ee* **P2**(%)[d]
1	**21b**	4	84	14	83
2	**21w**	24	55	11	-
3	**23b**	4	75	14	17
4	**64b**	4	94	20	34
5	**65b**	4	100	9	66
6	**65a**	4	60	17	17
7	**66b**	4	100	10	73
8	**67b**	2	90	7	82
9	**67a**	2	60	13	2
10	**89b**	2	75	17	79
11	**87b**	2	70	15	77
12	**87w**	24	25	15	-

[a] All reactions were run at room temperature: 0.5 mol % $[PdCl(\eta^3\text{-}C_3H_5)]_2$; Pd/L = 1: 1.1; THF as solvent. [b] Conversion percentage of 1-phenyl-3-acetoxy-propene determined by 1H-NMR. [c] Regioselectivity to the branched product determined by ^{1}H-NMR. [d] Enantiomeric escesses determined by HPLC on a Chiralcel-OJ column.

The best results in the Pd-allylic alkylation of **S2** using dimethyl malonate as the nucleophile were reported using bidentate ligand containing very different coordinating functions.[11, 28-30] Our results are in agreement with this observation, since the best enantioselectivities were obtained with ligands **21b**, **87b** and **89b** (*ee* up to 83%), which present the higher difference in bulkiness between positions C-3 and C-5.

Given the high preference for the formation of the achiral linear product in the Pd-allylic alkylation of **S2** using dimethyl malonate, we considered to use α-(ethoxycarbonyl)-cyclohexanone as nucleophile because it offered the possibility of inducing chirality in the nucleophilic moiety. Firstly, we studied the effect of the solvent.

Also in this case, three solvents [tetrahydrofuran (THF), dichlorometane (DCM) and toluene] were tested at room temperature with a Pd to L ratio of 1:1.1, substrate to Pd ratio of 100: 1 and using the catalyst Pd/**65b** (Figure 3.4). The reaction was monitorized and the effect of the solvent in the activity was also observed. The order of activity determined agrees with the previous observed in this article. Thus, total conversion was achieved in 1 h when the reaction was conducted in DCM, 4 h in toluene and in this time the conversion in THF was only 20% (Figure 3.4). Total regioselectivity to the linear product **P4** was achieved in the tree solvents.

However, only moderate enatioselectivities were achieved by using DCM and toluene, and very low enantioselectivity was obtained by in THF. Therefore, DCM was chosen as a solvent because provided the best combination of activity and selectivity.

In a previous work, Nemoto et al. proved that the use of acetate salt as additive influenced the enantioselectivity. The enantioselectivity increases in the order: Zn^{2+}> Mg^{2+} > Li^{+}.[34] Then, three additives, $Zn(OAc)_2$, KOAc and NaOAc, were tested (Figure 3.5). As observed Nemoto et al., the use of $Zn(OAc)_2$ derivates provided higher enantioselectivity (*ee* up to 30%) than KOAc and NaOAc (*ee* up to 20%).

In conclusion, the solvent and the additive used affected the activity and the enantioselectivity of the reaction, and the best combination was achieved by using DCM as a solvent and $Zn(OAc)_2$ as the additive. Then, the series of ligands **21b**, **23b**, **64b**, **65b**, **66b**, **67b** and **89b** were tested in this reaction in the optimized parameter conditions.

UNIVERSITAT ROVIRA I VIRGILI
1,3- DIPHOSPHITE LIGANDS WITH FURANOSIDE BACKBONE: A POWERFUL TOOL IN ASYMMETRIC CATALYSIS
Aitor Gual Gozalbo
DL: T-1535-2009/ISBN: 978-84-692-4554-5

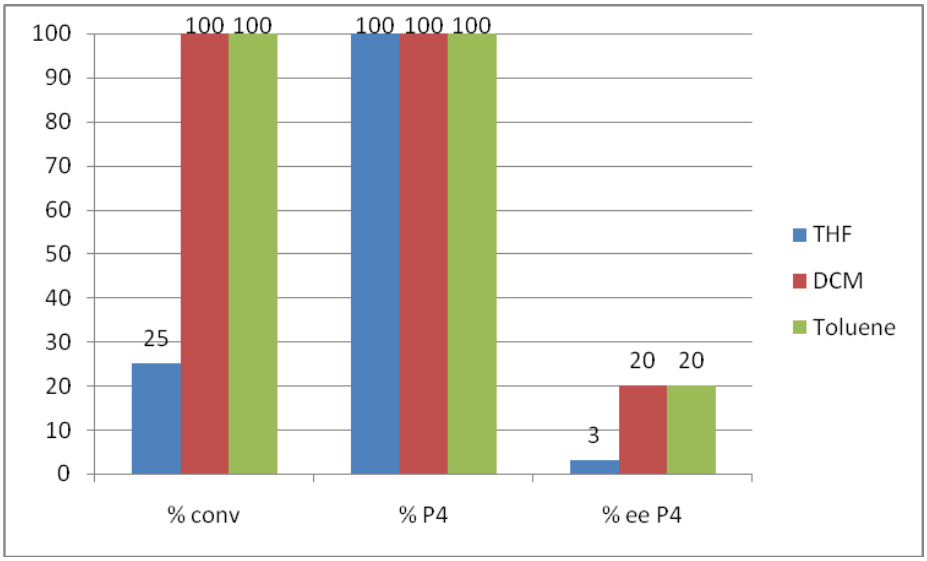

Figure 3.4. Pd-allylic substitution of **S2** using α-(ethoxycarbonyl)-cyclohexanone as nucleophile and the ligand **65b**. Effect of the solvent (THF, DCM and Toluene).

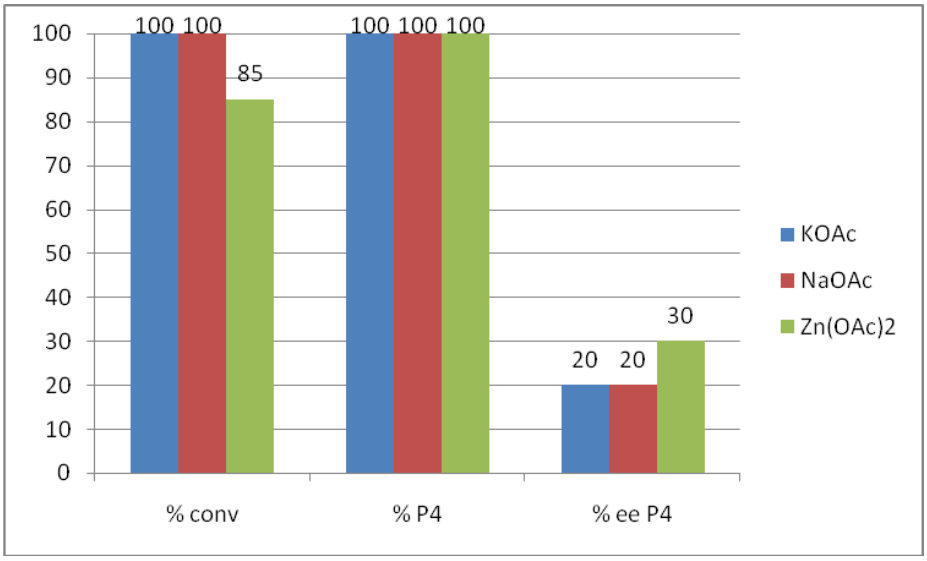

Figure 3.5. Pd-allylic substitution of **S2** using α-(ethoxycarbonyl)-cyclohexanone as a nucleophile and the ligand **65b**. Effect of the additive (KOAc, NaOAc and $Zn(OAc)_2$).

UNIVERSITAT ROVIRA I VIRGILI
1,3- DIPHOSPHITE LIGANDS WITH FURANOSIDE BACKBONE: A POWERFUL TOOL IN ASYMMETRIC CATALYSIS
Aitor Gual Gozalbo
DL: T-1535-2009/ISBN: 978-84-692-4554-5

Table 3.5. Pd-allylic alkylation of **S2** using α-(ethoxycarbonyl)-cyclohexanone as a nucleophile and the ligands **21b**, **23b**, **64b**, **65b**, **66b**, **67b** and **89b**.

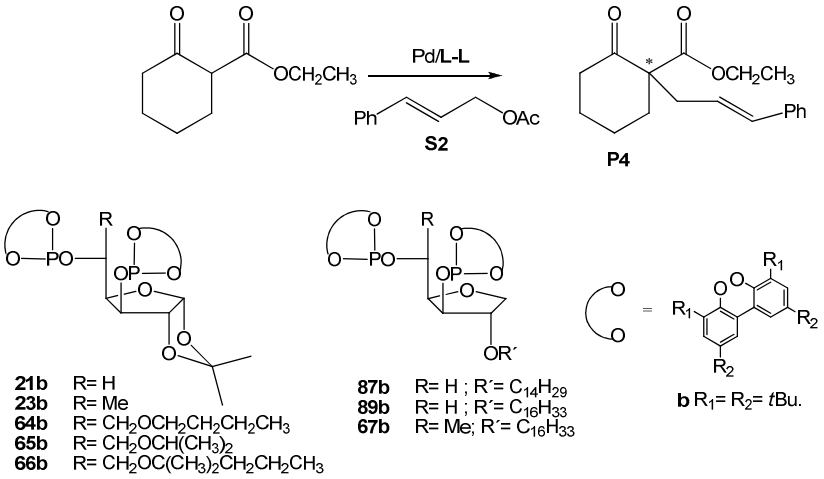

Entry[a]	Ligand	Time (h)	Conv.(%)[b]	**P4** (%)[c]	*ee* **P4**(%)[d]
1	**21b**	1	100	100	16
2	**23b**	1	100	100	10
3	**64b**	1	100	100	21
4	**65b**	1	100	100	30
5[e]	**65b**	24	40	100	32
6[f]	**65b**	24	20	100	38
7	**66b**	1	100	100	24
8	**67b**	1	100	100	13
9	**89b**	1	100	100	12

[a] All reactions were run at room temperature: 0.5 mol % $[PdCl(\eta^3\text{-}C_3H_5)]_2$; Pd/L = 1: 1.1; THF as solvent. [b] Conversion percentage of 1-phenyl-3-acetoxy-propene determined by 1H-NMR. [c] Regioselectivity to the linear product determined by ^{1}H-NMR. [d] Enantiomeric escesses determined by HPLC on a Chiralcel-OJ column. [e] T = -25 ºC. [f] T= -75 ºC.

When the reaction was performed a room temperature all the catalytic systems afforded total conversion in one hour with complete regioselectivity to the linear product (Entries 1-4 and 7-9). The enantioselectivity was in general low, although it can be observed several trends depending on the structure of the ligand. The best enantioselectivities were obtained with ligands modified in the C-6 positions (Entries 3-7) and the order **65b** > **66b** > **64b**. Ligands **21b**, **23b**, **67b** and

89b produced lower enantioselectivity than the ligands **64**-**66b** (Entries 1,2 and 8,9 vs. 3-7).

Since, the catalytic system Pd/**65b** provided the high enantioselectivity at room temperature the reaction was also tested at -25ºC (Entry 5). In these conditions, a 40% of conversion was achieved after 24 hours, with total regioselectivity to the linear product and a slight increase in the enantioselectivity (ee up to 32 %). Finally, the reaction temperature was decreased to -75ºC (Entry 6), but the enantioselectivity increased only slightly (ee up to 38%) and conversion decreased.

In conclusion, the 1,3-diphosphite carbohydrate backbone provided moderate to low enantioselectivity in the Pd-allylic alkylation of **S2** using -α-(ethoxycarbonyl)-cyclohexanone as the nucleophile. However, the results indicated that the introduction of bulky substituents in the C-6 positions allow to obtain higher enantioselectivities in this reaction.

Synthesis and Characterization of $[Pd(\eta^3\text{-}C_3H_5)(PP)]PF_6$ complexes

The results obtained in the Pd-allylic alkylation of 1,3-diphenyl-3-acetoxy-propene and 1-phenyl-3-acetoxy-propene suggested that the selective modification of the carbohydrate backbone highly affected the activity and the level of enantioselectivity. To understand this catalytic behaviour, the $[Pd(\eta^3\text{-}C_3H_5)(\mathbf{L})]PF_6$ complexes, where **L** = **65b** and **67b**, were synthesised and characterised by NMR (Scheme 3.15).

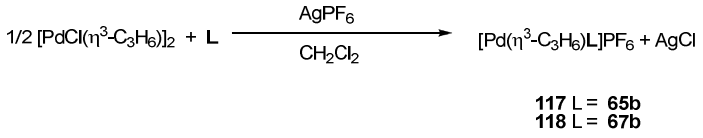

Scheme 3.15. Synthesis of $[Pd(\eta^3\text{-}C_3H_5)(\mathbf{L})]PF_6$ complexes **117** and **118**.

The NMR spectrum of complexes **117** and **118** in CD_2Cl_2, which respectively contain ligand **65b** and **67b**, shown a mixture of two isomers in equilibrium in a ratio 1:1 (See experimental section).

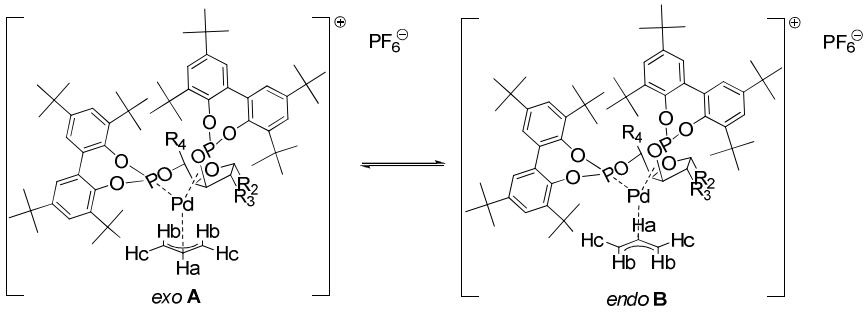

Scheme 3.16. Diastereomer complexes [Pd(η^3-C_3H_5)(**L**)]PF_6, where **L** is **65b** and **67b**.

Both isomers were characterized by NMR (^{1}H, ^{31}P, ^{13}C and HSQC) and their structure was attributed to the *exo* **A** and *endo* **B** (Scheme 3.16). The presence of these species in solution highly affected the enantioselectivity of the reaction because the chiral products obtained from structure **A** has the opposite configuration than those obtained from structure **B**.

It has been generally accepted that the enantioselectivity step in the Pd-catalyzed allylation is the nucleophilic attack.[1,2,3] Usually, nucleophilic attack occurs predominantly at the allyl terminus located trans to the ligand that is the better π-acceptor. For the homo-donor ligands **65b** and **67b**, it was assumed that the nucleophile attack predominantly occurs trans to the phosphite moiety attached to C-5. This hypothesis was formulated in a work by Dieguéz et al. about the influence of configurations at C-3 and C-5 in the enantioselectivity and is based on following facts:

(i) The configuration of the stereocenter C-3 strongly influences the enantioselectivity. Thus, using ligand **21b** with a *xylo*-configuration backbone, with (*R*)-configuration at C-3, give *ee´*s up to 90%, while with a *ribo*-configuration ligand **22b**, with (*S*)-configuration C-3, very low enantioselectivity is obtained.[22b]

(ii) The sense of the asymmetric induction obtained with 1,3-diphosphite ligands with a xylofuranoside backbone is the same than that obtained with heterodonor with the same carbohydrate backbone, for which the nucleophilic attack occurs *cis* to the phosphite moiety at C-3.[22b] Further proof for this hypothesis were found using related gluco-, allo-, ido- and talo-furanoside diphosphites which showed that the configuration of C-5 had little influence on the outcome of the reaction.[21,22,27]

In this work the influence of structural modifications of positions non-directly bonded to the phosphite moieties was studied and from the reported results it can be derived the following trends:

(iii) The removal of the 1,2-*O*-isopropylidene group and the introduction of the 2-*O*-alkyl chain (compound **21b** vs. **87b**, **89b** and **23b** vs. **67b**) caused a decrease in the enantioselectivity of the Pd-allylic alkylation of *rac*-**S1** using dimethyl malonate as nucleophile. Furthermore, the behaviour observed with diphosphite ligands **87b**, **89b** and **67b** was in agreement with the previous observation that the C-5 stereocenter has a little effect in the enantioselectivity. Interestingly, high dilution experiments showed that the catalytic system Pd/**67b** provided kinetic resolution of the substrate with excellent enantioselectivities to the product.

(iv) The introduction of several substituents in the C-6 position of the furanoside backbone of the diphosphite ligand produced a decrease (compound **21b** and **23b** vs. **64b**, **65b** and **66b**) in the enantioselectivity in the Pd-allylic alkylation of *rac*-**S1** using dimethyl malonate as nucleophile. Therefore, the presence of a non substituted methyl group in the position C-5 was revealed to an important factor to achieve high levels of enantioselectivity. It has to be noted, that the catalytic system Pd/**65b** in toluene produced an excellent kinetic resolution of the substrate with excellent enantioselectivity to the product.

(v) In the case of the Pd-allylic alkylation of **S2** using dimethyl malonate as nucleophile, the catalytic results shown that the stereogenic center C-3 determined also the enantioselectivity. In contrast to the reaction with *rac*-**S1**, the best results were obtained with the xylofuranose derivate ligand **21b**.

(vi) In the case of the reaction with **S2** to afford compound **P4**, the catalytic results shown that the presence of bulky substituents at C-6 positions allowed to obtain higher enantiomeric excesses. The high level of enantioselectivity was achieved with a ligand bearing a 6-O-isopropyl group.

3. 5. Conclusions

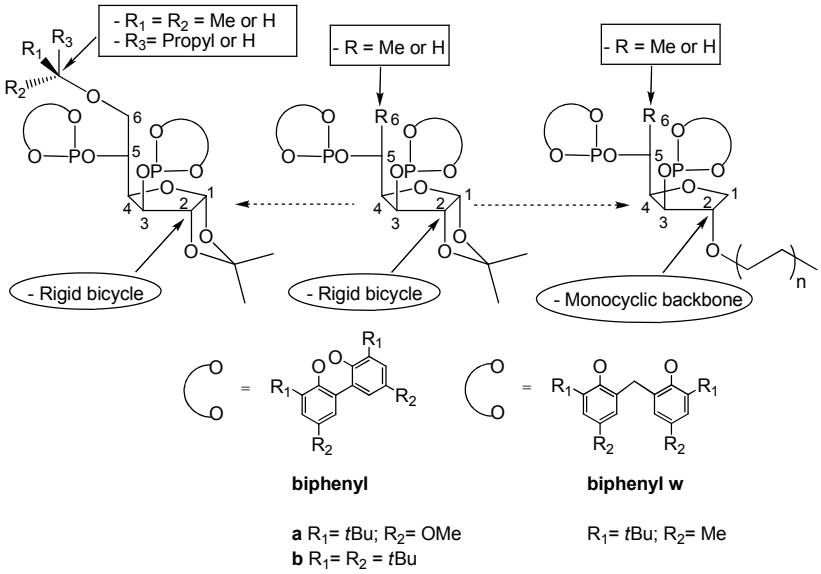

Figure 3.6. Structural diversity in 1,3-diphosphite ligands derived from carbohydrates with a furanoside (tetrahydrofuran) backbone prepared in this thesis.

A series of diphosphite ligands **21a**,**w**, **64b**, **65a,b**, **66b**, **67a**,**b**, **87b**,**w** and **89b** were applied in the Pd-allylic alkylation of *rac*-1,3-diphenyl-3-acetoxy-propen-1-ene and 1-phenyl-3-acetoxy-propene. The catalytic results provided useful information about the effect of the modification of the carbon stereocenters non-directly bonded to phosphite function of the carbohydrate backbone. Additionally, a new phosphite moiety **w**, containing a carbon bridge between the phenyl groups, was tested. The results indicated the importance of the biphenyl moiety in the activity and enantioselectivity of the reaction. Furthermore, the presence of an equilibrium between the *exo* **A** and *endo* **B** was confirmed by characterization of the $[Pd(\eta^3\text{-}C_3H_5)(\mathbf{L})]PF_6$ complexes, where **L** = **65b** and **67b**.

3.6. Experimental Section

General Considerations

All reactions were carried out using standard Schlenk techniques under an atmosphere of argon or nitrogen. Solvents were purified an dried by standard procedures. Diphosphite ligands **21a**,**w**, **64b**, **65a,b**, **66b**, **67a**,**b**, **87b**,**w** and **89b** were prepared using methods described in section 2.4.1 and 2.4.2. *rac*-1,3-diphenyl-3-acetoxy-propen-ene **S1** and achiral substrate 1-phenyl-3-acetoxy-propene **S2** were prepared as previously reported.[38, 39,40] ^{1}H, ^{13}C $\{^{1}H\}$ NMF and $^{31}P\{^{1}H\}$ NMR spectra were recorded using 400 MHz spectrometer. Chemical shifts are relative to $SiMe_4$ (^{1}H and ^{13}C) as internal standard or H_3PO_4 (^{31}P) as external standard.

Typical Procedure for the Allylic Alkylation of rac-1,3-diphenyl-3-acetoxy-propen-ene and achiral substrate 1-phenyl-3-acetoxy-propene using dimethyl malonate as a nucleophile

A degassed solution of $[PdCl(\eta^3\text{-}C_3H_6)]_2$ and the diphosphite ligand (1.1 equivs. to Pd) in dichlorometane (0.5 mL) was stirred for 30 min. Subsequently, a solution of substrate (0.5 mmol) in dichloromethane (1.5 mL), dimethyl malonate (171μL, 1.5 mmol), *N*,*O*-bis(trimethylsilyl)acetamide (370μL, 1.5 mmol) and a pinch of KOAc were added. The reaction mixture was stirred at room temperature. After the desired reaction time, the reaction mixture was diluted with Et_2O (5 mL) and saturated aqueous NH_4Cl solution (25 mL) was added. The mixture was extracted with Et_2O (3×10 mL) and the extract dried over $MgSO_4$. For *rac*-1,3-diphenyl-3-acetoxy-propen-ene, conversion was measured by ^{1}H NMR and enantiomeric excess was determined by HPLC (Chiralcel-OJ, 10% 2-propanol/hexane, flow 0.7 mL/min). For 1-phenyl-3-acetoxy-propene, conversion and regioselectivity to the branched product were measured by ^{1}H NMR and enantiomeric excess was determined by HPLC (Chiralcel-OJ, 13% 2-propanol/hexane, flow 0.7 mL/min).

Typical Procedure for the Pd-Allylic Alkylation of 1-phenyl-3-acetoxy-propene using α-(ethoxycarbonyl)-cyclohexanone as a nucleophile

A degassed solution of $[PdCl(\eta^3\text{-}C_3H_6)]_2$ and the diphosphite ligand (1.1 equivs. to Pd) in dichlorometane (0.5 mL) was stirred for 30 min. Subsequently, a solution of substrate (0.5 mmol) in dichloromethane (1.5 mL), *α*-(ethoxycarbonyl)-cyclohexanone (233μL, 1.5 mmol), *N*,*O*-bis(trimethylsilyl)acetamide (370μL, 1.5 mmol) and a pinch of KOAc were added. The reaction mixture was stirred at room temperature. After the desired reaction time, the reaction mixture was diluted with Et_2O (5 mL) and saturated aqueous NH_4Cl solution (25 mL) was added. The mixture was extracted with Et_2O (3 × 10 mL) and the extract dried over MgSO4. The conversion and regioselectivity to the linear product were measured by ^1H NMR and enantiomeric excess was determined by HPLC (Chiralcel-OJ, 10% 2-propanol/hexane, flow 0.7 mL/min).

General procedure for the preparation of the $[Pd(\eta^3\text{-}C_3H_6)(PP)]PF_6$.
A degassed solution of the corresponding $[PdCl(\eta^3\text{-}C_3H_6)]_2$ (0.025 mmol) and the diphosphite ligand (0.05 mmol) in dichlorometane (0.5 mL) was stirred at room temperature under argon atmosphere for 30 min. Subsequently, $AgPF_4$ (0.05 mmol) was added and the solution was stirred for 30 min. Thereafter, the solution was filtered over Celite under argon and the resulting solutions were analyzed by NMR. After the NMR analysis, the complexes were precipitated adding hexane as a pale yellow solid.

$[Pd(\eta^3\text{-}C_3H_6)(65b)]PF_6$ (117). By using general procedures, complex **117** was synthesised starting from $[PdCl(\eta^3\text{-}C_3H_6)]_2$ (0.025 mmol) and the diphosphite ligand **65b** (0.05 mmol). The complex **117** was characterised by NMR analysis, and precipitated as a pale yellow solid in 52% of yield (40 mg, 0.032 mmol). **^1H NMR** (CD_2Cl_2, 400 MHz) δ: 0.78 (d, *J* = 6Hz, 12H, $OCH(CH_3)_2$), 1.08 (s, 6H, $O_2C(CH_3)_2$), 1.43-1.23 (m, 150H, $O_2C(CH_3)_2$, *t*Bu), 2.59 (m, 1H, CH_2CHCH_2), 2.68 (m, 3H, 1H, CH_2CHCH_2), 2.98 (m, 4H, $OCH(CH_3)_2$), 3.55 (m, 4H, 6-H), 3.56 (m, 1H, CH_2CHCH_2), 3.77 (d, *J*= 3.6 Hz, 1H, 2-H), 3.90 (d, *J*= 3.6 Hz, 1H, 2-H), 3.92 (m, 2H, CH_2CHCH_2), 4.16 (m, 1H, CH_2CHCH_2), 4.49 (m, 2H, 5-H), 4.60 (m, 2H, 4-H), 4.90 (dd, *J*= 2.4, 9.6 Hz, 1H, 3-H), 4.99 (dd, *J*= 2.4, 9.6 Hz, 1H, H-3), 5.06 (m, 2H, CH_2CHCH_2), 5.60 (d, *J*= 3.6 Hz, 1H,1-H), 5.61 (d, *J*= 3.6Hz, 1H, 1-H), 7.80-7.20 (m, 32H, Aromatic) . **^{13}C NMR** (CD_2Cl_2, 100.6 MHz) δ: 21.8 ($OCH(CH_3)_2$), 21.9 ($OCH(CH_3)_2$), 26.8 ($O_2C(CH_3)_2$), 27.0 ($O_2C(CH_3)_2$), 32.4-

31.6 (*t*Bu), 35.4-35.3 (*t*Bu), 36.3-36.0 (*t*Bu), 67.0 (C-6), 71.3 (CH_2CHCH_2), 71.8 (CH_2CHCH_2), 72.5 ($OCH(CH_3)_2$), 73.0 (CH_2CHCH_2), 73.6 (CH_2CHCH_2), 75.8 (dd, *J*= 10.9, 6.8 Hz, C-5), 76.2 (C-4), 80.5 (dd, *J*= 8.4, 8.4 Hz, C-3), 84.2 (C-2), 106.1 (C-1), 113.9 ($O_2C(CH_3)_2$), 124.5 (CH_2CHCH_2), 150.7-126.2 (Aromatics). **^{31}P NMR** (CD_2Cl_2, 161.97 MHz) δ: 134.0 (d, *J*= 128.0 Hz, 1P(1)), 134.6 (d, *J*= 128.0 Hz, 1P (2)), 136.5 (d, *J*= 128.0 Hz, 1P (2)), 137.0 (d, *J*= 128.0 Hz, 1P(1)).

[Pd(η^3-C_3H_6)(67b)]PF_6 (118). By using general procedures, complex **118** was synthesised starting from $[PdCl(\eta^3\text{-}C_3H_6)]_2$ (0.025 mmol) and the diphosphite ligand **67b** (0.05 mmol). The complex **118** was characterised by NMR analysis, and precipitated as a pale yellow solid in 48% of yield (35 mg, 0.030 mmol). **^{1}H NMR** (CD_2Cl_2, 400 MHz) δ: 0.87 (t, *J* = 7.2Hz, 6H, $O(CH_2)_{15}CH_3$), 1.55-1.10 (m, 206H, *t*Bu, $O(CH_2)_{15}CH_3$, 6-H(1), 6-H(2)), 2.72 (m, 1H, CH_2CHCH_2), 2.84 (m, 3H, CH_2CHCH_2), 3.15 (m, 2H, $O(CH_2)_{15}CH_3$), 3.21 (m, 4H, 2-H, $O(CH_2)_{15}CH_3$), 3.64 (d, *J* = 9.6 Hz, 2H, CH_2CHCH_2), 3.85 (m, 4H, 1-H), 3.94 (m, 2H, 4-H), 4.05 (m, 1H, CH_2CHCH_2), 4.27 (m, 1H, CH_2CHCH_2), 4.65 (m, 1H, 5-H), 4.77 (m, 1H, 5-H), 5.01 (dd, *J*= 3.2, 9.6 Hz, 1H, 3-H), 5.08 (dd, *J*= 2.8, 7.2 Hz, 1H, 3-H), 5.12 (m, 2H, CH_2CHCH_2), 7.57-7.08 (m, 16H, Aromatic). **^{13}C NMR** (CD_2Cl_2, 100.6 MHz) δ: 14.4 ($O(CH_2)_{15}CH_3$), 20.5 ($O(CH_2)_{15}CH_3$), 23.2 ($O(CH_2)_{15}CH_3$), 26.5 (C-6), 32.5-29.8 (*t*Bu, $O(CH_2)_{15}CH_3$), 36.2-35.3 (*t*Bu), 70.8 ($O(CH_2)_{15}CH_3$), 71.5 (CH_2CHCH_2), 72.1 (CH_2CHCH_2), 72.5 (CH_2CHCH_2), 73.0 (CH_2CHCH_2), 73.2 (C-1), 73.6 (dd, *J*= 6.1, 10.5 Hz, C-5), 80.8 (dd, *J*= 8.6, 14.5 Hz, C-3), 82.7 (d, *J*= 7.2 Hz, C-4), 84.1 (C-2), 124.5 (CH_2CHCH_2), 150.6-125.3 (Aromatics). **^{31}P NMR** (CD_2Cl_2, 161.97 MHz) δ: 133.3 (d, *J*= 127.0 Hz, 1P(1)), 134.0 (d, *J*= 128.0 Hz, 1P (2)), 136.5 (d, *J*= 128.0 Hz, 1P (2)), 137.2 (d, *J*= 127.0 Hz, 1P(1)).

DL: T-1535-2009/ISBN: 978-84-692-4554-5

[1] S. A. Godleski, *Comprensive Organic Synthesis*, B. M. Trost, I. Fleming, M. F. Semmelhack, Eds.; Pergamon Press: Oxford, vol 4, Chapter 3.3, **1990**.

[2] a) S. Ma, Z. Lu, Angew. *Chem. Int. Ed.* **2008**, *47*, 258; b) M. Braun, T. Meier, *Angew. Chem. Int. Ed.* **2006**, *45*, 6952; c) S.-L. You, L. –X. Dai, *Angew. Chem.* **2006**, *118*, 5372; d) H. Yorimitsu, K. Oshima, Angew. Chem. 2005, 117, 4509; e) C. Bruneau, J. L. Renaud, B. Demerseman, *Chem. Eur. J.* **2006**, *12*, 5178;f) H. Miyabe, Y. Takemoto, *Synlett*, **2005**, 1641.

[3] a) B. M. Trost, *J. Org. Chem.* **2004**, *69*, 5813; b) B. M. Trost, M. L. Crawley, *Chem. Rev.* **2003**, *103*, 2921; c) B. M. Trost, D. L. Van Vranken, *Chem. Rev.* **1996**, *96*, 395; d) B. M. Trost, *Acc. Chem. Res.* **1996**, *96*, 395.

[4] B. M. Trost, F. D. Toste, *J. Am. Chem. Soc.*, **1999**, *121*, 4545.

[5] a) S. Hanessian, *Total Synthesis of Natural Products. The Chiron Approach*. Pergamon Press, Oxford, **1983**; b) K. Totami, K.-i. Tabao and K.-i. Tadano, Synlett, **2004**, 2006.

[6] M. T. Reetz, S. Sostmann, *J. Organomet. Chem.* **1999**, *64*, 9735.

[7] L. G. Bonnet, R. E. Douthwaite, B. M. Kariuki, *Organometallics*, **2003**, *22*, 4187.

[8] a) H. Aït-Haddou, O. Hoarau, D. Cramailére, F. Pezet, J. C. Daran, G. G. A. Balavoine, *Chem. Eur. J.* **2004**, *10*, 699; b) J. Bayardon, D. Sinou, M. Guala, G. Desimoni, *Tetrahedron: Asymmetry*, **2004**, *15*, 3195; c) J. Bayardon, D. Sinou, *J. Org. Chem.* **2004**, *69*, 3121; d) M. A. Pericàs, C. Puigjaner, A. Riera, A. Vidal-Ferran, M. Gómez, F. Jiménez, G. Muller, M. Rocamora, *Chem. Eur. J.* **2002**, *8*, 4164; e) M. Glos, O. Reiser, *Org. Lett.* **2000**, *2*, 2045.

[9] J. L. Vasse, R. Straanne, R. Zalubovskis, C. Gayet, C. Moberg, *J. Org. Chem.* **2003**, *68*, 3258.

[10] a) T. Hayashi, T. Suzuka, A. Okda, M. Kawatsura, *Tetrahedron: Asymmetry*, **2004**, *15*, 545; b) T. Fukuzumi, N. Shibata, M. Sugiura, H. Yashui, S. Nakamura, T. Toru, *Angew. Chem. Int. Ed.* **2006**, *45*, 4973; c) N. Kinoshita, T. Kawabata, K. Tsubaki, M. Bando, K. Fuji, *Tetrahedron*, **2006**, *62*, 1756; d) T. D. Weib, G. Helmchen, U. Kazmaier, *Chem. Comm.* **2002**, 1270; e) N. F. K. Kaiser, U. Bremberg, M. Larhed, C. Moberg, A. Hallberg, *J. Organomet. Chem.* **2000**, *603*, 2; C. J. Martin, D. J. Rawson, J. M. J. Williams, *Tetrahedron: Asymmetry*, **1998**, *9*, 3723; f) A. Frölander, S. Lutsenko, T. Privalov, C. Moberg, *J. Org. Chem.* **2005**, *70*, 9882; g) D. Liu, Q. Dai, X. Zhang, *Tetrahedron*, **2005**, *61*, 6460; h) A. Sudo, K. Saido, *J. Org. Chem.* **1997**, *62*, 5508.

[11] O. Pàmies, M. Diéguez, C. Claver, *J. Am. Chem. Soc.* **2005**, *127*, 3646.

[12] Y. Mata, M. Diéguez, O. Pàmies, C. Claver, *Adv. Synth. Catal.* **2005**, *347*, 1943.

DL: T-1535-2009/ISBN: 978-84-692-4554-5

[13] M. Tollabi, E. Framery, C. Goux-Henry, D. Sinou, *Tetrahedron: Asymmetry*, **2003**, *14*, 3329.

[14] a) M. Raghumath, X. Zhang, *Tetrahedron Lett*. **2005**, *46*, 8213; b) M. Braun, F. Laicher, T. Meier, *Angew. Chem. Int. Ed.* **2000**, *39*, 3494; c) I. D. G. Watson, S. A. Styler, A. K. Yudin, *J. Am. Chem. Soc.* **2004**, *126*, 5086; d) Y. Wang, K. Ding, *J. Org. Chem.* **2001**, *66*, 3228; e) H. Kodama, T. Taiji, T. Otha, I. Furukawa, *Synlett*, **2001**, 385; f) T. Otha, H. Sasayama, O. Nakajima, N. Kurahashi, T. Fujii, I. Furukuwa, *Tetrahedron: Asymmetry*, **2003**, *14*, 537; g) X. Chen, R. Guo, Y. Li, G. Chen, C. H. Yeunga, S. C. Chan, *Tetrahedron: Asymmetry*, **2004**, *15*, 213.

[15] a) M. Lotz, G. Kramer, P. Knochel, *Chem. Commun.* **2001**, 2546; b) S. Lee, J. H. Koh, J. Park, *J. Organomet. Chem.* **2001**, *637-639*, 99; c) J. Kang, J. H. Lee, J. S. Choi, *Tetrahedron: Asymmetry*, **2001**, *12*, 33; d) M. Raghumath, W. Gao, X. Zhang, *Tetrahedron: Asymmetry*, **2005**, *16*, 3676; e) M. Ogasawar, K. Yoshida, T. Hayashi, *Organometallics*, **2001**, *20*, 3913.

[16] a) D. Zhao, K. Ding, *Org. Lett.* **2003**, *5*, 1349; b) D. Zhao, J. Sun, K. Ding, *Chem. Eur. J.* **2004**, *10*, 5952.

[17] G. Malaisé, S. Ramdeehul, J. A. Osborn, L. Barloy, N. Kyrisakas, R. Graff, *Eur. J. Inorg. Chem*. **2004**, 3987.

[18] Y. Y. Yan, T. B. RajanBabu, *Org. Lett.* **2000**, *2*, 199.

[19] a) B. M. Trost, R. Radinov, *J. Am. Chem. Soc.* **1997**, *119*, 5962; b) B. M. Trost, G. M. Schroeder, *J. Am. Chem. Soc.* **2000**, *122*, 3785; c) B. M. Trost, J. P. Surivet, *J. Am. Chem. Soc.* **2000**, *122*, 3252.

[20] a) S. G. Lee, C. W. Lim, C. E. Song, K. M. Kim, C. H. Jun, *J. Org. Chem.* **1999**, *64*, 4445; b) S. G. Lee, S. H. Lee, C. E. Song, B. Y. Chung, *Tetrahedron: Asymmetry*, **1999**, *10*, 1795.

[21] M. Diéguez, O. Pàmies, C. Claver, *J. Org. Chem.* **2005**, *70*, 3363.

[22] a) M. Diéguez, S. Jansat, M. Gómez, A. Ruiz, G. Muller, C. Claver, *Chem. Commun.* **2001**, 1132; b) O. Pàmies, G.P.F Van Strijdonck, M. Diéguez, S. Deerenberg, G. Net, A. Ruiz, C. Claver, P.C.J. Kamer, P.W.N.M. Van Leeuwen, *J. Org. Chem.* **2001**, *66*, 8867.

[23] A. Balanta Castillo, I. Favier, E. Teuma, S. Castillón, C. Godard, A. Aghmiz, C. Claver, M. Gómez, *Chem. Commun.* **2008**, 6197.

[24] E. Raluy, C. Claver, O. Pàmies, M. Diéguez, *Org. Lett.* **2007**, *9*, 49.

[25] a) J. D. Oslob, B. Akermark, P. Helquist, P. O. Norby, *Organometallics*, **1997**, *16*, 3015; b) M. P. T. Sjören, S. Hansson, B. Akermark, A. Vitagliano, *Organometallics*, **1994**, *13*, 1963.

[26] J. W. Faller, J. C. Wilt, *Org. Lett.* **2005**, *7*, 633.

[27] M. Diéguez, O. Pàmies, C. Claver, *Adv. Synth. Catal.* **2005**, *347*, 1257.

[28] T. Hayashi, M. Kawatsura, Y. Uozumi, *J. Am. Chem. Soc.* **1998**, *120*, 1681.

[29] a) R. Prétôt, A. Pfaltz, *Angew. Chem. Int. Ed.* **1998**, *37*, 323; b) R. Hilgraf, A. Pfaltz, *Synlett*, **1999**, 1814.

[30] S. L. You, X. Z. Zhu, Y. M. Luo, X. L. Hou, L. X. Dai, *J. Am. Chem. Soc.* **2001**, *123*, 7471.

[31] B. Bartels, G. Helmchen, *Chem. Commun.* **1999**, 741.

[32] C. García-Yebra, J. P. Janssen, F. Rominger, G. Helmchen, *Organometallics*, **2004**, *23*, 5459.

[33] T. Hayashi, A. Okada, T. Suzuka, M. Kawatsura, *Org. Lett.* **2003**, *5*, 1713.

[34] T. Nemoto, T. Matsumoto, T. Masuda, T. Hitomi, K. Hatano, Y. Hamada, *J. Am. Chem. Soc.* **2004**, *126*, 3690.

[35] M. Nakoji, T. Kanayama, T. Okino, Y. Takemoto, *J. Org. Chem.*, **2002**, *67*, 7418.

[36] a) R. Kuwano, R. Nishio, Y. Ito, *Org. Lett.*, **1999**, *6*, 837; b) M. Ogasawara, H. L. Ngo, T. Sakamoto, T. Takahashi, W. Lin, *Org. Lett.* **2005**, *14*, 2881.

[37] R. Kuwano, K. Uchida, Y. Ito, *Org. Lett.*, **2003**, *5*, 2177.

[38] P. R. Auburn, P. B. Mackenzie, B. Bosnich, *J. Am. Chem. Soc.* **1985**, *107*, 2033.

[39] C. Jia, P. Müller, H. Mimoun, *J. Mol. Cat. A: Chem.* **1995**, *101*, 127.

[40] J. Lehman, G. C. Lloyd-Jones, *Tetrahedron*, **1995**, *51*, 8863.

Chapter 4

Synthesis of metal nanoparticles stabilized by chiral diphosphites and their use as catalysts in the hydrogenation of pro-chiral monocyclic arenes

4.1 Introduction to nanoscience

Science aims at discovering what already exists, but is still unknown.[1] Specifically, nanoscience refers to the knowledge that comes from the study of the matter behaviour and properties at the nanometer size scale. There are many examples in the nature that can be considered nanostructures. For example: DNA, viruses, colloids, etc.

Scientists have been compiling information about these systems during a large period of time and now, below the nanoscience concept, all this information being reconsidered and complemented.

In a parallel way, industrial progress seems to be in a good extent accompanied by the ability to produce smaller and smaller devices with higher and higher precision. Recently, the interest in the nanotechnology was receiving growing interest. However, nanotechnology should not be considered only the next stage of the miniaturisation progress. An additional and central aspect of nanotechnology is that when shrinking objects to nanometer dimensions their physical and chemical properties start to differ markedly form macroscopic ones.[2] Nanostructures are in a range of sizes (from a few nanometers to less than 100 nanometers) in which quantum phenomena would be expected to be significant.[3,4] Therefore, if a metal particle with bulk properties is reduced to the size of a few dozen or a few hundred atoms, the density of states in the valence band and the conductivity band, respectively, decreases to such an extent that the electronic properties change dramatically (Figure 4.1). It was noteworthy that the separation between the bands increases when the size of the material decreases.

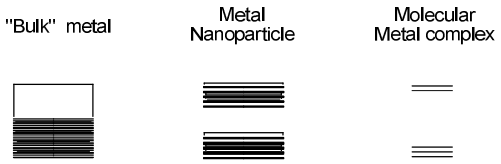

Figure 4.1. Illustration of the typical electronic structure in (a) the typical band structure of the bulk metal particle, (b) a small band gap of the metal nanoparticle with cubic close-packed, (c) separated bonding and antibonding molecular orbitals in a molecular metal complex.

Then, the control the particle size, shape, organisation and the nature of the chemical species on surface was necessary to develop new materials with intermediate physical and chemical properties.[5,6] Modern transition-metal nanoclusters differ form the classical colloids in several important features. They are generally: (a) smaller (1-10 nm in diameter) than classical colloids (>10 nm), (b) isolable and redissolvable, unlike classical colloids (c) soluble in organic solvents (classical colloid chemistry is typically aqueous) and (d) with well defined composition. In addition modern transition-metal nanoclusters have: (e) narrower size dispersion, (f) clean surfaces, (g) reproducible synthesis and (h) reproducible catalytic results.[7]

In fact, these special characteristics of nanostructures would provide interesting catalytic properties in terms of activity and selectivity in front of the classical colloids.

In this section, the synthesis of metal nanoparticles (NPs) using stabilizing agents and their successfully use in some asymmetric processes is introduced.

4. 2. Synthesis of modern metal colloids

The word colloid [8] implied the suspension of a phase (solid or liquid) into a second phase, and was used for a suspension that neither settled nor deposited spontaneously.

"Modern nanoclusters" or "nanoparticles" can be distinguished from traditional colloids in the fact that control can be exerted over their composition, size, surface covering, and over desired properties. The methods used to synthesise metal nanoparticles (NPs) are commonly classified as "top-down" and "bottom-up" approaches. In the top-down approach, photolithography and related techniques are used to pattern features (typically in two-dimensions) over length scales approximately 4 orders of magnitude larger (in linear dimensions) than an individual structure.[9] This approach is subject to drastic limitations for dimensions smaller than 100 nm. The size restriction and its high cost make the bottom-up approach an alternative and most promising strategy.

The bottom-up approximation consists in the synthesis of Metal-NPs starting from inorganic metallic molecules by "stabilization of metal nanoparticles procedures".[1]

The Metal-NPs have to be stabilized because they are unstable with respect to agglomeration to the bulk. At short interparticle distances, and in the absence of any repulsive effect, the van der Waals forces will attract two metallic particles to each other. The agglomeration problem can become more serious if magnetic forces are present. Hence it is necessary the use of capping agents to provide stable nanoparticles in solution.[7-10]

Nanoclusters stabilization is usually discussed in terms of two general categories: (i) electrostatic stabilization and (ii) steric stabilization.

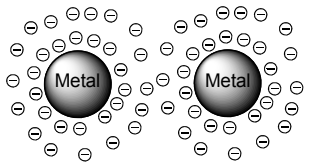

Figure 4.2. Schematic representation of the electrostatic stabilization in metal nanoparticles.

Ionic compounds such halides, carboxylates, or polyoxoanions, in (generally aqueous) solution can perform the electrostatic stabilization of metal nanoparticles.[7-10] The presence of these compounds and their related counterions surrounding the metallic surface will generate an electrical double-layer around the particles(Figure 4.2). This results in a Coulombic repulsion between the particles. If the electric potential associated with the double layer is high enough, then the electrostatic repulsion will prevent particle aggregation.

Colloidal suspensions stabilized by electrostatic repulsion are very sensitive to any change in the medium that enables to disrupt the double layer, like changes in ionic strength or thermal motion (Figure 4.3).Thus the control of these parameters is essential to guarantee and effective electrostatic stabilization.

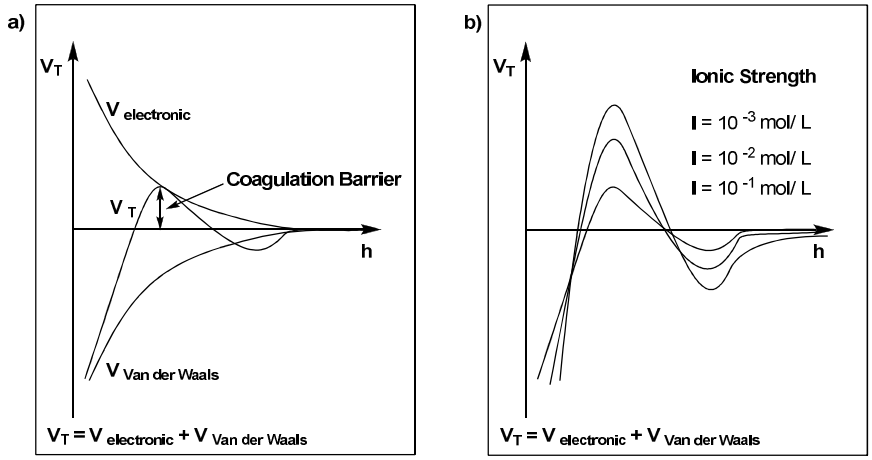

Figure 4.3. (a) Plot of energy ($\mathbf{V_T}$) *vs* interparticular distance (**h**) for electrostatic stabilization, (b) Influence of the ionic strength (**I**).

In the case of steric stabilization, organic molecules which present coordinating groups in its molecular structure can prevent particle aggregation by providing a protective layer.[7-10] These molecules will be restricted in motion in the nanoparticles surface and in the interparticle space. Then, it causes a decrease in entropy and thus and increase in free energy (Figure 4.4).

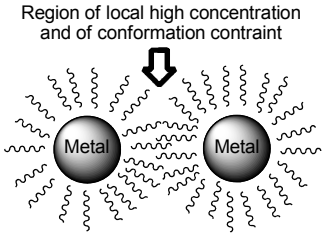

Figure 4.4. Schematic representation of the steric stabilization in metal nanoparticles.

A second effect is caused by the local increase in concentration because the two protective layers begin to interpenetrate.[7-10] This fact produces an osmotic repulsion, and therefore the media restores the equilibrium by diluting the macromolecules and thus separating the particles. The variation of potential energy versus interparticle distance is shown in Figure

4.5a. In contrast to the electrostatic stabilization, which is mainly used in aqueous media, the steric stabilization can be used in organic or in aqueous phase. Nevertheless, the length and/or the nature of the macromolecules used influence the thickness of the protective layer and can thus modify the stability of the colloidal metal particles.

It has been reported that nanoparticles can also be stabilized by the sole effect of the coordinating solvent molecules.[11,12] However, it has not been entirely established if in these cases there is a complete lack of other stabilizing agents such as anions or cations involved in the process. Sometimes, the elemental composition of the stabilised NPs shows that potentially coordinating halides still remain.[13]

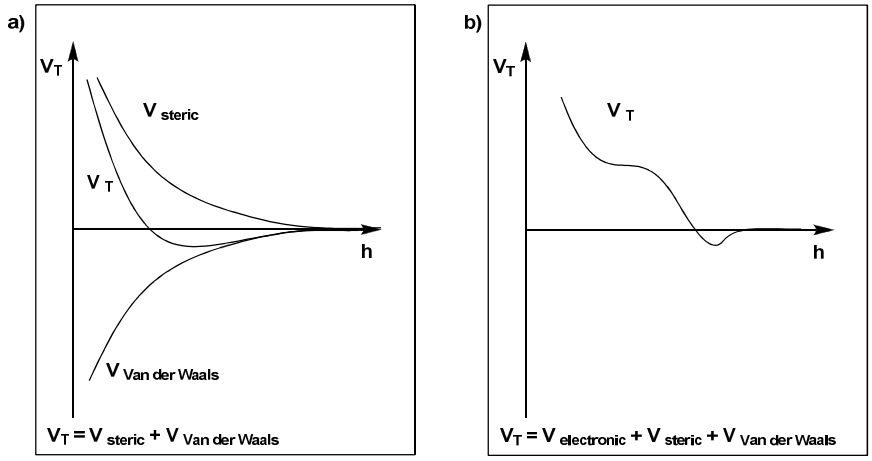

Figure 4.5. (a) Plot of energy ($\mathbf{V_T}$) *vs* interparticular distance (**h**) for steric stabilization, (b)Plot of energy ($\mathbf{V_T}$) *vs* interparticular distance (**h**) for electrosteric stabilization.

Finally, the electrostatic and steric stabilization can be combined to maintain metallic nanoparticles stable in solution. [7,8] This kind of stabilization is generally provided by ionic surfactants, which contain a polar group able to generate an electronic double layer and a lipophylic side chain able to provide steric repulsion (Figure 4.5b).

Therefore, metal nanoparticles are synthesized by using stabilizing agents which prevents the aggregation processes. An important variable in the synthesis of metal nanoparticles is the use of methods that allow control

over the particle size and composition. Furthermore, the particles synthesized by these methods have to be easily isolable and redissolvable, and the procedure has to be reproducible. Chemical methods, which generally provide a reproducible synthesis of metal nanoparticles with small size and narrow dispersion, are preferred in front of the physical methods (Figure 4.6).

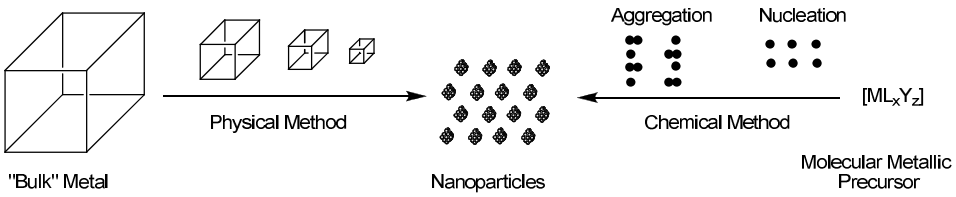

Figure 4.6. Schematic representation of the preparative methods for the synthesis of metal nanoparticles (M-NPs).

The method chosen to synthesize metal nanoparticles essentially depends on the metal oxidation state in the molecular precursor.[8] If metal appears in an oxidised state (M^{n+}), the presence of a reducing agent becomes necessary to obtain the desired metal colloids. This reducing agent can be or not generated in situ. For example, it can be the solvent, the stabilizer, a reducing gas as H_2 or CO, and also hydrides or other reducing compounds. The metallic precursor can also be reduced by electrolysis or by the presence of free reducing radicals generated in situ when ultrasounds or radiation were used. Electrochemical methods are also suitable in the case of easily oxidized metals. Metal vapours co-condensed with organic and electrochemical methods are also suitable to synthesise metal nanoparticles. In any case, enough energy has to be given to the system to allow nucleation and growth. If the precursor already contains the metal in low valence state, metal colloids can be generated through ligand displacement by reduction or by thermal induction.[8,10]

The organometallic approach to synthesise metal nanoparticles through ligand displacement by reduction was developed by Chaudret et al.[8,10].This synthesis of the metal nanoparticles consists in the decomposition of an organometallic precursor, mainly zerovalent organometallic complexes, in an organic solvent and under mild conditions.

This method provides nanoparticles with clean surface because a reducing gas (dihydrogen or carbon monoxide) was used to decompose the organometallic precursor (Figure 4.7).

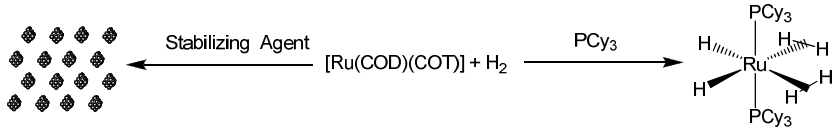

Figure 4.7. Synthesis of ruthenium nanoparticles by decomposition of [Ru(COD)(COT)] precursor through ligand displacement by reduction with dihydrogen.

Furthermore, this methodology offers the possibility to stabilize metal nanoparticles with a high degree of control on the size, shape and surface environment. The ideal precursor are zerovalent olefinic metal complexes, such as [Ru(COD)(COD)] (COD: 1,5-cyclooctadiene, COT: 1,3,5-cyclooctatriene). However, these procedures were also carried out using metal precursors which contain allylic groups, such as $[Rh(\eta^3\text{-}C_3H_5)_3]$, and organometallic complexes which contain another ligand able to be deplaced by hydrogenolisis, such as $[Rh(\mu\text{-}OMe)(COD)]_2$. It is important to note that the olefinic ligands are hydrogenated during the decomposition of the organometallic precursor to form alkanes, and they are unable to form strong bonds with the growing metal surface. Concerning to the stabilizing agent, polymers, solvents or ligands can be used to synthesise metal nanoparticles by this approach.[8,10]

4. 3. Metal nanoparticles and their application in catalysis

The use of metal nanoparticles in catalysis is a field of growing interest. To date, the metal nanoparticles were revealed to be efficient catalysts in several processes typically homogeneous or heterogeneous, and in some cases interesting results in terms of activity and selectivity were achieved. However, the nature of the "true" active catalytic specie was in some cases controversial [8,14,15] In this section, the application of metal nanoparticles in several catalysed asymmetric processes were introduced:

Reactions catalysed by metal nanoparticles

Hydrogenation reactions can be performed using metal nanoparticles as catalyst. Even greater, nanocatalysts were able to achieve high levels of chemoselectivity. For example, Liu and co-workers in 1999 achieved the chemoselective reduction of cinnamaldehyde into cinnamic alcohol with Pt-nanoparticles stabilised by PVP as catalyst. (Scheme 4.1).[16]

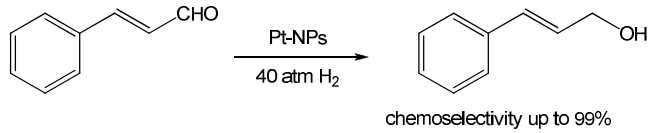

Scheme 4.1. Pt-NPs catalysed chemoselective reduction of cinnamaldehyde.

Recently, the selective hydrogenation of monosubstituted over disubstituted double bonds was reported.[17] Interestingly, the authors observed that the selectivity of this reaction increases with smaller nanoparticles.

Furthermore, the use of metal nanoparticles in the hydrogenation of arenes is an area of growing interest because their produced improved catalytic properties than the "classical" colloid catalysts. [7,8,18,19,20,21,22,23] The discussion about this reaction is introduced in section 4.4.

The use of metal nanoparticles for catalysis in reactions generating a carbon-carbon bonds is an interesting field, specially in the case of coupling reactions as Heck[14,24, 25], Stille type[25,26,27], Sonogashira[27 ,28], and Suzuki cross-coupling reactions[14]. Reetz and co-workers reported one of the pioneering works in the Suzuki cross-coupling, where Pd- or Pd/Ni-(giving a better conversion rate) nanoparticles stabilized by tetrabutylammonium bromide were used as catalysts (Scheme 4.2).[29]

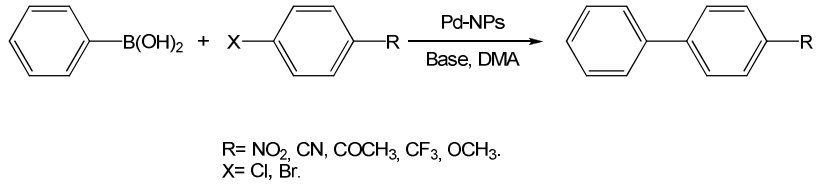

Scheme 4.2. Pd-NPs catalysed Suzuki Coupling Reaction.

Another interesting application of metal nanoparticles was developed by Schmid et al. They applied Pt-Nanoparticles and Pt/Au or Pt/Pd bimetallic colloids supported on alumina to catalyse the hydosilylation of 1-octene with heptamethyltrisiloxane (HMTS) as it is shown in Scheme 4.3.[30]

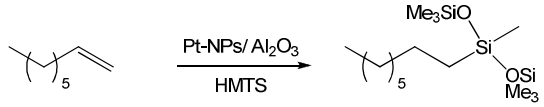

Scheme 4.3. Pt-NPs catalysed hydrosilylation of 1-octene.

The use of metal nanoparticles to catalyse oxidation reaction was also described. Thosima et al. used Ag-nanoparticles stabilised by poly(*N*-vinyl-2-pyrrolidone) (PVP) or by sodium poly(sodium acrylate) to oxidize ethene (Scheme 4.5).[31]

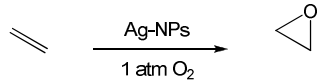

Scheme 4.4. Ag-NPs catalysed epoxidation of ethene.

Furthermore, the use of supported gold nanoparticles was revealed to be very effective catalyst to oxidize alkanes, alkenes and alcohols, to hydrogenate alkenes and to reduce nitro compounds in the presence of other reducible functions.[32] Recently, the use of Au-nanoparticles as efficient and selective catalysts in the reaction of diboration of terminal and internal alkenes was described by Fernandez et al. (Scheme 4.4).[33]

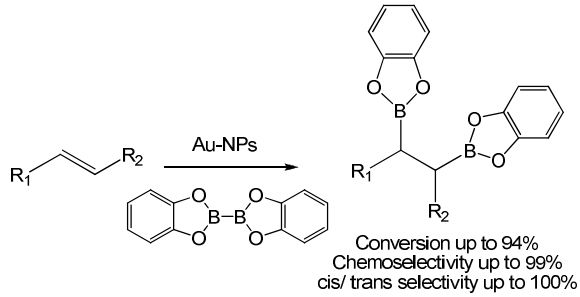

Scheme 4.5. Au-NPs catalysed diboration of terminal and internal alkenes.

Additionally, several examples of Pauson-Khand reactions catalysed by Co or Co/Rh-nanoparticles were reported by Chung and co-workers.[34] Other

carbonylation reactions such as the carbonylation of methanol have been described by Liu using Rh nanoparticles stabilized by PVP.[35] The use of Ru-nanoparticles was revealed to be a very selective catalyst in the Fischer-Trops reaction to form C_{10}-C_{20} hydrocarbons.[36]

Asymmetric reactions catalysed by metal nanoparticles

The first successful example of asymmetric reaction catalysed by metal nanoparticles was reported by Bönneman et al. (Scheme 4.6).[37]

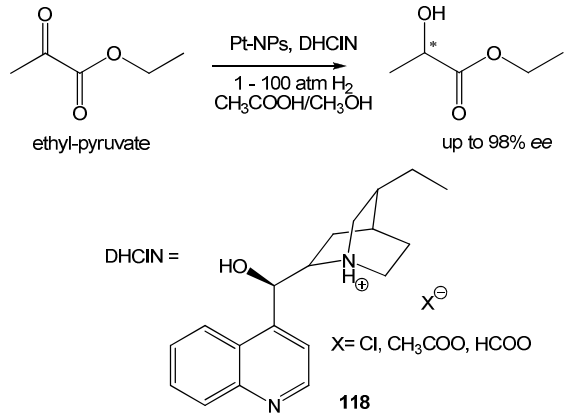

Scheme 4.6. Pd-cinchonidine and Pt-cinchonidine nanoparticles catalysed enantioselective hydrogenation of ethyl pyruvate.

They described the synthesis of Pd- and Pt-nanoparticles stabilised by dihydrocinchonidine salts (DHCIN) **118** and their use in liquid phase or immobilised on a support (in charcoal or silica). The hydrogenation of ethyl pyruvate provided (*R*)-ethyl lactate with enatiomeric excess up to 80%. The enantioselectivity of the reaction was later improved up to 98% by using Pt-nanoparticles stabilised by PVP and modified with cinchonidine.[38] Additionally, several examples using Rh-[39] and Ir-[40]nanoparticles modified with cinchonidine derivates were reported in the enantioselective hydrogenation of α-ketosters (*ee* up to 75%) and acetophenone (*ee* up to 80%), respectively.

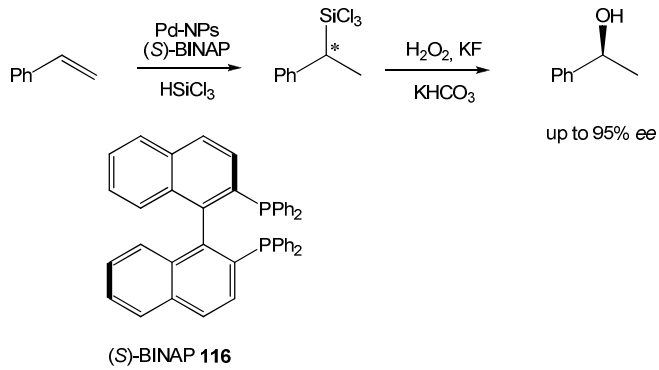

Scheme 4.7. Pd-NPs modified with ligand BINAP **116** catalysed the hydrosilylation of styrene.

Fujimara and co-workers reported the use of 2,2´-bis(diphenylphosphino)-1,1´-binaphthyl (BINAP) **116** as stabilizing agent in the synthesis of Pd nanoparticles, and their use as nanocatalyst in the asymmetric hydrosilylation of styrene under mild conditions (Scheme 4.7). High conversions and high enantioselectivity (up to 95%) were achieved with the Pd-BINAP nanocatalyst system. In contrast, the Pd-BINAP mononuclear complex was inactive in this reaction.[41]

Chang et al. reported the synthesis of Co/Rh nanoparticles modified with C_2-simmetrical chiral diphosphine ligands and their use as catalysts in the intramolecular Pauson-Khand type reaction using aldehydes as carbonyl source. High enantioselectivity (*ee* up to 87%) was achieved in this reaction.[42]

In 2004, the Chaudret, Gómez and Claver et al. reported the use of chiral diphosphite ligand **21b** as stabilizing agent in the synthesis of Pd nanoparticles, and their use as nanocatalysts in the enantioselective allylic alkylation of *rac*-1,3-diphenyl-3-acetoxy-propen-1-ene using dimethyl malonate as nucleophile (Figure 4.8). High enantioselectivity (*ee* up to 97%) in the product and in the substrate (*ee* up to 89%) were achieved.[43]

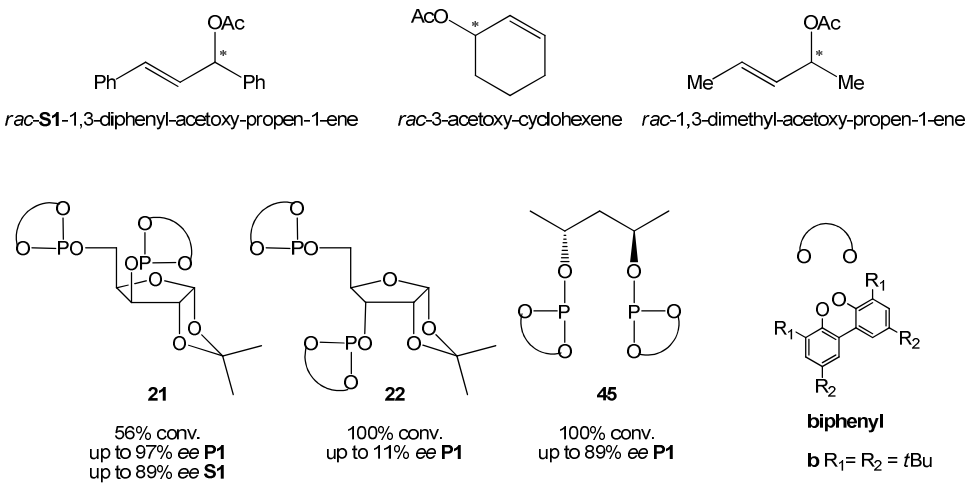

Figure 4.8. Pd-NPs stabilised by ligands **21b**, **22b** and **45b** catalysed asymmetric allylic substitution.

More recently, the same authors reported the use of diphosphite ligands **22b** and **45b**, related to **21b**, to stabilize Pd nanoparticles and their application in the asymmetric allylic alkylation reaction of 1,3-diphenyl-3-acetoxy-propen-1-ene, 3-acetoxy-cyclohexenene and 1,3-dimethyl-3-acetoxy-propen-1-ene with dimethyl malonate as nucleophile (Figure 4.7).[44] Nanoparticle colloids Pd/**21b** and Pd/**22b** were both well dispersed. These results are not very surprising since the stabilizing ligand **21b** and **22b** only differ in the configuration of carbon atom C-3 of their carbohydrate backbone. In contrast, the colloid Pd/**45b** contained nanoparticles with larger mean diameter and size distribution than the colloids Pd/**21b** and Pd/**22b**. The results showed a clear influence of the substrate on the catalytic activity. No conversion was achieved in the allylic alkylation of 3-acetoxy-cyclohexenene and 1,3-dimethyl-3-acetoxy-propen-1-ene. However, the 1,3-diphenyl-3-acetoxy-propen-1-ene is converted. The authors suggested that this fact is in agreement with the strong preference shown by metallic surfaces for aryl groups, probably due to π-coordination between the metallic surface and the aromatic group whereas alkyl groups can only lead to weak agostic interactions.[44]

It should be noted that the elucidation of the nature of the "true" active catalyst in processes in which both the homogenous molecular complexes and the nanoparticles are active is a very complex task.[7] A variety of

experiments have been used to distinguish homogeneous catalysis from nanocatalysis. The most convincing studies use a combination of experiments before reaching a compelling conclusion. To elucidate the true nature of the catalyst is necessary to perform two types of experiments: a) experiments that provide information about kinetics, they are crucial for determining the identity of the true catalyst; b) control experiments using heterogeneous catalysts or homogeneous catalysts can be important.

Interestingly, metal nanoparticles, either preformed or generated in situ, can also act as a reservoir of active molecular complexes. This is the case of palladium-nanoparticles when they are applied in the Heck coupling reactions.[45]

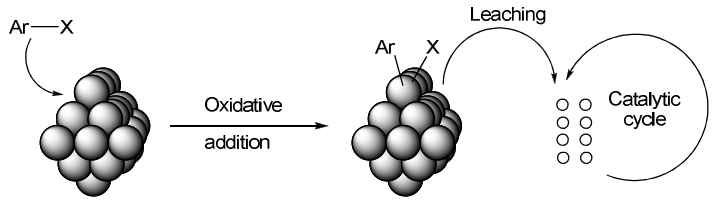

Figure 4.9. Schematic representation of the accepted mechanism for Heck coupling with Pd-NPs as catalytic precursor.

The accepted mechanism involves the following elementary steps: oxidative addition to the aryl halide substrate to the nanoparticle surface, leaching of Pd(II) molecular species that enter the catalytic cycle and then reforming of the nanoparticles at the end of the reaction (Scheme 4.9).

In this way, van Leeuwen et al.[46] stabilised palladium-nanoparticles with phosphite-oxazoline ligands derived from carbohydrates and applied them as catalysts in allylic alkylations and Heck reactions. The results found in these reaction were compared with those obtained using the related homogeneous monometallic catalysts. The obtained activities and enantioselectivities using the Pd-nanoparticles were lower than those obtained using the Pd homogeneous catalysts. Furthermore, the results using a continuous-flow membrane reactor (CFMR), Transmission Electron Microscopy (TEM), poisoning and kinetic measurements show that the formation of active molecular species can account for the catalytic results. The CFMR experiments proved to be crucial to elucidate that the leached

molecular palladium species containing oxazolinyl-phosphite ligands were the true active catalyst.

4. 4. Hydrogenation of arenes

To date, the hydrogenation of monocyclic arenes is an active area of research.[47] The production of cyclohexanes from the corresponding substituted arenes is a goal of this research. The hydrogenation of benzene to cyclohexane is probably the most important industrially practiced arene hydrogenation reaction, the cyclohexane being used primarily in the production of adipic acid, a precursor of nylon. Another interesting applications of the arene hydrogenation are: (a) the partial arene hydrogenation to cyclohexenes, (b) the treatment of diesel to obtain low-aromatic-content diesel fuels, (c) the hydrogenation of aromatic polymers enabled to produce new material with new interesting properties, and (d) the synthesis of enantiomerically enriched chiral cyclohexanes, which were useful in organic synthesis for the production of pharmaceuticals and biologically active compounds.

The hydrogenation of arenes is much more difficult to catalyse than the hydrogenation of simple olefins.[48] This is as expected because at least some fraction of the resonance stabilization energy that is lost during arene hydrogenation appears in the transition state of the rate-determininig step. Herein a distinction is made between monocyclic arenes and polycyclic arenes because, at least under mild conditions monocyclic arenes are more difficult to hydrogenate.[49]

Several reports described the hydrogenation of monocyclic arene using homogeneous, single-metal-complex catalyst.[50] Unfortunately, these catalysts typically have poor catalytic activity, and several such claimed mononuclear "homogeneous" catalysts have more recently shown to be soluble nanoparticles catalysts.[47,50] To date, only organometallic complexes based on Nb or Ta were demonstrated to catalyse as true homogeneous species, for instance the Nb^{V} and Ta^{V} hydrido aryloxide complexes developed by Rothwell[51] and the cylcohexadienyl Nb^{III} catalyst developed by Fryzuk[52].

The use of heterogeneous catalytic systems in the hydrogenation of monocyclic arenes is preferred, because they are more active than the

homogeneous catalytic systems. These catalysts are typically based on Group VIII metals. The catalytic activity of such metals for the hydrogenation of benzene and alkylbenzenes decreases in the order Rh > Ru > Pt > Ni > Pd > Co.[53] The use of colloidal catalytic systems based on metal sufides, such as MoS_2 and WS_2, has also been described, however they are much less active than the catalyst based on metals of group VIII.[54]

Nowadays, the introduction of the use of nanoparticles as catalyst provided a highly interesting way to improve the catalytic properties of the "classical" colloidal systems. The chemical and physical properties of these new systems provided excellent opportunities to explore a non-typically selective reaction, such as hydrogenation of arenes. Several types of selectivity were studied: (a) the chemoselectivity, (b) *cis/trans* selectivity and (c) enantioselectivity.

Chemoselectivity

The chemoselectivity of these reactions refers to the hydrogenation of arenes in front other function. For example, side reactions as the hydrogenolysis of substituents can compete with the arene hydrogenation. Generally hydrogenolysis is slow compared to the hydrogenation reaction. However, there are exception to this rule in the literature, such as the hydrogenation of dibenzo-18-crown-6 ether with Rh(0) nanoclusters. Lemaire an co-workers found that under certain conditions the main product is a hydrogenolysis product.[55]

Another interesting feature involved in the chemoselectivity of the reaction was the possibility to reduce selectively aromatic compounds to cyclohexenes. In the industry this reaction is typically performed by Asahi Chemical Industry in Japan using heterogeneous Ru catalyst. However, to date only three nanocatalytic systems yielding observable amounts of partial hydrogenated products have been reported reported. In the first report, Blum et al.[56] observed the formation of cyclohexenes in the hydrogenation of very sterically hindered substrates like durene (1,2,4,5-tetramethylbenzene). This fact was explained because the sterically bulky substrates dissociate more readily from the catalyst surface and, therefore,

favour partial hydrogenation. In the second report, Finke et al.[57] described 30% of selectivity to the partial hydrogenation of anisoleee at very low conversions (up to 8%) by using Rh-nanoparticles stabilised with polyoxoanion-and tetrabutylamonoium. In the last report, Dupont et al.[58] described selectivities to the partial hydrogenation of benzene using Ru nanocatalyst stabilised by imidazolium ionic liquids, obtaining selectivities up to 39% at very low conversion (up to 2%). It was interesting to note that the solubility differences in the ionic liquid can be used for the extraction of cyclohexene during benzene hydrogenation, because ciclohexene was less soluble in the ionic liquid than the benzene.

cis/*trans* Selectivity

In the hydrogenation of di-or multi-substituted monocyclic arenes with soluble metal nanocatalysts the formation of *cis* distereomer the formation of *cis* diastereomer is usually observed. Arenes hydrogenated with metal particles are known to favour formation of the thermodynamically less favourable all-*cis*-diastereomer.[59] This selectivity is rationalized by a continuous coordination of the substrate to the catalyst during hydrogenation, leading to the addition of hydrogen to only one "face" of the arene.[50, 60]

The studies of nanocluster catalysis have typically used di-substituted benzenes such as *o*-methylanisole or xylenes. Without exception, the all-*cis*-diasteromers are the major product; *trans*-diastereomers, commonly observed as minor products, are formed when partially hydrogenated intermediate dissociates from the catalyst surface and then re-associates with the opposite "face" before further hydrogenation (see Scheme 4.8).[53]

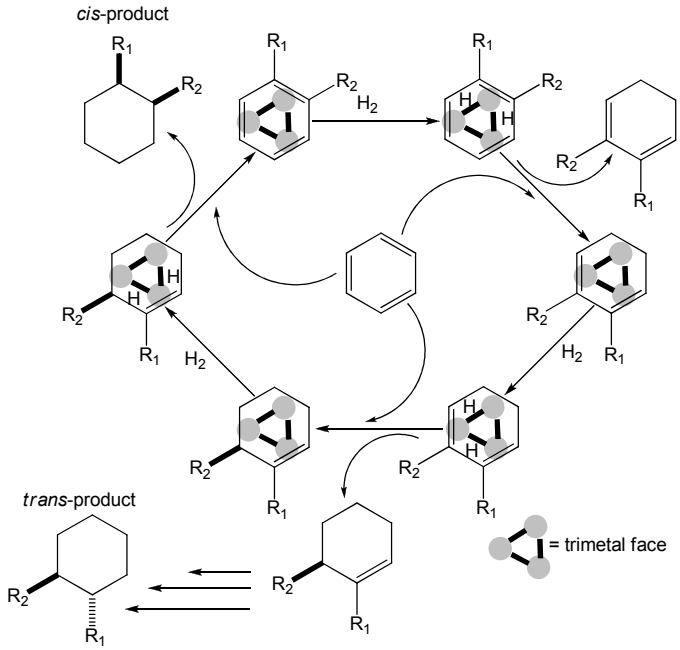

Scheme 4.8. Proposed arene-exchange mechanism that could operate at a metal face in a homogeneous cluster or heterogeneous catalyst.

Several examples involving methylanisole as a substrate were reported in the literature (Scheme 4.9).

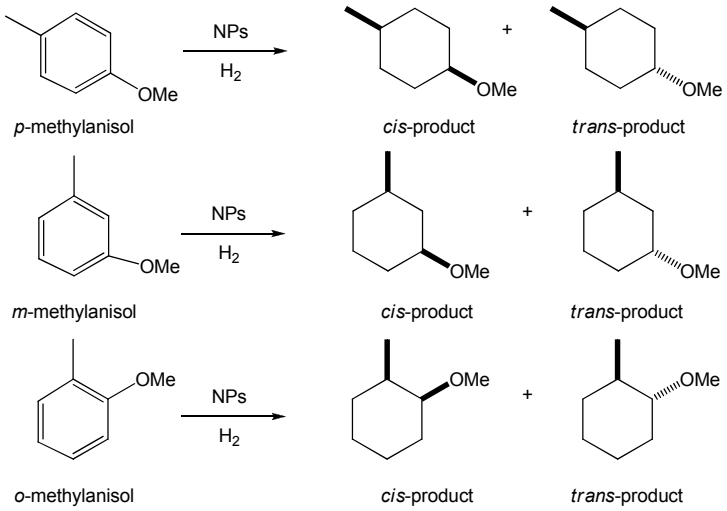

Scheme 4.9. Hydrogenation of *p*-, *m*- and *o*-methylanisole catalysed by metal nanoparticles.

For example, Halper et al. found only the *cis*-product when the *p*-methylanisole was hydrogenated using Rh-nanocatalyst.[61] Furthermore, Lemaire et al. found *cis*-selectivities up to 97% in the hydrogenation of *o*-mehtylanisole using Rh- and Ru-nanocatalyst.[62]

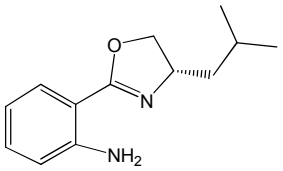

119

Figure 4.9. Ru-nanoparticles stabilised by oxazoline ligand **119** provided high trans-selectivity.

The synthesis of Ru-nanoparticles stabilised by chiral oxazoline ligand **119** and their use in the hydrogenation of *p*-methylanisole and *o*-methylanisole was recently reported (Figure 4.9). It is interesting to noted that in this case the major product obtained is the *trans*-product, with 65% of *trans*-selectivity in the hydrogenation of *p*-methylanisole and 95% of *trans*-selectivity in the hydrogenation of *o*-methylanisole.[63] Traditional heterogeneous metal particle catalysts are known to favour the formation of the *cis*-diastereomer but it is not so clear if this trend will hold for metal soluble nanocatalyst.

Enantioselectivity

As far as we know, only one report described the use of metal nanocatalyst in the hydrogenation of pro-chiral arenes, such as methylanisoles and its derivates. Lemaire and co-workers described the use of Rh nanocatalyst stabilised by chiral amines, such as *R*-(-)-dioctylcyclohexyl-1-ethylamine (DOCEA) **120**, and their use as catalyst in the hydrogenation of *o*-methylanisole and *o*-methyl-*O*-trimethylsilyl-benzene achieving low enantioselectivities, *ee* of 3% and 6%, respectively (Scheme 4.10).[62]

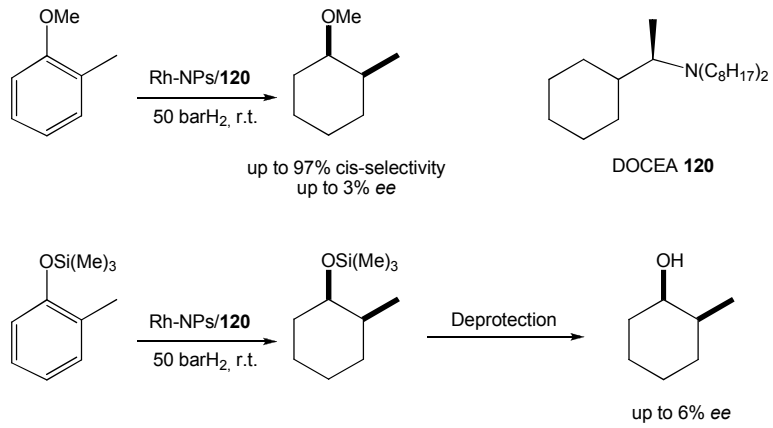

Scheme 4.10. Rh-nanoparticles stabilized by chiral amine **120** produced low enantioselectivities in the hydrogenation of *o*-methylanisole and *o*-methyl-*O*-trimethylsilyl-benzene.

Lemaire also described diastereoselectivities up to 10% in the hydrogenation of *o*-methylanisole derivate **121** by covalently binding a chiral auxiliary, such as methoxy-acetic acid, to the substrate.[62] Nowadays, much effort has been directed to the design of chiral auxiliaries (see compounds **122-124**, Figure 4.9) in order to obtain the hydrogenated product in high diastereoselectivities (*de* up to 96%).[64]

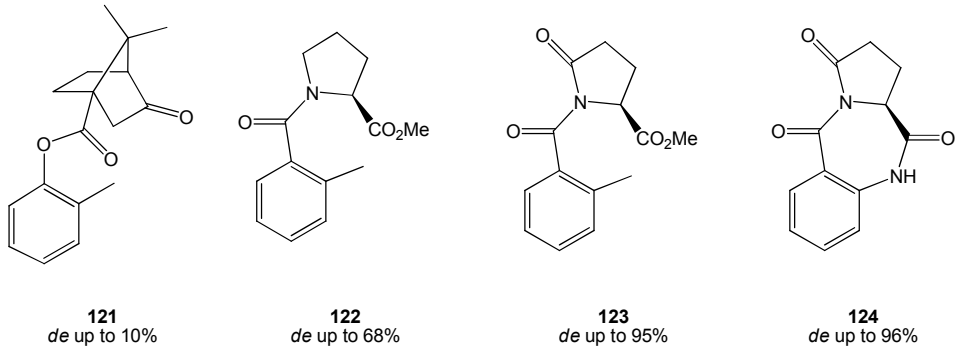

121 *de* up to 10% | **122** *de* up to 68% | **123** *de* up to 95% | **124** *de* up to 96%

Figure 4.10. Hydrogenation of substrates that contain a chiral auxiliaries.

However, the use of the chiral auxiliaries has a very limited scope of substrates (Figure 4.10). Therefore, future work in this area is required in order to obtain effective nanocatalyst for the hydrogenation of pro-chiral arenes.

4. 4. Results and Discussion

The use of series of chiral 1,3-diphosphites in the stabilization of metal-nanoparticles and their use as nanocatalysts provided excellent opportunities to study the effect of the stabilizing agent structure by selective modification of the electronic and the steric properties of the 1,3-diphosphite moieties.

In this chapter is introduced the use of series of chiral 1,3-diphosphite ligands in the synthesis of Ru-, Rh- and Ir-nanoparticles, and their use in the hydrogenation of pro-chiral *m*-and *o*-methylanisole.

The effect of the 1,3-diphosphite moieties in the mean diameter and size distribution of the synthesised nanoparticles was extensively studied by selective modification of the carbohydrate backbone and the biphenyl moiety.

This work was carried out in collaboration with the Prof. Bruno Chaudret and Prof. Alain Roucoux.

1,3-Diphosphite ligands derived from carbohydrates as chiral stabilizers for transition metal nanoparticles: promising catalytic systems for the asymmetric hydrogenation of ortho- and meta-methylanisoles

This work has been published:

A. Gual, M.R. Axet, K. Philippot, B. Chaudret, A. Denicourt-Nowicky, A. Roucoux, S. Castillón, C. Claver, *Chem. Commun.* **2008**, 2759.

A. Gual, C. Godard, K. Philippot, B. Chaudret, A. Denicourt-Nowicki, A. Roucoux, S. Castillón, C. Claver, *ChemSusChem.* **2009**, Submitted.

Summary

Metallic nanoparticles (NPs) based on Ru, Rh and Ir were prepared by decomposition of organometallic precursors under H_2 pressure in the presence of 1,3-diphosphites derived from carbohydrates as stabilising agents. Interestingly, structural modifications of the diphosphite backbone influence the nanoparticle size and dispersion as well as their catalytic activity. In the hydrogenation of o,m-methylanisole, the Rh-NPs showed higher activity than the corresponding Ru-NPs. As expected, the Ir-NPs presented the lowest activity of the series. Hydrogenation of *o*-methylanisole gave rise to a total selectivity in the *cis*-product, although the product *ee* was only up to 6 %. With *m*-methylanisole up to 73 % *cis*-selectivity without asymmetric induction was achieved. Finally, the catalytic results showed that they are clearly affected by the substrate, the diphosphite ligand and the metal nanoparticle.

Design and synthesis of new stabilizing agents

As previously mentioned the design of the stabilizing agent is a key step to allow effective nanocatalyst. The use of amines bearing long-alkyl chains, such as *N*,*N*-dimethyl-*N*-cetyl-*N*-(2-hydroxyethyl)ammonium chloride salt (HEA16Cl) **125** (Figure 4.11), was demonstrated to produce small and better dispersed Ru-, Rh- and Ir-nanocatalyst. These nanocatalyst were active in the hydrogenation of arenes in the hydrogenation of arenes in aqueous media[65] or in organic media, such as ionic liquids [66].

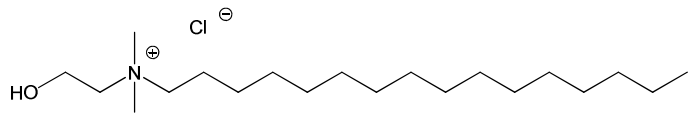

HEA16Cl **125**

Figure 4.11. Long chain amine previously reported for the stabilisation of NPs.

The length of the alkyl chain was shown to contribute to the stabilization of smaller and better dispersed metallic nanoparticles.[67] Additionally, the selective modification of the phosphite structure allow us to design a series of stabilizing agents in order to accomplish a complete study about their effect in the nanoparticle mean diameter and size distribution, as well as their catalytic properties.

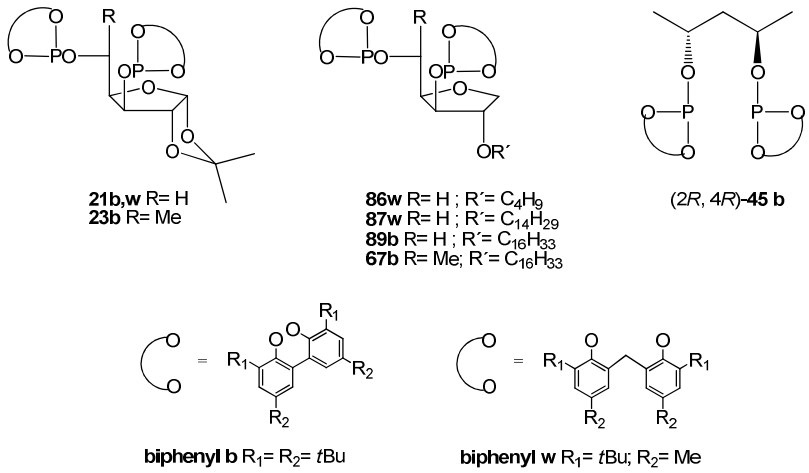

Figure 4.12. 1,3-diphosphite ligands applied as stabilizing agents in the synthesis of metallic nanoparticles.

To achieve our objective of preparing new ligands specifically designed to stabilize metallic nanoparticles, two structural modifications of the 1,2-*O*-isopropyliden-α-*D*-xylofuranose and 1,2-*O*-isopropyliden-α-*D*-glucofuranose backbones were carried out (Figure 4.12): a) Introduction of 3-*O*-alkyl chain in the carbohydrate backbone, b) Increase of the steric bulk of the phosphite moiety using the highly hindered bis-phenol **w**, and c) Study of

the effect of the carbohydrate backbone in the stabilization of the nanoparticles and in their catalytic properties by comparison with the related 1,3-diphosphite derived from (2*R*,5*R*)-pentanediol.

The synthetic procedures to introduce the *O*-alkyl chain function in C-2 position of the carbohydrate backbone and the synthesis of the 1,3-diphosphite ligands **21b,w**, **23b**, **86w**, **87w**, **89b** and **67b** were described in section 2.4.1. and 2.4.2. The 1,3-diphosphite ligand **45b** was synthesised by literature procedures.[68]

Stabilization of Metal-Nanoparticles

The synthesis of metal nanoparticles by olefin reduction and displacement from organometallic compounds was previously reported and was shown to provide nanoparticles with good size and dispersion under mild conditions.[10,69]

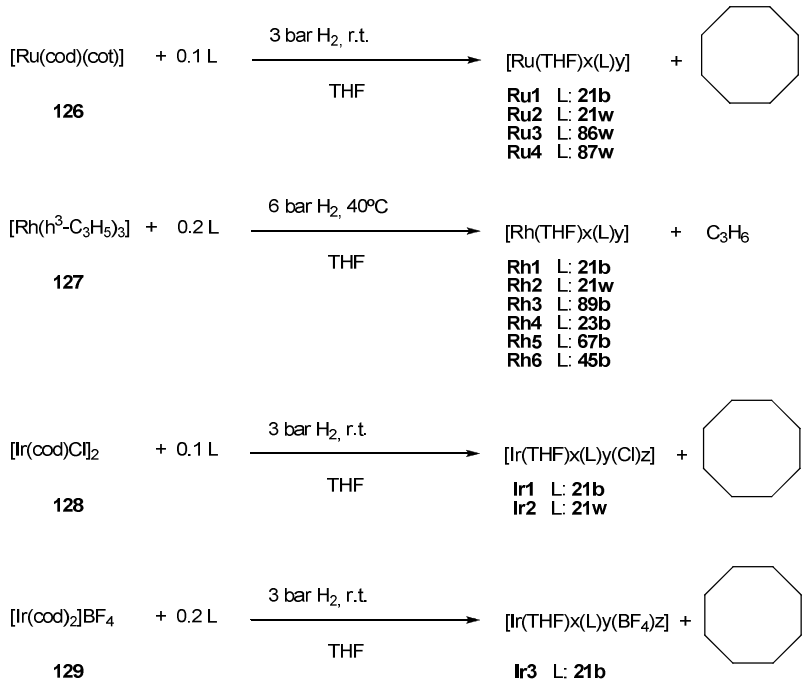

Scheme 4.11. Synthesis of metallic NPs through decomposition of organometallic precursors in the presence of diphosphite ligands.

The Rh, Ru and Ir nanoparticles described here were obtained by decomposition of [Ru(cod)(cot)] (**126**), [Rh(η^3-C_3H_5)$_3$] (**127**), and

$[Ir(cod)(\mu\text{-}Cl]_2$ (**128**) or $[Ir(COD)_2][BF_4]$ (**129**), respectively. These organometallic precursors were synthesised following described methods.[70] It is noteworthy that the Ir precursors used here contain non-alkene ligands that could interact with the surface of the resulting nanoparticles, as suggested by the ICP analysis results and as previously described by Dupont et al.[23]

As a standard procedure, the decomposition of each organometallic precursor (Scheme 4.11) was carried out as previously reported in a Fischer-Porter bottle under H_2 atmosphere in the presence of sub-stoichoimetric quantities of the corresponding diphosphite ligand (L) with THF as solvent.[43,44,71] During the course of the synthesis, the initial solutions were observed to slowly turn black, confirming the decomposition of the complexes. Finally, the NPs were isolated as black powders after precipitation with pentane. The NPs were characterized by transmission electron microscopy (TEM) and the metal and phosphorous contents determined by Induced Coupled Plasma (ICP).

As described in Figure 4.13, spherical shaped Ru-NPs were obtained using ligands **21b**, **21w**, **86w** and **87w** as stabilizers. The mean diameter of **Ru1** stabilised by ligand **21b** was larger than those of **Ru2**, stabilised by ligand **21w**. Interestingly, **Ru4**, which were stabilised by ligand **87w** bearing an *O*-tetradecyl chain, were smaller and better dispersed than the **Ru2** and **Ru3**, which were respectively stabilised by ligands **21w** and **86w**. Thus, the structure of the ligand clearly influences the NPs size.

The right column of figure 4.14 shows the TEM micrographs and size histograms of samples **Rh1**, **Rh2** and **Rh3**, respectively stabilized by ligands **21b**, **21w** and **89b**. All these Rh-NPs were found to have mean diameters inferior to 2.5 nm, with a spherical shape and narrow distribution. A few agglomerates consisting of small groups of individual nanoparticles were also observed. Mean diameters of ca. 1.8 nm, 2.4 nm and 1.6 nm were found for the **Rh1**, **Rh2** and **Rh3**, respectively. Comparing the results with the same ligand (namely **21b** and **21w**), we could observe that Rh-NPs possess smaller size than Ru-NPs.

The differences in mean diameter and size dispersion for these 3 samples clearly indicate that the ligand structure is a key parameter to obtain small and well dispersed nanocolloids. The NPS obtained with ligands **21b**,**w** showed that stabilization using the more rigid diphosphite moiety **b** leads to

a better size control during the growth step, thus yielding smaller and better dispersed Rh-NPs than the biphenyl moiety **w** (**Rh1** vs. **Rh2**). The greater flexibility induced by the presence of a methylene bridge between the two phenol moieties in **w** could reduce the steric hindrance of the ligand and thus explain this difference. The steric hindrance induced by the substituents in *para*-position of the phenol group could also explain this result. Furthermore, **Rh3** NPs, stabilised by ligand **89b**, are even smaller than **Rh1** and present a narrower size distribution, indicating that the *O*-hexadecyl group in the carbohydrate backbone increases the steric hindrance and improves their stabilisation properties.

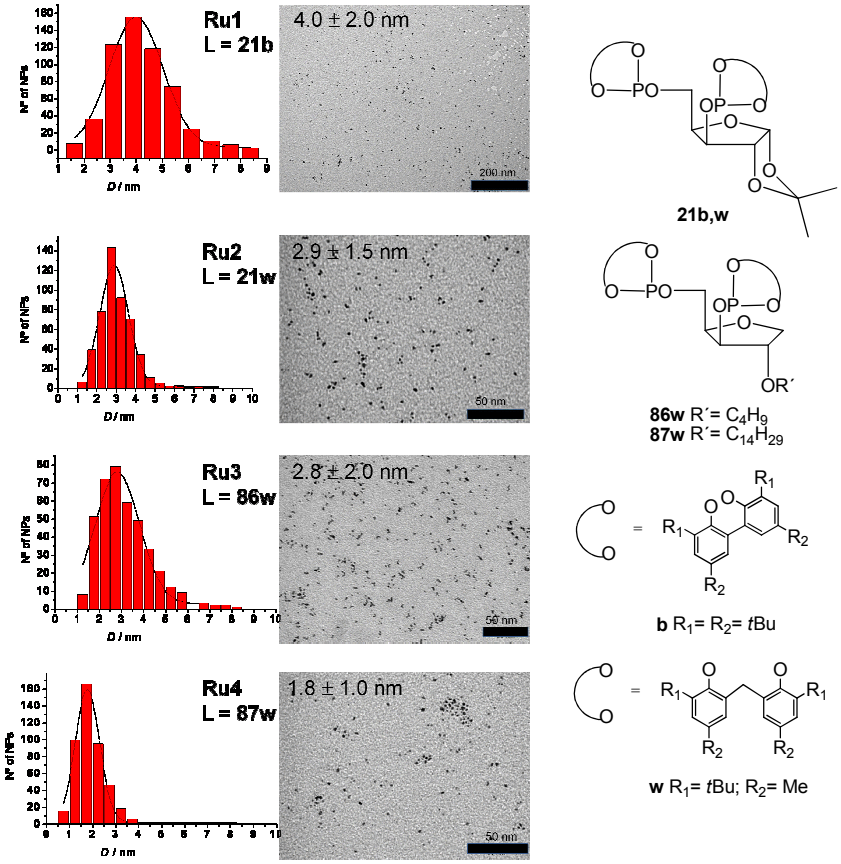

Figure 4.13. TEM micrographs and size histograms for Ru-NPs **Ru1**-**Ru4**.

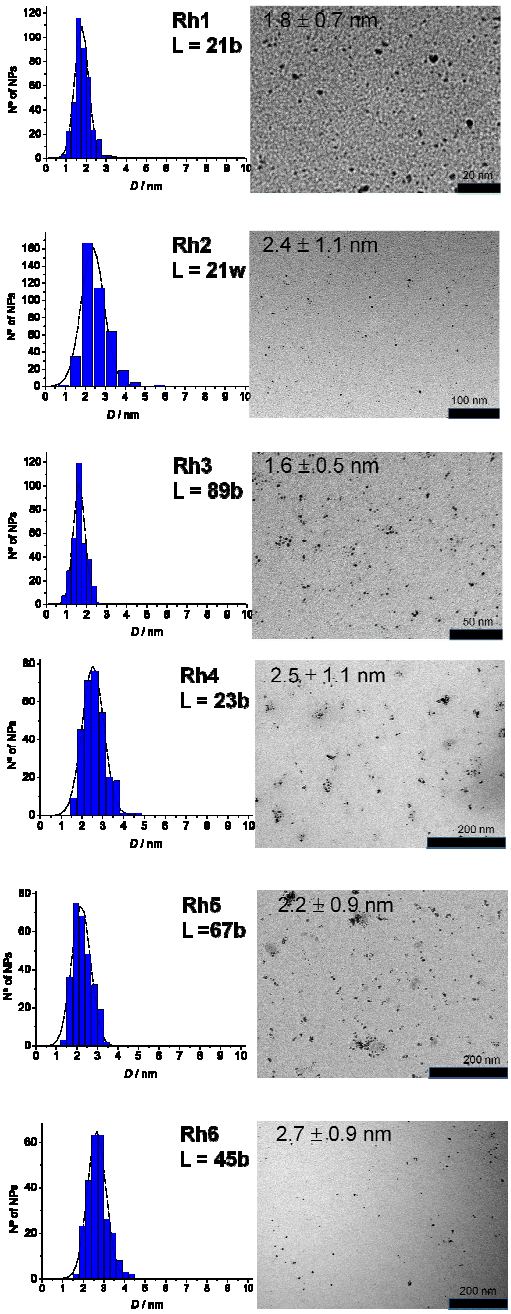

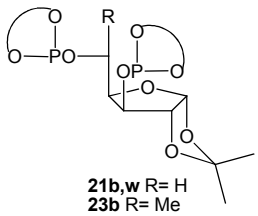

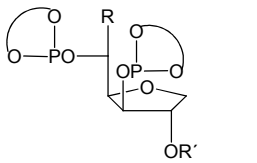

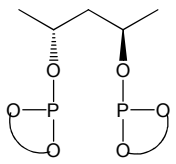

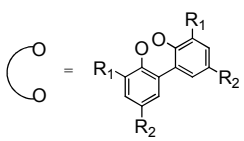

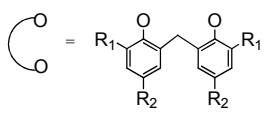

Figure 4.14. TEM micrographs and size histograms for Rh-NPs **Rh1**-**Rh6**.

The left column of figure 4.14 presents the TEM micrographs and size histograms of **Rh4**, **Rh5** and **Rh6** NPs, which are respectively stabilized by ligands derived from 6-*O*-deoxy-glucofuranose, **23b** and **67b**, and **45b**

(derived from (3*R*,5*R*)-pentanediol). These nanoparticles are similar, possessing a small size, a spherical shape and good size dispersions. Some small agglomerates consisting of a few individual nanoparticles were also observed. Mean diameters of ca. 2.5 nm were found for all these Rh-NPs. A small increase in size and dispersion was observed, when compared to those stabilised by xylofuranose based ligands (Figure 7 vs. Figure 8). This effect was attributed to the increased steric hindrance at C5-position of ligands **23b** and **67b** (and the related ligand **45b**) which contain a methyl substituent close to the phosphorus function and must therefore alter the coordination properties of these ligands to the NPs metal surface. Thus, the presence of a methyl group on the ligand leads to the formation of larger NPs, due to an enhanced steric hindrance, which could hamper the coordination. As previously mentioned for Ru-NPs, the presence of a long alkyl chain in the ligands improves both the mean diameter and the size dispersion of the NPs (**Rh4** vs. **Rh5**, Figure 8). The **Rh6** NPs, stabilised by the pentanediol based ligand **45b**, revealed to be slightly larger than those bearing carbohydrate derived ligand, showing that such ligand skeleton is well appropriate to favour small size NPs.

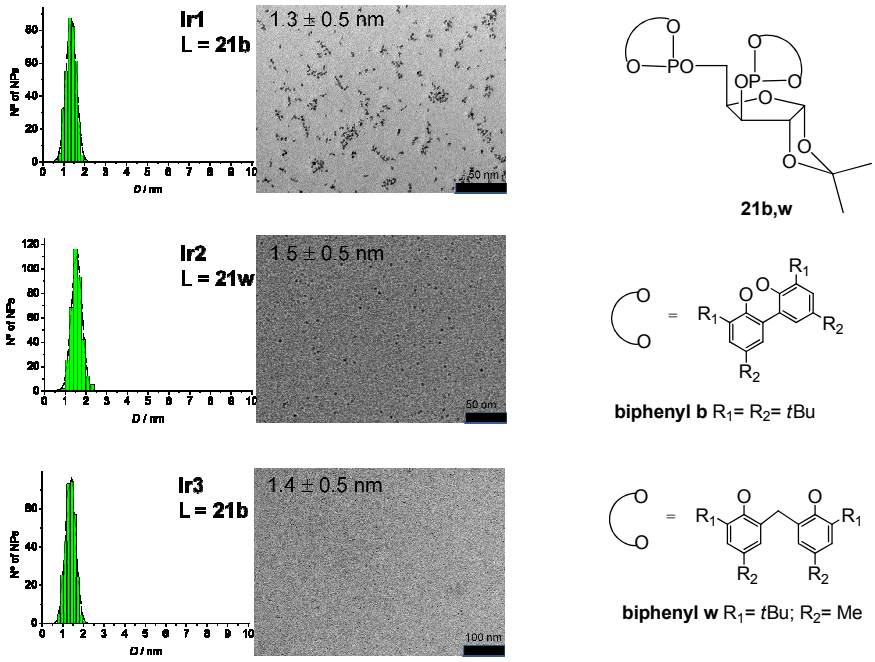

Figure 4.15. TEM micrographs and size histograms for Ir-NPs **Ir1**-**Ir3**.

Ligands **21b** and **21w** were also used to stabilise Ir-NPs (Figure 4.15), for which two precursors, namely $[Ir(\mu\text{-}Cl)(COD)]_2$ **128** and $[Ir(COD)_2][BF_4]$ **129** were probed. Samples **Ir1** and **Ir3**, are both stabilized with **21b**, while **Ir2** is stabilized with **21w**.

Figure 4.14 presents the TEM micrographs and size histograms of **Ir1**, **Ir2** and **Ir3**.These NPs were found to have a spherical shape, with a mean diameter of ca. 1.5 nm with narrow size dispersion. The NPs stabilised with ligand **21b** were found to be slightly smaller than those bearing **21w** (**Ir1** vs. **Ir2**). No obvious effect of the metal precursor on the size and shape of the NPs was observed, as previously reported by Dupont and co-workers.[23]

Hydrogenation of *m*- and *o*-methylanisoles

The main objective of this study was to probe the catalytic activity and selectivity of different metallic NPs stabilised by chiral diphosphite ligands in the enantioselective hydrogenation of disubstituted arenes. The results of the enantioselective hydrogenation of *m*-methylanisole and *o*-methylanisole catalysed by **Ru1**, **Ru2** and **Ru4**-NPs are listed in Table 4.1. The results obtained with Rh and Ir-NPs in this reaction are also described and compared to those obtained using Ru-NPs. The effect of the ligand structure on the catalytic results is also studied. The conversion and the selectivity were determined by chiral gas chromatography analysis. Several parameters, such as the solvent, the ligand, the pressure, have been optimized.

First, concerning the solvent, no conversion was observed in THF and CH_3CN (Entries 1 and 2, Table 4.1), whereas **Ru1** NPs have shown an efficient activity in pentane (Entry 3, Table 4.1). This difference was explained by a competitive adsorption between the substrate and the solvent (THF and CH_3CN) at the NPs surface, preventing the reaction. The influence of the ligand structure was thus explored in pentane. Higher conversions were obtained with **Ru2** system (Entry 3 vs Entry 5 and Entry 9 vs Entry 11) for both substrates *m*-methylanisole and *o*-methylanisole under the same conditions. Addition of 1 eq. of free ligand to the **Ru1** catalytic system (Entries 4 and 10) leads to a decrease in the activity,

which was attributed to a competitive coordination between the free ligand and the arene substrates at the NPs surface.

Table 4.1. Hydrogenation of *m*-methylanisole (**M**) and *o*-methylanisole (**O**) with Ru-NPs.

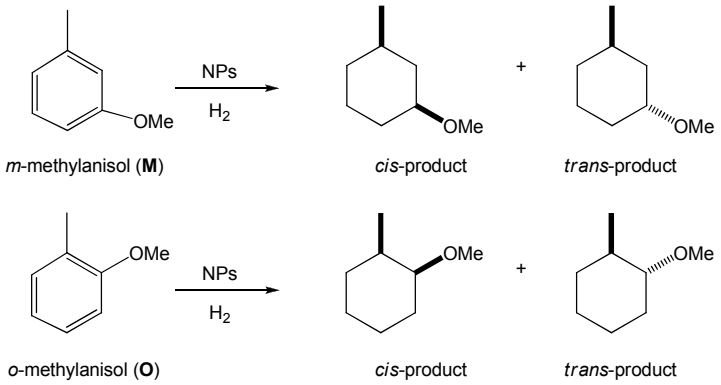

Entry [a][b]	NPs	Mean Size (nm)	Subs tr.	P (bar)	Conv (%)	%*cis* [c]	*ee* (%)	TON [d]
1[e]	**Ru1**	4.0	**M**	40	0	-	-	-
2[f]	**Ru1**	4.0	**M**	40	0	-	-	-
3[g]	**Ru1**	4.0	**M**	40	39	78	-	444
4[h]	**Ru1**	4.0	**M**	40	13	78	-	148
5	**Ru2**	2.9	**M**	40	100	79	-	750
6	**Ru2**	2.9	**M**	10	13	81	-	97
7	**Ru4**	1.8	**M**	10	100	79	-	497
8	**Ru4**	1.8	**M**	2	48	73	-	238
9	**Ru1**	4.0	**O**	40	14	100	4	160
10[h]	**Ru1**	4.0	**O**	40	7	100	5	79
11	**Ru2**	2.9	**O**	40	100	100	6	750
12	**Ru2**	2.9	**O**	10	65	100	4	487
13	**Ru4**	1.8	**O**	10	77	100	4	382
14	**Ru4**	1.8	**O**	2	39	100	4	193

[a] Substrate/metal = 100, methylanisole = 1.24 mmol, 10 mL solvent, T = r.t.; t= 15h. [b] Substrate conversion and selectivity determined by GC analysis using a chiral column Chiralsil-Dex CB. [c] % *cis*-product. [d] TON= moles of H_2 consumed/ moles of metal on the nanoparticle surface. [e] solvent = THF. [f] solvent= CH_3CN. [g] Solvent= pentane. [h] 1 eq. of the corresponding diphosphite ligand per metal total mol in the nanoparticle was added.

This result confirmed the NPs nature of the active catalytic species. When *m*-methylanisole was used as substrate, 39% conversion was obtained with **Ru1** while **Ru2** yielded 100 % conversion. In contrast, the *cis* selectivity (ca. 80%) was identical using both systems and no enantioselectivity was obtained in the reaction products. With *o*-methylanisole as substrate, 14% conversion was achieved with **Ru1**, while **Ru2** leads to a total conversion.

In addition, with this substrate, total selectivity to the *cis* product was observed although low enantioselectivity (ca. 6%) was achieved using either **Ru1** or **Ru2** as catalyst. This difference in activity was explained by the influence of the diphosphite moiety of the stabilising ligands.

Next, the effect of the pressure was also investigated. When the total pressure was decreased to 10 bar the nanocatalyst **Ru2** exhibited lower activity (Entry 5 vs Entry 6 and Entry 11 vs Entry 12). Furthermore, the nanocatalyst **Ru4**, which possesses smaller nanoparticles, showed higher activity than **Ru2** (Entry 6 vs Entry 7 and Entry 12 vs Entry 13). Finally, the total pressure was decreased to 2 bar in order to test the most active nanocatalyst **Ru4** under mild reaction conditions (Entry 7 vs Entry 8 and Entry 13 vs Entry 14). Lower activities were obtained with lower pressure but the conversions are similar to those obtained with the other catalytic systems under high pressure conditions.

In terms of selectivity, high selectivity to the *cis*-product in the hydrogenation of *m*-methylanisole (ca. 81%) and total selectivity to the *cis*-product in the hydrogenation of *o*-methylanisole were achieved. Furthermore, no asymmetric induction was observed in the case of the *cis*-product formed in the hydrogenation of *m*-methylanisole and low values in the *cis*-product formed in the hydrogenation of *o*-methylanisole. Interestingly, no effect of the variation of the total pressure, the added quantities of ligand or the ligand structure over the *cis*-and enantioselectivity was observed.

In Table 4.2, the results obtained in the enantioselective hydrogenation of *m*-methylanisole and *o*-methylanisole catalysed by the **Rh1**-, **Rh2**-, **Rh3**-, **Rh4**- and **Rh6**-NPs are presented. These nanocatalysts were tested at room temperature using pentane as a solvent.

Firstly, when **Rh1** was used as catalyst under 40 bar of H_2 at room temperature, moderate conversions were observed (Entries 1 and 8, Table 4.2). Decreasing the H_2 pressure to 2 bar (Entries 2 and 9), comparable

conversion and selectivity were achieved. This result confirmed that the H_2 pressure has no effect over the *cis*/*trans* selectivity. When the catalytic reaction was carried out in the presence of 1 eq. of ligand **21b** per mol of Rh (Entry 3 and 10), the conversion was found to decrease, while the selectivity to the *cis* product slightly increased. As for Ru systems, this effect can be explained by competitive coordination between the free ligand and the substrate at the Rh-NPs surface.

Afterwards, the results obtained for the enantioselective hydrogenation of *m*-methylanisoleee are hereafter discussed in order to rationalize the catalytic results using the Rh nanocatalyst with the modified ligand structures.

When **Rh2** was used as catalyst under 2 bar of H_2 (Entry 4, Table 4.2), 97% conversion was achieved with similar *cis* selectivity to the one obtained with **Rh1**. This increase in activity was unexpected considering the larger mean size of these NPs (ca. 2.4 nm), and is attributed to an effect of the diphosphite moiety.

Using **Rh3** as catalyst under the same conditions (Entry 5, Table 4.2), 100% conversion was achieved, together with 64% selectivity to the *cis* product. The increase in activity compared to that of **Rh1**, bearing the unmodified xylofuranose derived diphosphite **21b**, could be attributed to the introduction of a long chain alkyl substituents which avoids aggregation of the nanocatalysts. When **Rh4**, bearing the glucofuranose based ligand **23b**, was used (Entry 6), a drastic decrease in conversion (17%) was observed while the *cis*-selectivity slightly increased. However, when **Rh5** was used as catalyst (Entry 7), an increase in conversion (43%) was observed, although no change in *cis* selectivity was obvious. Once more, this increase in catalyst activity was attributed to a ligand effect, due to the similarity in size, shape and dispersion of the NPs **Rh4**- and **Rh6**-NPs. It is noteworthy that although chiral ligands were used to stabilise these nanocatalysts, the hydrogenated product was in all cases detected as a racemic mixture.

Comparing the results obtained with Rh-and Ru-NPs, it should be noted that lower selectivities in the *cis*-product were obtained with Rh-NPs. In all cases, no asymmetric induction in the *cis*-product obtained in the hydrogenation of *m*-methylanisoleee was detected.

Table 4.2. Hydrogenation of *m*-methylanisole (**M**) and *o*-methylanisole (**O**) with Rh-NPs.

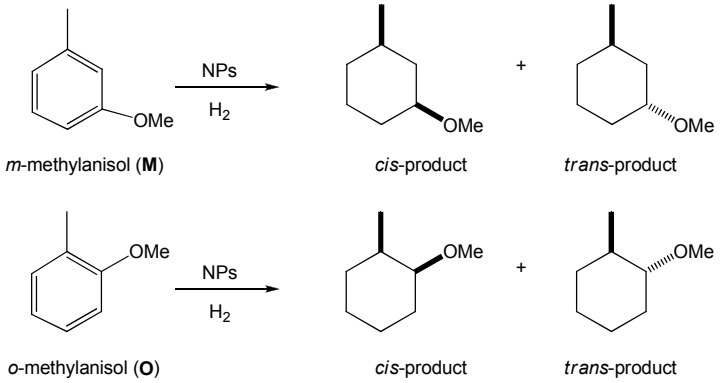

Entry [a][b]	NPs	Mean Size (nm)	Subs tr.	P (bar)	Conv (%)	%*cis* [c]	*ee* (%)	TON [d]
1[e]	**Rh1**	1.8	**M**	40	45	65	-	325
2	**Rh1**	1.8	**M**	2	42	68	-	304
3[f]	**Rh1**	1.8	**M**	2	28	73	-	202
4	**Rh2**	2.4	**M**	2	97	65	-	862
5	**Rh3**	1.6	**M**	2	100	64	-	762
6	**Rh4**	2.5	**M**	2	17	72	-	207
7	**Rh6**	2.7	**M**	2	43	71	-	470
8[e]	**Rh1**	1.8	**O**	40	25	100	5	181
9	**Rh1**	1.8	**O**	2	100	100	6	723
10[f]	**Rh1**	1.8	**O**	2	18	100	4	130
11	**Rh2**	2.4	**O**	2	25	100	6	222
12	**Rh3**	1.6	**O**	2	100	100	6	762
13	**Rh4**	2.5	**O**	2	30	100	5	366
14	**Rh6**	2.7	**O**	2	35	100	0	383

[a] Substrate/ Metal = 150, methylanisole = 1.24 mmol, 10 mL pentane, T = r.t., t= 15h. [b] Substrate conversion and selectivity determined by GC analysis using a chiral column Chiralsil-Dex CB. [c] % *cis*-product . [d] TON= moles of H_2 consumed/ moles of metal on the nanoparticle surface. [e] t= 3h. [f] 1 eq. of the corresponding diphosphite ligand per metal total mol in the nanoparticle was added.

The results of the enantioselective hydrogenation of *o*-methylanisole are discussed in the next paragraphs, since it is interesting to compare the

effect of the ligand structure over the catalytic hydrogenation of *o*-substituted and *m*-substituted arenes.

When **Rh2** was used as catalyst (Entry 11, Table 4.2), 25% conversion was obtained and total selectivity to the *cis*-product obtained in the hydrogenation of *o*-methylanisole was measured. This decrease in activity is in contrast with the results obtained using *m*-methylanisole as substrate (Entries 2 and 4 vs. 9 and 11, Table 4.2). This result suggests that the interactions between the ligand and the substrate at the metal surface are strongly influenced by the position of the substituents of the aromatic ring and thus, that these interactions govern the catalytic activity of these nanocatalysts. When the reaction was performed in the presence of **Rh3** (Entry 12), total conversion to the *cis* product was achieved in 15h with 6 % *ee*. This result confirms the positive effect of the alkyl chain of the ligand on the catalytic activity of the system. In contrast with the results obtained using *m*-methylanisole as the substrate, similar results were obtained using **Rh4** and **Rh6** as catalysts (Entries 6 and 7 vs. 13 and 14) with ca. 30% conversion and a total selectivity to the *cis* product.

Interestingly, the *cis*-selectivity in the hydrogenation of *o*-methylanisole was not affected by the use of Ru- or Rh-NPs. In both cases total *cis*-selectivity was measured. In addition, as for Ru systems, a low but reproducible asymmetric induction was observed in the *cis*-product formed in the hydrogenation of *o*-methylanisole with Rh-NPs.

It is noteworthy that the **Rh6** system did not induce any enantioselectivity in the product. This indicates that the carbohydrate backbone is responsible for the asymmetric induction observed in this reaction with the systems **Rh1**-**Rh4**.

In view of these promising results, the hydrogenation of disubstituted arenes was performed using Ir-NPs, as this metal gives interesting results in hydrogenation reactions.[72] In Table 4.3, the results obtained in the enantioselective hydrogenation of *m*-methylanisole and *o*-methylanisole catalysed by the **Ir1**-**Ir3**-NPs are described. It should be noted that, due to the lower activity of these Ir systems, the substrate to metal ratio was lowered to 40 and the H_2 pressure increased to 40 bars.

When the **Ir1** system was used as catalyst for the hydrogenation of *m*- and *o*-methylanisole under 40 bar of H_2 during 24 h (Entries 1 and 5, Table 4.3), high conversions (87 and 96%, respectively) and high selectivity to

the *cis* products were achieved (81 and 100 %, respectively). However, both *cis* and *trans* products did not present any *ee*. Using the **Ir2** system (Entries 2 and 6) stabilised by ligand **21w**, low conversions were obtained (14 and 4%, respectively) although similar *cis* selectivity was measured (75 and 100%, respectively).

Table 4.3. Hydrogenation of *m*-methylanisole (**M**) and *o*-methylanisole (**O**) with Ir-NPs.

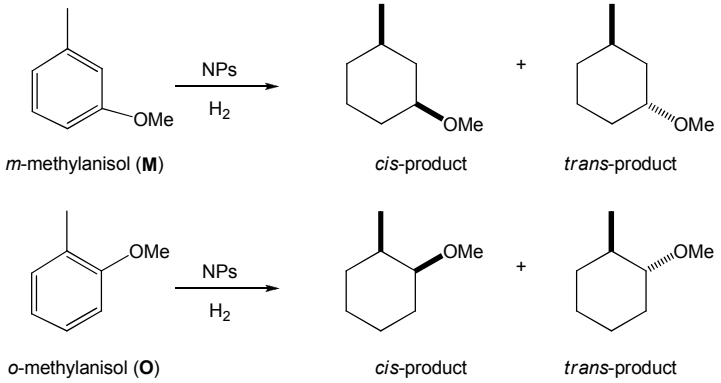

Entry [a][b]	NPs	Mean Size (nm)	Subs tr.	P (bar)	Conv (%)	%*cis* [c]	*ee* (%)	TON [d]
1	**Ir1**	1.3	**M**	40	87	81	-	70
2	**Ir2**	1.5	**M**	40	14	75	-	12
3	**Ir3**	1.4	**M**	40	0	-	-	-
4[e]	**Ir3**	1.4	**M**	40	0	-	-	-
5	**Ir1**	1.3	**O**	40	96	100	1	77
6	**Ir2**	1.5	**O**	40	4	100	2	3
7	**Ir3**	1.4	**O**	40	0	-	-	-
8[e]	**Ir3**	1.4	**O**	40	0	-	-	-

[a] Substrate/ Metal = 40, methylanisole = 1.24 mmol , 10 mL pentane, T = r.t., t= 24h. [b] Substrate conversion and selectivity determined by GC analysis using a chiral column Chiralsil-Dex CB. [c] % *cis*-product . [d] TON= moles of H_2 consumed/ moles of metal on the nanoparticle surface. [e] t= 3h. [f] 1 eq. of the corresponding diphosphite ligand per metal total mol in the nanoparticle was added.

No enantioselectivity was again obtained using this catalyst. The differences in activity between the two catalytic systems **Ir1** and **Ir2**, which exhibit very similar mean diameter and size dispersion are unexpected. The

stabilising ligands for these nanocatalysts, **21b** and **21w**, which only differs by the phosphite moieties, are considered responsible for this difference in activity. Such a strong effect of the diphosphite moiety was previously mentioned in this manuscript using Ru- and Rh-NPs stabilised by ligands **21b** and **21w** as catalysts (Table 4.1, 4,2 and 4.3).

Using **Ir3**, which was synthesised through decomposition of a cationic Ir precursor in presence of **21b** as stabilising ligand, no conversion could be observed (Entries 4 and 7). When the reaction in the presence of 1 eq. of free ligand, no conversion was again measured (Entries 4 and 8). Comparing these results obtained with **Ir1** and **Ir3**, both stabilised with ligand **21b**, it could be concluded that the nature of the metal precursor used for the synthesis of metal nanoparticles is also of great importance to produce nanocatalysts of interest. More precisely the surface state of the NPs needs to be clean and may differ depending on the metal precursor used and the coordinating effect of the stabilising counter-ion.[23]

Comparison of Rh, Ir and Ru nanocatalysts

To compare as accurately as accurately the different metal nanoparticles used in this study, we focused on the nanocatalysts stabilised by ligands **21b** and **21w**, which only differ by the structure of their diphosphite moiety. Comparison of the catalytic activity will be purely qualitative, due to the difference of reaction conditions used in the hydrogenation reactions.

It is noteworthy that the stabilising ligands could have an effect on the crystal-phase of the nanoparticles, which in turns would also have a profound effect on the catalytic properties of the resulting catalysts. In this case, the ligands would only play a stabilising role, thus explaining the small differences in selectivity observed for the series of ligands described here. However, the determination of the crystal-phase of the NPs described here would be extremely difficult due to their small size. Such an effect can therefore not be discarded.

In Table 4.4, the main features of these systems are summarised. The diphosphite ligands **21b** and **21w** were shown to successfully stabilise metallic nanoparticles of Rh, Ru and Ir, which were all active in the hydrogenation of *m*- and *o*-methylanisoles. These ligands were shown to have an effect on both the size and the catalytic activity of the resulting

nanoparticles. In terms of size, the Rh and Ir systems were found to have smaller mean diameter and better size dispersion when **21b** was the stabilising ligand, than those using **21w** (Entry 1 vs 2, Entry 3 vs 4). However, the opposite trend was observed in the case of Ru systems (Entry 5 vs 6), which both displayed larger mean size than their Rh and Ir counterparts. This latter observation can be explained by the nature of the organometallic source used for their synthesis. The Ru-NPs were formed from a Ru(0) species while the Rh- and Ir-NPs were formed from Rh(III) and Ir(I) complexes.

Table 4.4. Metallic NPs stabilised by ligands **21b** and **21w** catalysed the hydrogenation of *m*-methylanisole (**M**) and *o*-methylanisole (**O**).

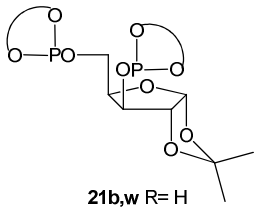

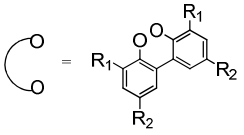

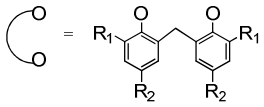

Entry[a]	NPs	Ligand	L /M	P (bar)	Substr./M	Mean size (nm)	TON (%*cis*):	
							M	**O**
1[b]	**Ru1**	**21b**	0.46	40	100	4.0	444 (78)	160 (100)
2[b]	**Ru2**	**21w**	0.38	40	100	2.9	750 (79)	750 (100)
3[c]	**Rh1**	**21b**	0.49	2	150	1.8	305 (68)	723 (100)
4[c]	**Rh2**	**21w**	0.66	2	150	2.4	862 (65)	222 (100)
5[d]	**Ir1**	**21b**	0.04	40	40	1.3	70 (81)	77 (100)
6[d]	**Ir2**	**13b**	0.05	40	40	1.5	12 (75)	3 (100)

[a] methylanisole = 1.24 mmol, 10 mL solvent, T = r.t. [b] Substrate/metal = 100, P = 40 bar; t= 15h. [c] Substrate/ Metal = 150, P = 2 bar, t= 15h. [d] Substrate/ Metal = 40, P = 40 bar, t= 24h.

In terms of catalytic activity, the expected trend was observed with Rh> Ru > Ir. However, the effect of the stabilising ligands was surprising since drastic differences were observed. In contrast, the size of the nanocatalysts did not affect the catalytic activity to a great extent. The Ru catalyst bearing ligand **21b** is less active than that bearing ligand **21w** for both substrates (Entry 1 vs 2). In contrast, the Ir systems, which size and dispersion were quite similar (Entry 5 vs 6), showed considerable differences in catalytic activity depending on the ligand used for their stabilisation. The Ir-NPs stabilised by ligand **21b** were much more active than those with **21w** for the hydrogenation of both *m*-and *o*-methylanisoles. Finally, the case of Rh systems is somewhat intermediate since the nanocatalysts stabilised by ligand **21b** were more active for the hydrogenation of *o*-methylanisole while higher conversion of substrate m-methylanisole was achieved using NPs stabilised by ligand **21w** (Entry 3 vs 4).In terms of *cis*-selectivity, the use of these diphosphite ligands provided excellent results when *m*-methylanisole was used as substrate (ca. 75%, Entries 1-6). When *o*-methylanisole was used as substrate, total selectivity to the *cis* product was achieved (Entries 1-6). In the hydrogenation of *m*-methylanisole, no clear effect of the ligand structure was observed although the use of Ir and Ru based catalysts (ca. 80%, Entries 3-6) were shown to be slightly more selective than the Rh nanocatalysts (ca.70%, Entries 1 and 2).In terms of enantioselectivity, chiral induction was only achieved in the hydrogenation of *o*-methylanisole, and not with *m*-methylanisole. Although very low *ee*'s were obtained, the Rh systems provided the highest value reported to date (6%) for the hydrogenation of *o*-methylanisole. It is noteworthy that the diphosphite ligand derived from pentanediol did not provide any chiral induction while those derived from carbohydrates all yielded non-racemic mixtures when *o*-methylanisole was the substrate. Within the series of carbohydrate ligands used in this study, no substantial effect of the ligand structure was observed on the enantioselectivity of the reaction. The Ir-NPs provided the weakest chiral induction in the hydrogenation of *o*-methylanisole, which can be related to the low ligand to metal surface atoms ratio (<0.04) measured in these nanocatalysts with respect to the corresponding Ru (ca. 0.4) and Rh (ca. 0.6) catalysts (Table 4.4, Entries 5 and 6 vs Entries 1-2 and 3-4).

2.6. Conclusions

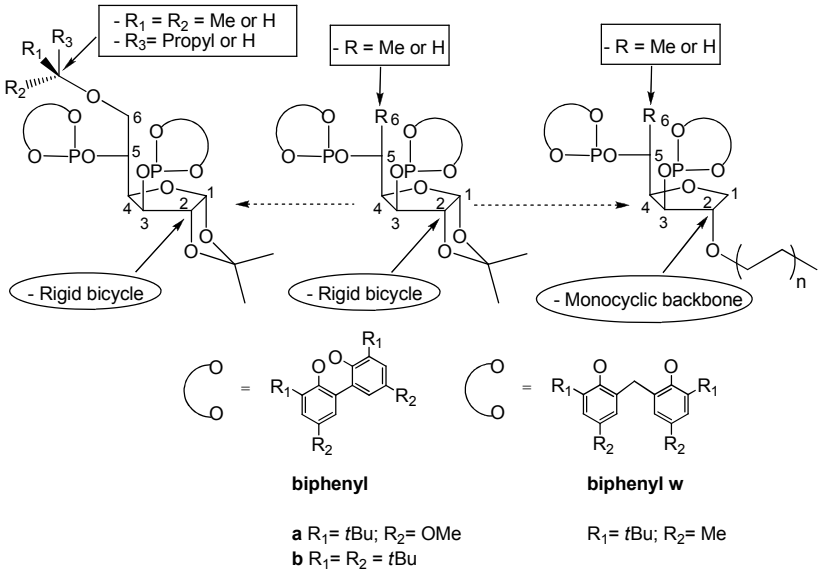

Figure 4.16. Structural diversity in 1,3-diphosphite ligands derived from carbohydrates with a furanoside (tetrahydrofuran) backbone prepared in this thesis.

New diphosphite ligands derived from carbohydrates containing a long alkyl chain were prepared. These ligands were successfully used to stabilise small metallic nanoparticles based on Rh, Ru and Ir displaying small mean size diameters and narrow size distributions. These NPs were shown to be active in the hydrogenation of m- and o-methylanisoles. The order of activity was as following: Rh> Ru > Ir, with all systems yielding high *cis* selectivity. The structure of the stabilising ligand appeared to have a drastic effect on the catalytic activity. These results demonstrate that such NPs based catalytic systems are of great interest for the hydrogenation of arenes and that ligand design is of crucial importance to obtain NPs with specific catalytic properties. Furthermore, the modular nature of the carbohydrate derived diphosphites should allow a systematic approach to achieve efficient chiral nanocatalysts.

2.7 Experimental Section

General methods. All syntheses were performed using standard Schlenk techniques under N_2 or Ar atmosphere. Solvents were purified by standard procedures. All other reagents were used as received. 1,2-*O*-isopropylidene-*α*-*D*-xylofuranose **2** and (3*R*, 5*R*)-pentanediol were purchased from Sigma-Aldrich. Ligands **21b**,**w**, **23b**, **67b**, **86w**, **87w** and **89b** were prepared by procedures described in section 2.4.1 and 2.4.2. Ligand **45b** was synthesised by previously described literature procedures.[68] $[Ir(cod)Cl]_2$ (**128**) and $[Ir(COD)_2][BF_4]$ (**129**) were synthesised by previous reported procedures.[70c-d] Elemental analyses of the organic compounds were performed on a Carlo Erba EA-1108 instrument. Optical rotation was measured at room temperature in 10 cm cell. ^1H, $^{13}C\{^1H\}$ and $^{31}P\{^1H\}$ NMR spectra were recorded on a Varian Gemini 400 MHz spectrometer. Chemical shifts are relative to $SiMe_4$ (^1H and ^{13}C) as internal standard or H_3PO_4 (^{31}P) as external standard. All NMR spectral assignments were determined by COSY and HSQC spectra. TEM samples were prepared by slow evaporation of a drop of each colloidal solution deposited under an argon atmosphere onto a holey carbon-covered copper grid. The TEM experiments were performed at the "Unitat de Microscopia dels Serveis Cientificotècnics de la Universitat Rovira I Virgili" (TEM-SCAN) in Tarragona with Zeiss 10 CA electron microscope operating at 100 kV with resolution of 3 Å. The particles size distributions were determined by a manual analysis of enlarged images. At least 300 particles on a given grid were measured in order to obtain a statistical size distribution and a mean diameter. The %metal and % Phosphorus were determined by Induced Coupled Plasma (ICP) at the "Unitat d´Anàlisi Elemental dels Serveis Cientificotècnics de la Universitat de Barcelona" in Barcelona with "Perkin Elmer" Optima 3200 RL spectrometer.

Synthesis of [Ru(cod)(cot)] (126). $RuCl_3 \cdot xH_2O$ (4.0 g, 17.1 mmol) was completely dissolved in methanol (45 mL) under nitrogen. 1,5-cyclooctadiene (cod) (107 mL, 0.86 mol), previously deoxygenated and filtered through alumina, and zinc powder (6.7 g, 0.10 mol) were added and the solution was heated 80ºC for 4h. The resulting solution was filtered and the residue was washed with toluene (3×27 mL). The filtrate

was evaporated to dryness under reduced pressure at room temperature and the solid residue obtained was extracted with pentane (2 × 50 mL). The solution was concentrated and passed through alumina using pentane. The yellow pentane solution was concentrated to 5 mL and cooled to -78ºC giving yellow crystals in 20% of yield (1.2 g, 3.8 mmol). The resulting highly sensitive yellow crystals were stored under argon at -30ºC.

Synthesis of [Rh(η^3-C_3H_5)$_3$] (127). $RhCl_3 \cdot xH_2O$ (1.1 g, 5.3 mmol) was completely dissolved in THF (93 mL) under nitrogen. The solution was cooled to -10ºC and thereafter allylmagnesium chloride (17.5 mL of 2M solution, 35 mmol) was slowly added. The solution lost its yellow-brown colour as the $RhCl_3 \cdot xH_2O$ disappeared over a period of about 1 hour. The solution was then allowed to warm at 10ºC and stirred for an additional 16 hours. The THF was removed under reduced pressure and the residue extracted with pentane (3 × 50 mL). The yellow pentane extracted was filtered though celite and the pentane was removed under reduced pressure. The bright yellow residue was sublimed onto a water-cooled prove over a period of 2h using static vacuum (50-60ºC/ 10^{-4}torr). The resulting highly sensitive yellow crystals were recovered in 42% of yield (0.4 g, 2.2 mmol) and they were stored under argon.

General procedure for the synthesis of Ruthenium Nanoparticles from the [Ru(cod)(cot)] (126) precursor. As a standard procedure, [Ru(cod)(cot)] (150mg, 0.476 mmol) was dissolved under an atmosphere of argon at -110ºC (ethanol/N_2 bath) in tetrahydrofuran (150 mL) containing the chosen ligand (0.1 eq.) in a closed pressure bottle. The Fischer-Porter reactor was then pressurized at r.t. under dihydrogen (3 bar) for 30 min. The initial yellow solution became black after 1h. Vigorous magnetic stirring was maintained for 18 h. After that period of time, the hydrogen pressure was eliminated, and a drop of the colloidal solution was deposited under an argon atmosphere on a holey carbon-covered copper grid for electron microscopy analysis. Precipitation with a tetrahydrofurane/pentane mixture at low temperatures gave rise to black precipitates that were washed with cold pentane (3 × 5 mL) and dried under vacuum.

Ru1. The synthesis of **Ru1** was completed according to the general procedure by using the **21b** (51 mg, 0.0476 mmol) as stabilizing agent. The product was isolated as a black powder (60 mg). Mean diameter= 4.0 ± 2.0 nm.%(w/w) Ru = 21.3, P = 1.9. $[Ru_{2057}(THF)_x(\mathbf{21b})_{299}]$.

Ru2. The synthesis of **Ru2** was completed according to the general procedure by using the **21w** (44 mg, 0.0476 mmol) as stabilizing agent. The product was isolated as a black powder (50 mg). Mean diameter= 2.9 ± 1.5 nm. %(w/w) Ru = 25.7, P = 2.3. $[Ru_{923}(THF)_x(\mathbf{21w})_{135}]$.

Ru3. The synthesis of **Ru3** was completed according to the general procedure by using the **86w** (44 mg, 0.0476 mmol) as stabilizing agent. The product was isolated as a black powder (50 mg). Mean diameter= 2.8 ± 2.0 nm. %(w/w) Ru = 25.6, P = 2.2. $[Ru_{923}(THF)_x(\mathbf{86w})_{129}]$.

Ru4. The synthesis of **Ru4** was completed according to the general procedure by using the **87w** (58 mg, 0.0476 mmol) as stabilizing agent. The product was isolated as a black powder (60 mg). Mean diameter= 1.8 ± 1.0 nm. %(w/w) Ru = 29.1, P = 1.8. $[Ru_{309}(THF)_x(\mathbf{87w})_{31}]$.

General procedure for the synthesis of Rhodium Nanoparticles from the $[Rh(\eta^3\text{-}(C_3H_5)_3]$ (127) precursor. As a standard procedure, $[Rh(\eta^3\text{-}(C_3H_5)_3]$ (75mg, 0.332 mmol) was dissolved under an atmosphere of argon at -110ºC (ethanol/N_2 bath) in tetrahydrofuran (75 mL) containing the chosen ligand (0.2 eq.) in a closed pressure bottle. The Fischer-Porter reactor was then pressurized at 40ºC under dihydrogen (6 bar) for 30 min. The initial yellow solution became black after 1h. Vigorous magnetic stirring was maintained for 18 h. After that period of time, the hydrogen pressure was eliminated, and a drop of the colloidal solution was deposited under an argon atmosphere on a holey carbon-covered copper grid for electron microscopy analysis. Precipitation with a tetrahydrofurane/pentane mixture at low temperatures gave rise to black precipitates that were washed with cold pentane (3 × 5 mL) and dried under vacuum.

Rh1. The synthesis of **Rh1** was completed according to the general procedure by using the **21b** (70 mg, 0.066 mmol) as stabilizing agent. The

product was isolated as a black powder (77 mg). Mean diameter= 1.8 ± 0.7 nm. %(w/w) Rh= 25.9, P = 4.0. $[Rh_{309}(THF)_x(\mathbf{21b})_{79}]$.

Rh2. The synthesis of **Rh2** was completed according to the general procedure by using the **21w** (61 mg, 0.066 mmol) as stabilizing agent. The product was isolated as a black powder (60 mg). Mean diameter= 2.4 ± 1.1 nm. %(w/w) Rh = 24.6, P = 4.4. $[Rh_{561}(THF)_x(\mathbf{21w})_{167}]$.

Rh3. The synthesis of **Rh3** was completed according to the general procedure by using the **89b** (81 mg, 0.066 mmol) as stabilizing agent. The product was isolated as a black powder (136 mg). Mean diameter= 1.6 ± 0.5 nm. %(w/w) Rh = 20.3, P = 3.3. $[Rh_{147}(THF)_x(\mathbf{89b})_{40}]$.

Rh4. The synthesis of **Rh4** was completed according to the general procedure by using the **23b** (71 mg, 0.066 mmol) as stabilizing agent. The product was isolated as a black powder (72 mg). Mean diameter=2.5 ± 1.1 nm. %(w/w) Rh= 17.9, P= 3.1. $[Rh_{561}(THF)_x(\mathbf{23b})_{172}]$.

Rh5. The synthesis of **Rh5** was completed according to the general procedure by using the **67b** (82 mg, 0.066 mmol) as stabilizing agent. The product was isolated as a black powder (87 mg). Mean diameter= 2.2 ± 0.9 nm. %(w/w) Rh = 19.8, P = 2.5. $[Rh_{471}(THF)_x(\mathbf{67b})_{118}]$.

Rh6. The synthesis of **Rh6** was completed according to the general procedure by using the **45b** (65 mg, 0.066 mmol) as stabilizing agent. The product was isolated as a black powder (48 mg). Mean diameter= 2.7 ± 0.9 nm. %(w/w) Rh = 22.9, P = 2.1. $[Rh_{923}(THF)_x(\mathbf{45b})_{141}]$.

General procedure for the synthesis of Iridium Nanoparticles from the Ir precursor. As a standard procedure, iridium precursor was dissolved under an atmosphere of argon at -110ºC (ethanol/N_2 bath) in tetrahydrofuran (40 mL) containing the chosen ligand in a closed pressure bottle. The Fischer-Porter reactor was then pressurized at r.t. under dihydrogen (3 bar) for 30 min. The initial yellow solution became black after 1h. Vigorous magnetic stirring was maintained for 18 h. After that period of time, the hydrogen pressure was eliminated, and a drop of the

colloidal solution was deposited under an argon atmosphere on a holey carbon-covered copper grid for electron microscopy analysis. Precipitation with a tetrahydrofurane/pentane mixture at low temperatures gave rise to black precipitates that were washed with cold pentane (3 × 5 mL) and dried under vacuum.

Ir1. The synthesis of **Ir1** was completed according to the general procedure by using the $[Ir(cod)Cl]_2$ **128** (118 mg, 0.175 mmol) as precursor and **21b** (75 mg, 0.07 mmol) as stabilizing agent. The product was isolated as a black powder (30 mg). Mean diameter = 1.3 ± 0.5 nm. %(w/w) Ir = 72.3, P = 0.57. $[Ir_{147}(THF)_x(\mathbf{21b})_4Cl_z]$.

Ir2. The synthesis of **Ir2** was completed according to the general procedure by using the $[Ir(cod)Cl]_2$ **128** (118 mg, 0.175 mmol) and **21w** (65 mg, 0.07 mmol) as stabilizing agent. The product was isolated as a black powder (28 mg). Mean diameter = 1.4 ± 0.5 nm. %(w/w) Ir = 75.4, P = 0.9. $[Ir_{147}(THF)_x(\mathbf{21w})_5Cl_z]$.

Ir3. The synthesis of $_{Ir3}$ was completed according to the general procedure but using $[Ir(COD)_2][BF_4]$ **129** (120 mg, 0.24 mmol) as precursor and **21b** (52 mg, 0.05 mmol) as stabilizing agent. The product was isolated as a black powder (40 mg). Mean diameter = 1.5 ± 0.5 nm. %(w/w) Ir = 76.2, P = 0.8 . $[Ir_{147}(THF)_x(\mathbf{21b})_5(BF_4)_z]$.

Hydrogenation of *m*- and *o*-methylanisoleee. The Ru-, Rh- and Ir-nanoparticles were used as catalysts in the asymmetric hydrogenation of pro-chiral arenes.

In a typical experiment, methylanisole (154 μL, 1.24 mmol) and the corresponding quantities of nanoparticles (Substrate/Ru= 100/1, Substrate/Rh= 150/1, Substrate/Ir= 40/1) were dissolved in 10 mL of the desired solvent in an autoclave. Molecular hydrogen was then introduced until the desired pressure was attained. The reaction was stirred and after the desired reaction time, the autoclave was cooled to room temperature and depressurized. Finally, the solution was filtered over celite and the solution analyzed. The conversion, the *cis*-selectivity and the enantiomeric excess of the *cis*-product were determined by GC analysis.

Chromatographic analyses were run with Fisons Instrument (GC 9000 series) equipped with a Chirasil Dex CB column. Parameters were as follows: temperature, 80ºC; injector temperature, 220ºC; detector temperature, 250ºC.

DL: T-1535-2009/ISBN: 978-84-692-4554-5

[1] V. Balzani, *Small*, **2005**, *1*, 278.

[2] P. Gröning, *Advanced Engineering Materials*, **2005**, *7*, 279.

[3] G. M. Whitesides, *Small*. **2005**, *1*, 172.

[4] E. Roduner, *Chem. Soc. Rev.* **2006**, *35*, 583.

[5] A. R. Tao, S. Habas, P. Yang, *Small*, **2008**, *4*, 310.

[6] J. K. Norskov, T. Bligaard, B. Hvolbaek, F. Abild-Pedersen, I. Chokendorff, C. H. Chirstensen, *Chem. Soc. Rev.* **2008**, *37*, 2163.

[7] a) J. D. Aiken III, R. G. Finke, *J. Mol. Catal. A: Chem.* **1999**, *145*, 1; b) J. A. Widegren, R. G. Finke, *J. Mol. Catal. A: Chem.* **2003**, *191*, 187.

[8] A. Roucoux, J. Schulz, H. Patin, *Chem. Rev.* **2002**, *102*, 3757.

[9] B. Gates, Q. Xuo, M. Stewart, D. Ryan, G. Willson, G. M. Whitesides, *Chem. Rev.* **2005**, *105*, 1171.

[10] a) B. Chaudret, *C. R. Physique*, **2005**, *6*, 117; b) K. Philippot, B. Chaudret, *C. R. Chimie*, **2003**, *6*, 1019-1034.

[11] O. Vidoni, K. Philippot, C. Amiens, B. Chaudret, O. Balmes, J.O. Balm, F. Senocq, M. J. Casanove, *Angew. Chem. Int. Ed.* **1999**, *38*, 4.

[12] L.Starkey, R. G. Finke, *Inorg. Chem.* **2006**, *45*, 8382.

[13] H. Bönneman, G. Braun, W. Bnjoux, R. Brinkmann, A. Shculze Tilling, K. Seevogel, K. Siepen, *J. Organomet. Chem.* **1996**, *520*, 143.

[14] M. Moreno-Mañas, R. Pleixats, *Acc. Chem. Res.* **2003**, *36*, 638.

[15] D. Astruc, F. Lu, J. A. Aranzaes, *Angew. Chem. Int. Ed.* **2005**, *44*, 7852.

[16] a) W. Yu, H. Liu, X. An, X. Ma, Z. Liu, L. Qiang, *J. Mol Catal. A: Chem.* **1999**, *147*, 73; b) W. Yu, H. Liu, Q. Tao, *J. Mol. Catal. A: Chem.* **1999**, *138*, 273; c) H. Feng; H. Liu, *J. Mol. Catal. A: Chem.* **1997**, *126*, L5; d) W. Yu, Y. Wang, H. Liu, W. Zheng, *J. Mol. Catal. A: Chem.* **1996**, *112*, 105.

[17] S. Bhattacharjee, D. M. Dotzauer, M. L. Bruening, *J. Am. Chem. Soc.* **2009**, *131*, 3601.

[18] L. M. Rossi, G. Machado, *J. Mol. Cat. A. Chem.***2009**, *298*, 69.

[19] V. Cimpeanu, M. Kocevar, V. I. Parvulescu, W. Leiner, *Angew. Chem. Int. Ed.* **2009**, *48*, 1085.

[20] S. Boujday, J. Blanchard, R. Villaneau, J. M. Kraft, C. Geantet, C. Louis, M. Breysse, A. Proust, *ChemPhysChem*, **2007**, *8*, 2636.

[21] C. Hubert, A. Denicourt-Nowicki, A. Roucoux, D. Landy, B. Leger, G. Crowyn, E. Monflier, *Chem. Commun.* **2009**, 1128.

[22] B. Léger, A. Denicourt-Nowicki, A. Roucoux, H. Olivier-Bourbigou, *Adv. Synth. Catal.* **2008**, *350*, 153.

[23] a) P. Wigowski, J. Dupont, *Chem. Eur. J.* **2007**, *13*, 32; b) G.S. Fonseca, G. Machado; S.R. Teixeira, G.H. Fecher, J. Morais, M.C.M. Alves, J. Dupont, *J. Coll. Int. Sci.* **2006**, *301*, 193.

[24] a) M. Beller, H. Fisher, K. Kühlein, C. P. Reisinger, W. A. Hermann, *J. Organomet. Chem.* **1996**, *520*, 257; b) M. T. Reetz, G. Lohmer, *Chem. Commun.* **1996**, 1921; c) S. Klingelhöfer, W. Heitz, A. Greiner, S. Oestreich, S. Föster, M. Antonietti, *J. Am. Chem. Soc.* **1997**, *119*, 10166.

[25] L. Wu, Z. W. Li, F. Zhang, Y. M. He, Q. H. Fan, *Adv. Synth. Catal.* **2008**, *350*, 846.

[26] a) S. Pathak, M. T. Greci, R. C. Kwong, K. Mercado, G. K. S. Prakash, G. A. Olah, M. E. Thompson, *Chem. Mater.* **2000**, *12*, 1985; b) V. Kogan, Z. Aizenshtat, R. Popovitz-Biro, R. Neumann, *Org. Lett.* **2002**, *4*, 3529.

[27] B. M. Choudary, S. Madhi, N. S. Chowdary, M. L. Kantam, B. Sreedhar, *J. Am. Chem. Soc.* **2002**, *124*, 14127.

[28] R. R. Deshmukh, R. Rajagopal, K. V. Srinivasan, *Chem. Commun.* **2001**, *17*, 1544.

[29] a) M. T. Reetz, R. Breinbauer, K. Wanninger, *Tetrahedron Lett.* **1996**, *37*, 4499; b) M. T. Reetz, G. Lohmer, *Chem. Comm.* **1996**, 1921.

[30] G. Schmid, H. West, H. Mehles, A. Lehnert, *Inorg. Chem.* **1997**, *36*, 891.

[31] a) Y. Shiraishi, N. Toshima, *J. Mol. Catal. A: Chem.* **1999**, *141*, 187; b) Y. Shirashi, N. Toshima, *Coll. Surf. A.* **2000**, *169*, 59.

[32] A. Corma, H. Garcia, *Chem. Soc. Rev.* **2008**, *37*, 2096.

[33] J. Ramírez, M. Sanaú, E. Fernández, *Angew. Chem. Int. Ed.* **2008**, *47*, 5194.

[34] a) S. Kim, S. U. Son, S. S. Lee, T. Hyeon, Y. K. Chung, *Chem. Commun.* **2001**, *21*, 2212; b) S. U. Son, K. H. Park, Y. K. Chung, *J. Am. Chem. Soc.* **2002**, *124*, 6838; c) S. U. Son, S. I. Lee, Y. K. Chung, S. Kim, T. Hyeon, *Org. Lett.* **2002**, *4*, 277; d) S. U. Song, S. I. Lee, Y. K. Chung, S. Kim, T. Hyeon, *Org. Lett.* **2002**, *4*, 3938; e) K. H. Park, I. G. Jung, Y. K. Chung, *Org. Lett.* **2004**, *6*, 1183.

[35] Q. Wang, H. Liu, M. Han, X. Li, D. Jiang, *J. Mol. Catal. A: Chem.* **1997**, *118*, 145.

[36] J. Kang, S. Zhang, Q. Zhang, Y. Wan, *Angew. Chem. Int. Ed.* **2009**, *48*, 2565.

[37] H. Bönnemann, G. A. Braun, *Chem. Eur. J.* **1997**, *3*, 1200.

[38] a) J. U. Köhler, J. S. Bradley, *Langmuir*, **1998**, *14*, 2730; b) X. Zuo, H. Liu, D. Guo, X. Yang, *Tetrahedron*. **1999**, *55*, 7787; c) M. Studer, H. U. Blaser, C. Exner, *Adv. Synth. Catal.* **2003**, *345*, 45.

[39] F. Hoxha, N. van Vegten, A. Urakawa, F. Krumeich, T. Mallat, A. Baiker, *J. Catal.* **2009**, *261*, 224.

[40] C. Yang, H. Y. Jiang, J. Feng, H. Y. Fu, R. X. Li, H. Chen, X. J. Li, *J. Mol. Catal. A. Chem.* **2009**, *300*, 98.

[41] M. Tamura, H. Fujihara, *J. Am. Chem. Soc.* **2003**, *125*, 15742.

[42] K. H. Park, Y. K. Chung. *Adv. Synth. Catal*. **2005**, *347*, 854.

[43] S. Jansat, M. Gómez, K. Philippot, G. Muller, E. Guiu, C. Claver, S. Castillón, B. Chaudret, *J. Am. Chem. Soc.* **2004**, *126*,1592-1593.

[44] I. Favier, M. Gómez, G. Muller, M.R. Axet, S. Castillón, C. Claver, S. Jansat, B. Chaudret, K. Philippot, *Adv. Synth. Catal.* **2007**, *349*, 2459-2469.

[45] a) D. Astruc, *Inorg. Chem.* **2007**, *251*, 1281; b) M. Moreno-Mañas, R. Pleixats, *Acc. Chem. Res.* **2003**, *36*, 638; c) J. Durand, E. Teuma, M. Gómez, *Eur. J. Inorg. Chem.* **2008**, 3577.

[46] M. Dieguez, O. Pamies, Y. Mata, E. Teuma, M. Gomez, F. Ribaudo, P. W. N. M. van Leeuwen, *Adv. Synth. Catal.* **2008**, *350*, 2583.

[47] J. A. Widegren, R. G. Finke, *J. Mol. Catal. A: Chem*, **2003**, *191*, 187.

[48] J. March, *Advanced Organic Chemistry: Reaction, Mechanism and Structure*, Wiley-Interscience, New York, **1992**.

[49] R. J. Fessenden, J. S. Fessenden, *Organic Chemistry*, Brooks/Cole Publishing Copmpany, Pacific Grove, **1993**.

[50] P. J. Dyson, *Dalton Trans*. **2003**, 1964.

[51] I. P. Rothwell, *Chem. Commun*, **1997**, 1331.

[52] M. D. Fryzuk, C. M. Kozak, M. R. Bowdridge, B. O. Patrick, *Organometallics*, **2002**, *21*, 5047.

[53] R. L. Augustine, *Heterogeneous Catalysis for the Synthetic Chemist*, Marcel Dekker, New York, **1996**.

[54] B. C. Gates, *Catalytic Chemistry*, Willey, New York, **1992**.

[55] P. Drognat Landré, M. Lemaire, D. Richard, P. Gallezot, *J. Mol. Catal.* **1992**, *78*, 257.

[56] J. Blum, I. Amer, K. P. C. Vollhardt, H. Schwarz, G. Hoehne, *J. Org. Chem.* **1987**, *52*, 2804.

[57] J. A. Widegren, R. G. Finke, *Inorg. Chem.* **2002**, *41*, 1558.

[58] E. T. Silveira, A. P. Umpierre, L. M. Rossi, G. Machado, J. Morais, G. V. Soares, I. J. R. Baumvol, S. R. Teixeira, P. F. P. Fichtner, J. Dupont, *Chem. Eur. J.* **2004**, *10*, 3734.

[59] P. Drognat Landré, D. Richard, M. Draye, P. Gallezot, M. Lemaire, *J. Catal.* **1994**, *147*, 214.

[60] T. Q. Hu, B. R. James, S. J. Retting, C. L. Lee, *Can. J. Chem.* **1997**, *75*, 1234.

[61] K. R. Januszkiewicz, H. Alper, *Organometallic*, **1983**, *2*, 1055.

[62] K. Nasar, F. Fache, M. Lemaire, J. C. Beziat, M. Besson, P. Gallezot, *J. Mol. Catal.* **1994**, *87*, 107.

[63] S. Jansat, D. Picurelli, K. Pelzer, K. Philippot, M. Gómez, G. Muller, P. Lecante, B. Chaudret, *New. J. Chem.* **2006**, *30*, 115.

[64] a) V.S. Ranade, R. Prins, *J. Catal.* **1999**, *185*, 479; b) V.S. Ranade, G. Consiglio, R. Prins, *Catal. Lett.* **1999**, *58*, 71; c) L.A.M.M. Barbosa, P. Sautet, *J.*

Catal. **2003**, *217*, 23; d) M. Besson, P. Gallezot, S. Neto, C. Pinel, *Chem. Commun.* **1998**, 1431; e) M. Besson, B. Blanc, M. Champelet, P. Gallezot, K. Nasar, C. Pinel, *J. Catal.* **1997**, *170*, 254.

[65] a) A. Nowicki, V. Le Boulaire, A. Roucoux, *Adv. Synth. Catal.* **2007**, *349*, 2326; b) V. Mévellec, A. Roucoux, E. Ramirez, K. Philippot, B. Chaudret, *Adv. Synth. Catal.* **2004**, *346*, 72; c) J. Schulz, S. Levigne, A. Roucoux, H. Patin, *Adv. Synth. Catal.* **2002**, *344*, 266.

[66] V. Mévellec, B. Léger, M. Mauduit, A. Roucoux, *Chem. Comm.* **2005**, 2838.

[67] a) C. Pan, K. Pelzer, K. Philippot, B. Chaudret, F. Dassenoy, P. Lecante, M. J. Casanove, *J. Am. Chem. Soc.* **2001**, *123*, 7584; b) E. Ramírez, L. Eradés, K. Philippot, P. Lecante, B. Chaudret, *Adv. Funct. Mater.* **2007**, *17*, 2219.

[68] G.J.H. Buisman, M.E. Martin, E.J. Vos, A. Klootwijk, P.C.J. Kamer, P.W.N.M. van Leeuwen, *Tetrahedron: Asymmetry*, **1995**, *6*, 719.

[69] a) C. H. Hagen, J. A. Widegren, P. M. Maitlis, R. G. Finke, *J. Am. Chem. Soc.* **2005**, *127*, 4423; b) M. Hagen, L. Vieille-Petit, G. Laurenzy, G. Süs-Fink, G. Finke, *Organometallics*, **2005**, *24*, 1819; c) J. A. Widegren, M. A. Bennet, R. G. Finke, *J. Am. Chem. Soc.* **2003**, *125*, 10301.

[70] a) M. D. Fryzuk, w. E. Piers, in *Organometallic Synthesis*, Elsevier, Amsterdam, **1996**; b) W. A. Herrmann, in *Synthetic Methods of Organometallic and Inorganic Chemistry*, Thieme, Stuttgart, **1996**; c) P. Pertici, G. Vitulli, *Inorg. Synth.* **1983**, *22*, 17; d) J.L. Herde, J.C. Lambert, C.V. Senoff, Inorg. Synth. 1979, 15, 18-XX; e) M. Green, T.A. Kuc, S. H. Taylor, *J. Chem. Soc. A.* **1971**, 2334.

[71] M.R. Axet, S. Castillón, C. Claver, K. Phillipot, P. Lecante, B. Chaudret, *Eur. J. Inorg. Chem.* **2008**, 3460.

[72] J.D. Scholten, J. Dupont, in *Iridium complexes in Organic Synthesis*, Ed. L. Oro and C. Claver, Wiley-VCH, Weinheim, **2009** (Chapter 15).

Conclusions

UNIVERSITAT ROVIRA I VIRGILI
1,3- DIPHOSPHITE LIGANDS WITH FURANOSIDE BACKBONE: A POWERFUL TOOL IN ASYMMETRIC CATALYSIS
Aitor Gual Gozalbo
DL: T-1535-2009/ISBN: 978-84-692-4554-5

General conclusion

The structural modifications of the backbone as well as the biphenyl moiety in carbohydrate derivatives 1,3-diphosphites allows the optimization of catalytic systems in the following reactions:

-Rhodium catalyzed styrene and dihydrofurans hydroformylation.

-Palladium catalyzed allylic alkylation.

-Arene hydrogenation using rhodium, ruthenium and iridium nanoparticles stabilized by those diphosphite ligands.

Detailed conclusions

- Novel 1,3-diols with furanoside backbone were synthesised by structural modification of the 1,2-*O*-isopropyliden-α-D-xylofuranose and 1,2-*O*-isopropyliden-α-D-glucofuranose. These new diol backbones incorporate the following modifications: a) higher substitution at position C-6 of the sugar to increase the steric hindrance of the coordinating phosphorus atom, b) absence of 1,2-*O*-isopropylidene ring in order to increase the conformational freedom.
- Novel 1,3-diphosphite ligands were synthesised by treatment of the 1,3-diols with phosphorochloridites derived from bis-phenols **a**, **b** and **w**.
- These ligands were applied in the Rh-asymmetric hydroformylation of styrene. The best results were obtained with the ligand **67a**. This ligand provided moderate conversions with very good enantioselectivities (*ee* up to 83% (*S*)) at 20ºC. Additionally, the ligands **64**-**66a** containing bulky substituents in the positions C-6 provided lower enantioselectivities. The catalytic systems Rh/**21w** and Rh/**67w** were inactive under standard reaction conditions.
- In the Rh-asymmetric hydroformylation of vinyl acetate the best results were obtained using the ligand **23a**. This ligand produced moderate conversion and excellent regioselectivities with 73% of *ee* at 20ºC.
- The Rh-asymmetric hydroformylation of 2,5-dihydrofuran and 2,3-dihydrofuran were also carried out using these new 1,3-diphosphite

ligands. In the case of 2,5-dihydrofuran, the best results were achieved using the ligand **67b** at 20ºC. This ligand provided moderate conversion with total selectivity to the tetrahydro-3-carbaldehyde product with 88% of *ee* (*S*). It has to be noted that the presence of bulky substituents in the position C-6 of the carbohydrate backbone produced lower enantioselectivity because these ligands favour the β-elimination of the product to form 2,3-dihydrofuran and the Rh-asymmetric hydroformylation of 2,3-dihydrofuran preferment formed the opposite enantiomer of tetrahydro-3-carbaldehyde product. In the Rh-asymmetric hydroformylation of 2,3-dihydrofuran the best results were obtained using the catalytic systems Rh/**64b** and Rh/**65b** at 45ºC. The ligand **64b** provided higher conversion but both systems afforded similar results in terms of reigoselectivity (up to 78%) and enantioselectivity (up to 84%).

- The $[RhH(CO)_2(L)]$ (L = **21w**, **65b** and **67a,b**) species were characterised by HP-NMR techniques. The formation of the **eq-eq** $[RhH(CO)_2(L)]$ (L = **21w**) specie under hydroformylation conditions was confirmed by NMR techniques. It has to be noted that this ligand didn't produce any activity under standard hydroformylation conditions and therefore the formation of this species is not a limiting step of the reaction. The $[RhH(CO)_2(L)]$ species, where L= **65b** and **67a,b**, were characterised by NMR demonstrating that these ligands **65b** and **67a,b** coordinate to the Rh centre in an **eq-eq** fashion in these hydride complexes. The complex $[RhH(CO)_2($**65b**$)]$ was detected as a single isomer with characteristic features of **eq-eq** coordination. However, the broadening of the corresponding signals indicated that this species is rapidly interchanging in solution. The absence of signals for the second species involved did not permit to undoubtedly determine the nature of this exchange process, although an equilibrium between **eq-eq** and **eq-ax** coordinations is likely. In contrast, complex $[RhH(CO)_2($**67a** or **67b**$)]$ was detected as a mixture of two isomers at low temperature, and that both contained the diphosphite ligand in an **eq-eq** fashion. In this case, the increased flexibility of ligand **67b** with a monocyclic backbone is thought to

be responsible for the formation of two conformational isomers of this complex.

- 1,3-diphosphite ligands with a furanoside backbone prepared in the chapter 2, were applied in the Pd-allylic alkylation of 1,3-diphenyl-3-acetoxy-propen-1-ene using dimethyl malonate as a nucleophile. The reaction conditions were optimized for each family of 1,3-diphosphite ligands. The catalytic systems Pd/**65a**,and Pd/**65b** provided and efficient kinetic resolution when working in the standard conditions and short reactions times. The enantioselectivities in the product (95 %, Pd/**65a**; 94%, Pd/**65b**) and in the substrate (99.9%, Pd/**65a**; 94% Pd/**65b**) were excellent at 50% of conversion. Furthermore, Pd/**67b** catalytic system provided also excellent results working in high diluted solutions and longer reaction times, achieving a 98.4% *ee* in the product and 95% *ee* in the substrate.
- The use of ligands with incorporate biphenyl moiety **w** produced much lower activities with very low selectivities.
- The novel 1,3-diphosphite were also applied in the Pd-allylic alkylation of 1-phenyl-3-acetoxy-propene using dimethyl malonate as a nucleophile. The effect of the solvent was studied and THF was chosen as a solvent. In this reaction, the ligands derived from xylofuranose **21b**, **87b** and **89b** provided good enantioselectivity (up to 83%) with a poor regioselectivity (17%).
- The Pd-allylic alkylation of 1-phenyl-3-acetoxy-propene using α-(ethoxycarbonyl)-cyclohexanone as a nucleophile and the 1,3-diphosphite ligands was also tested. The best results were achieved using dichloromethane as a solvent, $Zn(OAc)_2$ as a additive and the ligand **65b**. Moderate conversion with total selectivity to the chiral linear product and enantioselectivities up to 38% were achieved.
- The $[Pd(\eta^3\text{-}C_3H_5)(L)]PF_6$ complexes, where L = **65b** and **67b**, were synthesised and characterised by NMR. The NMR spectrum of both complexes in CD_2Cl_2 showed a mixture of two isomers in equilibrium in a ratio 1:1. Both isomers were characterized by NMR and their structure was attributed to the *exo* and *endo* isomers.

- Ligands **21b,w**, **23b**, **67b**, **86w**, **87w** and **89b** were used to stabilize Ru, Rh, and Ir nanoparticles. Ligands **67b**, **86w**, **87w** and **89b**, which incorporate in their backbone alkyl chains, were specifically designed to stabilise nanoparticles.
- The effect of the biphenyl moiety in the stabilization of metal nanoparticles was studied by preparing Rh-, Ru- and Ir-nanoparticles stabilised with ligands **21b** and **21w**. The biphenyl moiety **b** produced smaller Rh- (1.8 *vs.* 2.4 nm) and Ir- (1.3 *vs.* 1.5 nm) nanoparticles, while the biphenyl moiety **w** produced smaller Ru-(4.0 *vs.* 2.9 nm) nanoparticles.
- These Rh-, Ru- and Ir-nanocatalysts stabilized with 1,3-diphosphite ligands were active in the hydrogenation of *o*-methylanisole and *m*-methylanisole. In the hydrogenation of *m*-methylanisole a *cis* selectivity of 65-80% with no asymmetric induction were achieved. Whereas for *o*-methylanisole selectivity in the *cis* product was total but enantioselectivities (6% *ee*) were very low. It has to be noted, that the structure of the stabilising 1,3-diphophite ligand appeared to have a drastic effect on the catalytic activity.

UNIVERSITAT ROVIRA I VIRGILI
1,3- DIPHOSPHITE LIGANDS WITH FURANOSIDE BACKBONE: A POWERFUL TOOL IN ASYMMETRIC CATALYSIS
Aitor Gual Gozalbo
DL: T-1535-2009/ISBN: 978-84-692-4554-5

Summary/Resum

UNIVERSITAT ROVIRA I VIRGILI
1,3- DIPHOSPHITE LIGANDS WITH FURANOSIDE BACKBONE: A POWERFUL TOOL IN ASYMMETRIC CATALYSIS
Aitor Gual Gozalbo
DL: T-1535-2009/ISBN: 978-84-692-4554-5

UNIVERSITAT ROVIRA I VIRGILI
1,3- DIPHOSPHITE LIGANDS WITH FURANOSIDE BACKBONE: A POWERFUL TOOL IN ASYMMETRIC CATALYSIS
Aitor Gual Gozalbo
DL: T-1535-2009/ISBN: 978-84-692-4554-5

Summary

The demand for chiral compounds in pharmaceutical, agrochemical and the flavour and fragrance industry has encouraged the development of methods for synthesizing such compounds. Three basic strategies make possible the production of enantiomerically pure compounds: a) the use of optically active natural molecules as building blocks, b) optical resolution via resolving agents and c) asymmetric synthesis. Asymmetric synthesis is commonly used to prepare chiral compounds. The basic principle of this method is to form a new chiral centre under the influence of a chiral group. Asymmetric catalysis is part of this preparative method and makes possible the transformation of a pro-chiral or racemic substrate into a chiral product using catalytic amounts of the compounds which contain the chiral information.

Homogeneous catalysis involves a catalytic system in which the substrates and the catalyst components are brought together in one phase, most often liquid, where the catalyst is usually a metal complex modified with ligands. Therefore, the ligand effects are extremely important in homogeneous catalysis by metal complexes. In enantioselective homogeneous metal catalysis the design of new ligands is perhaps the most crucial step to achieve the highest levels of reactivity and selectivity. In this optimisation process, careful selection and design of the chiral ligands are perhaps the most crucial steps, since the best ligand strongly depends on each particular reaction. Carbohydrates, together with aminoacids, are the most prominent members of the "chiral pool". Carbohydrates have many advantages: they are readily available, highly functionalised and contain several stereogenic centres. Carbohydrates have been mainly used as chiral templates for the synthesis of enantiomerically pure organic compounds by using stereoselective transformations (the "chiron" approach). The presence of hydroxyl functions in carbohydrate derivates facilitates the synthesis of series of chiral phosphorus ligands such as phosphines, phosphinites, phosphonites and phosphites. Furthermore, the possibility to introduce easy modification in the carbohydrate contributes to the rational design of ligands in the search for high activities and selectivities for each particular reaction.

In addition, most carbohydrates, and in particular the most commonly used pentoses and hexoses, can be easily and selectively obtained in the pyranose or the furanose form.

Ligands with a furanoside backbone are usually prepared from xylose or glucose. The main structural features of furanoside ligands are the following: a) The anomeric position is usually blocked with a 1,2-*O*-isopropylidene group to give a bicycle, which restricts the conformational freedom; b) phosphorus functions can be attached to 3,5-OH (xylose and glucose derivates) and 5,6-OH (glucose derivates) to give their corresponding 1,2 or 1,3-phosphorus derivatives. One of the main limitations of using natural products as precursors for ligands is that often only one for the enantiomers (in the case of carbohydrates, the *D* series) is readily available. However, this limitation can be overcome by using pseudo-enantiomer ligands or by suitable ligand tuning of the 1,3-diol furanoside carbohydrate backbone.

The ligands derived with a 1,2-*O*-isopropylidene-α-*D*-furanoside backbone derived from xylose and glucose have been successfully applied in several transition metal catalyzed processes. However, the influence of several structural parameters of these types of ligands on the catalytic results was not outstanding.

This thesis focus on the development and application in asymmetric catalysis of new 1,3-diphosphite with furanoside backbone. As mentioned in the section 1.1, the synthesis of series 1,3-diols with 1,2-O-isopropylidene-α-*D*-furanose backbone by varying the configuration of the stereocentres directly bonded to the phosphorus function is a crucial step in the design of most efficient bidentate ligands. Thus, in chapter 2 was introduced the design and synthesis of new 1,3-diol with furanoside bicyclic backbone related to the well-known 1,2-*O*-isopropylidene-α-*D*-xylofuranose and 6-*O*-deoxy-1,2-*O*-isopropylidene-α-*D*-glucofuranose backbones. The modifications of these 1,3-diol backbones were carried out in two directions: a) Introduction of *O*-alkyl substituents in the positions C-6 of the furanoside bicyclic backbone, and b) reduction of the 1,2-*O*-isopropylidene ring in order to obtain 1,3-diol with furanoside monocyclic backbones and introduction of *O*-alkyl substituent in the C-2 position. The synthetic work carried out to achieve these new diol backbones was introduced in chapter 2.

New 1,3-diphosphite ligands with the biphenyl moieties **a** and **b** were synthesised starting from the new 1,3-diols with furanoside backbone. The phosphite moieties **a** and **b** were selected because their versatility in several asymmetric processes. Additionally, the use of biphenyl moiety **w** was also tested. Recently, this biphenyl moiety was probed to be efficient in the Ir-catalysed hydrogenation of ketimines by using 1,2-phosphinite-phosphite ligands with manitol derived backbone. The synthesis of these new 1,3-diphosphite ligands were placed in chapter 2.

The application of the new 1,3-diphosphite ligands series in the Rh-asymmetric hydroformylation of monosubstituted alkenes, such as styrene and vinyl acetate, and disubstituted internal alkenes, 2,5-dihydrofuran and 2,3-dihydrofuran, was described in chapter 2. Additionally, in collaboration with the Prof. Dr. Dieter Vogt these ligands were applied in the Rh-asymmetric hydroformylation of 1,1-disubstituted alkenes, such as methyl methacrylate and α-methylstyrene. The effect of the structural modifications of these 1,3-diphosphite ligands on the catalytic results was studied and the results were introduced in chapter 2. The catalytic systems Rh/**21w** and Rh/**67w** were inactive under standard reaction conditions. The best results in the Rh-asymmetric hydroformylation of styrene were obtained with the ligand **67a**. This ligand provided moderate conversions with excellent enantioselectivities (*ee* up to 83% (*S*)) at 20ºC. In the Rh-asymmetric hydroformylation of vinyl acetate the best results were obtained using the ligand **23a**. This ligand produced moderate conversion and excellent regioselectivities with 73% of *ee* at 20ºC. In the case of 2,5-dihydrofuran, the best results were achieved using the ligand **67b** at 20ºC. This ligand provided moderate conversion with total selectivity to the tetrahydro-3-carbaldehyde product with 88% of ee (*S*). In the Rh-asymmetric hydroformylation of 2,3-dihydrofuran the best results were obtained using the catalytic systems Rh/**64b** and Rh/**65b** at 45ºC. The ligand **64b** provided higher conversion but both systems provided similar results in terms of reigoselectivity (up to 78%) and enantioselectivity (up to 84%). The ligand **65a** produced the best results in the Rh-asymmetric hydroformylation of methyl methacrylate and α-methylstyrene. In the case of α-methyl styrene, moderate to low conversion and good regioselectivity with 36% of *ee* were achieved at 80ºC. In the case of methyl methacrylate, moderate to low conversion and good regioselectivity with 71% of *ee* were

achieved at 60ºC. The [$RhH(CO)_2(L)$] (L = **21w**, **65b** and **67a,b**) species were characterised by HP-NMR techniques. The [$RhH(CO)_2(L)$] species, where L= **21w**, **65b** and **67a,b**, were characterised by NMR demonstrating that these ligands **65b** and **67a,b** coordinate to the Rh centre in an **eq-eq** fashion in these hydride complexes.

Next, the effect of the structural modification of these 1,3-diphosphite ligands on the catalytic results of the Pd-allylic alkylation of phenyl-allyl compounds was described in chapter 3. In this section was studied the Pd-allylic alkylation of *rac*-1,3-diphenyl-3-acetoxy-propene using dimethyl malonate as nucleophile and the Pd-allylic alkylation of 1-phenyl-3-acetoxy-propene using dimethyl malonate and α-(ethoxycarbonyl)-cyclohexanone as nucleophiles. The reaction conditions in the Pd-allylic alkylation of *rac*-1,3-diphenyl-3-acetoxy-propene using dimethyl malonate as nucleophile were optimized for each family of 1,3-diphosphite ligands. The ligand **65a** provided the best results under the following reaction conditions: Substrate/Pd = 100/1, Pd/L = 1/ 1.1, toluene as solvent and t= 5 min. This ligand produced excellent enantioselectivity in the product (*ee* up to 95 %) and in the substrate (*ee* up to 99.9%). The ligand **65b** provided excellent results under the following reaction conditions: Substrate/Pd = 100/1, Pd/L = 1/ 2.0, toluene as solvent and t= 5 min. Excellent enantioselectivities in the product (*ee* up to 94%) and in the substrate (*ee* up to 94%) were achieved by using the Pd/**65b** catalytic system. Furthermore, the ligand **67b** provided also excellent results in the following reaction conditions: Substrate/Pd = 1000/1, Pd/L = 1/ 2.0, dichloromethane as solvent and t= 90 min. The catalytic system Pd/**67b** produced excellent enantioselectivities in the product (*ee* up to 98.4 %) and in the substrate (*ee* up to 95%). The use of ligands with incorporate biphenyl moiety **w** produced much lower activities with very low selectivities. The effect of the solvent was studied in the Pd-allylic alkylation of 1-phenyl-3-acetoxy-propene using dimethyl malonate as a nucleophile and THF was chosen as a solvent. In this reaction, the ligands derived from xylofuranose **21b**, **87b** and **89b** produced the best results in terms of regioselectivity (up to 17%) and enantioselectivity (up to 83%). The best results in the Pd-allylic alkylation of 1-phenyl-3-acetoxy-propene using α-(ethoxycarbonyl)-cyclohexanone as a nucleophile were achieved using dichloromethane as a solvent, $Zn(OAc)_2$ as a additive and the ligand **65b**. Moderate conversion

with total selectivity to the chiral linear product and enantioselectivities up to 38% were achieved. The $[Pd(\eta^3\text{-}C_3H_5)(L)]PF_6$ complexes, where L = **65b** and **67b**, were synthesised and characterised by NMR. The NMR spectrum of both complexes in CD_2Cl_2 showed a mixture of two isomers in equilibrium in a ratio 1:1. Both isomers were characterized by NMR and their structure was attributed to the *exo* and *endo* .

The stabilization of metal nanoparticles and their use as nanocatalysts were described in chapter 3. The metal nanoparticles are active in processes in which the homogeneous catalysts are not active. Therefore, we decided to apply the series of 1,3-diphosphites to stabilize metal nanoparticles (ruthenium, rhodium and iridium nanoparticles) and to study the effect of their selective structural modification in the size, shape and dispersion of the nanoparticles. The synthesised nanocatalysts were tested in the hydrogenation of pro-chiral monocyclic arenes, such as *o*-methylanisole and *m*-methylanisole. Rh-, Ru- and Ir- nanoparticles were stabilised the ligands **21b** and **21w**. The effect of the biphenyl moiety in the stabilization of metal nanoparticles was studied. The biphenyl moiety **b** produced smaller Rh- and Ir- nanoparticles, while the biphenyl moiety **w** produced smaller Ru-nanoparticles. The ligands which incorporate in their backbone alkyl chains were successfully applied in the stabilization of Rh- and Ru-nanoparticles. The Rh-, Ru- and Ir-nanocatalysts synthesised by stabilization with the novel 1,3-diphosphite ligands were active in the hydrogenation of *o*-methylanisole and *m*-methylanisole. Moderate to high cis-selectivity (65-80%) with any asymmetric induction were achieved in the hydrogenation of *m*-methylanisole using these nanocatalysts. In the case of *o*-methylanisole, total selectivity to the *cis* product with very low enantioselectivities (6% *ee*) were achieved.

Resum

La demanda de compostos quirals per part de l'industrià de disseny de fragàncies, agroquímica i farmacèutica estimula el desenvolupament de mètodes per sintetitzar aquestos compostos. Tres estratègies bàsiques fan possible la producció productes enantiomèricament purs: a) l'ús de molècules naturals òpticament actives com a "building blocks", b) resolució òptica gastant agents de resolució, c) síntesi asimètrica. La síntesi asimètrica es el mètode mes comú per preparar compostos quirals. El principi basic d'aquest mètode es la formació de nous centres quirals baix la influencia de grups quirals. Aquesta es part d'un mètode preparatiu i fa possible la transformació de substrats pro-chiral o racèmic en productes quirals mitjançant l'ús de quantitats catalítiques de compostos que contenen informació quiral.

La catàlisi homogènia inclou els sistemes catalítics amb el que el substrats i el component catalític estan mesclats en una fase, freqüentment en fase líquida, on el catalitzador es usualment un complex metàl·lic modificat amb lligands. Per tant, els efectes dels lligands son d'extrema importància en el complexos metàl·lics emprats en catàlisi homogènia. En els processos homogenis enantioselectius catalitzats per complexes metàl·lics el disseny de nous lligands es l'etapa clau per obtenir alts nivells de reactivitat i selectivitat. En aquest procés d'optimització, la selecció i disseny dels lligands quirals es l'etapa més important, perquè el millor lligand extremadament depèn de cada reacció. Els carbohidrats, juntament amb el aminoàcids, son els més prominent membres de la "chiral pool". Els carbohidrats tenen moltes avantatges: ells son molts accessibles, altament funcionalitats i contenen centres estereógenics. Els carbohidrats s'han gastat principalment com a models quirals per a la síntesi de compostos orgànics enantiomèricament purs mitjançant transformacions estereoselectives (the "chiron" approach). La presencia de funcions hidroxil en els derivats de carbohidrats facilita la síntesi de series de lligands fosforats quirals com per exemple: fosfines, fosfinits, fosfonits i fosfits. A més, la possibilitat de introduir fàcilment modificacions a l'estructurà del carbohidrat contribueix al disseny racional de lligands per tal de cercar de altes activitats i selectivitats per a cada reacció en particular.

A més, molts dels carbohidrats, i en particular les pentoses i hexoses més habitualment emprades, poden ser obtinguts en la seua forma piranosa of furanosa.

Els lligands amb el esquelet furanosa son usualment preparats partint de xilosa o glucosa. Les característiques estructurals dels lligands furanòsids son les següents: a) La posició anomèrica es usualment bloquejada amb el grup 1,2-*O*-isopropylideno, que restringeix la llibertat conformacional; b) les funcions fosforades poden ser introduïdes en les posicions 3,5-OH (derivats de xilosa o glucosa) i 5,6-OH (derivats de glucosa) per donar els corresponents derivats 1,2 o 1,3-forforats. Una de les principals limitacions a l'hora de gastar productes naturals com a precursors de lligands es que quasi sempre nomes un dels enantiòmers (en el cas dels carbohidrats, la sèrie *D*) es accessible. Encara que aquesta limitació pot ser superada emprant lligands pseudo-enantiomerics o pel adequat disseny del esquelet 1,3-diol del lligand.

Els lligands amb 1,2-*O*-isopropylidene-α-*D*-furanòsid esquelet derivats de xilosa i glucosa han sigut aplicats amb èxit en varis processos catalitzats per metalls de transició. Fins ara la influencia de varis paràmetres estructurals d'aquest tipus de lligands sobre els resultats catalítics no ha sigut destacada.

Aquest tesis esta enfocada en el desenvolupament i aplicació en catàlisi asimètrica de nous lligands 1,3-difosfit amb esquelet furanòsid. Com a sigut mencionat en la secció 1.1, la síntesis de series de 1,3-diosl amb esquelet 1,2-O-isopropylidene-α-*D*-furanòsid mitjançant la selectiva variació de la configuració dels stereocentres directament enllaçats a la funció fosforada es una etapa important en el disseny dels lligands bidentats mes eficients. Llavores, el disseny i la síntesis de nous 1,3-diols amb esquelet furanòsid, relacionat amb els ben coneguts esquelets 1,2-*O*-isopropilidene-α-*D*-xylofuranosa i 6-*O*-deoxy-1,2-*O*-isopropilidene-α-*D*-glucofuranosa, es descrit al capítol 2. Aquestes modificacions foren dutes a termes en dues direccions: a) Introducció de substituents *O*-alquilo en las posicions C-6 del esquelet furanòsid amb estructura bicíclica, i b) la reducció del anell 1,2-*O*-isopropylidene per tal d'obtenir 1,3-diols amb esquelet furanòsid i estructura monocíclica, i la introducció de substituents O-alquilo en la posició C-2 d'aquestos esquelets. El treball sintètic dut a terme per tal d'obtenir aquestos nous 1,3-diols es descrit al capítol 2.

Nous lligands 1,3-difosfit que contenen les funcions bifenil **a** i **b** han sigut sintetitzats partint dels nous 1,3-diols amb esquelet furanòsid. Les funcions bifenil **a** i **b** varen ser seleccionades per la versatilitat d´aquestos grup en varis processos asimètrics. A més, s'han sintetitzat nous lligands 1,3-difosfit que contenen les funcions bifenil **w**. Recentment, aquesta funció fosfit ha provat la seva eficiència a la hidrogenació de ketimines catalitzada per complexos d'iridi modificats amb lligands 1,2-fosfinit-fosfit amb esquelet derivat de mannitol. La síntesi d'aquestos nous 1,3-difosfits es descrita en el capítol 2.

La aplicació d'aquestos nous lligands 1,3-difosfot a la hidroformilació asimètrica de alquens monosubstituïts, com es el cas de l'estirè i l'acetat de vinil, i alquens interns disubstituïts, com es el cas del 2,5-dihidofuan i 2,3-dihidrofuran, es descrit al capítol 2. A més, en col·laboració amb el Prof. Dr. Dieter Vogt, aquestos nous lligands varen ser aplicats en la hidroformilació de alquens 1,1-disustituits, com es el cas del metil metacrilat i α-metilestire. L'efecte de les modificacions estructural del nous lligands 1,3-difosfit sobre els resultats catalítics va ser estudiada. Els resultats obtinguts en aquestos experiments son introduïts en el capítol 2. Els catalitzadors **21w** i **67w** son inactius baix condicions de reacció standard. Els millors resultats en la hidroformilació asimètrica d'estirè catalitzada per rodi foren obtingut amb el lligant **67a**. Aquest lligand produeix conversions moderades amb excel·lents enantioselectivitats (*ee* fins a 83% (*S*)) a 20ºC. En la hidroformilació asimètrica d'acetat de vinil catalitzada per rodi els millors resultats foren obtinguts emprant lligand **23b**. Aquest lligand produeix moderades conversions amb excel·lent regioselectivitat i 73% de *ee* a 20ºC. En el cas del lligand 2,5-dihidrofuran, els millors resultats es van obtenir emprant el lligand 67b a 20ºC. En aquest cas moderades conversions amb total selectivitat per donar el tetrahydro-3-carbaldehyde amb 88% de *ee* (*S*). En la hidroformilació asimètrica de 2,3-dihidrofuran, els millors resultats foren obtinguts emprant els sistemes catalítics Rh/**64b** i Rh/**65b** a 45ºC. El lligand **64b** permet obtenir conversions mes elevades que el lligand 65b, encara que els dos sistemes catalítics produeixen resultats similars en termes de regioselectivitat (fins a 78%) i enantioselectivitat (fins a 84%). Finalment, el lligand **65a** produeix els millors resultats en la hidroformilació asimètrica de metil metacrilat i α-metilestiré. En el cas de α-metilstiré, moderades conversions i bones

regioselectivitats amb 36% de *ee* va ser obtingut a 80ºC. En el cas metil metacrilat, moderades conversions i bones regioselectivitats amb 71% de *ee* va ser obtingut a 60ºC. Els complexos $[RhH(CO)_2(L)]$ (L = **21w**, **65b** i **67a,b**) van ser caracteritzats mitjançant tècniques de HP-RMN. Aquestes especies $[RhH(CO)_2(L)]$, on L= **21w**, **65b** i **67a,b**, va ser caracteritzats mitjançant RMN demostrant que aquestos lligands es coordinen al rodi en les posicions **eq-eq**.

Per altra part, l'efecte de les modificacions estructurals d'aquestos lligands 1,3-difosfit sobre els resultats catalítics en l'alquilació al·lílica de compostos al·lílic amb grups fenils catalitzada per compostos de pal·ladi es descrita al capítol 3. En aquesta secció es estudiada l'alquilació al·lílica catalitzada per pal·ladi de *rac*-1,3-difenil-3-acetoxi-propè emprant dimetil malonat com a nucleòfil i l'alquilació al·lílica catalitzada per pal·ladi de 1-fenil-3-acetoxi-propè emprant dimetil malonat i α-(etoxicarbonil)-cyclohexanona com a nucleòfils. Les condicions de reacció en l'alquilació al·lílica catalitzada per pal·ladi de *rac*-1,3-difenil-3-acetoxi-propè emprant dimetil malonat com a nucleòfil van ser optimitzades per a cada família de lligands. El lligand **65a** produeix els millors resultats baix les següents condicions de reacció: substrat/Pd = 100/1, Pd/L = 1/ 1.1, toluè com a solvent i t= 5 min. Aquet lligand produeix excel·lents enantioselectivitats en el producte (*ee* fins a 95 %) i en el substrat (*ee* fins a 99.9%). El lligand **65b** produeix resultats baix les següents condicions de reacció: substrat/Pd = 100/1, Pd/L = 1/ 2.0, toluè com a solvent i t= 5 min. Excel·lents enantioselectivitats en el producte (*ee* fins a 94%) i en el substrat (*ee* fins a 94%) van ser obtingudes. A més el lligand **67b** produeix excel·lents resultats en les següents condicions de reacció: substrat/Pd = 1000/1, Pd/L = 1/ 2.0, diclorometà com a solvent i t= 90 min. El sistema catalític Pd/**67b** produeix excel·lents enantioselectivitats en el producte (*ee* fins a 98.4 %) i en el substrat (*ee* fins a 95%). Els lligands que posseeixen en la seua estructura la funció fosfit **w** produeixen activitats i selectivitats molt baixes. L'efecte del sovent va ser estudiat en l'alquilació al·lílica catalitzada per pal·ladi de 1-fenil-3-acetoxi-propè emprant dimetil malonat com a nucleòfil i THF va ser seleccionat com el solvent més adequat. En aquesta reacció, els lligands derivats de xilofuranosa **21b**, **87b** i **89b** produeixen els millors resultats en termes de regioselectivitat (fins a 17%) i enantioselectivitat (fins a 83%). Els millors resultats en l'alquilació al·lílica catalitzada per pal·ladi de 1-fenil-

3-acetoxy-propè emprant α-(etoxicarbonil)-ciclohexanone com a nucleòfil van ser descrits emprant diclorometà com a solvent, $Zn(OAc)_2$ com a additiu i el lligand **65b**. Conversions moderades amb total selectivitat per a la formació del producte linear i enantioselectivitats fins a 38% van ser obtingudes. Els complexes $[Pd(\eta^3\text{-}C_3H_5)(L)]PF_6$, on L = **65b** i **67b**, van ser sintetitzats i caracteritzats per RMN. Els espectres de RMN dels dos complexes en CD_2Cl_2 revelen la presencia de una mescla de dos isòmers en equilibri amb una relació 1:1. Els dos isòmers varen ser caracteritzats per RMN i la seua estructura va ser atribuïda a les estructures *exo* i *endo*.

L'estabilització de nanopartícules metàl·liques i el seu us com a nanocatalitzadors es descrit al capítol 3. Les nanopartícules metàl·liques son actives en processos en els que els catalitzadors homogenis no ho son. Per tant, es van emprar les noves series de lligands 1,3-difosfit a l'estabilització de nanopartícules metàl·liques (ruteni, rodi i iridi) i es va estudiar l'efecte de les modificacions estructurals dels lligands sobre la sobre el diàmetre, la forma i la dispersió de diàmetres de les nanopartícules. Els nanocatalitzadors sintetitzats van ser emprats a la hidrogenació d'arens monocíclics pro-quirals, com es *o*-metilanisol i *m*-metilanisol. Rh-, Ru- i Ir- nanopartícules varen ser estabilitzades amb els lligands **21b** i **21w**. L'efecte de la funció fosfit emprada en l'estabilització de les nanopartícules va ser estudiat. La funció fosfit **b** produeix Rh- i Ir-nanopartícules més petites, mentre que la funció fosfit **w** produeix Ru-nanopartícules més petites. Els lligands que incorporaven en la seua estructura cadenes alquíliques van ser aplicats amb èxit en l'estabilització de Rh- i Ru-nanopartícules. Els Rh-, Ru- i Ir-nanocatalitzadors sintetitzats per estabilització amb els nous lligands 1,3-difosfit son actius en la hidrogenació de *o*-metilanisol i *m*-metilanisol. *Cis*-selectivitats moderades a altes (65-80%) sense enantioselectivitats van ser obtingudes en la hidrogenació de *m*-metilanisol. En el cas del *o*-metilanisol, total selectivitats al producte *cis* amb enantiosectivitats molt baixes (6% *ee*) varen ser descrites.

UNIVERSITAT ROVIRA I VIRGILI
1,3- DIPHOSPHITE LIGANDS WITH FURANOSIDE BACKBONE: A POWERFUL TOOL IN ASYMMETRIC CATALYSIS
Aitor Gual Gozalbo
DL: T-1535-2009/ISBN: 978-84-692-4554-5

STAGES:

▪June **2008** and May-June **2007**: Short training stage at the "Ecole Nationale Superieure de Chimie", Rennes, France

▪June **2006**: Short training stage at the "Laboratoire de Chimie de Coordination-CNRS", Toulouse, France

MEETING CONTRIBUTIONS:

▪Oral presentation at "4th Nanometcat Meeting"; Montpellier, November **2006**.

Title: *Asymmetric Catalysis: From carbohydrate ligands to metal nanoparticle catalysts*.

▪Poster at "XXII International Conference on Organometallic Chemistry"; Zaragoza, July **2006**.

Title: *Diphosphite ligands derived from carbohydrates. Application in Rh catalysed asymmetric hydroformylation and stabilization of Ru nanoparticles*.

▪Poster at "International Symposium on Homogeneous Catalysis, ISCH 2006"; Johanesburg, August **2006**

Title: *Diphosphite ligands derived from carbohydrates. Application in Rh catalysed asymmetric hydroformylation and stabilization of Ru nanoparticles*.

▪Poster at "COST Chemistry D40, Innovative Catalysis: New Processes and Selectivities."; Tarragona, April **2008**

Title: *Diphosphite Ligands Derived From Carbohydrates as Stabilizers for Ruthenium Nanoparticles: Promising Catalytic Systems in Arene Hydrogenation*.

▪Poster at "XXIII International Conference on Organometallic Chemistry"; Rennes, July **2008**

Title: *Diphosphite Ligands Derived From Carbohydrates as Stabilizers for Ruthenium Nanoparticles: Promising Catalytic Systems in Arene Hydrogenation.*

LIST OF PUBLICATIONS:

1. Diphosphite ligands derived from carbohydrates as stabilizers for ruthenium nanoparticles: promising catalytic systems in arene hydrogenation; A. Gual, M.R. Axet, K. Philippot, B. Chaudret, A. Denicourt-Nowicky, A. Roucoux, S. Castillón, C. Claver, *Chem. Commun.* **2008**, 2759.
2. C1-Symmetry Diphosphite Ligands Derived From Carbohydrates. Influence of Structural Modifications on the Rh-Catalyzed Asymmetric Hydroformylation of Styrene; A. Gual; C. Godard; C. Claver; S. Castillón, *Eur. J. Org. Chem.* **2009**, 1191.
3. New chiral diphosphites derived from substituted 9,10-dihydroanthracene. Applications in asymmetric catalytic processes; D. Sanhes, A. Gual, S. Castillon, C. Claver, M. Gómez, E. Teuma, *Tetrahedron: Asymmetry*, **2009**, in press.
4. 1,3-Diphosphite ligands derived from carbohydrates as chiral stabilizers for transition metal nanoparticles: promising catalytic systems for the hydrogenation of ortho- and meta-methylanisole; A. Gual, C. Godard, K. Philippot, B. Chaudret, A. Denicourt-Nowicki, A. Roucoux, S. Castillón, C. Claver, *ChemSusChem*. **2009**, submitted.
5. *Highly enantioselective Rh-catalysts for the asymmetric hydroformylation of vinyl- and allylethers using C1-Symmetry Diphosphite Ligands*; A. Gual, C. Godard, C. Claver, S. Castillón, *Chem. Eur. J.* **2009**, in preparation.
6. *Selective Hydroformylation of 2,2´-Disubstituted Alkenes using Chiral Diphosphites*; L. Cornelissen, C. Muller, A. Gual, S. Castillón, C. Claver, D. Vogt, *Chem. Eur. J.* **2009**, in preparation.
7. *Pd-Allylic Alkylation Provides Easy Access to Chiral Compounds. Searching the Best C-1 Symmetric Furanoside Diphosphite Ligand For These Reactions*; A. Gual, O. Pamies, M. Diéguez, S. Castillón, C. Claver, in preparation.
8. *New chiral diphosphites and their application in asymmetric catalytic processes*; F. Fernandez, A. Gual, S. Castillon, C. Claver, M. Gómez, E. Teuma, in preparation.